Advanced Mathematical Methods in Theoretical Physics

Wintersemester 2017/2018
Technische Universität Berlin

PD Dr. Gernot Schaller

March 15, 2021

This lecture aims at providing physics students and neighboring disciplines with a heuristic toolbox that can be used to tackle all kinds of problems. As time and resources are limited, we will explore only small fractions of different much wider fields, and students are invited to take the lecture only as a starting point.

The lecture will try to be as self-contained as possible and aims at providing rather recipes than strict mathematical proofs. It is not an original contribution but an excerpt of many papers, books, other lectures, and own experiences. Only a few of these have been included as references (footnotes describing famous scientists originate from Wikipedia and solely serve for better identification).

As successful learning requires practice, the lecture (Mondays) will be accompanied by exercises. Students should turn in individual solutions to the exercises at the beginning of Wednesday seminars (computer algebra may be used if applicable). Students may earn points for the exercise sheets, to be admitted to the final exam, they should have earned 50% of the points. After passing the final exam, the students earn in total six ECTS credit points. To get these credit points, students therefore need to get 50 % of the exercise points and 50 % to pass the final exam.

The lecture script will be made available online at

http://www1.itp.tu-berlin.de/schaller/.

Corrections and suggestions for improvements should be addressed to

gernot.schaller@tu-berlin.de.

The tentative content of the lecture is as follows:

- Integration
- Integral Transforms
- Ordinary Differential Equations
- Partial Differential Equations
- Statistics
- Operators

Contents

Chapter 1

Integration of Functions

In this chapter, we first briefly review the properties of complex numbers and functions of complex numbers. We will find that these properties can be used to solve e.g. challenging integrals in an elegant fashion.

1.1 Heuristic Introduction into Complex Analysis

Complex analysis treats complex-valued functions of a complex variable, i.e., maps from $\mathbb{C}$ to $\mathbb{C}$. As will become obvious in the following, there are fundamental differences compared to real functions, which however can be used to simplify many relationships extremely. In the following, we will therefore for a complex-valued function $f(z)$ always use the partition

$$\begin{aligned} z &= x + \mathrm{i}y &&: \quad \{x, y \in \mathbb{R}\} \\ f(z) &= u(x,y) + \mathrm{i}v(x,y) &&: \quad \{u, v : \mathbb{R}^2 \to \mathbb{R}\}, \end{aligned} \tag{1.1}$$

where x and y denote real and imaginary part of the complex variable z, and u and v the real and imaginary part of the function $f(z)$, respectively.

1.1.1 Differentiation over $\mathbb{C}$

The differentiability of complex-valued functions is treated in complete analogy to the real case. One fundamental difference however is that the limit

$$f'(z) := \lim_{z' \to z} \frac{f(z') - f(z)}{z' - z} \tag{1.2}$$

has in the complex plane an infinite number of ways to approach $z' \to z$, whereas in the real case there are just two such paths (left and right limit). In analogy to the real case we define the derivative of a complex function $f(z)$ via the difference quotient when the limit in Eq. (1.2)

a.) exists and

b.) is independent of the chosen path.

In this case, the function $f(z)$ is then called in z **complex differentiable**. If $f(z)$ is complex-differentiable in a U_ε-environment of z_0, it is also called **holomorphic** in z_0.

Demanding that a function is holomorphic has strong consequences, see Fig. 1.1. It implies

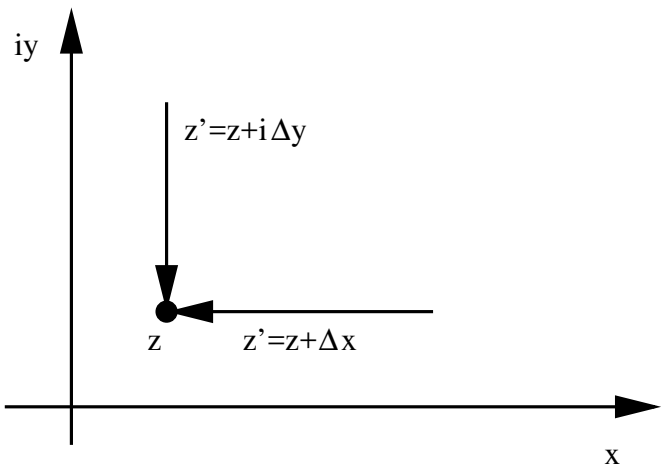

Figure 1.1: For the complex-differentiable function $f(x+\mathrm{i}y) = u(x,y) + \mathrm{i}v(x,y)$ we consider the path $z' \to z$ once parallel to the real and once parallel to the imaginary axis. For a complex-differentiable function, the result must be independent of the chosen path.

that the derivative can be expressed by

$$\begin{aligned} f'(z) &= \lim_{\Delta x\to 0} \frac{u(x+\Delta x,y) + iv(x+\Delta x,y) - u(x,y) - \mathrm{i}v(x,y)}{\Delta x} \\ &= \lim_{\Delta x\to 0} \frac{u(x+\Delta x,y) - u(x,y)}{\Delta x} + \mathrm{i} \lim_{\Delta x\to 0} \frac{v(x+\Delta x,y) - v(x,y)}{\Delta x} \\ &= \frac{\partial u}{\partial x} + \mathrm{i}\frac{\partial v}{\partial x}\,. \end{aligned} \tag{1.3}$$

On the other hand one must also have

$$\begin{aligned} f'(z) &= \lim_{\Delta y\to 0} \frac{u(x,y+\Delta y) + \mathrm{i}v(x,y+\Delta y) - u(x,y) - \mathrm{i}v(x,y)}{i\Delta y} \\ &= \lim_{\Delta y\to 0} \frac{u(x,y+\Delta y) - u(x,y)}{\mathrm{i}\Delta y} + \mathrm{i} \lim_{\Delta y\to 0} \frac{v(x,y+\Delta y) - v(x,y)}{\mathrm{i}\Delta y} \\ &= -\mathrm{i}\frac{\partial u}{\partial y} + \frac{\partial v}{\partial y}\,, \end{aligned} \tag{1.4}$$

since $f(z)$ has been assumed complex differentiable. Now, comparing the real and imaginary parts of Eqns. (1.3) and (1.4) one obtains the

Cauchy [1]-Riemann [2] differential equations

$$\frac{\partial u}{\partial x} = \frac{\partial v}{\partial y}\,, \qquad \frac{\partial u}{\partial y} = -\frac{\partial v}{\partial x}\,, \tag{1.5}$$

which – in essence – generate the full complex analysis.

The following theorem holds regarding complex differentiability:

Box 1 (Complex differentiability) *The function $f(z) = u(x,y) + \mathrm{i}v(x,y)$ is in z_0 complex differentiable if and only if:*

[1] Augustin-Louis Cauchy (1789–1857) was an extremely productive french mathematician with pioneering contributions to analysis and functional calculus. He is regarded as the first modern mathematician since he strict methodical approaches to mathematics.

[2] Georg Friedrich Bernhard Riemann (1826–1866) was a german mathematician with numerous contributions to analysis, differential geometry, functional calculus and number theory.

1. *real part $u(x_0, y_0)$ and imaginary part $v(x_0, y_0)$ are in (x_0, y_0) totally differentiable and*
2. *the Cauchy-Riemannschen differential equations ($u_x = v_y$, $u_y = -v_x$) in (x_0, y_0) hold.*

Then, the derivative is given by
$f'(z_0) = u_x(x_0, y_0) + \mathrm{i}v_x(x_0, y_0) = v_y(x_0, y_0) - \mathrm{i}u_y(x_0, y_0)$.

Many functions can be analytically continued from the real case to the full complex plane $\mathbb{C}$:

- the sine function (holomorphic in the full complex plane)

$$\sin(z) = \sum_{n=0}^{\infty} \frac{(-1)^n z^{2n+1}}{(2n+1)!} \tag{1.6}$$

- the cosine function (holomorphic in the full complex plane)

$$\cos(z) = \sum_{n=0}^{\infty} \frac{(-1)^n z^{2n}}{(2n)!} \tag{1.7}$$

- the exponential function (holomorphic in $\mathbb{C}$)

$$\exp(z) = \sum_{n=0}^{\infty} \frac{z^n}{n!}\,, \tag{1.8}$$

$$\cos(z) + \mathrm{i}\sin(z) = \sum_{n=0}^{\infty} \left(\frac{(\mathrm{i}z)^{2n}}{(2n)!} + \frac{(\mathrm{i}z)^{2n+1}}{(2n+1)!} \right) = \exp(\mathrm{i}z) \tag{1.9}$$

The last relation reduces for $z \in \mathbb{R}$ to the well-known Euler [3]- Moivre [4] formula.

We would like to summarize a few properties of the complex derivative:

1. Since the definition is analogous to the real derivative we also have in the complex plane $\mathbb{C}$ the product rule, quotient rule, and the chain rule.
2. Real- and Imaginary part of holomorphic functions obey the Laplace [5] equation: $u_{xx} + u_{yy} = 0 = v_{xx} + v_{yy}$. This is a direct consequence of the Cauchy-Riemann differential equations (1.5). This also implies that when a holomorphic function is known at the boundary of an area $G \subset \mathbb{C}$, it is fixed for all $x \in G$.
3. It is easy to show that all polynomials in z are in $\mathbb{C}$ holomorphic.
4. There are fundamental differences to $\mathbb{R}^2$. For example, the function $f(z) = z^* z = x^2 + y^2$ is totally differentiable in $\mathbb{R}^2$ but not holomorphic, since the Cauchy-Riemann differential equations (1.5) are not obeyed.

[3] Leonhard Euler (1707–1783) was a swiss mathematician with important contributions to analysis. His son Johann Albrecht Euler also became a mathematician but contributed also to astronomy.

[4] Abraham de Moivre (1667–1754) was a french mathematician most notably known for the formula $[\cos(z) + \mathrm{i}\sin(z)]^n = \cos(nz) + \mathrm{i}\sin(nz)$.

[5] Pierre-Simon (Marquis de) Laplace (1749–1827) was a french mathematician, physicist and astronomer. He contributed greatly to astronomy and physics, which forced him to developed new mathematical tools, which are still important today.

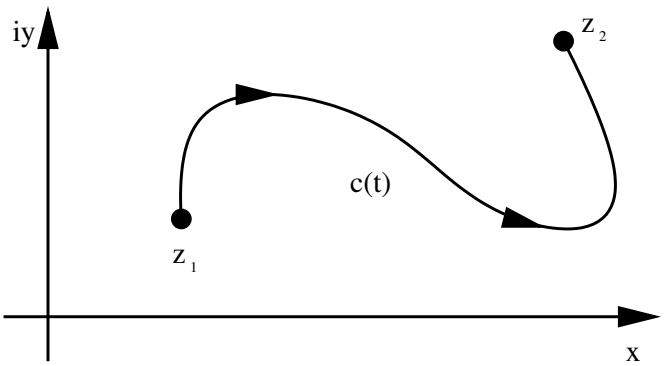

Figure 1.2: In contrast to the real numbers a path between points z_1 and z_2 in the complex plane must be specified to fix the integral. This can be conveniently done by choosing a parametrization of a contour $c(t) = x(t) + \mathrm{i}y(t)$ with parameter t.

1.1.2 Integration in the complex plane $\mathbb{C}$

As was already the case with differentiation, also for the integration a path must be fixed – in stark contrast to the real case, see Fig. 1.2. As in the real case the integral along a contour is defined via the Riemann sum. For its practical calculation however one uses a parametrization of the integration contour c by a curve $c(t) : [\alpha, \beta] \subset \mathbb{R} \to c \subset \mathbb{C}$ in the following way:

$$\int_c f(z)dz = \int_\alpha^\beta f[c(t)]\dot{c}(t)dt\,. \tag{1.10}$$

This maps complex integrals to real ones.

Fundamental example of complex calculus

We consider the closed integral in counterclockwise (mathematical) rotation along a circle with radius R and center z_0 over the function $f(z) = (z - z_0)^n : n \in \mathbb{Z}$. The parametrization of the contour is given by $z(t) = z_0 + Re^{\mathrm{i}t} : t = 0 \ldots 2\pi$. This implies

$$\begin{aligned}
\oint_{S_R(z_0)} (z - z_0)^n dz &= \mathrm{i}\int_0^{2\pi} R^{n+1} e^{\mathrm{i}(n+1)t} dt \\
&= \begin{cases} \frac{R^{n+1}}{n+1}\, e^{\mathrm{i}(n+1)t}\Big|_0^{2\pi} & : \quad n \neq -1 \\ 2\pi\mathrm{i} & : \quad n = -1 \end{cases} \\
\oint_{S_R(z_0)} (z - z_0)^n dz &= \begin{cases} 2\pi\mathrm{i} & : \quad n = -1 \\ 0 & : \quad \text{else} \end{cases} \qquad (n \in \mathbb{Z})\,.
\end{aligned} \tag{1.11}$$

For $n \neq -1$ the vanishing of the integral follows from the periodicity of the exponential function (1.8). For $n = -1$ the function is just constant along the contour, such that the value of the integral is given by the length of the path. Many theorems of complex calculus may be traced back to this fundamental example.

In the complex plane the integral has similiar properties as in the real case:

1. Since contour integrals are mapped to real integrals via parametrizations of the path it follows that the integral is linear.

2. For the same reason, the sign of an integral changes when the contour is traversed in the opposite direction (e.g. clockwise in the fundamental example).

3. The analogy to path integrals in $\mathbb{R}^3$ (for example regarding the work $W = \int_c \vec{F}d\vec{r}$) leads to the valid question:

   When are complex integrals independent of the chosen path?

1.1.3 Cauchy integral theorem

Box 2 (Cauchy's integral theorem) *Let $G \subset \mathbb{C}$ be a bounded and simply connected (no holes) area. Let f in G be holomorphic and let c be a closed curve that is fully contained in G. Then one has:*

$$\oint_c f(z)dz = 0\,. \tag{1.12}$$

A vanishing integral over a closed curve does of course also imply that the integral between two points is independent on the path (simply form a closed curve by adding two baths between two points). Here, we would just like to sketch the proof of Cauchy's theorem. First we separate real and imaginary parts:

$$\oint_c f(z)dz = \oint_c [u(x,y)dx - v(x,y)dy] + \mathrm{i}\oint_c [u(x,y)dy + v(x,y)dx]\ . \tag{1.13}$$

To both integrals we can apply the two-dimensional Stokes theorem

$$\oint_{\partial A} \vec{F}d\vec{r} = \oint_{\partial A} [F_x(x,y)dx + F_y(x,y)dy] = \iint_A \left(\frac{\partial F_y}{\partial x} - \frac{\partial F_x}{\partial y}\right) dxdy\,. \tag{1.14}$$

When we do now in Eq. (1.13) identify in the first integral $F_x = u(x,y), F_y = -v(x,y)$ and in the second integral $F_x = v(x,y), F_y = u(x,y)$ we obtain

$$\oint_c f(z)dz = \iint_{A(c)} dxdy \left(-\frac{\partial v}{\partial x} - \frac{\partial u}{\partial y}\right) + \mathrm{i}\iint_{A(c)} dxdy \left(\frac{\partial u}{\partial x} - \frac{\partial v}{\partial y}\right)\ . \tag{1.15}$$

The terms in round brackets vanish for holomorphic functions $f(z)$, since they constitute nothing but the Cauchy-Riemann differential equations (1.5).

Cauchy's integral theorem is useful for the calculation of many contour integrals. Consider, for example, the function $f(z) = (z - z_0)^{-1}$. It is holomorphic for all $z \neq z_0$ but has at $z = z_0$ a pole. When now z_0 is not enclosed by the integration contour c, one has $\oint_c (z - z_0)^{-1}dz = 0$. If, in contrast, z_0 is inside the contour specified by c, the pole can be cut out by a modified integration path c' (as depicted in Fig. 1.3) to render f holomorphic in the area surrounded by c'. Then, the area enclosed by the modified curve $c' = c + c_1 + \bar{S}_\varepsilon(z_0) + c_2$ does no longer contain a pole of f. Furthermore, for a closed path c and a closed circle $\bar{S}_\varepsilon(z_0)$ the integrals over c_1 and c_2 mutually cancel as $f(z)$ is continuous and these paths are traversed with opposite direction. Since the circle $\bar{S}_\varepsilon(z_0)$ is traversed with negative (clockwise) orientation, one obtains – with the fundamental example (1.11) – for the complete integral

$$\oint_{c'} f(z)dz = 0 = \int_c f(z)dz + \int_{\bar{S}_\varepsilon(z_0)} f(z)dz = \int_c f(z)dz - 2\pi\mathrm{i}\,. \tag{1.16}$$

This implies for arbitrary integration contours c:

$$\oint_c (z - z_0)^{-1}dz = \begin{cases} 0 & : \quad z_0 \notin c \\ 2\pi\mathrm{i} & : \quad z_0 \in c \end{cases}\ , \tag{1.17}$$

i.e., whereas the fundamental example was only valid for a circular contours, the above result is much more general.

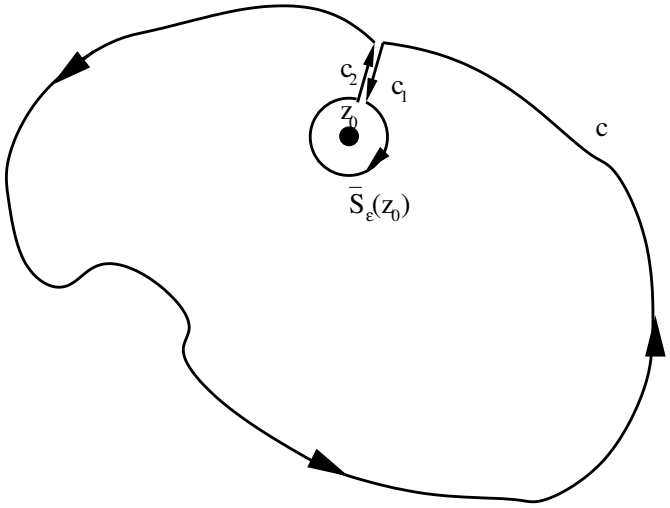

Figure 1.3: Appropriate excision of a singularity at $z = z_0$. The modified curve $c' = c + c_1 + \bar{S}_\varepsilon(z_0) + c_2$ does no longer enclose a singularity. In addition, it is directly obvious that the contributions c_1 and c_2 cancel each other since the are traversed at opposite orientation. Therefore, one actually has $\oint_c f(z)dz + \oint_{\bar{S}_\varepsilon(z_0)} f(z)dz = 0$.

1.1.4 Cauchy's integral formula

Box 3 (Cauchy's integral formula) *Let $G \subset \mathbb{C}$ be bounded and f in G be holomorphic and continous at the boundary ∂G. Let G be bounded by a finite number of disjoint curves c_i. Then one has:*

$$\oint_{\partial G} \frac{f(z)}{z - z_0} dz = \begin{cases} 2\pi \mathrm{i} f(z_0) & : \quad z_0 \in G \\ 0 & : \quad z_0 \notin G \end{cases} . \tag{1.18}$$

Also here we would like to provide a sketch for the proof: Since the case $z_0 \notin G$ can be mapped to Cauchy's integral theorem we will only consider the interesting case $z_0 \in G$. Then, the integrand has a pole at $z = z_0$, which – compare Fig. 1.3 – is excised by a small circle from G. In analogy to the previous example one obtains following Cauchy's integral theorem

$$\begin{aligned} \oint_{\partial G} \frac{f(z)}{z - z_0} dz &= -\lim_{\varepsilon \to 0} \int_{2\pi}^{0} \frac{f(z_0 + \varepsilon e^{\mathrm{i}\varphi})}{\varepsilon e^{\mathrm{i}\varphi}} \mathrm{i}\varepsilon e^{\mathrm{i}\varphi} d\varphi \\ &= \mathrm{i} \int_0^{2\pi} \lim_{\varepsilon \to 0} f(z_0 + \varepsilon e^{\mathrm{i}\varphi}) d\varphi \\ &= \mathrm{i} \int_0^{2\pi} f(z_0) d\varphi = 2\pi \mathrm{i} f(z_0) \,. \end{aligned} \tag{1.19}$$

A first observation regarding Eq. (1.18) is that all values of the function $f(z)$ in G are completely determined by its values at the boundary. This is a consequence of the Cauchy-Riemann differential equations as these imply that $f(x, y)$ is a solution to the Laplace equation (which is completely determined by given boundary conditions $[f(\partial G)]$). Therefore, Eq. (1.18) can be regarded a useful method to solve two-dimensional boundary problems on Laplace's equation.

Eq. (1.18) can be easily generalized to poles of higher order. Particularly interesting is of course only the case $z_0 \in G$. By performing multiple derivatives $\frac{\partial}{\partial z_0}$ on both sides of Eq. (1.18)

one obtains

$$\begin{aligned} 2\pi\mathrm{i}f'(z_0) &= 1\cdot\oint_{\partial G}\frac{f(z)}{(z-z_0)^2}dz\,, \\ 2\pi\mathrm{i}f''(z_0) &= 1\cdot 2\cdot\oint_{\partial G}\frac{f(z)}{(z-z_0)^3}dz\,, \\ 2\pi\mathrm{i}f'''(z_0) &= 1\cdot 2\cdot 3\cdot\oint_{\partial G}\frac{f(z)}{(z-z_0)^4}dz \qquad \ldots \end{aligned} \tag{1.20}$$

For the n-th derivative one obtains **Cauchy's general integral formula**:

$$\oint_{\partial G}\frac{f(z)}{(z-z_0)^{n+1}}dz = \frac{2\pi\mathrm{i}}{n!}f^{(n)}(z_0) \qquad (n=0,1,2,\ldots)\,, \tag{1.21}$$

which holds of course only for $z_0 \in G$. With this formula also integrals around higher-order poles can be calculated.

1.1.5 Examples

Cauchy's integral theorem and Cauchy's integral formula are often used to calculate real-valued integrals – these just have to be suitably continued into the complex plane. In the following, we will demonstrate this analytic continuation with some examples.

1. The integral

$$I = \int_{-\infty}^{\infty}\frac{dx}{x^2+1} \qquad \text{with} \qquad f(x) = \frac{1}{x^2+1} \tag{1.22}$$

has the solution π, since the antiderivative of $f(x)$ is arctan. However, also without knowing this one can find the solution directly with Eq. (1.18). The analytic continuation of $f(x)$ to the full complex plane is given by

$$f(z) = \frac{1}{z^2+1} = \frac{1}{(z-\mathrm{i})(z+\mathrm{i})}\,. \tag{1.23}$$

Obviously, there exist two poles at $z = \pm\mathrm{i}$. When we supplement the integral along the real axis with the semicircle in the upper complex half-plane as depicted in Fig. 1.4, we see that only one pole ($z = +\mathrm{i}$) resides inside the integration contour. In the limit $\lim_{R\to\infty}$ however the upper semicircle does not contribute, since $f(z)$ decays in the far-field as R^{-2}, whereas the length of the semicircle only grows linearly in R. This implies

$$\begin{aligned} I &= \int_{-\infty}^{\infty}\frac{dx}{x^2+1} = \oint_c\frac{F(z)}{z-\mathrm{i}}dz \qquad \text{with} \qquad F(z) = \frac{1}{z+\mathrm{i}} \\ &= 2\pi\mathrm{i}F(\mathrm{i}) = \frac{2\pi\mathrm{i}}{2\mathrm{i}} = \pi\,. \end{aligned} \tag{1.24}$$

2. When we consider the integral over the parametrization of a conic section, i.e., over an ellipse

$$I = \int_0^{2\pi}\frac{d\varphi}{1+\varepsilon\cos\varphi} = \int_0^{2\pi}\frac{d\varphi}{1+\frac{\varepsilon}{2}\left(e^{\mathrm{i}\varphi}+e^{-\mathrm{i}\varphi}\right)} \qquad : \qquad 0\le\varepsilon<1 \tag{1.25}$$

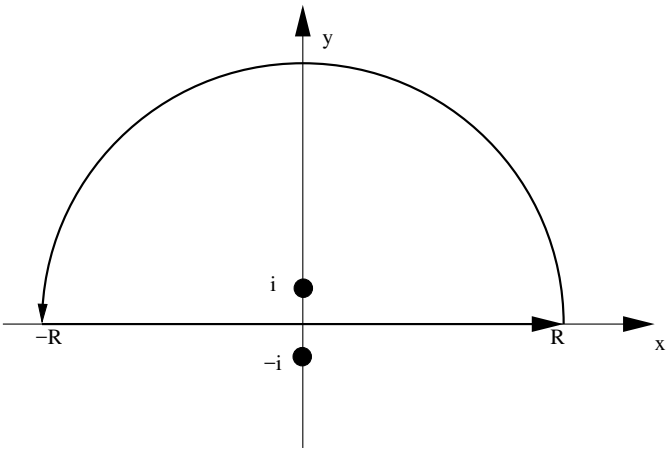

Figure 1.4: Closure of a complex integral in the upper complex half-plane. It is essential to verify that the integrand vanishes in the upper arc of radius R faster than $1/R$ as $R \to \infty$, since otherwise its contribution cannot be neglected.

we can use the substitution $z(\varphi) = e^{\mathrm{i}\varphi}$ to map the integral to a closed integral along the unit circle around the origin

$$\begin{aligned} I &= \frac{1}{\mathrm{i}} \oint_{S_1(0)} \frac{dz}{z + \frac{\varepsilon z}{2}\left(z + \frac{1}{z}\right)} = \frac{2}{\varepsilon \mathrm{i}} \oint_{S_1(0)} \frac{dz}{z^2 + \frac{2}{\varepsilon} z + 1} \\ &= \frac{2}{\varepsilon \mathrm{i}} \oint_{S_1(0)} \frac{dz}{(z - z_1)(z - z_2)} , \end{aligned} \tag{1.26}$$

$$\begin{aligned} \text{where} \quad z_1 &= -\frac{1}{\varepsilon} + \sqrt{\frac{1}{\varepsilon^2} - 1} \quad : \quad \text{inside } S_1(0) \\ z_2 &= -\frac{1}{\varepsilon} - \sqrt{\frac{1}{\varepsilon^2} - 1} \quad : \quad \text{outside } S_1(0) \end{aligned} \tag{1.27}$$

With Eq. (1.18) it follows that

$$I = \frac{2}{\varepsilon i} 2\pi \mathrm{i} \frac{1}{z_1 - z_2} = \frac{2\pi}{\varepsilon} \frac{1}{\sqrt{\frac{1}{\varepsilon^2} - 1}} = \frac{2\pi}{\sqrt{1 - \varepsilon^2}} . \tag{1.28}$$

3. The integral

$$I = \int_0^\infty \frac{dx}{(x^2 + a^2)^2} = \frac{1}{2} \int_{-\infty}^\infty \frac{dx}{(x^2 + a^2)^2} = \frac{1}{2} \int_{-\infty}^\infty \frac{dz}{(z + ia)^2 (z - ia)^2} \;:\; a > 0 \tag{1.29}$$

can as before be closed by a semicircle in the complex plane, see Fig. 1.5. Here, the integrand vanishes even faster than in our first example, such that the contribution of the upper semicircle need not be considered for the same reasons. However, here we have a second order pole residing at $z = +\mathrm{i}a$, such that Cauchy's general integral formula should be used

$$\begin{aligned} I &= \frac{1}{2} \lim_{R \to \infty} \oint_c \frac{dz}{(z + \mathrm{i}a)^2 (z - \mathrm{i}a)^2} = \frac{1}{2} 2\pi \mathrm{i} \frac{1}{1!} \frac{d}{dz} \left. \frac{1}{(z + \mathrm{i}a)^2} \right|_{z = \mathrm{i}a} \\ &= \left. \frac{-2\pi \mathrm{i}}{(z + \mathrm{i}a)^3} \right|_{z = \mathrm{i}a} = \frac{\pi}{4a^3} . \end{aligned} \tag{1.30}$$

We note that the result is an odd function of a, whereas the true solution to the integral must be an even function of a. This can be resolved by the fact that if a were negative, we could e.g. consider the same residue by closing the contour in the lower complex plane. Eventually, this would include a different orientation and thereby lead to a negative sign.

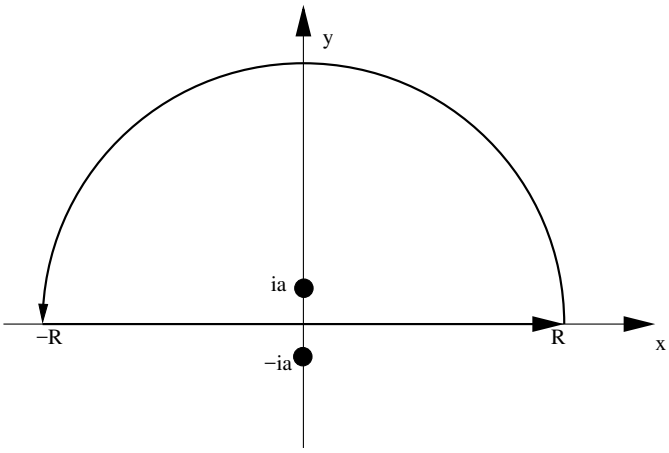

Figure 1.5: Closure of a contour in the upper complex plane. We have implicitly assumed here that $a > 0$.

4. Using the same contour as before we can also solve the integral (assuming $k > 0$)

$$I = \int_{-\infty}^{\infty} \frac{\cos(kx)dx}{x^2 + a^2} = \Re \int_{-\infty}^{\infty} \frac{e^{\mathrm{i}kz}dz}{z^2 + a^2} = \int_{-\infty}^{\infty} \frac{e^{\mathrm{i}kz}dz}{(z + \mathrm{i}a)(z - \mathrm{i}a)}\,, \tag{1.31}$$

which e.g. shows up in the calculation of many Fourier [6] transforms. Above, we have already used that the integral over the imaginary part vanishes due to symmetry arguments (odd function). Here, we have just as in Fig. 1.5 two poles, but of first order at $z = \pm \mathrm{i}a$. Furthermore, in contrast to the previous cases we have to be cautious: The contour should be closed in the upper half-plane, since in the lower half-plane ($y < 0$) the exponential function ($\exp(\mathrm{i}kz) = \exp(\mathrm{i}kx)\exp(-ky)$) would not be bounded. When we would close in the lower half-plane, the contribution from the semi-circle would therefore not vanish. Closing therefore in the upper half-plane, we obtain

$$I = 2\pi\mathrm{i}\, \frac{e^{\mathrm{i}kz}}{z + \mathrm{i}a}\bigg|_{z=\mathrm{i}a} = \frac{\pi}{a} e^{-ka}\,. \tag{1.32}$$

For $k < 0$ we would have to choose the opposite contour, but the symmetry of the cos function suggests that the result must be the same and we simply have to replace $k \to |k|$ in the result.

1.1.6 The Laurent Expansion

Box 4 (Laurent Expansion) *Let $f(z)$ be holomorphic inside the annulus (doughnut) $K(z_0, r, R) = \{z \in \mathbb{C} \,:\, 0 \le r < |z - z_0| < R \le \infty\}$. Then define for all ρ with $r < \rho < R$*

$$a_k = \frac{1}{2\pi\mathrm{i}} \oint_{S_\rho(z_0)} \frac{f(z)}{(z - z_0)^{k+1}} dz \qquad \forall k \in \mathbb{Z} \tag{1.33}$$

Then one has:

a. The a_k do not depend on ρ and

[6] Jean Baptiste Joseph Fourier (1768–1830) was a french mathematician and physicist. He was interested in heat conductance properties of solids (Fourier's law) and his Fourier analysis is a basis of modern physics and technology.

b. for all $z \in K(z_0, r, R)$ it follows that f is given by

$$f(z) = \sum_{n=-\infty}^{\infty} a_n (z - z_0)^n \,. \tag{1.34}$$

The above expansion is also called **Laurent** [7] **-Expansion**. In contrast to the conventional Taylor [8] expansion we also observe terms with poles (a_k with $k < 0$). From the definition of the coefficients above it furthermore follows that the Laurent-expansion is unique.

This in turn implies that in case $f(z)$ can at $z = z_0$ be expanded into a Taylor-Series, then this Taylor series is also the Laurent-series. In this case it just happens that many coefficients vanish $a_{k<0} = 0$.

Here, we just want to show that the calculation of the expansion coefficients a_k is self-consistent. For this we insert the expansion (1.34) in Eq. (1.33)

$$a_k = \frac{1}{2\pi \mathrm{i}} \sum_{l=-\infty}^{\infty} a_l \oint_{S_\rho(z_0)} \frac{(z - z_0)^l}{(z - z_0)^{k+1}} dz = \frac{1}{2\pi \mathrm{i}} \sum_{l=-\infty}^{\infty} a_l \oint_{S_\rho(z_0)} (z - z_0)^{l-k-1} dz \,. \tag{1.35}$$

Using the fundamental example of complex calculus from Eq. (1.11) it follows that all terms except one (for $l - k - 1 = -1$, i.e., for $l = k$) in the sum vanish. This leads to

$$a_k = \frac{1}{2\pi \mathrm{i}} 2\pi \mathrm{i} \sum_{l=-\infty}^{\infty} a_l \delta_{kl} = a_k \,. \tag{1.36}$$

This shows that the definition of the expansion coefficients is self-consistent.

The Laurent-expansion is often used to classify isolated singularities. Isolated singularities have in their U_ε-environment no further singularity – a typical counter-example is the function $f(z) = \sqrt{z}$, which is non-holomorphic on the complete negative real axis (where it has no isolated singularities).

To summarize, it is said that $f(z)$ has at $z = z_0$ a

- **curable singularity**, when the limit $\lim_{z \to z_0} =: f(z_0)$ exists and is independent on the approaching path. In the Laurent series all coefficients $a_{k<0}$ vanish in this case. A popular example for this situation is $\sin(z)/z$, which has a curable singularity at $z = 0$.

- **pole of order** m, when in the Laurent series of $f(z)$ around z_0 the first non-vanishing coefficient is a_{-m}, i.e., when $a_{-m} \neq 0$, $a_{k<-m} = 0$. For example, the function $f(z) = 1/(z - \mathrm{i})^3$ has a third order pole at $z = \mathrm{i}$.

- **essential singularity**, when in the Laurent series expansion of $f(z)$ there is no first non-vanishing coefficient, as is e.g. the case for $f(z) = \exp(1/z)$ at $z = 0$.

[7] Pierre Alphonse Laurent (1813–1854) was a french mathematician working as an engineer in the french army. His only known contribution – the investigation of the convergence properties of the Laurent series expansion – was published post mortem.

[8] Brook Taylor (1685–1731) was a british mathematician. He found his expansion already in 1712 but its importance for differential calculus was noted much later.

1.1.7 The Residue Theorem

Box 5 (Residue) *Let the Laurent expansion of a function $f(z)$ be known around z_0. Then, the expansion coefficient a_{-1} is called the* **residue of f at z_0**, *i.e.,*

$$\operatorname*{Res}_{z=z_0} f(z) = a_{-1} = \frac{1}{2\pi \mathrm{i}} \oint_{S_\rho(z_0)} f(z) dz \,. \tag{1.37}$$

Obviously, we have for the fundamental example with $f(z) = (z-z_0)^{-1}$ for the residue $\operatorname*{Res}_{z=z_0} f(z) = 1$. Furthermore, the integral theorem by Cauchy also implies that the residue vanishes at places where $f(z)$ is holomorphic. The **residue theorem** combines all theorems stated before and is one of the most important tools in mathemetics.

Box 6 (Residue Theorem) *Let $G \subset \mathbb{C}$ be an area bounded by a finite number of piecewise continuous curves. Let furthermore f be at the boundary ∂G and also inside G holomorphic – up to a finite number of isolated singularities $\{z_1, z_2, \ldots, z_{n-1}, z_n\}$ that are all in G. Then one has:*

$$\oint_{\partial G} f(z) dz = 2\pi \mathrm{i} \sum_{k=1}^{n} \operatorname*{Res}_{z=z_k} f(z) \,. \tag{1.38}$$

Here we would also like to provide a sketch of the proof. We will need the Laurent expansion and Cauchy's integral theorem. To obtain an area within which the function is completely holomorphic we excise the singularities as demonstrated in Fig. 1.6.

The ρ_k have to be chosen such that the Laurent-expansion of f around z_k converges on the circle described by $S_{\rho_k}(z_k)$. Now we insert at each singularity for $f(z)$ the Laurent expansion around the respective singularity $f(z) = \sum_l a_l^{(k)} (z - z_k)^l$

$$\begin{aligned} \oint_{\partial G} f(z) dz &= \sum_{k=1}^{n} \sum_{l=-\infty}^{\infty} a_l^{(k)} \oint_{S_{\rho_k}(z_k)} (z - z_k)^l dz = \sum_{k=1}^{n} \sum_{l=-\infty}^{\infty} a_l^{(k)} 2\pi \mathrm{i} \delta_{l,-1} \\ &= 2\pi \mathrm{i} \sum_{k=1}^{n} \operatorname*{Res}_{z=z_k} f(z) \,, \end{aligned} \tag{1.39}$$

where we have used the fundamental example of complex calculus (1.11).

Therefore, the residue theorem allows one do calculate path integrals that enclose multiple singularities. Very often, poles show up in these integrals, and the formula for the calculation of residues in Eq. (1.37) is rather unpractical for this purpose, since it requires the parametrization of an integral. Therefore, we would like to discuss a procedure that allows the efficient calculation of residues at poles of nth order.

Let $f(z)$ have at $z = z_0$ a pole of order m. Then, $f(z)$ can be represented as

$$f(z) = \frac{a_{-m}}{(z - z_0)^m} + \ldots + \frac{a_{-2}}{(z - z_0)^2} + \frac{a_{-1}}{(z - z_0)} + a_0 + \ldots \,. \tag{1.40}$$

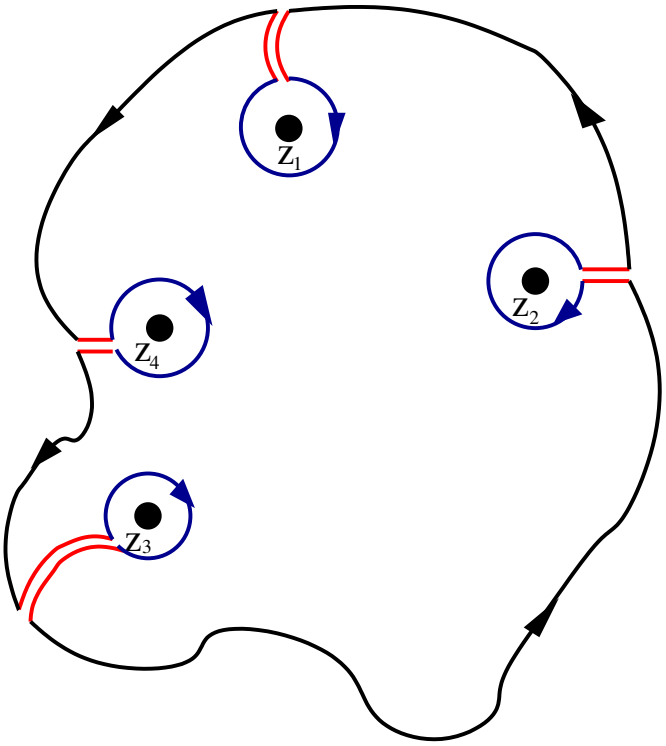

Figure 1.6: The singularities in G can be excised with circles of radii ρ_k, which implies $\oint_{\partial G} f(z)dz = -\sum_{k=1}^{n} \oint_{\bar{S}_{\rho_k}(z_k)} f(z)dz = +\sum_{k=1}^{n} \oint_{S_{\rho_k}(z_k)} f(z)dz$. Here, $\bar{S}_{\rho_k}(z_k)$ denote the clockwise orientation as depicted and $S_{\rho_k}(z_k)$ the positive orientation (counterclockwise), which compensates the sign. The two integral contributions along each cut (red) cancel each other as they are traversed with opposite orientation.

We are mainly interested in the coefficient a_{-1}. Therefore we first multiply the above equation with $(z-z_0)^m$ and then $(m-1)$ times perform the derivative for z, i.e.,

$$\begin{aligned}(z-z_0)^m f(z) &= a_{-m} + \ldots + a_{-2}(z-z_0)^{m-2} + \quad a_{-1} \quad (z-z_0)^{m-1} + a_0(z-z_0)^m + \ldots \\ \frac{d^{m-1}}{dz^{m-1}}(z-z_0)^m f(z) &= (m-1)! \quad a_{-1} \quad + \frac{m!}{1!}a_0(z-z_0) + \ldots . \end{aligned} \tag{1.41}$$

When in addition we do now also perform the limit $z \to z_0$ we see that all unwanted terms vanish and we obtain a formula for the fast calculation of residues of poles of m-th order.

Box 7 (Convenient calculation of residues) *Given that the function $f(z_0)$ has at $z = z_0$ a pole of order m, the residue can be obtained via*

$$\operatorname*{Res}_{z=z_0} f(z) = \frac{1}{(m-1)!} \lim_{z \to z_0} \frac{d^{m-1}}{dz^{m-1}}(z-z_0)^m f(z)\,. \tag{1.42}$$

In the following, we will discuss the residue theorem with the help of a few examples

1. The Laurent expansion of the function $f(z) = z^{-4}e^z$ around $z = 0$ can be directly found from the Taylor expansion of the exponential function

$$\begin{aligned} z^{-4}e^z &= z^{-4}\sum_{n=0}^{\infty}\frac{z^n}{n!} = z^{-4}\left(1 + z + \frac{1}{2}z^2 + \frac{1}{6}z^3 + \frac{1}{24}z^4 + \ldots\right) \\ &= \frac{1}{z^4} + \frac{1}{z^3} + \frac{1}{2z^2} + \frac{1}{6z} + \frac{1}{24} + \ldots \end{aligned} \tag{1.43}$$

and we can directly read off $\operatorname{Res}_{z=0} f(z) = 1/6$. This implies that e.g. for the closed integral along the unit circle centered at the origin (which contains the pole at $z = 0$)

$$\oint_{S_1(0)} \frac{e^z}{z^4} dz = 2\pi \mathrm{i} \operatorname{Res}_{z=0} f(z) = \frac{\pi \mathrm{i}}{3} . \tag{1.44}$$

2. For the integral

$$I = \oint_{S_7(\pi)} \frac{\cos(z)}{z^3 (z-\pi)^2} dz = \oint_{S_7(\pi)} f(z) dz \tag{1.45}$$

one has to calculate the residues at two poles, since both poles are enclosed by the integration contour $S_7(\pi)$. It is therefore useful to employ formula (1.42). At $z = 0$ we have a third-order pole, i.e.,

$$\begin{aligned} \operatorname{Res}_{z=0} f(z) &= \lim_{z\to 0} \frac{1}{2!} \frac{d^2}{dz^2} (z-0)^3 \frac{\cos(z)}{z^3 (z-\pi)^2} \\ &= \frac{1}{2} \lim_{z\to 0} \left(\frac{-\cos(z)}{(z-\pi)^2} + \frac{4\sin(z)}{(z-\pi)^3} + \frac{6\cos(z)}{(z-\pi)^4} \right) = \frac{6-\pi^2}{2\pi^4} . \end{aligned} \tag{1.46}$$

Analogously we proceed at $z = \pi$, where we have a second order pole

$$\begin{aligned} \operatorname{Res}_{z=\pi} f(z) &= \lim_{z\to \pi} \frac{1}{1!} \frac{d}{dz} (z-\pi)^2 \frac{\cos(z)}{z^3 (z-\pi)^2} \\ &= \lim_{z\to \pi} \left(\frac{-\sin(z)}{z^3} + \frac{-3\cos(z)}{z^4} \right) = \frac{3}{\pi^4} . \end{aligned} \tag{1.47}$$

Together we obtain

$$I = \oint_{S_7(\pi)} \frac{\cos(z)}{z^3 (z-\pi)^2} dz = 2\pi \mathrm{i} \frac{12-\pi^2}{2\pi^4} = \frac{(12-\pi^2)\mathrm{i}}{\pi^3} . \tag{1.48}$$

3. The Fourier transform

$$F(k) = \int_{-\infty}^{\infty} \frac{e^{-\mathrm{i}kx}}{(x^2+a^2)(x^2+b^2)} dx = \int_{-\infty}^{\infty} \frac{e^{-\mathrm{i}kz}}{(z-\mathrm{i}a)(z-\mathrm{i}b)(z+\mathrm{i}a)(z+\mathrm{i}b)} dz \tag{1.49}$$

can be calculated using the residue theorem. First we assume just for simplicity $a > 0$, $b > 0$, and $k > 0$: Symmetry arguments suggest that the value of the integral can only depend on $|a|$, $|b|$, and $|k|$ (the latter comes in since the imaginary part of the integral vanishes). When choosing the integration contour we have to be cautious, since $\exp(-\mathrm{i}kz) = \exp(-\mathrm{i}kx)\exp(+ky)$ for $k > 0$ is bounded only for z with negative real part $y < 0$. Therefore, we have to close the Fourier integral in the lower complex half-plane, see Fig. 1.7. Inside this contour we have two poles of first order at $z = -\mathrm{i}a$ und $z = -\mathrm{i}b$, and from Eq. (1.42) we obtain

$$\begin{aligned} \operatorname*{Res}_{z=-\mathrm{i}a} f(z) &= \lim_{z\to -\mathrm{i}a} \frac{e^{-\mathrm{i}kz}}{(z^2+b^2)(z-\mathrm{i}a)} = \frac{-e^{-ka}}{2\mathrm{i}a(b^2-a^2)} , \\ \operatorname*{Res}_{z=-\mathrm{i}b} f(z) &= \lim_{z\to -\mathrm{i}b} \frac{e^{-\mathrm{i}kz}}{(z^2+a^2)(z-\mathrm{i}b)} = \frac{e^{-kb}}{2\mathrm{i}b(b^2-a^2)} . \end{aligned} \tag{1.50}$$

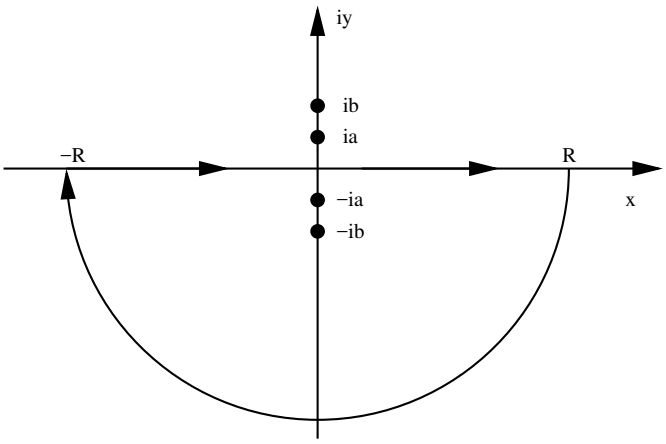

Figure 1.7: The contour integral (1.49) must be closed in the lower complex plane, as otherwise the contribution due to the semicircle would not vanish. Two poles are enclosed by the contour.

From the residue theorem we therefore obtain

$$\begin{aligned} F(k) &= \int_{-\infty}^{\infty} \frac{e^{-\mathrm{i}kx}}{(x^2+a^2)(x^2+b^2)} dx = -2\pi\mathrm{i} \frac{ae^{-kb} - be^{-ka}}{2\mathrm{i}ab(b^2-a^2)} \\ &= \frac{-\pi}{ab(b^2-a^2)} \left(ae^{-kb} - be^{-ka}\right) , \end{aligned} \tag{1.51}$$

where the sign arises from the negative orientation of the contour. With different assumptions on a, b, and k we might have to choose a different contour, direct inspection of the original integral however tells us that the result can only depend on the absolute values $|a|$, $|b|$, and $|k|$ of these parameters.

Many popular Fourier transforms can be calculated with the residue theorem, e.g. that of a Lorentz [9] function.

1.1.8 Principal Value integrals

On the real axis, the (Cauchy) Principal value is a way to assign finite solutions to sums of separately divergent integrals. A popular example is the integral ($a > 0$)

$$0 = \mathcal{P} \int_{-a}^{+a} \frac{dx}{x} , \tag{1.52}$$

where $\mathcal{P}$ denotes the $\mathcal{P}$rincipal value. We can split the integral into one contribution over negative numbers and another one over positive numbers, and each contribution is divergent. However, from simple symmetry considerations we can conclude that the integral must vanish, as the integrand is an odd function and the integration interval is symmetric with respect to $x = 0$. Therefore, one would assign the value 0 to the integral. Putting it more formally, we arrive at the following definition

[9] Hendrik Antoon Lorentz (1853–1928) was a dutch physicist known for the theoretical explanation of the Zeeman effect and for the transformation equations in special relativity. The distribution is sometimes however also called Breit-Wigner distribution or Cauchy distribution.

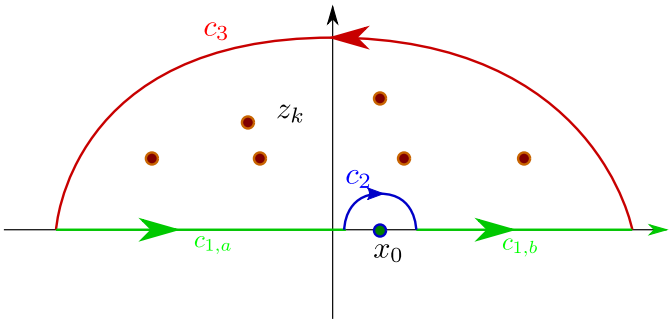

Figure 1.8: A contour integral can be used to calculate the Cauchy principal value of an integral with an isolated pole on the real axis. The green contours $c_{1,a}$ and $c_{1,b}$ yield the principal value integral, and by adding the semicircles around the pole on the real axis c_2 and the infinite semicircle in the upper complex plane c_3, the total contour becomes closed, such that the residue theorem applies.

Box 8 (Cauchy Principal Value) *Let the function $g(x)$ be defined in the interval $[a,b]$, with the exception of c with $a<c<b$. Then, the principal value is defined as*

$$\mathcal{P}\int_a^b g(x)dx = \lim_{\epsilon\to 0^+}\left[\int_a^{c-\epsilon} g(x)dx + \int_{c+\epsilon}^b g(x)dx\right]. \tag{1.53}$$

Clearly, when $g(x)$ has a curable singularity at $x=c$, the principal value is just the ordinary integral value. However, interesting applications arise when $g(x)=\frac{f(x)}{x-x_0}$, with $f(x)$ having no poles on the real axis. In the following, we will also consider $a\to-\infty$ and $b\to+\infty$. If furthermore $f(x)$ decays sufficiently fast in the upper or lower complex plane, we can use the residue theorem to calculate principal value integrals, see Fig. 1.8. We can construct a closed contour by supplementing the principal value contribution with two semicircles, which yields

$$\mathcal{P}\int\frac{f(x)}{x-x_0}dx + \int_{c_2}\frac{f(z)}{z-x_0}dz + \int_{c_3}\frac{f(z)}{z-x_0}dz = 2\pi\mathrm{i}\sum_{k=1}^N \operatorname*{Res}_{z=z_k}\frac{f(z)}{z-x_0}. \tag{1.54}$$

When $f(x)$ decays sufficiently fast in the upper complex plane, we can neglect the corresponding contribution $\int_{c_3}\frac{f(z)}{z-x_0}dz=0$. The remaining contour that goes around the pole on the real axis however needs to be evaluated explicitly by parametrizing $z=x_0+Re^{+\mathrm{i}\phi}$

$$\int_{c_2}\frac{f(z)}{z-x_0}dz = \lim_{R\to 0}\int_\pi^0 \frac{f(x_0+Re^{+\mathrm{i}\phi})}{Re^{+\mathrm{i}\phi}}\mathrm{i}Re^{+\mathrm{i}\phi}d\phi = -\pi\mathrm{i}f(x_0), \tag{1.55}$$

where we have used that the function $f(x)$ is holomorphic at x_0. Therefore, we can solve for the principal value as follows

$$\mathcal{P}\int\frac{f(x)}{x-x_0}dx = \pi\mathrm{i}f(x_0) + 2\pi\mathrm{i}\sum_{k=1}^N \operatorname*{Res}_{z=z_k}\frac{f(z)}{z-x_0}. \tag{1.56}$$

Alternatively, we could have closed the contour around the pole at x_0 by using a contour $\bar{c}_2$ in the lower complex plane. Then, the residue theorem would apply as well, with the difference that one additional pole is enclosed and that the small semicircle is traversed in opposite direction, and we would get

$$\mathcal{P}\int\frac{f(x)}{x-x_0}dx + \int_{\bar{c}_2}\frac{f(z)}{z-x_0}dz = 2\pi\mathrm{i}\operatorname*{Res}_{z=x_0}\frac{f(z)}{z-x_0} + 2\pi\mathrm{i}\sum_{k=1}^N \operatorname*{Res}_{z=z_k}\frac{f(z)}{z-x_0}. \tag{1.57}$$

We now get $\int_{\bar{c}_2} \frac{f(z)}{z-x_0} dz = +\pi \mathrm{i}$, and solving for the principal value contribution yields with considering that $\operatorname{Res}_{z=x_0} \frac{f(z)}{z-x_0} = f(x_0)$ the same result as Eq. (1.56). Effectively, we therefore get that the residue arising from the first order pole on the real axis counts only half

$$\mathcal{P} \int \frac{f(x)}{x-x_0} dx = \pi \mathrm{i} \operatorname{Res}_{z=x_0} \frac{f(z)}{z-x_0} + 2\pi \mathrm{i} \sum_{k=1}^{N} \operatorname{Res}_{z=z_k} \frac{f(z)}{z-x_0} \,. \tag{1.58}$$

As a first example, we consider ($a > 0$)

$$I = \int \frac{\sin(ax)}{x} dx = -\mathrm{i}\mathcal{P} \int \frac{e^{+\mathrm{i}ax}}{x} dx \,, \tag{1.59}$$

where we have used the symmetry argument that $\int \frac{\cos(ax)}{x} dx = 0$. In the original integral, we have at $x_0 = 0$ a curable singularity, whereas on the r.h.s. we have a first order pole. For $a > 0$, we can close the contour in the upper complex plane – there the integrand decays exponentially – and add a small semicircle excising the pole at $x_0 = 0$, leading to

$$\mathcal{P} \int \frac{e^{+\mathrm{i}ax}}{x} dx - \pi \mathrm{i} = 0 \,, \tag{1.60}$$

since no further poles are enclosed. Altogether, we therefore obtain

$$I = \pi \,. \tag{1.61}$$

A second example would be

$$I = \mathcal{P} \int \frac{\Gamma\delta^2}{(\omega-\epsilon)^2 + \delta^2} \frac{1}{\omega - \Omega} d\omega \tag{1.62}$$

with $\Omega \in \mathbb{R}$. The integrand has first order poles at $z_{1,2} = \epsilon \pm \mathrm{i}\delta$ and a first order pole on the real axis at $\omega = \Omega$. The integral therefore becomes

$$\begin{aligned} I &= \pi \mathrm{i} \frac{\Gamma\delta^2}{(\Omega-\epsilon)^2 + \delta^2} + 2\pi \mathrm{i} \left. \frac{\Gamma\delta^2}{(z-\epsilon+\mathrm{i}\delta)(z-\Omega)} \right|_{z=\epsilon+\mathrm{i}\delta} \\ &= \mathrm{i} \frac{\pi\Gamma\delta^2}{(\Omega-\epsilon)^2 + \delta^2} + \frac{\pi\Gamma\delta}{\epsilon - \Omega + \mathrm{i}\delta} = \frac{(\epsilon-\Omega)\pi\Gamma\delta}{(\epsilon-\Omega)^2 + \delta^2} \,. \end{aligned} \tag{1.63}$$

1.2 Useful Integration Tricks

Very often, integrals cannot be obviously solved by standard methods. Before one has to revert to numerical methods, there are a few well-known tricks to solve integrals or to map them to well-known standard integrals, which we will summarize here.

1.2.1 Standard Integrals

1. The integral ($a > 0$, $b \in \mathbb{R}$)

$$\begin{aligned} I_1(a,b) &= \int e^{-ax^2+bx} dx = \int e^{-\left(\sqrt{a}x - \frac{b}{2\sqrt{a}}\right)^2 + \frac{b^2}{4a}} \\ &= e^{\frac{b^2}{4a}} \int e^{-y^2} \frac{dy}{\sqrt{a}} = \sqrt{\frac{\pi}{a}} e^{\frac{b^2}{4a}} \end{aligned} \tag{1.64}$$

is a well-known standard, since it corresponds to a non-normalized Gaussian [10] distribution centered at $x^* = \frac{b}{2a}$. We note that the integral does not converge for $a <= 0$.

2. We can use Cauchy's integral formula to solve the integral over a Lorentzian function ($a \in \mathbb{R}$, $b > 0$ for simplicity)

$$\begin{aligned} I_2(a,b) &= \int \frac{1}{(x-a)^2+b^2}dx = \int \frac{1}{(x-a+\mathrm{i}b)(x-a-\mathrm{i}b)}dx \\ &= 2\pi\mathrm{i}\left.\frac{1}{x-a+\mathrm{i}\delta}\right|_{x=a+\mathrm{i}b} = \frac{\pi}{b}\,. \end{aligned} \tag{1.65}$$

The result of the integral is of course the same when $b < 0$, such that the more general expression would be $I_2(a,b) = \frac{\pi}{|b|}$.

3. The half-sided integral ($b > 0$)

$$I_3(b) = \int_0^\infty e^{-bx}dx = \frac{1}{b} \tag{1.66}$$

is readily solved as the antiderivative is well-known.

1.2.2 Integration by Differentiation

As many known integrals involve parameters, it is a popular method to see how these integrals transform when we consider derivatives with respect to these parameters. Here, we generalize the integrals introduced before.

1. Since the exponential function mainly reproduces itself under differentiation, we observe that performing a derivative with respect to the parameter b produces a factor of x in front of the exponential. We therefore directly conclude that for any polynomial $\mathcal{P}(x) = a_0 + a_1x + \ldots + a_Nx^N$, integrals of the type ($a > 0$, $b \in \mathbb{R}$)

$$I_1(a,b) = \int \mathcal{P}(x)e^{-ax^2+bx}dx = \mathcal{P}\left(\frac{\partial}{\partial b}\right)\sqrt{\frac{\pi}{a}}e^{\frac{b^2}{4a}}\,, \tag{1.67}$$

where we have used Eq. (1.64).

2. Similarly, we can solve the integral over higher powers of our second standard example ($a \in \mathbb{R}$, $b > 0$, $n \in \mathbb{N}$)

$$\begin{aligned} I_2(a,b) &= \int \left(\frac{1}{(x-a)^2+b^2}\right)^n dx = (-1)^{n-1}\frac{1}{(n-1)!}\left(\frac{\partial}{\partial B}\right)^{n-1}\int \frac{1}{(x-a)^2+B}dx\Bigg|_{B=b^2} \\ &= (-1)^{n-1}\frac{1}{(n-1)!}\left(\frac{\partial}{\partial B}\right)^{n-1}\left.\frac{\pi}{\sqrt{B}}\right|_{B=b^2}\,, \end{aligned} \tag{1.68}$$

where we have used Eq. (1.65). Alternatively, we might have solved this using the residue theorem.

[10] Johann Carl Friedrich Gauß (1777–1855) was a german mathematician, astronomer, physicist and geodesist. His extreme mathematical talent was soon recognized. Since he only published results after he was convinced that the theory was complete, many important contributions were discovered in his diary after his death.

3. Also half-sided integrals with polynomials $\mathcal{P}(x) = a_0 + a_1 x + \ldots + a_N x^N$ can be solved by differentiation

$$I_3(b) = \int_0^\infty \mathcal{P}(x) e^{-bx} dx = \mathcal{P}\left(-\frac{\partial}{\partial b}\right) \frac{1}{b} \,. \tag{1.69}$$

1.2.3 Saddle point approximation

Sometimes, series expansions of the integrand (or parts of it) lead to analytically solvable integrals.

Here, we will consider the series expansion of the integral

$$I = \int g(x) e^{\alpha f(x)} dx \,, \tag{1.70}$$

where $\alpha \gg 1$ is a real parameter, and $f(z)$ has a single maximum along the contour on the real axis. Clearly, for convergence we require that $g(x)$ decays sufficiently fast at $x \to \pm\infty$ and that $f(x)$ is negative at $x \to \pm\infty$. Furthermore, $f(z)$ and $g(z)$ should be holomorphic inside a region enclosing the real axis, and $g(z)$ should vary only slowly. Then, the main idea of the saddle point approximation is that the major contribution to the integral value comes from the region where $f(x)$ is maximal.

We therefore analytically continue $f(x)$ toward the complex plane and expand it around its maximum, defined by $f'(z_0) = 0$

$$f(x) \to f(z) \approx f(z_0) + \frac{1}{2} f''(z_0)(z - z_0)^2 \,. \tag{1.71}$$

Particularly, demanding that we expand around a maximum requires that $f''(z_0) < 0$. Using the holomorphic assumptions on $f(z)$ and $g(z)$, we may deform the integration contour without changing the value of the integral, such that the maximum of $f(z)$ lies on the contour. Then, the integral becomes

$$I \approx e^{\alpha f(z_0)} \int_c g(z) e^{\frac{\alpha}{2} f''(z_0)(z-z_0)^2} dz \approx e^{\alpha f(z_0)} g(z_0) \sqrt{\frac{-2\pi}{\alpha f''(z_0)}} \,. \tag{1.72}$$

In the last equality sign, we have used that for $\alpha \gg 1$, the integrand approaches a sharper and sharper Gaussian function, which for $\delta \to \infty$ approaches a δ-distribution.

As an example we consider the integral

$$I = \int \frac{e^{-\alpha x^2} \cos(2\alpha x)}{\sqrt{4 + x^2}} dx = \Re \int \frac{dz}{\sqrt{4 + z^2}} e^{\alpha(-z^2 + 2\mathrm{i}z)} = \int \frac{dz}{\sqrt{4 + z^2}} e^{\alpha(-z^2 + 2\mathrm{i}z)} \,. \tag{1.73}$$

In the last line, we have used that the imaginary part of the integrand is an odd function along the real axis and that the corresponding integral contribution vanishes. We first analyze the singularities of the integrand. These are beginning at the solution to $4 + z^2 = 0$, which corresponds to two branchcuts starting at $z = \pm 2\mathrm{i}$. However, as we see, these branchcuts are sufficiently far away from the real axis. The maximum of $f(z) = -z^2 + 2\mathrm{i}z$ is solved by $-2z_0 + 2\mathrm{i} = 0$, such that we have $z_0 = \mathrm{i}$. Furthermore, we get $f''(z_0) = -2$, and we remark that for this particular example we have no further terms, i.e.,

$$f(z) = -1 - (z - \mathrm{i})^2 \,. \tag{1.74}$$

Deforming the contour via $z = \mathrm{i} + s$, we can write the integral as

$$I = \int \frac{ds}{\sqrt{4+(\mathrm{i}+s)^2}} e^{-\alpha(1+s^2)} = e^{-\alpha} \int ds \frac{e^{-\alpha s^2}}{\sqrt{4+(\mathrm{i}+s)^2}} \approx e^{-\alpha} \frac{1}{\sqrt{4+\mathrm{i}^2}} \int ds e^{-\alpha s^2} = \frac{e^{-\alpha}}{\sqrt{3}} \sqrt{\frac{\pi}{\alpha}} \quad (1.75)$$

Higher order contributions can be taken into account by expanding the root around the stationary point z_0 as well.

Approximations of similar spirit can be applied to integrands that are given by a product of a simple weight function (which in our previous example was the Gaussian) and a complicated function (which was the exponential of the remainder before). For example, the current through a single quantum dot can be represented by the following integral

$$I = \frac{\Gamma_L \Gamma_R}{\Gamma_L + \Gamma_R} \int \left[f_L(\omega) - f_R(\omega) \right] \frac{1}{\pi} \frac{\Gamma/2}{(\omega - \epsilon)^2 + (\Gamma/2)^2} d\omega \,, \quad (1.76)$$

where Γ_α and $f_\alpha(\omega) = \left[e^{\beta_\alpha(\omega - \mu_\alpha)} + 1 \right]^{-1}$ are bare tunneling rates and Fermi functions of lead $\alpha \in \{L, R\}$, held at inverse temperatures β_α and chemical potentials μ_α. The abbreviation $\Gamma = \Gamma_L + \Gamma_R$ thus describes the overall coupling strength. Clearly, the current vanishes in equilibrium when both temperatures and chemical potentials are equal. Moreover, we note with using that for small coupling strength we can approximate the Lorentzian function by a Dirac-Delta distribution

$$\delta(x) = \lim_{\epsilon \to 0} \frac{1}{\pi} \frac{\epsilon}{x^2 + \epsilon^2} \,, \quad (1.77)$$

it becomes obvious that for weak couplings we can approximate the current by

$$I \approx \frac{\Gamma_L \Gamma_R}{\Gamma_L + \Gamma_R} \left[f_L(\epsilon) - f_R(\epsilon) \right] \,, \quad (1.78)$$

which is also the result of a simple master equation approach.

1.3 The Euler MacLaurin summation formula

Sums and Integrals are obviously related. For summations over integers, this relation can be made explicit by the Euler-MacLaurin [11] summation formula, which enables to calculate integrals by sums or sums by integrals.

1.3.1 Bernoulli functions

We first introduce the **Bernoulli** [12] **numbers** as expansion coefficients of the series

$$\frac{x}{e^x - 1} = \sum_{n=0}^{\infty} \frac{B_n}{n!} x^n \,, \quad (1.79)$$

[11] Colin Maclaurin (1698–1746) was a scottish mathematician, physicist and geodesist. He published the series in 1742 in a treatise on Newton's infinitesimal calculus.

[12] Jakob I. Bernoulli (1655–1705) was one of many famous members of the Bernoulli family with contributions to probability theory, variational calculus and power series.

where it is easy to show that the smallest Bernoulli numbers are given by

$$\begin{aligned} B_0 &= 1\,, \qquad B_1 = -\frac{1}{2}\,, \qquad B_2 = \frac{1}{6}\,, \qquad B_3 = 0\,, \qquad B_4 = -\frac{1}{30}\,, \qquad B_5 = 0\,, \\ B_6 &= \frac{1}{42}\,, \qquad B_7 = 0\,, \qquad B_8 = -\frac{1}{30}\,, \qquad B_9 = 0\,, \qquad B_{10} = \frac{5}{66}\,, \qquad \dots \end{aligned} \tag{1.80}$$

We note that all odd Bernoulli numbers $B_{n\geq 3}$ vanish. The Bernoulli numbers can be conveniently calculated via a recursion formula (without proof)

$$B_n = -\frac{1}{n+1}\sum_{k=0}^{n-1}\left(\begin{array}{c} n+1 \\ k \end{array}\right) B_k\,, \qquad B_0 = 1\,. \tag{1.81}$$

We also note that the Laurent-expansion (1.33) also enables us to calculate the Bernoulli numbers via the contour integral

$$B_n = \frac{n!}{2\pi \mathrm{i}}\oint_{S_\epsilon(0)} \frac{z}{e^z-1}\frac{dz}{z^{n+1}}\,. \tag{1.82}$$

Now, we extend the generating function for the Bernoulli numbers by considering the function

$$F(x,s) = \frac{xe^{sx}}{e^x-1} = \sum_{n=0}^{\infty}\frac{B_n(s)}{n!}x^n\,, \tag{1.83}$$

which defines the **Bernoulli functions** $B_n(s)$ implicitly as Taylor expansion coefficients (recall that $F(x,s)$ has a curable singularity at $x=0$). These Bernoulli functions have interesting analytic properties, we first state the simple ones

1. It is obvious that $B_n(0) = B_n$.

2. When we consider the limit $s=1$, we can obtain a further relation between the Bernoulli functions and Bernoulli numbers

$$\begin{aligned} F(x,1) &= \frac{xe^x}{e^x-1} = \frac{x}{1-e^{-x}} = \frac{(-x)}{e^{(-x)}-1} = \sum_{n=0}^{\infty}\frac{B_n}{n!}(-x)^n = \sum_{n=0}^{\infty}\frac{(-1)^n B_n}{n!}x^n \\ &= \sum_{n=0}^{\infty}\frac{B_n(1)}{n!}x^n\,, \end{aligned} \tag{1.84}$$

   which – since this has to hold for all x – yields $B_n(1) = (-1)^n B_n$.

3. Considering the limit $x\to 0$, we can fix the first Bernoulli function

$$F(0,s) = 1 = B_0(s)\,. \tag{1.85}$$

4. A recursive relation between the Bernoulli functions can be obtained by considering the partial derivative

$$\begin{aligned} \frac{\partial}{\partial s}F(x,s) &= x\frac{xe^{sx}}{e^x-1} = \sum_{n=0}^{\infty}\frac{B_n(s)}{n!}x^{n+1} \\ &= \sum_{n=0}^{\infty}\frac{B_n'(s)}{n!}x^n = \sum_{n=1}^{\infty}\frac{B_n'(s)}{n!}x^n\,, \end{aligned} \tag{1.86}$$

where in the last step we have used $B_0(x) = 1$, implying that $B_0'(x) = 0$. Now, we can rename in the second equation the summation index $n = m + 1$, such that we can write

$$F(x,s) = \sum_{m=0}^{\infty} \frac{B'_{m+1}(s)}{(m+1)!} x^{m+1} = \sum_{n=0}^{\infty} \frac{B'_{n+1}(s)}{(n+1)!} x^{n+1} \,, \tag{1.87}$$

from which we infer the relation $B'_{n+1}(s) = (n+1)B_n(s)$.

Altogether, we summarize again

$$\begin{aligned} B_n(0) &= B_n \,, \qquad B_n(1) = (-1)^n B_n \,, \\ B_0(s) &= 1 \,, \qquad B'_{n+1}(s) = (n+1) B_n(s) \,. \end{aligned} \tag{1.88}$$

Together, these formulas can be used to calculate the Bernoulli functions recursively. For a recursive calculation of Bernoulli functions, we note that these are completely defined by the relation

$$B_0(s) = 1 \,, \qquad B'_n(s) = n B_{n-1}(s) \,, \qquad \int_0^1 B_n(s) ds \overset{n\geq 1}{=} 0 \,. \tag{1.89}$$

For completeness, we note the first few Bernoulli functions explicitly

$$\begin{aligned} B_0(x) &= 1 \,, \qquad B_1(x) = x - \frac{1}{2} \,, \qquad B_2(x) = x^2 - x + \frac{1}{6} \,, \qquad B_3(x) = x^3 - \frac{3}{2} x^2 + \frac{x}{2} \,, \\ B_4(x) &= x^4 - 2x^3 + x^2 - \frac{1}{30} \,. \end{aligned} \tag{1.90}$$

1.3.2 The Euler-MacLaurin formula

We want to represent the integral

$$I = \int_0^1 f(x) dx \,, \tag{1.91}$$

in terms of a sum involving only the derivatives of $f(x)$. It can be shown easily that any integral along a finite range can be mapped to the above standard form. Heuristically, we may insert the Bernoulli function $B_0(x) = 1 = B_1'(x)$

$$I = \int_0^1 f(x) B_0(x) dx = \int_0^1 f(x) B_1'(x) dx \,. \tag{1.92}$$

Integration by parts yields

$$I = \left[f(x) B_1(x) \right]_0^1 - \int_0^1 f'(x) B_1(x) dx = \frac{f(0) + f(1)}{2} - \int_0^1 f'(x) B_1(x) dx \,, \tag{1.93}$$

where we have – temporarily used $B_1(0) = -1/2$ and $B_1(1) = +1/2$ – to demonstrate that the first term simply yields combinations of $f(0)$ and $f(1)$. We can go on with this game by using

$B_n(x) = 1/(n+1)B'_{n+1}(x)$ and performing again an integration by parts

$$\begin{aligned} I &= [f(x)B_1(x)]_0^1 - \frac{1}{2}\int_0^1 f'(x)B'_2(x)dx \\ &= \left[f(x)B_1(x) - \frac{1}{2}f'(x)B_2(x)\right]_0^1 + \frac{1}{2\cdot 3}\int_0^1 f''(x)B'_3(x)dx \\ &= \left[f(x)B_1(x) - \frac{1}{2}f'(x)B_2(x) + \frac{1}{2\cdot 3}f''(x)B_3(x)\right]_0^1 - \frac{1}{4!}\int_0^1 f^{(3)}(x)B'_4(x)dx \\ &= \left[\sum_{m=1}^{n} f^{(m-1)}(x)B_m(x)\frac{(-1)^{m-1}}{m!}\right]_0^1 + \frac{(-1)^n}{n!}\int_0^1 f^{(n)}(x)B_n(x)dx\,, \end{aligned} \tag{1.94}$$

where in the last line we have generalized to arbitrary integers $n \geq 1$. We can further use properties of the Bernoulli numbers, e.g. that $B_3(0) = B_3 = 0$ and $B_3(1) = -B_3 = 0$ and similiar for all higher odd Bernoulli functions evaluated at either 0 or 1. Therefore, after separating the nonvanishing terms with $B_1(0/1)$, only the even contributions need to be considered

$$\begin{aligned} I &= \frac{f(0)+f(1)}{2} + \left[\sum_{p=1}^{q} f^{(2p-1)}(x)B_{2p}(x)\frac{(-1)^{2m-1}}{(2p)!}\right]_0^1 + \frac{(-1)^{2q}}{(2q)!}\int_0^1 f^{(2q)}(x)B_{2q}(x)dx \\ &= \frac{f(0)+f(1)}{2} - \sum_{p=1}^{q}\frac{B_{2p}}{(2p)!}\left[f^{(2p-1)}(x)\right]_0^1 + \frac{1}{(2q)!}\int_0^1 f^{(2q)}(x)B_{2q}(x)dx\,, \end{aligned} \tag{1.95}$$

which finally allows us to summarize the **Euler-MacLaurin formula**.

Box 9 (Euler-MacLaurin formula) *The Euler-MacLaurin formula relates the integral of a function $f(x)$*

$$\begin{aligned} I &= \int_0^1 f(x)dx \\ &= \frac{f(0)+f(1)}{2} - \sum_{p=1}^{q}\frac{B_{2p}}{(2p)!}\left[f^{(2p-1)}(1) - f^{(2p-1)}(0)\right] + \frac{1}{(2q)!}\int_0^1 f^{(2q)}(x)B_{2q}(x)dx\,, \end{aligned} \tag{1.96}$$

where $q > 1$ is an integer, with the values of $f(x)$ and its derivatives at the end points of the interval and an error term involving the Bernoulli functions.

The formula can be extremely useful in practice when cleverly applied, as will be outlined below.

1.3.3 Application Examples

1. In many cases, the remainder term $\epsilon(q) \equiv \frac{1}{(2q)!}\int_0^1 f^{(2q)}(x)B_{2q}(x)dx$ can be neglected once q is chosen large enough. This holds true exactly when $f(x)$ is a polynomial in x, since then

above a certain q all derivatives simply vanish. However, also when the derivatives of $f(x)$ decay sufficiently fast with q, one may argue that in

$$\int_0^1 f(x)dx = \frac{f(0)+f(1)}{2} - \sum_{p=1}^{q} \frac{B_{2p}}{(2p)!}\left[f^{(2p-1)}(1) - f^{(2p-1)}(0)\right] + \epsilon(q) \tag{1.97}$$

the error term $\epsilon(q)$ can be neglected, which is then termed **Euler-MacLaurin approximation**. This may of course fail in cases where the error term does not decay for large q, as can be seen in the elementary example[13] $f(x) = \ln(1+x)$: Although derivatives become smaller with q in the interval $x \in (0,1]$, they do not decay fast enough to justify the neglect of the remainder $\epsilon(q)$.

2. The Euler-MacLaurin formula is useful to evaluate series of the form $\sum_{m=a}^{b} f(m)$ (with integers $b > a$). To see this, we consider the integral instead

$$I = \int_a^b f(x)dx = \sum_{m=a}^{b-1} \int_m^{m+1} f(x)dx\,. \tag{1.98}$$

For each integration interval we can introduce the function $g_m(x) = f(m+x)$, such that one has for a single interval

$$\begin{aligned} \int_m^{m+1} f(y)dy &= \int_0^1 g(x)dx \qquad (1.99)\\ &= \frac{f(m)+f(m+1)}{2} + \sum_{p=1}^{q} \frac{B_{2p}}{(2p)!}\left[f^{(2p-1)}(m) - f^{(2p-1)}(m+1)\right] + \epsilon_m(q)\,. \end{aligned}$$

For the total integral this now implies

$$I = \sum_{m=a}^{b-1} \left\{ \frac{f(m)+f(m+1)}{2} + \sum_{p=1}^{q} \frac{B_{2p}}{(2p)!}\left[f^{(2p-1)}(m) - f^{(2p-1)}(m+1)\right] + \epsilon_m(q) \right\} \tag{1.100}$$

where we can now separately evaluate the terms. The values $f(m)$ combine to

$$\begin{aligned} \sum_{m=a}^{b-1} \frac{f(m)+f(m+1)}{2} &= \frac{f(a)}{2} + f(a+1) + f(a+2) + \ldots + f(b-1) + \frac{f(b)}{2} \\ &= -\frac{f(a)+f(b)}{2} + \sum_{m=a}^{b} f(m)\,, \end{aligned} \tag{1.101}$$

where we have of course implicitly assumed convergence of the series. All derivatives of $f(x)$ cancel when evaluated at intermediate integers

$$\sum_{m=a}^{b-1} \sum_{p=1}^{\infty} \frac{B_{2p}}{(2p)!}\left[f^{(2p-1)}(m) - f^{(2p-1)}(m+1)\right] = \sum_{p=1}^{\infty} \frac{B_{2p}}{(2p)!}\left[f^{(2p-1)}(a) - f^{(2p-1)}(b)\right]\,, \tag{1.102}$$

[13] A special thanks to Dr. Vito Lampret for pointing this out.

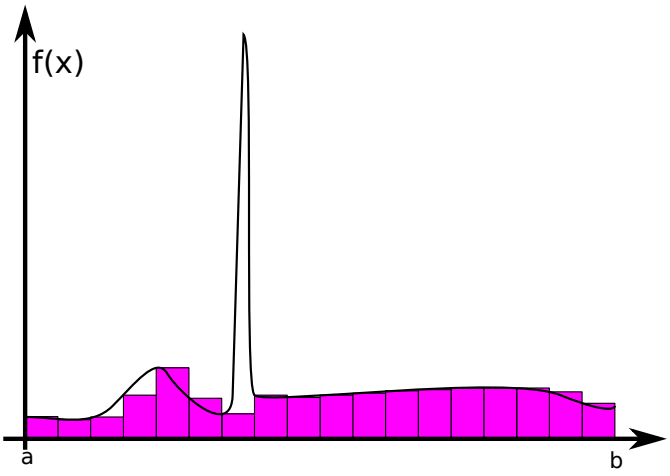

Figure 1.9: When the number of sampling points is finite, fine details (e.g. the peak) of the integrand may be missed. In regions where the integrand does not vary strongly, the number of sampling points could be reduced (to reduce the number of possibly expensive function calls). To maintain a high level of accuracy, the number of sampling points should be increased where the integrand changes strongly.

such that we can represent the sum by an integral as

$$\sum_{m=a}^{b} f(m) = \frac{f(a)+f(b)}{2} + \int_a^b f(x)dx - \sum_{p=1}^{q} \frac{B_{2p}}{(2p)!}\left[f^{(2p-1)}(a) - f^{(2p-1)}(b)\right] + \sum_m \epsilon_m(q) \quad (1.103)$$

The above formula is also useful to obtain asymptotic expansions of infinite series. When e.g. we consider the limit $b \to \infty$ and $a = 0$ and assume that all derivatives for the function vanish at infinity, one obtains the reduced version

$$\sum_{m=0}^{\infty} f(m) = \frac{f(0)}{2} + \int_0^{\infty} f(x)dx - \sum_{p=1}^{q} \frac{B_{2p}}{(2p)!} f^{(2p-1)}(0) + \sum_m \epsilon_m(q)\,. \quad (1.104)$$

3. Finally, we note here that the Euler-MacLaurin formula can be used to implement integrals numerically, which we will discuss in the next section.

1.4 Numerical Integration

If anything else (exact analytical solution, expansion of parts of the integrand, etc.) fails, one has to resort to numerical approaches. This is represented here as a last chance, since numerical integration may suffer from a variety of problems. The material in this section is a strongly-reduced excerpt from Ref. [1], which is available on-line at no cost. In particular, numerical integration is only useful when the integrand is sufficiently smooth and bounded and when the location of potential peaks is well known. The simplest approach to integrate a function numerically is to approximate it with a number of equally spaced sampling points

$$\int_a^b f(x)dx \approx \sum_{i=0}^{N} f\left(a + (b-a)\frac{i}{N}\right)\frac{b-a}{N}\,, \quad (1.105)$$

which becomes exact as the number of sampling points approaches infinity $N \to \infty$. Unfortunately, as numerical calculations should be performed in finite time, one will have to use a finite number of sampling points. Figure 1.9 demonstrates potential problems with numerical integration.

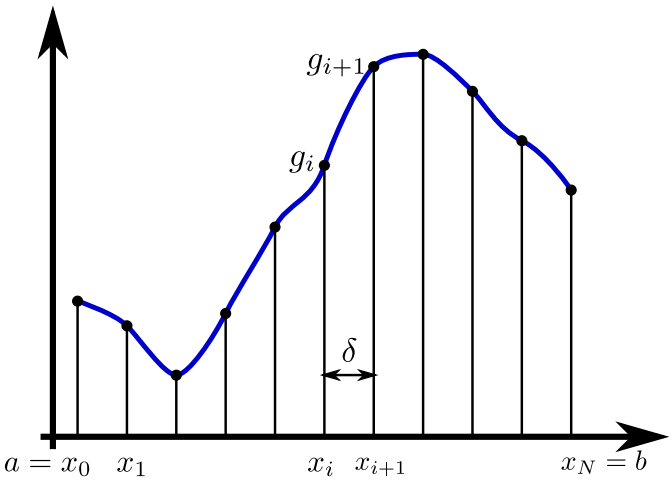

Figure 1.10: Sketch of a smooth function approximated by $N+1$ (here, $N=10$) sampling points separated by distance δ.

We further note here that solving the integral is equivalent to solving the differential equation

$$\frac{dy}{dx} = f(x)\,, \qquad \text{with} \qquad y(a) = 0 \tag{1.106}$$

for the solution $y(b)$. Methods for the solution of differential equations have been adapted to treat strongly varying $f(x)$. Therefore, if the integrand has many peaks – with positions of the peaks possibly unknown, a suitable solver for differential equations in combination with an adaptive stepsise is advisable.

Finally, we note that, to cope with such problems, modern computer algebra systems (e.g. Mathematica) provide several options regarding the integration method, the position of potential singularities or peaks, the required accuracy, the number of sampling points etc. It is usually a good idea to use them.

1.4.1 The Trapezoidal Rule

We will discuss the case of equally spaced sampling points here. For a short integration interval δ we can approximate any well-behaved function by a lower-order polynomial, such that the remainder term in the Euler-MacLaurin formula can be safely neglected as $q \to \infty$. Then we can apply the Euler-MacLaurin formula in Box 9 with $f(x) = g(x_i + x\delta)\delta$ and $y = x_i + x\delta$ and $q \to \infty$ (assuming that the remainder term vanishes) to yield

$$\int_{x_i}^{x_i+\delta} g(y)dy = \frac{g(x_i)+g(x_i+\delta)}{2}\delta - \sum_{p=1}^{\infty} \frac{B_{2p}}{(2p)!}\left[g^{(2p-1)}(x_i+\delta) - g^{(2p-1)}(x_i)\right]\delta^{2p}\,. \tag{1.107}$$

The factor δ^{2p} arises due to the chain rule. We note that δ becomes smaller when we increase the number of sampling points. Now we consider the discretization of the interval $[a,b]$ with N intervals such that $x_n = a + n\delta$ with $\delta = (b-a)/N$ and $n \in \{0,1,\ldots,N\}$, see Fig. 1.10. When applying the above equation to every interval, we see that for all internal points $x_1,\ldots,x_{N-1}$ the terms involving Bernoulli numbers cancel, and only the external contributions remain

$$\begin{aligned} I &= \int_a^b g(y)dy = \sum_{n=1}^{N} \int_{a+(n-1)\delta}^{a+n\delta} g(y)dy \\ &= \delta\left[\frac{g(a)+g(b)}{2} + \sum_{n=1}^{N-1} g(a+n\delta)\right] + \sum_{p=1}^{\infty}\left[g^{(2p-1)}(a) - g^{(2p-1)}(b)\right]\frac{(b-a)^{2p}}{N^{2p}}\,. \end{aligned} \tag{1.108}$$

First one can see that the second summation in the above equation can be neglected when $N \to \infty$, as for each power of $1/N$ only two terms remain. Then, the derivatives of $g(y)$ need not be computed. This is the essence of the trapezoidal rule.

Box 10 (Trapezoidal Rule) *The integral of a function $g(y)$ can be approximated by $N+1$ sampling points with interval spacings $\delta = (b-a)/N$*

$$I = \int_a^b g(y)dy = \delta \left[\frac{g(a)+g(b)}{2} + \sum_{n=1}^{N-1} g(a+n\delta) \right] + \mathcal{O}\{\frac{1}{N^2}\}\,. \tag{1.109}$$

- One obvious advantage of using the simple trapezoidal rule – where all mesh points are equally contributing to the integral – is that when we refine the grid at which $f(x)$ is evaluated, the previous result need not be discarded but can be used.

- Furthermore, the sum rule is extremely simple to implement, and one might have guessed this rule from the beginning by centering the integration intervals at the sampling points.

- We see that doubling the number of sampling points reduces the error by a factor of four.

1.4.2 The Simpson Rule

A further interesting observation stemming from the Euler-MacLaurin summation formula (or from the fact that the higher odd Bernoulli numbers vanish) is that only even powers of $\delta = (b-a)/N$ occur in Eq. (1.108), i.e., formally we can write for the integral approximation with N points

$$S_N = 2\delta \left[\frac{g(a)}{2} + \left[\sum_{n=1}^{N-1} g(a+n2\delta) \right] + \frac{g(b)}{2} \right] + \frac{\alpha}{N^2} + \mathcal{O}\{N^{-4}\}\,, \tag{1.110}$$

where we use $\Delta = (b-a)/N = 2\delta$. The fact that only even powers of $1/N$ occur has the beautiful consequence, that by cleverly combining summation results using the discretization width Δ and a half discretization width $\delta = \Delta/2$ as depicted in Fig. 1.11 we can eliminate the leading order error term. Formally, we can express the result for the half-width discretization as

$$S_{2N} = \delta \left[\frac{g(a)}{2} + \left(\sum_{n=1}^{2N-1} g(a+n\delta) \right) + \frac{g(b)}{2} \right] + \frac{\alpha}{4N^2} + \mathcal{O}\{N^{-4}\}\,. \tag{1.111}$$

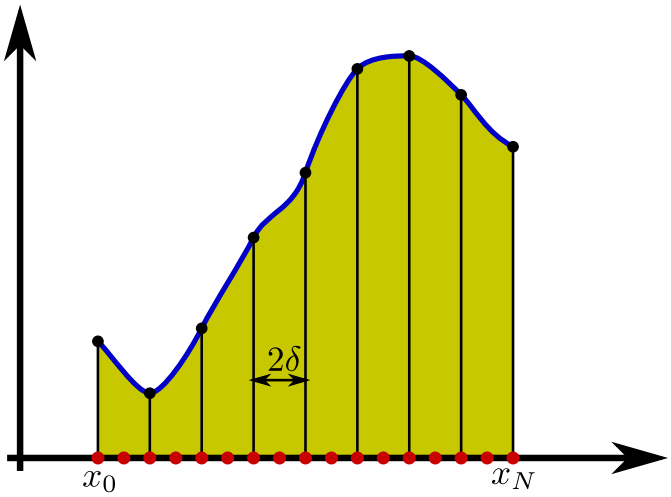

Figure 1.11: Sketch of the approximation of the integral in the shaded region with discretization width $\Delta = (b-a)/N$ (black circles) and $\delta = \Delta/2$ (red circles). The coarse discretization requires $N+1$ sampling points, whereas the finer grid has $2N+1$ sampling points.

Consequently, we see that in the combination of Eqns. (1.110) and (1.111)

$$\begin{aligned} S &= \frac{4}{3}S_{2N} - \frac{1}{3}S_N \\ &= \delta\Big[\left(\frac{4}{3}\frac{1}{2}g(a) - 2\frac{1}{3}\frac{1}{2}g(a)\right) + \left(\frac{4}{3}g(a+\delta)\right) + \left(\frac{4}{3}g(a+2\delta) - 2\frac{1}{3}g(a+2\delta)\right) + \dots \\ &\quad + \left(\frac{4}{3}g(a+(2N-2)\delta) - 2\frac{1}{3}g(a+(2N-2)\delta)\right) + \left(\frac{4}{3}g(a+(2N-1)\delta)\right) \\ &\quad + \left(\frac{4}{3}\frac{1}{2}g(b) - 2\frac{1}{3}\frac{1}{2}g(b)\right)\Big] + \mathcal{O}\{N^{-4}\} \\ &= \delta\Big[\frac{1}{3}g(a) + \frac{4}{3}g(a+\delta) + \frac{2}{3}g(a+2\delta) + \dots \\ &\quad + \frac{2}{3}g(a+(2N-2)\delta) + \frac{4}{3}g(a+(2N-1)\delta) + \frac{1}{3}g(b)\Big] + \mathcal{O}\{N^{-4}\}\,. \end{aligned} \tag{1.112}$$

Since there is no error contribution of power $1/N^3$, the actual error of this discretization approximation scales as $1/N^4$, which is a significant improvement over the trapezoidal rule.

Writing this as a sum of $M = 2N+1$ terms (where M is obviously always odd) we obtain an approximation for the integral that is known as **Simpson's rule** [14] .

Box 11 (Simpson's rule) *When one approximates the value of an integral with $M = 2N+1$ equally spaced sampling points, an efficient method is given by*

$$\begin{aligned} \int_a^b g(x)dx &= \delta\Big[\frac{1}{3}g(a) + \frac{4}{3}g(a+\delta) + \frac{2}{3}g(a+2\delta) + \frac{4}{3}g(a+3\delta) + \dots \\ &\quad + \frac{2}{3}g(a+(2N-2)\delta) + \frac{4}{3}g(a+(2N-1)\delta) + \frac{1}{3}g(b)\Big] + \mathcal{O}\{N^{-4}\}\,, \\ \delta &= \frac{b-a}{2N} = \frac{b-a}{M-1}\,. \end{aligned} \tag{1.113}$$

[14] Thomas Simpson (1710–1761) was a british mathematician with contributions to interpolation and numerical integration. It should be noted that the Simpson rule was actually introduced by Johannes Kepler already in 1615 who used it to estimate the content of wine barrels.

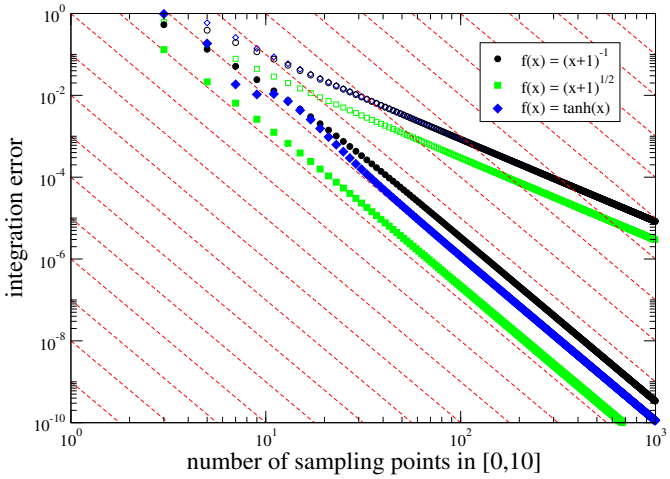

Figure 1.12: Scaling of the errors of the analytically solvable integrals $\int_0^{10} g(x)dx$ with the number of sampling points in the interval $[0, 10]$. Solid symbols denote the errors of the Simpson rule (compare Box 1.113), whereas hollow symbols show the errors resulting from the simple trapezoidal rule (Box 1.109) with the same number of sampling points. The functions chosen are analytic in the integration interval. Dashed lines in the background denote the N^{-4} scaling.

Fig. 1.12 demonstrates the scaling of the error that is obtained when comparing Simpson and trapezoidal rules with analytically solvable integrals. In particular, the superior scaling of the Simpson rule becomes visible when it is compared with the trapezoidal rule used with the same number of sampling points. Since it yields higher accuracy with the same number of sampling points, Simpson's rule should be given preference over the trapezoidal rule.

We finally note that when the stepsize is further reduced in a numerical algorithm, the previous results need not be discarded despite the fact that in the Simpson rule not all sampling points are treated equally. This can simply be achieved by separately treating contributions from boundary points, even and odd internal points

$$\begin{aligned} I_N^{\rm bdy} &= \frac{\delta_N}{3}\left[g(a)+g(b)\right] , \\ I_N^{\rm odd} &= \frac{4}{3}\delta_N\left[g(a+\delta_N)+\ldots+g(a+(2N-1)\delta_N)\right] , \\ I_N^{\rm evn} &= \frac{2}{3}\delta_N\left[g(a+2\delta_N)+\ldots+g(a+(2N-2)\delta_N)\right] , \end{aligned} \tag{1.114}$$

such that the integral is approximated by $I_N = I_N^{\rm bdy} + I_N^{\rm odd} + I_N^{\rm evn}$. For the refined calculation with half the discretization width $\delta_{2N} = \frac{1}{2}\delta_N$, one actually only has to sample the function at the new odd points, i.e., to calculate $I_{2N}^{\rm odd}$. The other contribution can be obtained from the previous results

$$\begin{aligned} I_{2N}^{\rm bdy} &= \frac{1}{2} I_N^{\rm bdy} , \\ I_{2N}^{\rm evn} &= \frac{1}{4} I_N^{\rm odd} + \frac{1}{2} I_N^{\rm evn} . \end{aligned} \tag{1.115}$$

Here, a factor of $1/2$ comes from the refinement of the integration mesh, and the different factor $1/4$ comes from the fact that additionally, some points previously considered odd will now become even points in the refined integration mesh. This can be used to recursively calculate new points of the function, starting e.g. with only three sampling points

$$\begin{aligned} \delta_1 &= \frac{b-a}{2} , \qquad S_1^{\rm bdy} = \frac{\delta_1}{3}\left[g(a)+g(b)\right] , \\ S_1^{\rm evn} &= 0 , \qquad S_1^{\rm odd} = \frac{4}{3}\delta_1 g(a+\delta_1) . \end{aligned} \tag{1.116}$$

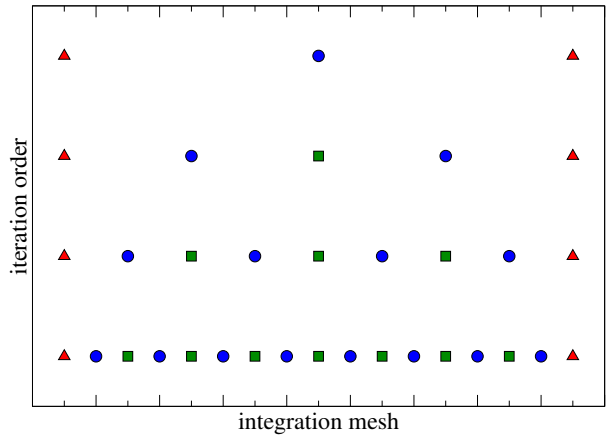

Figure 1.13: Illustration of the recursive application of Simpsons rule to the integration interval. Initially (top), only the boundary points (triangles) and an odd internal point (blue circle) are computed. After refinement, the previous odd points need not be computed again but become even points (green squares). In each refinement step, only the odd points (circles) need to be evaluated for the first time.

In the next step, the other contributions are iteratively calculated

$$\begin{aligned} \delta_n &= \frac{1}{2}\delta_{n-1}\,, \qquad S_n^{\rm bdy} = \frac{1}{2}S_{n-1}^{\rm bdy}\,, \\ S_n^{\rm evn} &= \frac{1}{4}S_{n-1}^{\rm odd} + \frac{1}{2}S_{n-1}^{\rm evn}\,, \qquad S_n^{\rm odd} = \frac{4}{3}\delta_n\left[g(a+\delta_n) + g(a+3\delta_n) + \ldots + g(b-3\delta_n) + g(b-\delta_n)\right]\,. \end{aligned} \tag{1.117}$$

The sum $I_n = S_n^{\rm bdy} + S_n^{\rm evn} + S_n^{\rm odd}$ then defines the approximation to the integral, and the absolute difference

$$\Delta = |I_{n+1} - I_n| \tag{1.118}$$

can be used as an error criterion to halt further refinements. Fig. 1.13 illustrates the iterative refinement of the integration mesh.

1.4.3 Monte-Carlo integration

The term Monte Carlo integration usually refers to a plethora of different schemes that all employ random numbers to estimate an integral. Here, we will only discuss the simplest schemes, see e.g. Ref. [1] for a longer introduction. Given a function $f(x)$ and an integration interval $[a,b]$, we would have previously partitioned the integration interval into equidistant sub-intervals, for which we can evaluate the value of $f(x)$. Alternatively, we could randomly generate a number of N points $x_i \in [a,b]$, and compute the average of the function evaluated at these points

$$\mu_f = \langle f \rangle = \frac{1}{N}\sum_{i=1}^{N} f(x_i)\,, \qquad \left\langle f^2 \right\rangle = \frac{1}{N}\sum_{i=1}^{N} f^2(x_i)\,. \tag{1.119}$$

From these quantities, we can also compute the variance

$$\sigma_f^2 = \left\langle f^2 \right\rangle - \langle f \rangle^2\,. \tag{1.120}$$

Assuming convergence, we would obtain an estimate of the integral by multiplying the average of the function with the width of the integration interval. Fig. 1.14 illustrates this procedure for the example of a Gaussian function. In addition, we can get from simple error propagation models an estimate on the numerical integration error. Assuming that the variance $\sigma_f^2 = \langle f^2 \rangle - \langle f \rangle$ provides something like an error estimate for the error of each data point, the error of the integral would

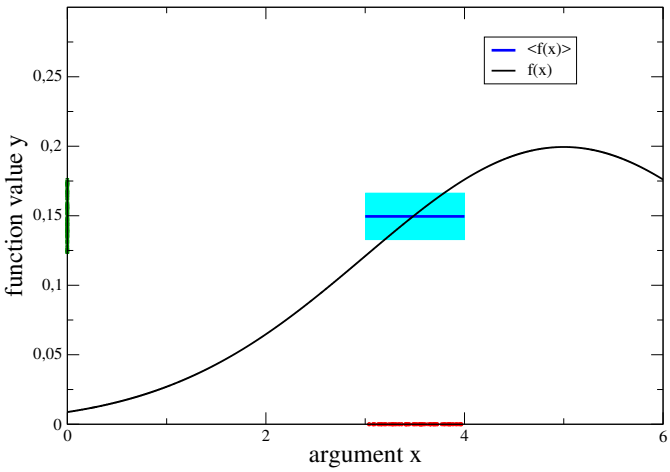

Figure 1.14: Illustration of a simple Monte Carlo integration routine for a Gaussian function with mean $\mu = 5$ and width $\sigma = 2$. The function is evaluated at $N = 100$ randomly distributed points in the inverval $x_i \in [3, 4]$ (red symbols), which yields the function values f_i (green symbols). From these, we can compute mean μ_f (blue) and variance σ_f (turquoise) of the function over the interval $[3, 4]$, the actual value of the integral is then estimated as $I = \int_a^b f(x)dx \approx (b-a)\mu_f \pm \frac{b-a}{\sqrt{N}}\sigma_f = 0.14954 \pm 0.00167$, close to the actual value of $I = 0.14988$.

be estimated by multiplying the individual errors σ_f with $(b-a)/\sqrt{N}$, such that the total integral and error estimate become

$$I = \int_a^b f(x)dx \approx (b-a)\langle f\rangle \pm (b-a)\sqrt{\frac{\langle f^2\rangle - \langle f\rangle^2}{N}} = (b-a)\mu_f \pm \frac{b-a}{\sqrt{N}}\sigma_f\,. \tag{1.121}$$

It should be noted that the error estimate comes from the expectation that the errors follow a Gaussian distribution, there is however no guarantee for that. We can directly generalize this formula to higher dimensions. Inside a volume V, the multi-dimensional integral becomes

$$I = \int f(\boldsymbol{x})dV \approx V\langle f\rangle \pm V\sqrt{\frac{\langle f^2\rangle - \langle f\rangle^2}{N}} = V\mu_f \pm \frac{V}{\sqrt{N}}\sigma_f\,. \tag{1.122}$$

We see that the convergence properties are therefore by far worse than e.g. Simpson rule integration in 1 dimension. However, the advantage of Monte Carlo integration is that it can be applied in a relatively simple and straightforward way also to multi-dimensional integrals, where other integration schemes will have trouble. Another advantage of Monte Carlo integration is that it is sometimes quite difficult even to parametrize the boundaries of the integration volume, e.g. when it is bounded by difficult shapes. Imagine, for example to integrate some function like an energy density over the shape of an airplane in three dimensions. If such difficult boundaries exist, one may define a function $g(x)$ in a simple-to-parametrize volume G that includes the region $F \supset G$ over which we want to integrate the function $f(x)$ that vanishes outside the boundary. With Monte-Carlo integration, it is no problem to integrate then the function $g(x)$ over the simple volume G, i.e., the non-analytic decay of the function $g(x)$ at the boundary of F is simple to implement.

Chapter 2

Integral Transforms

2.1 Fourier Transform

Fourier transforms are extremely important in modern science and technology. They are widely used in data and image analysis, image and sound compression.

2.1.1 Continuous Fourier Transform

There are multiple ways to define the Fourier transform of a function. They can all be transformed into each other with comparably little effort. Therefore, we will just pick one here that is convenient for us.

Box 12 (Fourier transform) *The Fourier transform of a function $f(t)$ is defined as*

$$F(\omega) = \frac{1}{\sqrt{2\pi}} \int f(t) e^{+\mathrm{i}\omega t} dt = \mathcal{F}[f(t)]\,. \tag{2.1}$$

The inverse Fourier transform is then given by

$$f(t) = \frac{1}{\sqrt{2\pi}} \int F(\omega) e^{-\mathrm{i}\omega t} d\omega = \mathcal{F}^{-1}[F(\omega)]\,. \tag{2.2}$$

We summarize a few properties of the Fourier Transform (FT)

1. The Fourier transform of a function exists when it is square-integrable, i.e., when $\int |f(t)|^2 dt < \infty$. This is a sufficient condition (but not necessary). One necessary (but not sufficient) condition for the existence of the FT is $\lim_{t\to\pm\infty} f(t) = 0$.

2. The Fourier representation of the Dirac [1] -Delta function is

$$\delta(\omega) = \frac{1}{2\pi} \int e^{+\mathrm{i}\omega t} dt\,. \tag{2.3}$$

[1] Paul Dirac (1902–1984) was an influential british theoretical physicist and one of the founders of quantum mechanics.

3. When $f(t)$ and $F(\omega)$ are FT pairs, it follows that the Fourier transform of the n-th derivative $f^{(n)}(t)$ is given by $(-\mathrm{i}\omega)^n F(\omega)$. This is directly visible from the inverse FT

$$f^{(n)}(t) = \frac{1}{\sqrt{2\pi}} \int F(\omega)(-\mathrm{i}\omega)^n e^{-\mathrm{i}\omega t} d\omega \,. \tag{2.4}$$

Altogether, we may write

$$F(\omega) = \mathcal{F}[f(t)] \Longrightarrow (-\mathrm{i}\omega)^n F(\omega) = \mathcal{F}[f^{(n)}(t)] \,. \tag{2.5}$$

A similar property exists of course for derivatives with respect to ω. This property will prove extremely important later-on, since it can be used to convert differential equations into algebraic ones. There, the basic idea is to solve the simpler algebraic equation in frequency space and perform an inverse Fourier transform.

4. Shifts in the time-domain imply a product with an exponential in the frequency domain

$$F(\omega) = \mathcal{F}[f(t)] \qquad \Longrightarrow \qquad e^{-\mathrm{i}a\omega} F(\omega) = \mathcal{F}[f(t-a)] \,. \tag{2.6}$$

5. The FT obeys the Parseval [2] relation

$$\begin{aligned} \int f(t) g^*(t) dt &= \frac{1}{2\pi} \int d\omega_1 \int d\omega_2 \int dt F(\omega_1) G^*(\omega_2) e^{-\mathrm{i}\omega_1 t} e^{+\mathrm{i}\omega_2 t} \\ &= \int d\omega_1 \int d\omega_2 F(\omega_1) G^*(\omega_2) \delta(\omega_1 - \omega_2) \\ &= \int F(\omega) G^*(\omega) d\omega \,. \end{aligned} \tag{2.7}$$

The above integral is nothing but a scalar product on the space of square-integrable functions. The Fourier transform leaves this scalar product invariant and is thus unitary. In particular when $f(t) = g(t)$, it reduces to $\int |f(t)|^2 dt = \int |F(\omega)|^2 d\omega$.

6. When $F(\omega)$ and $G(\omega)$ are Fourier transforms of $f(t)$ and $g(t)$, respectively, it follows that the FT of a product in the time-domain is a convolution

$$\begin{aligned} \sqrt{2\pi}\mathcal{F}[f(t)g(t)] &= \int f(t) g(t) e^{+\mathrm{i}\omega t} dt = \int d\omega_1 \int d\omega_2 \delta(\omega - \omega_1 - \omega_2) F(\omega_1) G(\omega_2) \\ &= \int F(\omega') G(\omega - \omega') d\omega' = \int F(\omega - \omega') G(\omega') d\omega' \,. \end{aligned} \tag{2.8}$$

This can be seen most easily by inserting the inverse FTs of $F(\omega)$ and $G(\omega)$ and using the Fourier representation of the Dirac Delta distribution. Likewise, it follows that the inverse FT of a product in the spectral domain is a convolution in the time domain

$$\sqrt{2\pi}\mathcal{F}^{-1}[F(\omega)G(\omega)] = \int f(t') g(t - t') dt' = \int f(t - t') g(t') dt' \,. \tag{2.9}$$

7. The FT is real-valued when complex conjugation implies the same as time inversion, i.e.,

$$f^*(t) = +f(-t) \qquad \Longrightarrow \qquad F(\omega) \in \mathbb{R} \,. \tag{2.10}$$

[2] Marc-Antoine Parseval (1755–1836) was a french mathematician who published this relation without proof, which he thought was obvious.

8. One can think of even stronger statements. For example, we can ask when the Fourier transform is not only real but even positive $F(\omega) \geq 0$. From the inverse Fourier transform we get that in this case

$$\sum_{ij} z_i^* f(t_i - t_j) z_j = \frac{1}{\sqrt{2\pi}} \int F(\omega) \left[\sum_i z_i^* e^{-\mathrm{i}\omega t_i}\right] \left[\sum_j z_j e^{+\mathrm{i}\omega t_j}\right] d\omega \geq 0\,, \tag{2.11}$$

which has to hold for all $\{t_i\} \in \mathbb{R}$ and $\{z_i\} \in \mathbb{C}$. This simply means that the matrix formed by $f(t_i - t_j)$ is positive semidefinite, and one generally calls functions obeying this property also positive definite. The converse, i.e., that the FT of a positive definite function is positive, can also be shown and is known as Bochners [3] theorem. This also generalizes to matrix Fourier transforms $F_{ij}(\omega)$ in a way that the FT of a positive function is a positive semi-definite matrix.

2.1.2 Important Fourier Transforms

- The Fourier Transform of a Gaussian is again a (not normalized) Gaussian

$$\begin{aligned} f(t) &= \frac{1}{\sqrt{2\pi}\sigma} e^{-(t-\mu)^2/(2\sigma^2)}\,, \\ F(\omega) &= \frac{1}{2\pi\sigma} \int e^{-(t-\mu)^2/(2\sigma^2)} e^{+\mathrm{i}\omega t} dt = \frac{1}{\sqrt{2\pi}} e^{-\mu^2/(2\sigma^2)} e^{+(\mu+\mathrm{i}\omega\sigma^2)^2/(2\sigma^2)} \\ &= \frac{e^{-\mu^2/(2\sigma^2)}}{\sqrt{2\pi}} e^{-\frac{\sigma^2}{2}\left(\omega - \mathrm{i}\frac{\mu}{\sigma^2}\right)^2}\,, \end{aligned} \tag{2.12}$$

where we note that the width of the Gaussian in the frequency domain is just the inverse of the width σ in the time domain. This holds more generally, and as a rule of thumb, this implies that the FT of a flat function is peaked whereas the FT of a peaked function is flat. An extreme case of this is the Dirac-Delta distribution.

- The FT of an exponentially decaying function is a Lorentzian

$$f(t) = \frac{1}{\sqrt{2\pi}} e^{-\mathrm{i}\epsilon t} e^{-\delta|t|}\,, \qquad F(\omega) = \frac{1}{\pi} \frac{\delta}{(\omega - \epsilon)^2 + \delta^2}\,. \tag{2.13}$$

Here, δ plays the role of a width in the frequency domain.

- The FT of of a rectangular function is a bandfilter function

$$f(t) = \begin{cases} 1 & : \quad \mu - \delta/2 \leq t \leq \mu + \delta/2 \\ 0 & : \quad \text{else} \end{cases}\,, \qquad F(\omega) = \frac{e^{+\mathrm{i}\omega\mu}}{\sqrt{2\pi}} \mathrm{sinc}\left(\frac{\delta\omega}{2}\right)\,, \tag{2.14}$$

where δ describes the width in the time domain.

- The FT of a Heaviside function can be deduced from its relation to the Dirac-Delta distribution $\Theta'(t) = \delta(t)$. We first relate the signum function $\mathrm{sgn}(t) = 2\Theta(t) - 1$ to the Dirac-Delta distribution via $\frac{d}{dt}\mathrm{sgn}(t) = 2\delta(t)$. From this, we conclude the FT of the signum function

$$\mathcal{F}[\mathrm{sgn}(t)] = \frac{2}{-\mathrm{i}\omega} \mathcal{F}[\delta(t)] = \frac{2\mathrm{i}}{\sqrt{2\pi}\omega} \to \mathcal{P}\frac{2\mathrm{i}}{\sqrt{2\pi}\omega}\,. \tag{2.15}$$

[3] Salomon Bochner (1899–1982) was an american mathematician, educated in Berlin.

Strictly speaking, this is not defined at $\omega = 0$, the expression only makes sense in integrals, where we have to take the principal value $\mathcal{P}$. This can be used in the previous identity to yield

$$\begin{aligned}\mathcal{F}[\Theta(t)] &= \frac{1}{2}\mathcal{F}[1] + \mathcal{P}\frac{1}{2}\frac{2\mathrm{i}}{\sqrt{2\pi}\omega} \\ &= \frac{1}{\sqrt{2\pi}}\left[\pi\delta(\omega) + \mathcal{P}\frac{\mathrm{i}}{\omega}\right] . \end{aligned} \tag{2.16}$$

2.1.3 Applications of the convolution theorem

An obvious application of the convolution theorem follows for partial Fts. For example, when the Fourier integral only involves a finite interval, e.g. the interval $[T^* - \delta/2, T^* + \delta/2]$ we can write this as a the FT of a product of two functions: the original function and the rectangular function $g(t)$ from Eq. (2.14). The FT over a finite interval is thus given by a convolution in the frequency domain

$$\frac{1}{\sqrt{2\pi}}\int_{T^*-\delta/2}^{T^*+\delta/2} f(t)e^{+\mathrm{i}\omega t}dt = \frac{1}{\sqrt{2\pi}}\int f(t)g(t)e^{+\mathrm{i}\omega t}dt = \frac{1}{2\pi}\int F(\omega-\omega')e^{+\mathrm{i}\omega' T^*}\mathrm{sinc}\left(\frac{\delta\omega'}{2}\right)d\omega' . \tag{2.17}$$

This justifies the name *bandfilter functions* for the sinc-function.

A second obvious consequence is that the convolution theorem can be used to to calculate the FT of a product of a simple periodic function and a decaying function. As a very simple example we consider here the functions ($\Omega \in \mathbb{R}$, $\delta > 0$)

$$f(t) = \sin(\Omega t) , \qquad g(t) = \frac{1}{\sqrt{2\pi}}e^{-\delta|t|} . \tag{2.18}$$

It is straightforward to deduce their FTs from our previous results

$$F(\omega) = \mathrm{i}\sqrt{\frac{\pi}{2}}\left[\delta(\omega-\Omega) - \delta(\omega+\Omega)\right] , \qquad G(\omega) = \frac{1}{\pi}\frac{\delta}{\omega^2+\delta^2} . \tag{2.19}$$

The evaluation of the convolution integral is thus particularly simple in this case

$$\begin{aligned} FG(\omega) &= \frac{1}{\sqrt{2\pi}}\int \sin(\Omega t)\frac{1}{\sqrt{2\pi}}e^{-\delta|t|}e^{+\mathrm{i}\omega t}dt \\ &= \frac{1}{\sqrt{2\pi}}\int F(\omega')G(\omega-\omega')d\omega' = \frac{\mathrm{i}}{\sqrt{2\pi}}\sqrt{\frac{\pi}{2}}\frac{1}{\pi}\int\left[\delta(\omega'-\Omega)-\delta(\omega'+\Omega)\right]\frac{\delta}{(\omega-\omega')^2+\delta^2}d\omega' \\ &= \frac{\mathrm{i}}{2\pi}\left[\frac{\delta}{(\omega-\Omega)^2+\delta^2} - \frac{\delta}{(\omega+\Omega)^2+\delta^2}\right] \\ &= \frac{\mathrm{i}}{2\pi}\frac{4\delta\omega\Omega}{\left[(\omega-\Omega)^2+\delta^2\right]\left[(\omega+\Omega)^2+\delta^2\right]} . \end{aligned} \tag{2.20}$$

Similar decompositions exist whenever the function $f(t)$ is periodic $f(t+T) = f(t)$ with $t = \frac{2\pi}{\Omega}$. In this case, one can use the decomposition of $f(t) = \sum_n f_n e^{+\mathrm{i}n\Omega t}$ into a Fourier series to compute the FT of $f(t)g(t)$.

Very often, half-sided Fourier transforms are used

$$\Gamma(\omega) = \frac{1}{\sqrt{2\pi}} \int_0^\infty f(t) e^{+\mathrm{i}\omega t} dt = \mathcal{F}[f(t)\Theta(t)]\,, \tag{2.21}$$

where $\Theta(t)$ denotes the Heaviside [4] function. Recalling the FT of the Heaviside function (2.16)

$$\mathcal{F}[\Theta(t)] = \frac{1}{\sqrt{2\pi}} \left[\pi\delta(\omega) + \mathcal{P}\frac{\mathrm{i}}{\omega}\right]\,, \tag{2.22}$$

we can apply the convolution theorem to separate the real and imaginary parts

$$\begin{aligned} \Gamma(\omega) &= \frac{1}{2\pi} \int F(\Omega) \left[\pi\delta(\omega-\Omega) + \mathcal{P}\frac{\mathrm{i}}{\omega-\Omega}\right] d\Omega \\ &= \frac{1}{2} F(\omega) + \frac{\mathrm{i}}{2\pi}\mathcal{P}\int \frac{F(\Omega)}{\omega-\Omega} d\Omega\,, \end{aligned} \tag{2.23}$$

which shows that half-sided FTs can be evaluated with full FTs and Cauchy principal value integrals.

2.1.4 Discrete Fourier Transform

When the function $f(t)$ has significant support only in a finite interval $[-\Delta/2, +\Delta/2]$, we can approximate the integral in the continuous Fourier transform by a sum of N terms (using $\delta = \Delta/(N-1)$)

$$\begin{aligned} F(\omega) &= \frac{1}{\sqrt{2\pi}} \int f(t) e^{+\mathrm{i}\omega t} dt \approx \frac{1}{\sqrt{2\pi}} \int_{-\Delta/2}^{+\Delta/2} f(t) e^{+\mathrm{i}\omega t} dt \\ &\approx \frac{1}{\sqrt{2\pi}} \sum_{k=-(N-1)/2}^{+(N-1)/2} f(k\delta) e^{+\mathrm{i}\omega k\delta}\delta\,, \end{aligned} \tag{2.24}$$

and the function $F(\omega)$ is then obtained from a number of discrete values $f_k = f(k\delta)$. Many natural signals are a priori discrete instead of continuous, and there is consequently also a unitary variant of the discrete Fourier transform.

Box 13 (Discrete Fourier Transform) *Let $\{a_0, a_1, \ldots, a_{N-1}\}$ be a list of N (complex-valued) numbers. Then, their discrete Fourier Transform (DFT) is given by*

$$\tilde{a}_k = \frac{1}{\sqrt{N}} \sum_{j=0}^{N-1} e^{+2\pi\mathrm{i}\frac{jk}{N}} a_j\,, \tag{2.25}$$

where $k \in \{0, 1, \ldots, N-1\}$. The original numbers can be recovered from the inverse DFT

$$a_j = \frac{1}{\sqrt{N}} \sum_{k=0}^{N-1} e^{-2\pi\mathrm{i}\frac{jk}{N}} \tilde{a}_k\,, \tag{2.26}$$

where $j \in \{0, 1, \ldots, N-1\}$.

[4] Oliver Heaviside (1850–1925) was a british physicist.

The reason why also the DFT is invertible lies in the identity

$$\delta_{k,0} = \frac{1}{N} \sum_{\ell=0}^{N-1} e^{2\pi \mathrm{i} \frac{\ell k}{N}} \,, \tag{2.27}$$

which can be shown by employing the finite geometric series

$$S_N = \sum_{\ell=0}^{N} x^\ell = \frac{1 - x^{N+1}}{1 - x} \,. \tag{2.28}$$

We note for completeness that the above relation holds for $x \neq 1$ and is evident from $S_{N+1} = 1 + xS_N = S_N + x^{N+1}$.

The DFT corresponds to the multiplication with an $N \times N$ unitary matrix, i.e., when we arrange the numbers in vectors $\tilde{\mathbf{a}} = (\tilde{a}_0, \ldots, \tilde{a}_{N-1})^{\mathrm{T}}$ and $\mathbf{a} = (a_0, \ldots, a_{N-1})^{\mathrm{T}}$, we have the relation $\tilde{\mathbf{a}} = U\mathbf{a}$ with the matrix

$$U = \frac{1}{\sqrt{N}} \begin{pmatrix} e^{2\pi \mathrm{i} \frac{1 \cdot 1}{N}} & e^{2\pi \mathrm{i} \frac{1 \cdot 2}{N}} & \ldots & e^{2\pi \mathrm{i} \frac{1 \cdot (N-1)}{N}} \\ e^{2\pi \mathrm{i} \frac{2 \cdot 1}{N}} & e^{2\pi \mathrm{i} \frac{2 \cdot 2}{N}} & & \vdots \\ \vdots & & \ddots & \vdots \\ e^{2\pi \mathrm{i} \frac{(N-1) \cdot 1}{N}} & \ldots & \ldots & e^{2\pi \mathrm{i} \frac{(N-1) \cdot (N-1)}{N}} \end{pmatrix} . \tag{2.29}$$

The inverse transformation is then given by $\mathbf{a} = U^\dagger \tilde{\mathbf{a}}$. Performing this matrix-vector multiplication would thus require $\mathcal{O}\{N^2\}$ multiplications of the numbers a_j. However, we just note here that when N is a power of two, i.e., $N = 2^n$, the DFT can be performed much more efficiently with complexity $\mathcal{O}\{N \ln N\}$. The corresponding algorithm is known as Fast Fourier Transform (FFT), and extensions of it have found widespread application in data analysis and image and sound compression (jpeg, mp3). Due to the similiar structure, we just note here that many properties of the continuous FT also hold for the DFT.

2.2 Laplace Transform

2.2.1 Definition

Box 14 (Laplace Transform) *The Laplace transform (LT) of a function $f(t)$ is given by*

$$F(s) = \int_0^\infty f(t) e^{-st} dt \,. \tag{2.30}$$

It exists when the integral converges, which defines a region of convergence $s \in S \subset \mathbb{C}$. For $t > 0$, it can be inverted via

$$f(t) = \frac{1}{2\pi \mathrm{i}} \int_{\gamma - \mathrm{i}\infty}^{\gamma + \mathrm{i}\infty} F(s) e^{+st} ds \,. \tag{2.31}$$

Here, $\gamma \in \mathbb{R}$ must be chosen such that the integration path lies within the region of convergence S.

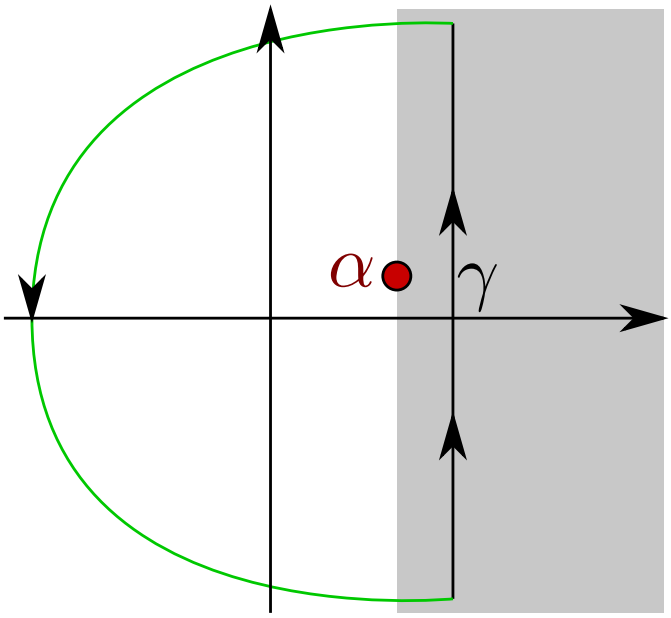

Figure 2.1: For a complex number α, the region of convergence for the Laplace transform of $f(t) = e^{+\alpha t}$ is given by all complex numbers with a larger real part than α (shaded area). It must not contain any singularities (by definition). The integration contour for the inverse Laplace transform must lie within this region of convergence $\gamma > \Re(\alpha)$. The inverse LT can be evaluated using the residue theorem when the contour is closed (green arc).

The integral of the inverse Laplace transform is also called Bromwich [5] integral. We note that unlike the FT, where forward and backward transformations are essentially of the same difficulty, computing the inverse LT may be much more tedious than computing the LT. Furthermore, since only positive times enter in the Laplace transform, the inverse LT can only be used to reconstruct the function $f(t)$ for $t > 0$. We start by considering some examples:

1. To elucidate what is meant with **region of convergence**, we consider the simple Laplace transform ($\alpha \in \mathbb{C}$)

$$f(t) = e^{\alpha t}\,, \qquad F(s) = \int_0^\infty e^{(\alpha - s)t} dt = \left. \frac{e^{(\alpha-s)t}}{\alpha - s} \right|_0^\infty \overset{\Re(s) > \Re(\alpha)}{=} \frac{1}{s - \alpha}\,. \tag{2.32}$$

   In this case, the region of convergence is defined by $S = \{s \in \mathbb{C} \;:\; \Re(s) > \Re(\alpha)\}$. By definition, it must not contain any poles or other singularities. The integration contour of the inverse LT must lie within this region of convergence, i.e., we have to choose γ such that also $\gamma > \Re(\alpha)\}$, see Fig. 2.1. We note that the inverse LT can be evaluated using the residue theorem once the integration contour is closed. For this, it is necessary to continue the LT $F(s)$ to the full complex plane and to close the contour in the left half plane, since in the right half plane the integrand $F(s)e^{st}$ is not suppressed. Provided that the Laplace transform has only a finite number of poles in the complex plane, we can use the residue theorem, which implies for the inverse Laplace transform

$$f(t) = \sum_i \operatorname*{Res}_{s=s_i} F(s) e^{st} = \sum_i e^{s_i t} \operatorname*{Res}_{s=s_i} F(s)\,, \tag{2.33}$$

   where s_i are the poles of the Laplace transform $F(s)$ – recall that e^{st} is analytic in $\mathbb{C}$ – that are contained by the integration contour. We note that when the poles of $F(s)$ have a vanishing or even negative real part, the above decomposition yields a convenient way to

[5] Thomas John I'Anson Bromwich (1875–1929) was a british mathematician and physicist with contributions to Maxwells equations.

approximate the long-term behaviour of the function $f(t)$. For our particular simple example this means

$$f(t) = \operatorname*{Res}_{s=\alpha} \frac{e^{st}}{s-\alpha} = e^{\alpha t}\,, \tag{2.34}$$

which demonstrates consistency.

2. As a second simple example we consider the function

$$f(t) = t^n e^{\alpha t} \tag{2.35}$$

with $n \in \{0, 1, 2, \ldots\}$ and $\alpha \in \mathbb{C}$. The Laplace transform exists for $\Re(s) > \Re(\alpha)$ and can be found by differentiation

$$F(s) = \int_0^\infty t^n e^{\alpha t} e^{-st} dt = \left(\frac{\partial}{\partial \alpha}\right)^n \frac{1}{s-\alpha} = \frac{n!}{(s-\alpha)^{n+1}}\,. \tag{2.36}$$

In the complex plane, it has a pole of order $n+1$ at $s = \alpha$. The residue necessary for the calculation of the inverse Laplace transform can be found by direct inspection

$$\frac{e^{st} n!}{(s-\alpha)^{n+1}} = e^{\alpha t} \frac{e^{(s-\alpha)t} n!}{(s-\alpha)^{n+1}} = e^{\alpha t} \sum_{m=0}^{\infty} \frac{n! t^m}{m!} (s-\alpha)^{m-n-1}\,, \tag{2.37}$$

which yields

$$\operatorname*{Res}_{s=\alpha} \frac{e^{st} n!}{(s-\alpha)^{n+1}} = e^{\alpha t} t^n \tag{2.38}$$

and thus consistently reproduces our original function.

3. As a more complex example, we consider the function $f(t) = \frac{1}{\sqrt{t}}$. First we consider the existence of the Laplace transform

$$F(s) = \int_0^\infty \frac{e^{-st}}{\sqrt{t}} dt \tag{2.39}$$

For large times, the integrand decays. In addition, we note that though for small times the integrand diverges, the integral is still finite, as it can be upper-bounded for $\Re(s) > 0$

$$\begin{aligned} |F(s)| &= \left| \int_0^1 \frac{e^{-st}}{\sqrt{t}} dt + \int_1^\infty \frac{e^{-st}}{\sqrt{t}} dt \right| \leq \left| \int_0^1 \frac{e^{-st}}{\sqrt{t}} dt \right| + \left| \int_1^\infty \frac{e^{-st}}{\sqrt{t}} dt \right| \\ &\leq \int_0^1 \frac{1}{\sqrt{t}} dt + \int_1^\infty e^{-st} dt = 2 + \frac{e^{-s}}{s}\,, \end{aligned} \tag{2.40}$$

where we have employed the triangle inequality $|z_1 + z_2| \leq |z_1| + |z_2|$ (which can be recursively applied to larger sums and therefore also holds for the integral). It is not difficult to show that the actual value of the integral is given by

$$F(s) = \int_0^\infty \frac{e^{-st}}{\sqrt{t}} dt = 2 \int_0^\infty e^{-sy^2} dy = \sqrt{\frac{\pi}{s}}\,. \tag{2.41}$$

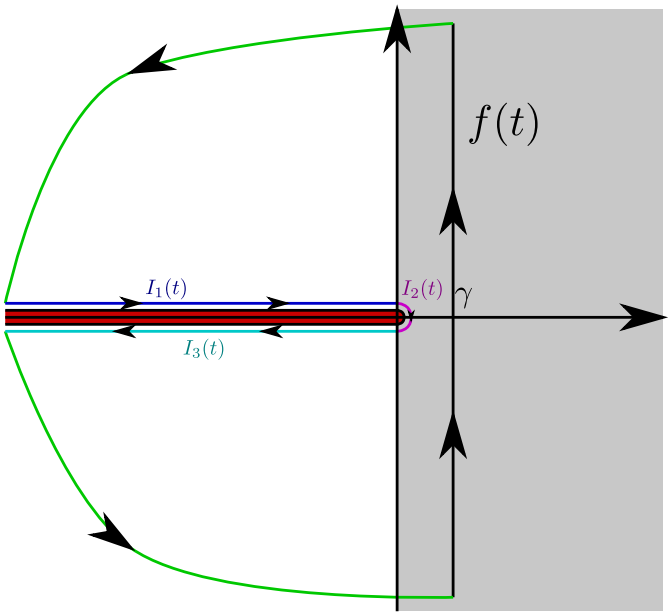

Figure 2.2: When the branch cut is excised, the contour encloses a region where the Laplace transform is holomorphic. Since in addition the green arcs do not contribute, the integral along the closed contour must vanish, and the Bromwich integral (solid black) can be represented as $f(t) = -I_1(t) - I_2(t) - I_3(t)$.

We note that $F(s)$ has no isolated singularity on the negative real axis but a full branch cut: By employing the polar representation $s = |s|e^{+\mathrm{i}\phi}$ we see that on the positive real axis we have

$$\lim_{\Im(s)\to 0^+} \sqrt{\frac{\pi}{s}} = \lim_{\Im(s)\to 0^-} \sqrt{\frac{\pi}{s}} = \lim_{\phi\to 0} \sqrt{\frac{\pi}{|s|e^{\mathrm{i}\phi}}} = \sqrt{\frac{\pi}{|s|}}\,. \tag{2.42}$$

However, on the negative real axis the two limits do not coincide

$$\begin{aligned} \lim_{\Im(s)\to 0^+} \sqrt{\frac{\pi}{s}} &= \lim_{\phi\to +\pi} \sqrt{\frac{\pi}{|s|}e^{-\mathrm{i}\phi}} = \sqrt{\frac{\pi}{|s|}}e^{-\mathrm{i}\pi/2} = -\mathrm{i}\sqrt{\frac{\pi}{|s|}}\,, \\ \lim_{\Im(s)\to 0^-} \sqrt{\frac{\pi}{s}} &= \lim_{\phi\to -\pi} \sqrt{\frac{\pi}{|s|}e^{-\mathrm{i}\phi}} = \sqrt{\frac{\pi}{|s|}}e^{+\mathrm{i}\pi/2} = +\mathrm{i}\sqrt{\frac{\pi}{|s|}}\,. \end{aligned} \tag{2.43}$$

To compute the inverse Laplace transform, we therefore have to excise the branch cut with a more complicated integration contour, see Fig. 2.2. The Bromwich integral can then be represented as

$$f(t) = \frac{1}{2\pi\mathrm{i}} \int_{\gamma-\mathrm{i}\infty}^{\gamma+\mathrm{i}\infty} \sqrt{\frac{\pi}{s}} e^{+st} ds = -I_1(t) - I_2(t) - I_3(t)\,, \tag{2.44}$$

where the individual contributions have to be parametrized explicitly. The first integral becomes

$$\begin{aligned} I_1(t) &= \lim_{\epsilon\to 0^+} \frac{1}{2\pi\mathrm{i}} \int_{-\infty}^{0} \sqrt{\frac{\pi}{x+\mathrm{i}\epsilon}} e^{+xt} dx = \frac{-1}{2\pi} \int_{-\infty}^{0} \sqrt{\frac{\pi}{-x}} e^{+xt} dx \\ &= \frac{1}{2\pi} \int_{+\infty}^{0} \sqrt{\frac{\pi}{y}} e^{-yt} dy = -\frac{1}{2\sqrt{\pi}} \int_0^\infty \frac{e^{-yt}}{\sqrt{y}} dy = \frac{-1}{2\sqrt{t}}\,, \end{aligned} \tag{2.45}$$

where in the last step we have used the previous result (2.41), this time assuming positive time. The integral along the arcs vanishes because at negative $\Re s$, the integrand is suppressed

exponentially, the path is so short, and the moderate divergence of the integrand at the origin cannot compensate for this

$$I_2(t) = \frac{1}{2\pi\mathrm{i}} \lim_{\rho\to 0^+} \int_{+\pi/2}^{-\pi/2} \sqrt{\frac{\pi}{\rho e^{+\mathrm{i}\phi}}} \exp\left\{\rho e^{+\mathrm{i}\phi} t\right\} \rho e^{+\mathrm{i}\phi} \mathrm{i} d\phi = 0\,. \tag{2.46}$$

Finally, the third integral yields the same contribution as the first one

$$\begin{aligned} I_3(t) &= \lim_{\epsilon\to 0^+} \frac{1}{2\pi\mathrm{i}} \int_0^{-\infty} \sqrt{\frac{\pi}{x-\mathrm{i}\epsilon}} e^{+xt} dx = \frac{1}{2\pi} \int_0^{-\infty} \sqrt{\frac{\pi}{-x}} e^{+xt} dx \\ &= -\frac{1}{2\sqrt{\pi}} \int_0^{\infty} \frac{e^{-yt}}{\sqrt{y}} dy = \frac{-1}{2\sqrt{t}}\,. \end{aligned} \tag{2.47}$$

The inverse Laplace transform therefore consistently becomes

$$f(t) = \frac{1}{\sqrt{t}}\,. \tag{2.48}$$

Inverting the Laplace transform may evidently become tedious when branch cuts are involved.

2.2.2 Properties

Since the exponential function occurs in the Laplace-transform, too, we observe that many interesting properties of the Fourier transform are also present in similiar form in the Laplace transform, some of which we summarize below

1. When $f(t)$ and $F(s)$ are Laplace transform pairs, the Laplace transform of the derivative $f'(t)$ is related to both $F(s)$ and the initial value $f(0)$

$$\mathcal{L}[f(t)] = \int_0^{\infty} f'(t) e^{-st} dt = f(t) e^{-st}\Big|_0^{\infty} + s \int_0^{\infty} f(t) e^{-st} dt = sF(s) - f(0)\,. \tag{2.49}$$

Applying this formula recursively we obtain

$$\mathcal{L}[f''(t)] = s^2 F(s) - sf(0) - f'(0)\,. \tag{2.50}$$

Similarly to the FT, the recursion depth yields formulas for higher derivatives

$$\mathcal{L}[f^{(n)}(t)] = s^n F(s) - \sum_{k=1}^{n} s^{k-1} f^{(n-k)}(0)\,. \tag{2.51}$$

As with the FT, this property also allows to convert differential equations into algebraic ones. However, as the main difference we see here that the initial values of $f(t)$ are also entering these equation. The LT therefore conveniently allows to solve initial value problems: The LT of an unknown function is computed formally and solved for in the spectral domain. Afterwards, the original solution to an initial value problem is computed via the inverse Laplace transform.

2. However, sometimes one does not need the full time-dependent solution but would be satisfied with initial $\lim_{t\to 0} f(t)$ or final values $\lim_{t\to\infty} f(t)$. To obtain these, the following properties may be helpful. The LT obeys the initial value theorem

$$\lim_{t\to 0} f(t) = \lim_{s\to\infty} sF(s)\,. \tag{2.52}$$

Provided that $f(t)$ has a Taylor expansion at $t = 0$, we can use our example in Eq. (2.36) for $\alpha = 0$ to see that

$$F(s) = \sum_{n=0}^{\infty} \frac{f^{(n)}(0)}{n!} \int_0^\infty t^n e^{-st} dt = \sum_{n=0}^{\infty} \frac{f^{(n)}(0)}{s^{n+1}}\,, \tag{2.53}$$

such that

$$\lim_{s\to\infty} sF(s) = f^{(0)}(0) + \lim_{s\to\infty} \left[\frac{f^{(1)}(0)}{s} + \frac{f^{(2)}(0)}{s^2} + \ldots\right] = f(0)\,. \tag{2.54}$$

3. Provided that the limit $\lim_{t\to\infty} f(t)$ exists, or that the Laplace transform has only a finite number of poles in the left complex half plane (with either negative real part or at $s = 0$), the Laplace transform obeys the final value theorem

$$\lim_{t\to\infty} f(t) = \lim_{s\to 0} sF(s)\,. \tag{2.55}$$

We consider the Laplace transform of a derivative to see this

$$\lim_{s\to 0} \int_0^\infty f'(t) e^{-st} dt = \lim_{s\to 0} \left[sF(s) - f(0)\right] = \lim_{s\to 0} sF(s) - f(0)\,. \tag{2.56}$$

Provided that the long-term limit exists, $f'(t)$ must vanish for large times, and we can exchange limit and integral. The above equation then becomes

$$\int_0^\infty \lim_{s\to 0} f'(t) e^{-st} dt = \int_0^\infty f'(t) dt = \lim_{t\to\infty} f(t) - f(0)\,, \tag{2.57}$$

and comparison with the previous Equation eventually yields the final value theorem (2.55).

4. The Laplace transform of an integral of a function can be easily computed once the LT of the original function is known, i.e., when $F(s) = \int_0^\infty f(t) e^{-st} dt$, we conclude

$$\int_0^\infty \left[\int_0^t f(t')dt'\right] e^{-st} dt = \frac{F(s)}{s}\,. \tag{2.58}$$

This can be seen by performing an integration by parts

$$\begin{aligned}
\int_0^\infty \left[\int_0^t f(t')dt'\right] e^{-st} dt &= \int_0^\infty \left[\int_0^t f(t')dt'\right] \left(\frac{-1}{s}\right) \left(\frac{d}{dt} e^{-st}\right) dt \\
&= \left[\left(\int_0^t f(t')dt'\right) \left(\frac{-1}{s}\right) e^{-st}\right]_0^\infty + \frac{1}{s} \int_0^\infty f(t) e^{-st} dt \\
&= \frac{F(s)}{s}\,,
\end{aligned} \tag{2.59}$$

where we have used that $\frac{d}{dt} \int_0^t f(t')dt' = f(t)$.

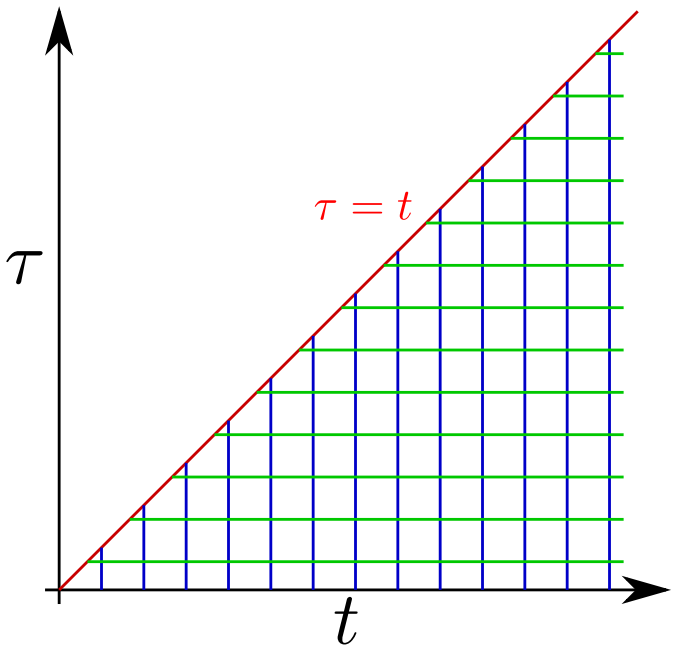

Figure 2.3: Sketch of the integration region in Eq. (2.62), which covers only the hatched area. The integrals $\int_0^\infty dt \int_0^t d\tau[\ldots]$ (vertical blue) and $\int_0^\infty d\tau \int_\tau^\infty dt[\ldots]$ (horizontal green) cover the same region.

5. Shifts in the time-domain ($a > 0$) imply a product with an exponential in the s-domain

$$\mathcal{L}[f(t-a)\Theta(t-a)] = \int_a^\infty f(t-a)e^{-s(t-a)}e^{-as}dt = \int_0^\infty f(\tau)e^{-s\tau}d\tau e^{-as} = e^{-as}F(s)\,, \quad (2.60)$$

where $\Theta(x)$ denotes the Heaviside-Theta function.

6. The Laplace transform of a convolution of two functions can be written as a simple product. First, we note that the Laplace transform only considers functions with a positive argument, so the convolution reduces to

$$(f * g)(t) = \int_{-\infty}^{+\infty} f(\tau)g(t-\tau)d\tau = \int_0^t f(\tau)g(t-\tau)d\tau\,. \quad (2.61)$$

The Laplace transform of such a convolution becomes

$$\begin{aligned} FG(s) &= \int_0^\infty (f*g)(t)e^{-st}dt = \int_0^\infty \left[\int_0^t f(\tau)g(t-\tau)d\tau\right] e^{-st}dt \\ &= \int_0^\infty dt \int_0^t d\tau f(\tau)g(t-\tau)e^{-st} = \int_0^\infty d\tau \int_\tau^\infty dt f(\tau)g(t-\tau)e^{-st}\,, \end{aligned} \quad (2.62)$$

where in the last step we have used that the two-dimensional integral covers the sector with $\tau, t \geq 0$ bounded by the lines $\tau = 0$, $\tau = t$ to change the order of the integration, see also Fig. 2.3. After substitution, we can relate the LT to the separate Laplace transforms

$$FG(s) = \int_0^\infty d\tau f(\tau)e^{-s\tau} \int_\tau^\infty dt g(t-\tau)e^{-s(t-\tau)} = F(s)G(s)\,. \quad (2.63)$$

The structure of the equations is thus considerably simplified, which justifies the importance of the Laplace transform for differential equations with a memory kernel.

7. The Laplace transform of a product of two functions in the time-domain can be written as a convolution of the Laplace-transformed functions

$$\begin{aligned} c(z) &\equiv \int_0^\infty a(t)b(t)e^{-zt}dt = \frac{1}{2\pi\mathrm{i}}\int_{\gamma-\mathrm{i}\infty}^{\gamma+\mathrm{i}\infty} a(\sigma)b(z-\sigma)d\sigma\,, \\ a(z) &= \int_0^\infty a(t)e^{-zt}dt\,, \qquad b(z) = \int_0^\infty b(t)e^{-zt}dt\,. \end{aligned} \tag{2.64}$$

Here, the contour parameter γ has to be chosen such that the integration contour lies within the region of convergence of $a(z)$, i.e., $\gamma > \gamma_a$. Furthermore, the region of convergence for $c(z)$ is defined such that $\Re(z) > \gamma_a + \gamma_b$. When $b(z)$ has poles at $z_i = b_i$, the poles of $b(z-\sigma)$ are now found at $\sigma_i = z - b_i$. From $\Re(z-\sigma) > \Re(b_i) \qquad \forall i$ it follows that $\Re(\sigma) < \Re(z-b_i) = \Re(\sigma_i)$. In practice, this has the consequence that the poles of $a(\sigma)$ lie left to the contour defined by γ, whereas the poles of $b(z-\sigma)$ lie right to the contour. Therefore, when solving the convolution integral (2.64) via the residue theorem we only need to evaluate the residues at the poles of e.g. $a(\sigma)$. The proof is rather straight, but requires some thought on necessary conditions

$$\begin{aligned} c(z) &= \left(\frac{1}{2\pi\mathrm{i}}\right)^2 \int_{\gamma_a-\mathrm{i}\infty}^{\gamma_a+\mathrm{i}\infty} dz_1 \int_{\gamma_b-\mathrm{i}\infty}^{\gamma_b+\mathrm{i}\infty} dz_2 a(z_1)b(z_2)\int_0^\infty e^{(z_1+z_2-z)t}dt \\ &= \left(\frac{1}{2\pi\mathrm{i}}\right)^2 \int_{\gamma_a-\mathrm{i}\infty}^{\gamma_a+\mathrm{i}\infty} dz_1 \int_{\gamma_b-\mathrm{i}\infty}^{\gamma_b+\mathrm{i}\infty} dz_2 a(z_1)b(z_2)\frac{-1}{z_1+z_2-z} \\ &= \frac{1}{2\pi\mathrm{i}}\int_{\gamma_a-\mathrm{i}\infty}^{\gamma_a+\mathrm{i}\infty} dz_1 a(z_1)b(z-z_1)\,. \end{aligned} \tag{2.65}$$

In the first line, we have simply inserted the inverse Laplace transforms of $a(t)$ and $b(t)$. Evaluating the integral over the exponential under the assumption that $\Re(z) > \Re(z_1)+\Re(z_2)$ then yields the second line. The last line then follows by closing the contour in the right half-plane such that the pole at $z_2 = z - z_1$ is contained.

2.2.3 Applications

Here, we briefly demonstrate the use of the Laplace transform for a few examples.

1. First we discuss the simple equation

$$\dot{x} = ax\,, \tag{2.66}$$

for which we know the solution is $x(t) = e^{at}x_0$. Formally performing the Laplace transform $F(s) = \int_0^\infty x(t)e^{-st}dt$ yields

$$sF(s) - x(0) = aF(s)\,, \tag{2.67}$$

which we can solve for the Laplace transform

$$F(s) = \frac{x_0}{s-a}\,, \tag{2.68}$$

which has a pole at $s = a$ in the complex plane. The inverse Laplace transform can be obtained from the residue theorem – Eq. (2.33) and yields

$$x(t) = e^{at}\operatorname*{Res}_{s=a}\frac{x_0}{s-a} = e^{at}x_0\,. \tag{2.69}$$

2. Now, we consider the well-known equation of motion for a harmonic oscillator of mass m, dampening constant γ_0, spring constant $\sqrt{\kappa_0}$, which is in addition subject to a periodic driving force of amplitude α_0 and frequency Ω

$$\ddot{x} + \frac{\gamma_0}{m}\dot{x} + \frac{\kappa_0}{m}x = \frac{\alpha_0}{m}\cos(\Omega t)\,, \tag{2.70}$$

where $x = x(t)$ denotes the time-dependent position of the oscillator. We perform the Laplace transform $F(s) = \int_0^\infty x(t)e^{-st}dt$ on the equation above and with $\gamma = \gamma_0/m$, $\kappa = \kappa_0/m$, and $\alpha = \alpha_0/m$ we obtain

$$\begin{aligned}\left[s^2F(s) - sx_0 - v_0\right] + \gamma\left[sF(s) - x_0\right] + \kappa F(s) &= \frac{\alpha}{2}\int_0^\infty \left[e^{-(s-\mathrm{i}\Omega)t} + e^{-(s+\mathrm{i}\Omega)t}\right]dt \\ &= \frac{\alpha}{2}\left(\frac{1}{s-\mathrm{i}\Omega} + \frac{1}{s+\mathrm{i}\Omega}\right) \\ &= \frac{\alpha s}{s^2+\Omega^2}\,,\end{aligned} \tag{2.71}$$

where we have used properties of the Laplace transform of a derivative and introduced initial position $x_0 = x(0)$ and initial velocity $v_0 = \dot{x}(0)$. In the above equation, we can now solve for the Laplace transform algebraically

$$F(s) = \frac{\alpha s}{(s^2+\Omega^2)\,(s^2+\gamma s+\kappa)} + \frac{s+\gamma}{s^2+\gamma s+\kappa}x_0 + \frac{1}{s^2+\gamma s+\kappa}v_0\,. \tag{2.72}$$

We denote the roots of the polynomial by

$$s_\pm = -\frac{\gamma}{2} \pm \sqrt{\left(\frac{\gamma}{2}\right)^2 - \kappa} = \frac{\gamma}{2}\left[-1 \pm \sqrt{1 - \frac{4\kappa}{\gamma^2}}\right]\,, \tag{2.73}$$

where we can see that the $s_\pm$ may have a large imaginary part (for weak dampening) or can also become purely real (for strong dampening). Since we can write the Laplace transform by using four poles

$$F(s) = \frac{\alpha s}{(s+\mathrm{i}\Omega)(s-\mathrm{i}\Omega)(s-s_+)(s-s_-)} + \frac{s+\gamma}{(s-s_+)(s-s_-)}x_0 + \frac{1}{(s-s_+)(s-s_-)}v_0 \tag{2.74}$$

its inverse is readily computed via the residue theorem – or Eq. (2.33) – to yield

$$\begin{aligned}x(t) &= e^{-\mathrm{i}\Omega t}\frac{\alpha(-\mathrm{i}\Omega)}{(-2\mathrm{i}\Omega)(-\mathrm{i}\Omega-s_+)(-\mathrm{i}\Omega-s_-)} + e^{+\mathrm{i}\Omega t}\frac{\alpha(+\mathrm{i}\Omega)}{(+2\mathrm{i}\Omega)(\mathrm{i}\Omega-s_+)(\mathrm{i}\Omega-s_-)} \\ &\quad + e^{+s_+t}\frac{\alpha s_+}{(s_++\mathrm{i}\Omega)(s_+-\mathrm{i}\Omega)(s_+-s_-)} + e^{+s_-t}\frac{\alpha s_-}{(s_-+\mathrm{i}\Omega)(s_--\mathrm{i}\Omega)(s_--s_+)} \\ &\quad + \left[e^{+s_+t}\frac{s_++\gamma}{(s_+-s_-)} + e^{+s_-t}\frac{s_-+\gamma}{(s_--s_+)}\right]x_0 \\ &\quad + \left[e^{+s_+t}\frac{1}{s_+-s_-} + e^{+s_-t}\frac{1}{s_--s_+}\right]v_0\,.\end{aligned} \tag{2.75}$$

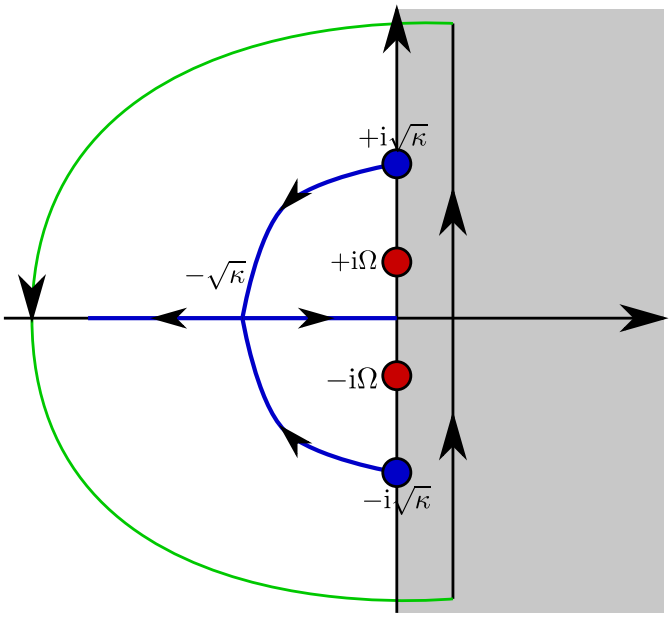

Figure 2.4: The Laplace transform of the damped and driven oscillator has four poles. With turning on damping γ, the two poles (blue) at the original oscillator eigenfrequencies $\pm i\sqrt{\kappa} = \pm i\omega_0$ move into the left half plane (arrows) until they collide at $s^* = -\sqrt{\kappa}$ when $\gamma = \sqrt{4\kappa}$. When damping is further increased, they move in opposite direction along the negative real axis. For physical parameters ($\kappa > 0$, $\gamma > 0$), none of the poles ever aquires a positive real part. For most parameter constellations, only the two poles arising from the driving (red) will have a vanishing real part.

Now, the dependence of the pole positions $s_\pm$ on the model parameters tells us what long-term dynamics can be expected, see also Fig. 2.4. Unless the dampening vanishes or is infinite, two poles will have a negative real part, and the corresponding contributions to the full solution will be negligible for large times. The asymptotic solution will in this case be given by

$$\begin{aligned} x(t) \quad &\to \quad \frac{\alpha}{2}\left[\frac{e^{-i\Omega t}}{(i\Omega + s_+)(i\Omega + s_-)} + \frac{e^{+i\Omega t}}{(i\Omega - s_+)(i\Omega - s_-)}\right] \\ &= \quad \frac{2(\kappa - \Omega^2)\cos(\Omega t) + 2\gamma\Omega \sin(\Omega t)}{\gamma^2\Omega^2 + (\kappa - \Omega^2)^2}\,. \end{aligned} \tag{2.76}$$

Noting that $\kappa = \kappa_0/m = \omega_0^2$ denotes the squared eigenfrequency of the undamped oscillator, it is clearly visible that the asymptotic oscillation amplitude may become large (resonance catastrophy) when the driving frequency matches the oscillator eigenfrequency.

3. As a third example we will consider an integro-differential equation

$$\dot{\rho} = \int_0^t g(\tau)\rho(t-\tau)d\tau\,, \tag{2.77}$$

where we simply note that the change of ρ at time t depends also on all previous values of $\rho(t)$. The function $g(\tau)$ – sometimes called memory kernel – weights these influences from the past. If $\rho(t)$ denotes a density matrix or some probability distribution, such equations are also called non-Markovian master equations, and their Markov [6] limit is obtained by letting $g(\tau) \to g\delta(\tau)$, which collapses the equation into a time-local version. The convolution property tells us

$$sF(s) - \rho_0 = G(s)F(s)\,, \tag{2.78}$$

[6] Andrei Andrejewitsch Markow (1856–1922) was a russian mathematician with contributions to probability calculus and analysis.

where

$$G(s) = \int_0^\infty g(\tau) e^{-s\tau} d\tau \tag{2.79}$$

denotes the Laplace transform of the kernel function. For simplicity we choose here a simple kernel of the form

$$g(\tau) = g_0 \tau e^{-\alpha\tau}\,, \qquad G(s) = \frac{g_0}{(s+\alpha)^2}\,. \tag{2.80}$$

The kernel peaks at $\tau = 1/\alpha$, which can then be considered as a characteristic delay time. The Laplace transform of the solution therefore becomes

$$F(s) = \frac{\rho_0}{s - G(s)} = \frac{\rho_0 (s+\alpha)^2}{s(s+\alpha)^2 - g_0} = \frac{\rho_0 (s+\alpha)^2}{(s-s_1)(s-s_2)(s-s_3)}\,, \tag{2.81}$$

where s_i denote the roots of the polynomial $s(s+\alpha)^2 - g_0$. Since the polynomial is only of third order, these can be computed exactly with the Cardano [7] formulas. However, the Cardano formulas are quite sophisticated. Therefore, we only aim at an approximate solution here. To do so, it is usually always a good idea to introduce dimensionless variables. Consequently, we can write the equation $0 = s(s+\alpha)^2 - g_0$ also as

$$0 = S(S+1)^2 - \gamma\,, \qquad S = \frac{s}{\alpha}\,, \qquad \gamma = \frac{g_0}{\alpha^3}\,, \tag{2.82}$$

which we intend to solve for small γ. For $\gamma = 0$ we get the lowest order contributions $\bar{S}_1 = 0$ and $\bar{S}_{2/3} = -1$. Using the ansatz $S_1 = 0 + a\gamma + b\gamma^2 + \mathcal{O}\{\gamma^3\}$ we obtain

$$\begin{aligned} 0 &= (a\gamma + b\gamma^2)(a\gamma + b\gamma^2 + 1)^2 - \gamma + \mathcal{O}\{\gamma^3\} \\ &= \gamma(a+b\gamma)(\gamma^2(a+b\gamma)^2 + 2\gamma(a+b\gamma) + 1) - \gamma + \mathcal{O}\{\gamma^3\} \\ &= \gamma\left[a-1\right] + \gamma^2\left[b + 2a^2\right] + \mathcal{O}\{\gamma^3\}\,, \end{aligned} \tag{2.83}$$

from which we can deduce $a = +1$ and $b = -2$, such that

$$s_1 = \alpha S_1 = \alpha\left[\left(\frac{g_0}{\alpha^3}\right) - 2\left(\frac{g_0}{\alpha^3}\right)^2 + \mathcal{O}\{\left(\frac{g_0}{\alpha^3}\right)^3\right]\,. \tag{2.84}$$

When treating the other solutions, it becomes obvious that a simple ansatz with integer powers of γ will not work, since there would be no first order contribution to cancel. The next obvious try is to expand in roots of γ: $S_{2/3} = -1 + a_{2/3}\gamma^{1/2} + b_{2/3}\gamma + \mathcal{O}\{\gamma^{3/2}\}$. When this expansion is inserted, ordering in powers of γ leads to the equation

$$0 \;=\; \gamma\left[-a_{2/3}^2 - 1\right] + \gamma^{3/2}\left[a_{2/3}^3 - 2a_{2/3}b_{2/3}\right] + \mathcal{O}\{\gamma^2\}\,, \tag{2.85}$$

such that we obtain $a_{2/3} = \pm\mathrm{i}$ and $b_{2/3} = -1/2$ yielding eventually

$$s_{2/3} = \alpha S_{2/3} = \alpha\left[-1 \pm \mathrm{i}\sqrt{\frac{g_0}{\alpha^3}} - \frac{1}{2}\frac{g_0}{\alpha^3} + \mathcal{O}\{\left(\frac{g_0}{\alpha^3}\right)^{3/2}\right]\,. \tag{2.86}$$

[7] Gerolamo Cardano (1501–1576) was an italian scholar who worked as a doctor, philosopher and mathematician. He is considered as one of the last polymaths.

We see that only s_1 has a positive real part and consequently, the residues originating from $s_{2/3}$ can be neglected in the long-term limit. While these expansions hold for weak coupling and little delay (large α), it is also possible to expand around the opposite limit by introducing $S = s/g_0^{1/3}$ and $\sigma = \alpha/g_0^{1/3}$ and considering the equation

$$0 = S(S+\sigma)^2 - 1 \tag{2.87}$$

for small σ (large delay and strong coupling). Eventually, we have the power series ansatz

$$s_1 = \frac{g_0}{\alpha^2} + \mathcal{O}\{g_0^{3/2}\}\,, \qquad s_{2/3} = -\alpha \pm \mathrm{i}\sqrt{\frac{g_0}{\alpha}} - \frac{g_0}{2\alpha^2} + \mathcal{O}\{g_0^{3/2}\}\,. \tag{2.88}$$

Consequently, we see that the long-term dynamics of the solution is dominated by the pole with the largest real part, and we find

$$\operatorname*{Res}_{s=s_1} F(s) = \frac{\rho_0(s_1+\alpha)^2}{(s_1-s_2)(s_1-s_3)}\,, \tag{2.89}$$

which implies for the long-term asymptotics

$$\rho(t) \to e^{s_1 t}\frac{\rho_0(s_1+\alpha)^2}{(s_1-s_2)(s_1-s_3)}\,. \tag{2.90}$$

4. Finally, we may also apply the convolution theorem to memories that have a strongly peaked delay kernel, e.g. to the differential equation

$$\dot\rho(t) = g_0\rho(t-\tau_D)\Theta(t)\,, \tag{2.91}$$

where $\tau_D > 0$ is a delay time. We can write the above equation also as a convolution

$$\dot\rho(t) = \int_0^t g(\tau)\rho(t-\tau)d\tau\,, \qquad g(\tau) = g_0\delta(\tau-\tau_D)\,. \tag{2.92}$$

The Laplace transform of the kernel function becomes

$$G(s) = g_0 e^{-s\tau_D}\,, \tag{2.93}$$

such that the Laplace transform of the solution is

$$F(s) = \frac{\rho_0}{s-G(s)} = \frac{\rho_0}{s-g_0e^{-s\tau_D}}\,. \tag{2.94}$$

The denominator now has infinitely many roots s_n (corresponding to first order poles) which in general will have to be determined numerically, and the full solution is then given by

$$\rho(t) = \sum_{n=-\infty}^{+\infty} e^{s_n t}\operatorname*{Res}_{s=s_n}\frac{\rho_0}{s-g_0e^{-s\tau_D}}\,. \tag{2.95}$$

In particular, only one pole – which we formally denote as s_0 – has a positive real part and will thus dominate the long-term dynamics

$$\rho(t) \overset{t\to\infty}{\to} e^{s_0 t}\operatorname*{Res}_{s=s_0}\frac{\rho_0}{s-g_0e^{-s\tau_D}}\,. \tag{2.96}$$

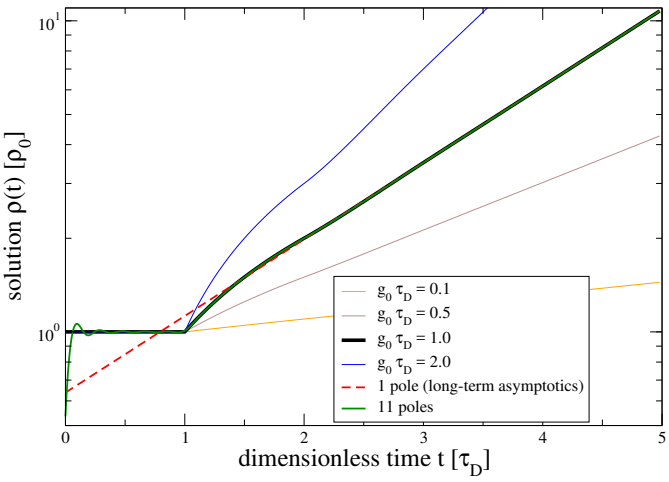

Figure 2.5: Plot of the full solution (2.99) (solid black, in units of ρ_0) versus time (in units of delay time τ_D). For times smaller than the delay time, nothing happens. Afterwards the growth dynamics is not immediately exponential but quickly approches the asymptotic limit obtained by considering the dominant pole (dashed red). For short times the dynamics is poorly captured if only a finite number of poles is considered in Eq. (2.95).

Alternatively, the full inverse LT for finite times can be obtained by expanding the Laplace transform

$$F(s) = \frac{\rho_0}{s}\frac{1}{1-\frac{g_0}{s}e^{-s\tau_D}} = \frac{\rho_0}{s}\sum_{n=0}^{\infty}\left(\frac{g_0}{s}\right)^n e^{-ns\tau_D} = \rho_0\sum_{n=0}^{\infty}\frac{g_0^n}{s^{n+1}}e^{-ns\tau_D}\,. \tag{2.97}$$

We can perform the inverse Laplace transform for each term separately

$$\mathcal{L}^{-1}\left(e^{-ns\tau_D}\frac{g_0^n}{s^{n+1}}\right) = \frac{g_0^n}{n!}(t-n\tau_D)^n\Theta(t-n\tau_D)\,, \tag{2.98}$$

where we have used previous results. The solution eventually becomes

$$\rho(t) = \sum_{n=0}^{\infty}\frac{g_0^n}{n!}(t-n\tau_D)^n\Theta(t-n\tau_D)\rho_0\,. \tag{2.99}$$

For significant delay, the solution can be quite different from simple exponential growth, see Fig. 2.5. In particular, it is straightforward to see that we can truncate the solution for short times after a few terms.

5. As the last example, we consider the Laplace transform of a product. Consider the following Laplace transform pairs (we assume that $\omega \in \mathbb{R}$ below)

$$\begin{aligned} a(t) &= e^{\alpha t}\,, \qquad a(z) = \frac{1}{z-\alpha}\,, \qquad \Re(z) > \Re(\alpha)\,, \\ b(t) &= e^{\beta t}\cos(\omega t)\,, \qquad b(z) = \frac{z-\beta}{(z-\beta)^2+\omega^2}\,, \qquad \Re(z) > \Re(\beta)\,. \end{aligned} \tag{2.100}$$

The Laplace transform of the product of both is given by

$$c(z) = \int_0^\infty e^{(\alpha+\beta-z)t}\cos(\omega t)dt = \frac{1}{2\pi\mathrm{i}}\int_{\gamma-\mathrm{i}\infty}^{\gamma+\mathrm{i}\infty}\frac{1}{\sigma-\alpha}\frac{z-\sigma-\beta}{(z-\sigma-\beta)^2+\omega^2}d\sigma\,, \tag{2.101}$$

where $\gamma > \alpha$, and it converges for $\Re(z) > \Re(\alpha) + \Re(\beta)$. The integrand has three poles, one at $\sigma_1 = \alpha$ (left to the contour defined by γ) and the other two at $\sigma_{2/3} = z - \beta \pm \mathrm{i}\omega$ (right to

the contour defined by γ). Closing the contour integral in the left half plane, such that only σ_1 is contained, we obtain

$$c(z) = \frac{z - \alpha - \beta}{(z - \alpha - \beta)^2 + \omega^2}\,, \tag{2.102}$$

as we would have obtained from the Laplace transform of $b(t)$.

Chapter 3

Ordinary Differential Equations

In short, any equation involving a function and also its derivatives with respect to a single variable may be called ordinary differential equation.

Box 15 (Ordinary differential Equation) *An ordinary differential equation (ODE) of order n is defined by the equation*

$$f(t, x(t), x'(t), x''(t), \ldots, x^{(n)}(t)) = 0\,, \tag{3.1}$$

where $f(t, x'(t), \ldots)$ is a function. When the equation can be solved for the highest derivative, i.e.,

$$x^{(n)}(t) = F(t, x(t), x'(t), \ldots, x^{(n-1)}(t)) \tag{3.2}$$

it is called **explicit**.

Any explicit m-th order ODE can always be mapped to a coupled system of first order ODEs. To see this, we introduce auxiliary variables

$$y_1(t) = x(t)\,, \qquad y_2(t) = x'(t)\,, \qquad \ldots\,, \qquad y_n(t) = x^{(n-1)}(t)\,, \tag{3.3}$$

which yields the system

$$\begin{aligned} y_1'(t) &= y_2(t)\,, \qquad y_2'(t) = y_3(t)\,, \qquad \ldots\,, \qquad y_{n-1}'(t) = y_n(t)\,, \\ y_n'(t) &= F(t, y_1(t), \ldots, y_n(t))\,. \end{aligned} \tag{3.4}$$

Above, only the first derivatives occur, but we now have a system of n equations instead of a single equation with n derivatives. As a simple example, we consider the harmonic oscillator

$$m\ddot{x} + \gamma\dot{x} + \kappa x = g(t)\,, \tag{3.5}$$

which by introducing

$$y_1(t) = x(t)\,, \qquad y_2(t) = \dot{x}(t) \tag{3.6}$$

can be converted into the system

$$\dot{y}_1(t) = y_2(t)\,, \qquad \dot{y}_2(t) = -\frac{\gamma}{m} y_2(t) + \frac{\kappa}{m} y_1(t) + \frac{g(t)}{m}\,. \tag{3.7}$$

There exist many types of ODEs and only few of them can be solved analytically.

A special case of ODEs occurs when the functions $y_i(t)$ occur only linearly in the ODE, i.e.,

$$\begin{pmatrix} \dot{y_1} \\ \vdots \\ \dot{y_n} \end{pmatrix} = \begin{pmatrix} a_{11}(t) & \dots & a_{1N}(t) \\ \vdots & & \vdots \\ a_{N1}(t) & \dots & a_{NN}(t) \end{pmatrix} \begin{pmatrix} y_1 \\ \vdots \\ y_n \end{pmatrix} + \begin{pmatrix} f_1(t) \\ \vdots \\ f_n(t) \end{pmatrix} . \tag{3.8}$$

Such a system is then called **homogeneous** when $f_i(t) = 0$. In what follows, we will switch to a vector representation (marked by bold symbols), where the linear ODE becomes

$$\dot{\boldsymbol{y}} = A(t)\boldsymbol{y} + \boldsymbol{f}(t) . \tag{3.9}$$

We can immediately exploit the linearity to deduce that when we have found two solutions to the homogeneous system, any combination of these will also be a solution of the homogeneous system. Furthermore, when $\boldsymbol{y_H}(t)$ denotes any solution (or the general solution) of the homogeneous system and $\boldsymbol{y_S}(t)$ any particular solution of the inhomogeneous system

$$\dot{\boldsymbol{y_H}} = A(t)\boldsymbol{y_H}(t) , \qquad \dot{\boldsymbol{y_S}} = A(t)\boldsymbol{y_S}(t) + \boldsymbol{f}(t) , \tag{3.10}$$

it is directly evident that the combination of both $\boldsymbol{y}(t) = \boldsymbol{y_H}(t) + \boldsymbol{y_S}(t)$ will also solve the differential equation (3.9).

3.1 Linear ODEs with constant coefficients

The case becomes much simpler when the coefficients in the linear system are constant $A(t) \to A$ and $\boldsymbol{f}(t) \to \boldsymbol{f}$. Then, the solution for the homogeneous system reads

$$\boldsymbol{y}_H(t) = e^{At}\boldsymbol{c} , \tag{3.11}$$

where $\boldsymbol{c}$ is any vector. A special solution of the inhomogeneous system can then be found by solving the time-independent equation $A\boldsymbol{y}_S + \boldsymbol{f} = 0$, and by using the initial condition $\boldsymbol{y}(0) = \boldsymbol{y}_0$ we can fix the vector $\boldsymbol{c}$. Thus, the solution is given by

$$\boldsymbol{y}(t) = e^{At}\boldsymbol{y}_0 + \left[1 - e^{At}\right] \boldsymbol{y_S} . \tag{3.12}$$

Evidently, the computation of the exponential of a matrix is important to calculate the solution of linear ODEs with constant coefficients.

3.1.1 Properties of the Matrix Exponential

The exponential of a matrix is defined via the power series expansion

$$e^A = \sum_{n=0}^{\infty} \frac{A^n}{n!} . \tag{3.13}$$

We summarize some properties of the matrix exponential

1. When two matrices commute $[A, B] = AB - BA = \mathbf{0}$ we have

$$e^{A+B} = e^A e^B \,. \tag{3.14}$$

It may seem trivial but is sadly often forgotten: Usually matrices do not commute, and the above property does not hold.

2. The matrix exponential is always invertible, and one has

$$\left(e^A\right)^{-1} = e^{-A} \,. \tag{3.15}$$

3. When there exists a similiarity transform $C = BAB^{-1}$ one can compute the matrix exponential via

$$e^C = Be^A B^{-1} \,. \tag{3.16}$$

This is particularly useful if e^A is simple to compute.

4. When the matrix if of block-diagonal form, its exponential can be computed by exponentiating the blocks separately

$$B = \begin{pmatrix} B_1 & & \mathbf{0} \\ & \ddots & \\ \mathbf{0} & & B_k \end{pmatrix} \qquad \Longrightarrow \qquad e^B = \begin{pmatrix} e^{B_1} & & \mathbf{0} \\ & \ddots & \\ \mathbf{0} & & e^{B_k} \end{pmatrix} , \tag{3.17}$$

which may significantly – in particular when the dimension of the blocks is one (diagonal matrix) – reduce the effort.

5. The determinant of a matrix exponential can be computed by exponentiating the trace

$$\det\left(e^A\right) = e^{\mathrm{Tr}\{A\}} \,. \tag{3.18}$$

6. One has

$$\frac{d}{dt} e^{At} = Ae^{At} \,. \tag{3.19}$$

Note that this does not hold when A is time-dependent.

In particular when two matrices do not commute but when their commutator is small or just a $\mathbb{C}$-number, the Baker[1]- Campbell[2]- Hausdorff[3] formula

$$\begin{aligned} e^X e^Y &= e^{Z(X,Y)} \,, \qquad \text{with} \\ Z(X,Y) &= X + Y + \frac{1}{2}\,[X,Y] + \frac{1}{12}\,[X,[X,Y]] - \frac{1}{12}\,[Y,[X,Y]] + \ldots \end{aligned} \tag{3.20}$$

[1]Henry Frederick Baker (1856–1956) was a british mathematician with contributions to algebraic geometry. He elaborated on the formula in 1902.

[2]John Edward Campbell (1862–1924) was a british mathematician who first introduced the formula in 1897.

[3]Felix Hausdorff (1868–1942) was a german mathematician who also acted as a philosopher and writer (under the pseudonym Paul Mongré). He systematized the formula geometrically in 1906.

may be useful. In particular when $[X,Y] \in \mathbb{C}$ we may exactly truncate the series. A simple consequence of the expansion is the Lie[4] product formula

$$e^{A+B} = \lim_{N\to\infty} \left(e^{A/N} e^{B/N}\right)^N , \tag{3.21}$$

which has applications e.g. in path integrals. Very often, one encounters transformations of the form $e^{+X} Y e^{-X}$. These can be conveniently treated with the decomposition

$$\begin{aligned} e^{+X} Y e^{-X} \quad &= \quad Y + [X,Y] + \frac{1}{2!}[X,[X,Y]] + \frac{1}{3!}[X,[X,[X,Y]]] + \ldots = \sum_{n=0}^{\infty} \frac{1}{n!} [X,Y]_n \\ &\text{with} \quad [X,Y]_m = \left[X,[X,Y]_{m-1}\right] , \qquad \text{and} \qquad [X,Y]_0 = Y . \end{aligned} \tag{3.22}$$

The above expansion is also known as nested commutator expansion for obvious reasons.

To prove it, we consider the parameter-dependent transformation

$$Y(\alpha) = e^{+\alpha X} Y e^{-\alpha X} , \tag{3.23}$$

such that $Y(0) = Y$ and $Y(1) = e^{+X} Y e^{-X}$ is the sought-after transformation. The derivative becomes

$$\frac{dY}{d\alpha} = XY(\alpha) - Y(\alpha)X = [X, Y(\alpha)] . \tag{3.24}$$

We can apply this recursively

$$\frac{d^n Y}{d\alpha^n} = [X, Y(\alpha)]_n . \tag{3.25}$$

The Taylor expansion of $Y(\alpha)$ around $\alpha = 0$ therefore becomes

$$Y(\alpha) = \sum_{n=0}^{\infty} [X, Y(0)]_n \frac{\alpha^n}{n!} . \tag{3.26}$$

At $\alpha = 1$, this becomes the nested commutator expansion.

Finally, we note that the matrix exponential can always be computed.

- When A is diagonalizable, we may directly compute the matrix exponential via the (simple) exponential of the diagonalized matrix – cf. Eq. (3.16).
- Even when A is not diagonalizable, it can be represented in Jordan[5] normal form

$$B = UAU^{-1} = \begin{pmatrix} J_1 & & \mathbf{0} \\ & \ddots & \\ \mathbf{0} & & J_k \end{pmatrix} \quad \text{with Jordan blocks} \quad J_i = \begin{pmatrix} \lambda & 1 & & \mathbf{0} \\ & \ddots & \ddots & \\ & & \ddots & 1 \\ \mathbf{0} & & & \lambda \end{pmatrix} . \tag{3.27}$$

  Since these Jordan blocks can be decomposed as $J_i = \lambda \mathbf{1} + N_i$ with nilpotent matrices N_i (meaning that $N_i^k = \mathbf{0}$ for sufficiently large exponent k), their exponential can be explicitly computed via $e^{J_i} = e^{\lambda} e^{N_i} = e^{\lambda} \left[\sum_{\ell=0}^{k} N_i^\ell / \ell!\right]$.

[4] Sophus Lie (1842–1899) was a norwegian mathematician best known for his contributions to continuous transformation (Lie-) groups.

[5] Marie Ennemond **Camille** Jordan (1838–1922) was a french mathematician who initially worked as an engineer and persued his mathematical studies in his spare time. He contributed to analysis, group theory, and topology.

3.1.2 Numerical Computation of the matrix exponential

The problem with using the Taylor series expansion (3.13) for direct numerical computation of the matrix exponential is that in general convergence is poor. In particular for matrices with a large norm, intermediate contributions to the series may become very large – possibly exceeding numerical ranges, and since very large numbers are used, also numerical roundoff errors become a serious issue. It has therefore become common practice to use other schemes to approximate the exponential of a matrix, here we will discuss the scaling and squaring algorithm in combination with Padé approximation and an algorithm for computing the inverse of a matrix.

Scaling and Squaring

To make all algorithms converge well, we require that the norm of the matrix is neither too small nor too large but rather in the order of one. We therefore make use of the property

$$e^A = \left(e^{A/\sigma}\right)^\sigma \,, \tag{3.28}$$

such that $\|A\|/\sigma \approx 1$. It is then particularly helpful to choose $\sigma = 2^N$ with integer N, since then – supposed one is given a suitable approximation

$$B_0 \approx e^{A/2^N} = e^{A/\sigma} \,, \tag{3.29}$$

it takes only N matrix multiplications to recover e^A from B_0

$$B_1 = B_0^2 = e^{A/2^{N-1}} \,, \qquad B_2 = B_1^2 = e^{A/2^{N-2}} \,, \qquad \ldots \qquad , B_N = B_{N-1}^2 = e^A \,. \tag{3.30}$$

Padé approximation

In principle, we could simply use the Taylor series once $\|A\|/\sigma$ is small. However, if speed is relevant, much can be gained by approximating the exponential by Padé[6] approximation. The basic idea is to approximate any function

$$f(x) = \sum_{n=0}^{\infty} c_n x^n \approx q_{km}^{-1}(x) p_{km}(x) \tag{3.31}$$

by the ratio of two polynomials – $p_{km}(x)$ being a polynomial of order k and q_{km} a polynomial of order m – such that

$$\begin{aligned} f(x) - \left[q_{km}(x)\right]^{-1} p_{km}(x) &= f(x) - \left[q_{km}^0 + q_{km}^1 x + \ldots + q_{km}^m x^m\right]^{-1} \left[p_{km}^0 + p_{km}^1 x + \ldots + p_{km}^k x^k\right] \\ &= \mathcal{O}\{x^{k+m+1}\} \,. \end{aligned} \tag{3.32}$$

Provided that computing the inverse of a matrix does not provide significant additional cost (see below), this method is particularly useful, since the Padé approximants to the exponential are explicitly known

$$\begin{aligned} p_{km}(x) &= \sum_{j=0}^{k} \frac{(k+m-j)!k!}{(k+m)!(k-j)!j!} (+x)^j \,, \\ q_{km}(x) &= \sum_{j=0}^{m} \frac{(k+m-j)!m!}{(k+m)!(m-j)!j!} (-x)^j \,. \end{aligned} \tag{3.33}$$

[6] Henri Eugène Padé (1863–1953) was a french mathematician who contributed approximation techniques using rational functions.

In particular, it is obvious that the trivial $m = 0$ case recovers the Taylor approximation. In practice, it is preferred to choose $k = m$. In particular, when $k = m$ is large, we note that $q_{mm}(X)$ approximates $\exp(-X/2)$, whereas $p_{mm}(X)$ approximates $\exp(+X/2)$. We can can see this by writing some of the factorials in the Padé approximants explicitly and grouping all terms

$$\begin{aligned}\frac{(2m-j)!}{(2m)!}\frac{m!}{(m-j)!} &= \frac{1}{2m(2m-1)\cdot\ldots\cdot(2m-j+1)}\frac{m(m-1)\cdot\ldots\cdot(m-j+1)}{1} \\ &= \underbrace{\frac{m}{2m}\frac{m-1}{2m-1}\cdot\ldots\cdot\frac{m-j+1}{2m-j+1}}_{j\times} \\ &\overset{m\to\infty}{\to} \frac{1}{2^j}\,. \end{aligned} \tag{3.34}$$

Equivalently, one can also use the Stirling approximation to the factorial

$$n! \approx \sqrt{2\pi n}\left(\frac{n}{e}\right)^n \tag{3.35}$$

to show this. Effectively, we therefore have $p_{mm}(X) \approx e^{X/2}$ and $q_{mm}(X) \approx e^{-X/2}$, such that $p_{mm}(X)$ may serve as a first guess to the inverse of $q_{mm}(X)$ in iterative algorithms (see below), provided m is chosen large enough.

Matrix inversion

Multiple algorithms for matrix inversion exist. They may become somewhat sophisticated but have an optimal complexity of $\mathcal{O}\{N^3\}$ (e.g. LU decomposition). Here, we are seeking for a simpler algorithm that is comparably easy to implement.

So let Q denote the matrix to be inverted and let M_0 be a first guess for its inverse. For the iteration to converge, the initial guess M_0 must be close to the true inverse. Defining the initial residual as $R = \mathbf{1} - M_0 Q$, which implies $M_0 Q = \mathbf{1} - R$, we use

$$\begin{aligned} Q^{-1} &= Q^{-1}(M_0^{-1}M_0) = (Q^{-1}M_0^{-1})M_0 = (M_0 Q)^{-1}M_0 = (\mathbf{1}-R)^{-1}M_0 \\ &= (\mathbf{1} + R + R^2 + R^3 + \ldots)M_0\,, \end{aligned} \tag{3.36}$$

where we have only used the geometric series – which converges only when the norm of the initial residual is small. When we now define the partial approximation as

$$M_n = \left[\sum_{k=0}^{n} R^k\right] M_0\,, \tag{3.37}$$

such that $M_\infty = Q^{-1}$, it is not difficult to find recursion relations between the M_n. One of them is a well-known iteration method for finding the inverse of a matrix Q

$$M_{2n+1} = 2M_n - M_n Q M_n\,, \tag{3.38}$$

which converges (quadratically) to the inverse of Q – provided that M_0 is sufficiently close to the true inverse. Trivially we see that for $M_n = Q^{-1}$ we also obtain $M_{2n+1} = Q^{-1}$ from Eq. (3.38). We can prove the recursion relation from realizing that $M_n Q = \sum_{k=0}^{n} R^k M_0 Q = \sum_{k=0}^{n} R^k(1-R) =$

$\mathbf{1} - R^{n+1}$. This does of course imply $R^{n+1} = (\mathbf{1} - M_n Q)$, and when one now splits the left hand side as

$$M_{2n+1} = \left[\sum_{k=0}^{n} R^k + \sum_{k=n+1}^{2n+1} R^k\right] M_0 = M_n + R^{n+1} M_n = M_n + (\mathbf{1} - M_n Q) M_n \,, \tag{3.39}$$

the iteration equation follows directly.

We finally note that the iteration will converge when the initial residual is small, i.e., when one already has a sufficiently good estimate of the inverse. In the general case, convergence is not guaranteed. However, the initial choice

$$M_0 = \frac{Q^\dagger}{\|Q\|_1 \|Q\|_\infty} \tag{3.40}$$

with the row and column norms

$$\|A\|_1 = \max_i \left(\sum_j |a_{ij}|\right) \,, \qquad \|A\|_\infty = \max_j \left(\sum_i |a_{ij}|\right) \tag{3.41}$$

will lead to (possibly slow) convergence of the iteration scheme (3.38). This follows from realizing that the initial residual

$$R = \mathbf{1} - M_0 Q = \mathbf{1} - \frac{Q^\dagger Q}{\|Q\|_1 \|Q\|_\infty} \tag{3.42}$$

has only eigenvalues ranging between zero and one.

3.2 The adiabatically driven Schrödinger equation

We consider the time-dependent Schrödinger [7] equation

$$\left|\dot{\Psi}\right\rangle = -\mathrm{i} H(t) \left|\Psi(t)\right\rangle \,. \tag{3.43}$$

Here, $|\Psi(t)\rangle$ denotes the normalized wave function, where the normalization is preserved as long as $H(t) = H^\dagger(t)$ is self-adjoint. In this sense, the results in this section apply to all time-dependent first order ODEs with a self-adjoint generator, which can be written in the form of Eq. (3.43).

Thanks to the hermiticity of $H(t)$, we can at each instant in time define an orthonormal energy eigenbasis of the instantaneous Hamiltonian

$$H(t) \left|n(t)\right\rangle = E_n(t) \left|n(t)\right\rangle \,. \tag{3.44}$$

Since the basis is complete $\sum_n |n(t)\rangle \langle n(t)| = \mathbf{1}$, we can always expand the state vector in this energy eigenbasis

$$|\Psi\rangle = \sum_n a_n(t) \exp\left\{-\mathrm{i} \int_0^t E_n(t')dt'\right\} |n(t)\rangle \,, \tag{3.45}$$

[7] Erwin Rudolf Josef Alexander Schrödinger (1887 – 1961) was an austrian physicist known as one of the founders of quantum mechanics.

where $a_n(t) \in \mathbb{C}$ and where the exponential integral factor has just been introduced for convenience The coefficients $a_n(t)$ tell us the distribution of the state vector over the different energy eigenstate. For example, the energy of the state is given by $\langle E \rangle = \sum_n E_n(t)|a_n(t)|^2$.

Inserting this in the Schrödinger equation one directly obtains

$$\dot{a}_m = -\sum_n a_n(t) \exp\left\{-\mathrm{i}\int_0^t [E_n(t') - E_m(t')]\, dt'\right\} \langle m(t)|\dot{n}(t)\rangle \ . \tag{3.46}$$

Since we aim at an expression quantifying the transitions between energy eigenstates, we pull the term with $n = m$ to the l.h.s., yielding

$$\begin{aligned} \dot{a}_m + a_m \langle m(t)|\dot{m}(t)\rangle &= -\sum_{n:n\neq m} a_n(t) \exp\left\{-\mathrm{i}\int_0^t [E_n(t') - E_m(t')]\, dt'\right\} \langle m(t)|\dot{n}(t)\rangle \\ &= -\sum_{n:n\neq m} a_n(t) \exp\left\{-\mathrm{i}\int_0^t [E_n(t') - E_m(t')]\, dt'\right\} \frac{\langle m(t)|\, \dot{H}\, |n(t)\rangle}{E_n(t) - E_m(t)} \end{aligned} \tag{3.47}$$

In the last step, we have assumed that the system is non-degenerate, i.e., $E_n(t) \neq E_m(t)$, which enables to obtain the used relation from the eigenvalue equation (3.44). Multiplying both sides with $e^{-\mathrm{i}\gamma_m(t)}$ with

$$\gamma_m(t) = \mathrm{i}\int_0^t \langle m(t')|\dot{m}(t')\rangle\, dt' \tag{3.48}$$

denoting the Berry [8] phase, we can also write this as

$$\frac{d}{dt}\left(a_m e^{-\mathrm{i}\gamma_m}\right) = -\sum_{n:n\neq m} a_n(t) e^{-\mathrm{i}\gamma_m(t)} \exp\left\{-\mathrm{i}\int_0^t [E_n(t') - E_m(t')]\, dt'\right\} \frac{\langle m(t)|\, \dot{H}\, |n(t)\rangle}{E_n(t) - E_m(t)} \tag{3.49}$$

Assuming that the r.h.s. is small (slow evolution), we aim at solving the equation perturbatively for slow evolutions. First, we formally integrate the equation, yielding

$$\begin{aligned} a_m(t)e^{-\mathrm{i}\gamma_m(t)} - a_m^0 &= -\sum_{n:n\neq m} \int_0^t dt' a_n(t') e^{-\mathrm{i}\gamma_m(t')} \exp\left\{-\mathrm{i}\int_0^{t'} [E_n(t'') - E_m(t'')]\, dt''\right\} \times \\ &\quad \times \frac{\langle m(t')|\, \dot{H}(t')\, |n(t')\rangle}{E_n(t') - E_m(t')} \\ &= -\mathrm{i}\sum_{n:n\neq m} \int_0^t dt' a_n(t') e^{-\mathrm{i}\gamma_m(t')} \frac{\langle m(t')|\, \dot{H}(t')\, |n(t')\rangle}{[E_n(t') - E_m(t')]^2} \times \\ &\quad \times \frac{d}{dt'} \exp\left\{-\mathrm{i}\int_0^{t'} [E_n(t'') - E_m(t'')]\, dt''\right\} . \end{aligned} \tag{3.50}$$

We can now perform an integration by parts on the r.h.s., leading to

$$\begin{aligned} a_m(t) &= a_m^0 e^{+\mathrm{i}\gamma_m(t)} \\ &\quad -\mathrm{i}e^{+\mathrm{i}\gamma_m(t)} \sum_{n:n\neq m} \left[a_n(t') e^{-\mathrm{i}\gamma_m(t')} \frac{\langle m(t')|\, \dot{H}(t')\, |n(t')\rangle}{[E_n(t') - E_m(t')]^2} \exp\left\{-\mathrm{i}\int_0^{t'} [E_n(t'') - E_m(t'')]\, dt''\right\} \right]_0^t \\ &\quad +\mathcal{O}\left\{ \frac{d}{dt'} a_n(t') e^{-\mathrm{i}\gamma_m(t')} \frac{\langle m(t')|\, \dot{H}(t')\, |n(t')\rangle}{[E_n(t') - E_m(t')]^2} \right\} . \end{aligned} \tag{3.51}$$

[8] Michael Victor Berry (born 1941) is a british physicist who discussed the phase in 1983.

Now, provided that the condition

$$\frac{\langle m(t')|\,\dot{H}(t')\,|n(t')\rangle}{[E_n(t')-E_m(t')]^2} \ll 1 \tag{3.52}$$

holds for $0 < t' < t$, the evolution is *locally adiabatic*, and we can neglect the term with the integral. In this case, the first-order correction yields

$$\begin{aligned} a_m(t) \;\approx\; & a_m^0 e^{+\mathrm{i}\gamma_m(t)} \\ & -\mathrm{i}\sum_{n:n\neq m} a_n(t)\frac{\langle m(t)|\,\dot{H}(t)\,|n(t)\rangle}{[E_n(t)-E_m(t)]^2}\exp\left\{-\mathrm{i}\int_0^t [E_n(t')-E_m(t')]\,dt'\right\} \\ & +\mathrm{i}e^{+\mathrm{i}\gamma_m(t)}\sum_{n:n\neq m} a_n^0\frac{\langle m(0)|\,\dot{H}(0)\,|n(0)\rangle}{[E_n(0)-E_m(0)]^2}\,. \end{aligned} \tag{3.53}$$

Essentially, when the adiabatic condition (3.52) holds also initially and finally, we see that for such slowly driven systems, the coefficient $a_m(t)$ just acquires a phase factor, and effectively, the system remains in its instantaneous energy eigenstate. This is the essence of the adiabatic theorem: Slowly driven quantum systems remain in their instantaneous energy eigenstates. It can be used to prepare desired quantum states as particular energy eigenstates of a final Hamiltonian (e.g. ground states) or even solve NP-hard problems by encoding the solutions to such problems in the ground state of the final Hamiltonian [2].

In particular, we can consider a situation where the system is initially in its ground state $a_n^0 = \delta_{n,0}$. Then, we get

$$a_0(t) \;\approx\; e^{+\mathrm{i}\gamma_0(t)} - \mathrm{i}\sum_{n\geq 1} a_n(t)\frac{\langle 0(t)|\,\dot{H}(t)\,|n(t)\rangle}{[E_n(t)-E_0(t)]^2}\exp\left\{-\mathrm{i}\int_0^t [E_n(t')-E_0(t')]\,dt'\right\}, \tag{3.54}$$

which immediately identifies an excitation amplitude.

As a simple example to illustrate this we consider a driven spin

$$H(t) = \Omega\boldsymbol{n}(t)\cdot\boldsymbol{\sigma} = \Omega\left[n_x(t)\sigma^x + n_y(t)\sigma^y + n_z(t)\sigma^z\right], \tag{3.55}$$

which has time-dependent eigenvalues and eigenvectors

$$\begin{aligned} \lambda_\pm(t) &= \pm\Omega|\boldsymbol{n}(t)|\,, \\ |v_\pm\rangle &= \frac{1}{\sqrt{(n_z\pm|\boldsymbol{n}|)^2+n_x^2+n_y^2}}\left[(n_z\pm|\boldsymbol{n}|)\,|0\rangle + (n_x+\mathrm{i}n_y)\,|1\rangle\right]. \end{aligned} \tag{3.56}$$

Without loss of generality we can consider the simplified case

$$n_x(t) = 1-\frac{t}{T}\,, \qquad n_y(t) = 0\,, \qquad n_z(t) = +\frac{t}{T}\,, \tag{3.57}$$

which is a quench from the initial Hamiltonian $H_I = \Omega\sigma^x$ to the final Hamiltonian $H_F = \Omega\sigma^z$. We can prepare the system in the ground state $\Psi(0) = |v_-(0)\rangle$, where we have $H_I\,|v_-(0)\rangle = -\Omega\,|v_-(0)\rangle$, and then solve the time-dependent Schrödinger equation for $0 \leq t \leq T$ numerically. For an infinitely slow evolution, the system will remain in the instantaneous eigenstate and we will thus prepare the ground state of the final Hamiltonian $H_F\,|v_-(T)\rangle = -\Omega\,|v_-(0)\rangle$, i.e., $a_-(0) = 1$ and

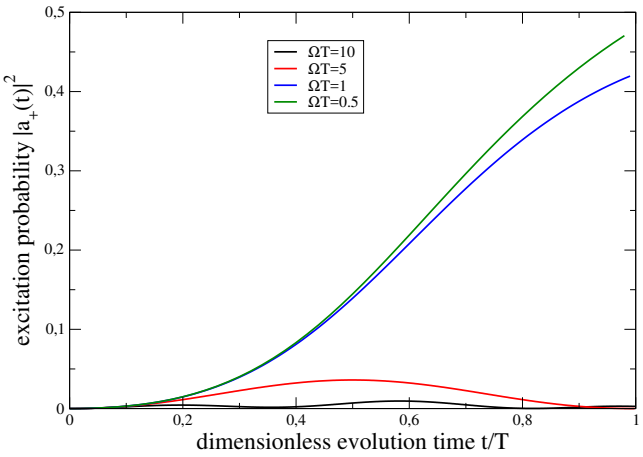

Figure 3.1: Plot of the excitation probability during a non-adiabatic transition for different total driving times T. For slow drivings, the system remains in its energy eigenstate throughout, but for very fast drivings, the transfer probability reaches 1/2.

$a_+(0) = 0$. For fast driving, a part of the amplitude will be transferred to the excited state, and the excitation probability after the quench is given by

$$P_{\text{ex}} = |\langle v_+(T)|\Psi(t)\rangle|^2 = |a_+(T)|^2 \,. \tag{3.58}$$

In the numerical solution we see that for very fast drivings (small T) one half of the probability of the incoming level is transferred to the other level, see Fig. 3.1. The fact that it is precisely 1/2 depends on the overlap between the eigenvectors of the initial Hamiltonian and those of the final Hamiltonian. This will differ from problem to problem.

3.3 Periodic Linear ODEs

We consider the problem of a first order ODE with time-dependent – periodically modulated – coefficients

$$\dot{\boldsymbol{x}} = A(t)\boldsymbol{x} \,, \qquad A(t+T) = A(t) \,. \tag{3.59}$$

Here, $T = 2\pi/\Omega$ denotes the period of the driving. A **fundamental matrix** $\Phi(t)$ of such homogeneous systems can be used to define the evolution depending on the initial condition, i.e., $\boldsymbol{x}(t) = \Phi(t)\boldsymbol{x}_0$, where we normalize the fundamental matrix $\Phi(0) = \mathbf{1}$. In essence, the fundamental matrix holds the linearly independent solutions to the homogeneous problem. In many physics applications, the fundamental matrix is just the time evolution operator. In particular, for periodic systems every **fundamental matrix** of this equation can be written as a product of a periodic matrix and the matrix exponential of a constant matrix, which is the theorem of Floquet [9].

Box 16 (Floquet theorem) *The fundamental matrix of the homogeneous equation $\dot{\boldsymbol{x}} = A(t)\boldsymbol{x}$ with time-periodic coefficients $A(t+T) = A(t)$ can be written as*

$$\Phi(t) = G(t)e^{+Rt} \,, \tag{3.60}$$

with a periodic matrix function $G(t+T) = G(t)$ and a constant matrix R. In particular, for a normalized fundamental matrix $\Phi(0) = \mathbf{1}$, the matrix e^{RT} is called monodromy matrix.

[9] Achille Marie Gaston Floquet (1847–1920) was a french mathematician with contributions to ODEs, astronomy, and mathematics.

In physics of closed quantum systems, the ODE is given by the driven time-dependent Schrödinger equation, where $A(t) \to -\mathrm{i}H(t)$

$$\left|\dot{\Psi}\right\rangle = -\mathrm{i}H(t)\left|\Psi(t)\right\rangle\,, \tag{3.61}$$

and the fundamental matrix becomes the corresponding time evolution operator

$$\Phi(t) \to U(t) = \hat{\tau}\exp\left\{-\mathrm{i}\int_0^t H(t')dt'\right\}\,. \tag{3.62}$$

The Floquet theorem tells us that there is a decomposition of the form

$$U(t) = U_{\mathrm{kick}}(t)e^{-\mathrm{i}\bar{H}t}\,, \qquad U_{\mathrm{kick}}(t+T) = U_{\mathrm{kick}}(t)\,, \tag{3.63}$$

where $\bar{H} = \mathrm{i}R$ is called the Floquet Hamiltonian, and $G(t) \to U_{\mathrm{kick}}(t)$ is in this context called kick operator (which is unitary as well).

Unfortunately, Floquet's theorem does not tell us how to get the fundamental matrix, it just states that the above decomposition exists. Furthermore, the matrices in the decomposition are of course not independent: Once we have the decomposition of the fundamental matrix, we can use the transformation $\boldsymbol{x} = G(t)\boldsymbol{y}$, which implies that $\boldsymbol{y}(t) = e^{Rt}\boldsymbol{x}_0$. Using this in the periodically driven ODE we find

$$\dot{\boldsymbol{y}} = G^{-1}(t)\left[A(t)G(t) - \dot{G}(t)\right]\boldsymbol{y}(t) \stackrel{!}{=} R\boldsymbol{y}\,, \tag{3.64}$$

which in quantum mechanics relates the Floquet Hamiltonian with the kick operator

$$\bar{H} = U_{\mathrm{kick}}^{\dagger}(t)\left[H(t)U_{\mathrm{kick}}(t) - \mathrm{i}\dot{U}_{\mathrm{kick}}(t)\right]\,. \tag{3.65}$$

The other way round, when we find a transformation that maps our periodically driven problem into a time-independent one, we have found the Floquet Hamiltonian, and the transformation defines the kick operator.

As an example, we consider the driven quantum harmonic oscillator, i.e., the Schrödinger equation with a driven Hamiltonian of the form

$$H(t) = \omega a^{\dagger}a + \frac{P}{2}e^{+\mathrm{i}\Omega t}a + \frac{P^*}{2}e^{-\mathrm{i}\Omega t}a^{\dagger}\,, \tag{3.66}$$

which could model a laser-driven cavity mode. We first transform the time-dependent Schrödinger equation $\left|\dot{\Psi}\right\rangle = -\mathrm{i}H(t)\left|\Psi\right\rangle$ into a time-independent frame via the transformation $\left|\Psi(t)\right\rangle = e^{-\mathrm{i}\Omega a^{\dagger}at}\left|\tilde{\Psi}(t)\right\rangle$, which obeys

$$\left|\dot{\tilde{\Psi}}\right\rangle = -\mathrm{i}\left[(\omega-\Omega)a^{\dagger}a + \frac{P}{2}a + \frac{P^*}{2}a^{\dagger}\right]\left|\tilde{\Psi}\right\rangle\,. \tag{3.67}$$

Here, we have used the identity

$$e^{+\mathrm{i}\Omega a^{\dagger}at}ae^{-\mathrm{i}\Omega a^{\dagger}at} = ae^{-\mathrm{i}\Omega t} \tag{3.68}$$

and similar for the hermitian conjugate operator. In this rotating frame, the Hamiltonian becomes time-independent, we can readily write down the solution, and the time-evolution operator in the original frame therefore becomes

$$U(t,0) = e^{-\mathrm{i}\Omega a^\dagger a t} \exp\left\{-\mathrm{i}\left[(\omega-\Omega)a^\dagger a + \frac{P}{2}a + \frac{P^*}{2}a^\dagger\right]t\right\} . \tag{3.69}$$

To stress the difference of Floquet Hamiltonian averages in contrast to the conventional average, we note the simple-averaged Hamiltonian $\frac{1}{T}\int_0 TH(t)dt = \omega a^\dagger a$. We also note that to determine the Floquet Hamiltonian from the time evolution over one period $e^{-\mathrm{i}\bar{H}T} = U(T,0)$, it is not allowed to simply perform a derivative, as $\bar{H} \neq \mathrm{i}\,\frac{d}{dT}U(T,0)\big|_{T=0}$. The reason is that the relation is defined stroboscopically, which conflicts with the derivative – otherwise we would always have $\bar{H} = H(0)$. We can nevertheless compute the Floquet Hamiltonian using that $e^{-\mathrm{i}\Omega a^\dagger a T} = e^{-\mathrm{i}2\pi a^\dagger a} = \mathbf{1}$, which can be seen by evaluating its matrix elements in Fock space. From Eq. (3.69), the time-averaged Floquet Hamiltonian then becomes

$$\bar{H} = (\omega-\Omega)\,a^\dagger a + \frac{P}{2}a + \frac{P^*}{2}a^\dagger = (\omega-\Omega)\left[a^\dagger + \frac{P}{2(\omega-\Omega)}\right]\left[a + \frac{P^*}{2(\omega-\Omega)}\right] - \frac{|P|^2}{4(\omega-\Omega)^2} , \tag{3.70}$$

from which we see that first, the Floquet average Hamiltonian is different from the conventional average Hamiltonian, and second, that its Bohr frequencies are integer multiples of $(\omega-\Omega)$.

Similarly, we see that the kick operator becomes in this case

$$G(t) = e^{-\mathrm{i}\Omega a^\dagger a t} = G\left(t + \frac{2\pi}{\Omega}\right) . \tag{3.71}$$

To show that the operator is periodic, we can consider any basis, as e.g. the Fock basis where $a^\dagger a\,|n\rangle = n\,|n\rangle$. Then, the matrix elements become

$$G_{nm}(t+T) = \langle n|\,G(t+T)\,|m\rangle = e^{-\mathrm{i}\Omega n t}e^{-\mathrm{i}n2\pi}\delta_{nm} = e^{-\mathrm{i}\Omega n t}\delta_{nm} = G_{nm}(t) , \tag{3.72}$$

such that their periodicity becomes manifest. This has to hold in any basis, such that the kick operator must be periodic.

We can furthermore directly confirm the relation between kick operator and Floquet Hamiltonian

$$\bar{H} = G^{-1}(t)H(t)G(t) - \mathrm{i}G^{-1}(t)\dot{G}(t) . \tag{3.73}$$

3.4 Nonlinear ODEs

In essence, nonlinear ODEs can only be solved in special cases, e.g. if certain symmetries are present.

3.4.1 Separable nonlinear ODEs

A special case appears when one only has a single first order nonlinear ODE that is separable, i.e., of the form

$$\dot{x} = \frac{dx}{dt} = f(x)g(t) , \tag{3.74}$$

where $f(x)$ is a function of x and $g(t)$ a function of time. Separating the differentials in the derivative yields

$$\frac{dx}{f(x)} = g(t)dt\,, \tag{3.75}$$

such that integrating the r.h.s. from t_0 to t yields with the substitution $x(t)$ the relation

$$\int_{x_0}^{x(t)} \frac{dx}{f(x)} = \int_{t_0}^{t} g(t)dt\,. \tag{3.76}$$

In population dynamics, for example, one models the growth in worlds with limited resources (e.g. nutrients, space) by the logistic growth equation

$$\frac{dN}{dt} = \alpha N(t)\left[1 - \frac{N(t)}{C}\right]\,, \tag{3.77}$$

where α is the initial growth rate and C denotes a carrying capacity.

3.4.2 Fixed-Point Analysis

When it is not possible to solve a nonlinear ODE exactly – which is the general case – some insight can still be gained when the ODE admits for the calculation of stationary states (which unfortunately is not always possible). So let there be in the ODE system without explicit time-dependence a stationary point $\bar{x}$

$$\dot{x}_i = f_i(x_1, \ldots, x_n)\,, \qquad \text{where} \qquad f_i(\bar{x}_1, \ldots, \bar{x}_n) = 0\,. \tag{3.78}$$

Then, we can learn about the dynamics around this stationary point by expanding linearly around that stationary point

$$x_i(t) = \bar{x}_i + y_i(t) + \mathcal{O}\{y_i^2(t)\}\,, \tag{3.79}$$

which yields

$$\dot{y}_i = \sum_j \frac{\partial f_i}{\partial x_j} y_j\,, \tag{3.80}$$

which constitutes a simple linear system

$$\dot{\boldsymbol{y}} = A\boldsymbol{y}\,, \qquad A = \left(\begin{array}{ccc} \frac{\partial f_1}{\partial x_1} & \cdots & \frac{\partial f_1}{\partial x_n} \\ \vdots & \ddots & \vdots \\ \frac{\partial f_n}{\partial x_1} & \cdots & \frac{\partial f_n}{\partial x_n} \end{array}\right)_{\boldsymbol{x}=\bar{\boldsymbol{x}}} \tag{3.81}$$

that has the simple solution $\boldsymbol{y}(t) = e^{At}\boldsymbol{y}_0$. Consequently, the eigenvalues of the matrix A can tell a lot about the behaviour of the solution. One can use these to classify the character of the fixed point, for example:

- When the real part of all eigenvalues is negative, the fixed point is called **attractive** or **stable**. Then, all solutions starting in the region where the linearization is valid (i.e., close to the fixed point) will decay towards the fixed point.

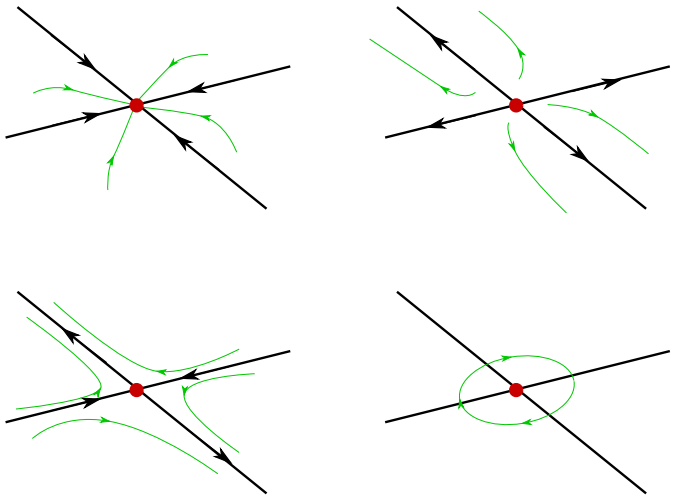

Figure 3.2: Sketch of different fixed points (red) in two dimensions. Solid straight lines represent the eigenvectors of the linearized systems, thin green curves represent sample trajectory solutions. A stable fixed point (top left) will attract all trajectories, whereas a repulsive one (top right) will repel them. When we have both positive and negative real parts in the eigenvalues (bottom left), the solution will be attracted in one direction and repelled in the other, whereas for vanishing real parts, we will have a periodic solution (bottom right).

- When the real part of all eigenvalues is positive, the fixed point is **repulsive**. In this case, all solutions that are initially close to the fixed point will eventually leave the linearization region. Very often however, when only one eigenvalue has a positive real part, whereas the others have a negative real part, the evolution will be repulsive in certain directions and attractive in others. Such a fixed point is also **unstable**.

- When the real part of all eigenvalues vanishes, the solution will oscillate in closed orbits around the fixed point. Therefore, the fixed point is then called **elliptic** or **neutrally stable**.

Fig. 3.2 provides a sketch of the situation in two dimensions. A very nice introduction into this research field can be found in the book by Strogatz [3].

Example: Lotka-Volterra model

We illustrate this classification with a simple example for a Lotka[10] -Volterra[11] model

$$\frac{dN}{dt} = N(a - bP)\,, \qquad \frac{dP}{dt} = P(cN - d)\,, \tag{3.82}$$

N and P denote populations of prey and predators, respectively. The positive constants can be interpreted as proliferation capability of prey (a), the impact of the predators on the prey population (b), the ability of predators to proliferate in presence of prey (c), and the death of predators in absence of prey (d). It is straightforward to identify the fixed points

$$\begin{aligned} \bar{N}_1 &= 0\,, \qquad \bar{P}_1 = 0\,, \\ \bar{N}_2 &= d/c\,, \qquad \bar{P}_2 = a/b\,, \end{aligned} \tag{3.83}$$

and the linearization $N = \bar{N}_i + n_i$ and $P = \bar{P}_i + p_i$ yields the linear systems

$$\frac{d}{dt}\begin{pmatrix} n_1 \\ p_1 \end{pmatrix} = \begin{pmatrix} +a & 0 \\ 0 & -d \end{pmatrix}\begin{pmatrix} n_1 \\ p_1 \end{pmatrix}, \qquad \frac{d}{dt}\begin{pmatrix} n_2 \\ p_2 \end{pmatrix} = \begin{pmatrix} 0 & -db/c \\ +ac/b & 0 \end{pmatrix}\begin{pmatrix} n_2 \\ p_2 \end{pmatrix}, \tag{3.84}$$

[10] Alfred James Lotka (1880–1949) was an austrian-american chemist.
[11] Vito Volterra (1860–1940) was an italian mathematician and physicist with contributions to integral equations.

and we see that the first fixed point is actually a saddle point, since in one direction (prey) it predicts unbounded growth and in the other direction (predators) exponential dampening. The eigenvalues for the second fixed point have only imaginary parts, such that it is classified as elliptic.

Since the model is particularly simple, we can obtain the trajectories exactly.

Example: Kepler model

Fixed point analysis can also be applied to the Kepler[12] problem of a point particle in a radially symmetric potential. Adjusting the coordinate system such that the dynamics only occurs in the $x-y$-plane, the equations of motions read

$$m\ddot{x} + \frac{\partial V(r)}{\partial x} = 0\,, \qquad m\ddot{y} + \frac{\partial V(r)}{\partial y} = 0\,, \tag{3.85}$$

and we could directly map it to a system of first-order differential equations with four variables. However, exploiting the radial symmetry of the potential it is favorable to use polar coordinates

$$x = r\cos(\phi)\,, \qquad y = r\sin(\phi)\,. \tag{3.86}$$

We can now express $\ddot{x}$ and $\ddot{y}$ in terms of derivatives of r and ϕ with respect to time, which yields the equations

$$0 = \ddot{r}\cos(\phi) - 2\dot{r}\dot{\phi}\sin(\phi) - r\ddot{\phi}\sin(\phi) - r\dot{\phi}^2\cos(\phi) + \frac{V'(r)}{m}\cos(\phi)\,, \tag{3.87}$$

$$0 = \ddot{r}\sin(\phi) + 2\dot{r}\dot{\phi}\cos(\phi) + r\ddot{\phi}\cos(\phi) - r\dot{\phi}^2\sin(\phi) + \frac{V'(r)}{m}\sin(\phi)\,. \tag{3.88}$$

At first glance, this does not seem a great improvement over the initial equations, but it is easy to see that by cleverly combining the above equations, the situation can be greatly simplified. The combination $\cos(\phi)(3.87) + \sin(\phi)(3.88)$ yields

$$\ddot{r} - r\dot{\phi}^2 + \frac{V'(r)}{m} = 0\,, \tag{3.89}$$

and when combining $\sin(\phi)(3.87) - \cos(\phi)(3.88)$ we obtain

$$-2\dot{r}\dot{\phi} - r\ddot{\phi} = -\frac{1}{r}\frac{d}{dt}\left(r^2\dot{\phi}\right) = 0\,, \tag{3.90}$$

which implies existence of the conserved quantity

$$r^2\dot{\phi} = C_0 = \text{const}\,, \tag{3.91}$$

which is just related to the conservation of angular momentum. Therefore, we can reduce the system to a single differential equation of second order for r

$$\ddot{r} - \frac{1}{r^3}\left(r^2\dot{\phi}\right)^2 + \frac{V'(r)}{m} = \ddot{r} - \frac{C_0^2}{r^3} + \frac{V'(r)}{m} = \ddot{r} + \frac{V'_{\text{eff}}(r)}{m} = 0\,, \tag{3.92}$$

[12] Johannes Kepler (1571–1630) was a german astronomer, philosopher, and theologist. He is best known for the Kepler laws describing the planetary motion.

where we have introduced the effective potential

$$V_{\text{eff}}(r) = V(r) + \frac{mC_0^2}{2r^2}\,. \tag{3.93}$$

Not knowing anything about theoretical mechanics, we would map this to two coupled first order ODEs via $y_1 = r$ and $y_2 = \dot{r}$

$$\dot{y}_1 = y_2\,, \qquad \dot{y}_2 = -\frac{1}{m}\frac{\partial V_{\text{eff}}(y_1)}{\partial y_1}\,, \tag{3.94}$$

and it is immediately obvious that at a fixed point, $y_2 = \dot{r} = 0$ and also the derivative of the effective potential should vanish $V'_{\text{eff}}(r) = 0$. When we insert the gravitational potential $V(r) = -\frac{\gamma}{r}$, we get

$$V_{\text{eff}}(y_1) = -\frac{\gamma}{y_1} + \frac{mC_0^2}{2y_1^2}\,, \tag{3.95}$$

which can be solved for its minimum

$$V_{\text{eff}}(\bar{y}_1) = 0\,, \qquad \bar{y}_1 = \frac{mC_0^2}{\gamma}\,, \tag{3.96}$$

such that we have a fixed point at $\bar{y}_1 = \frac{mC_0^2}{\gamma}$ and $\bar{y}_2 = 0$, which describes an orbit with a positive radius. Linearizing around this fixed point $y_i = \bar{y}_i + \tilde{y}_i$ we obtain the system

$$\frac{d}{dt}\begin{pmatrix} \tilde{y}_1 \\ \tilde{y}_2 \end{pmatrix} = \begin{pmatrix} 0 & 1 \\ -\frac{\gamma^4}{m^4 C_0^6} & 0 \end{pmatrix}\begin{pmatrix} \tilde{y}_1 \\ \tilde{y}_2 \end{pmatrix}\,. \tag{3.97}$$

The eigenvalues of this matrix now tell us with $\gamma^4/(m^4C_0^6) > 0$ that the fixed point is an elliptic one. This implies that e.g. the distance between earth and sun will not approach a stationary value but rather hover around a mean, which characterizes the elliptical orbit.

Furthermore, we note that the radial equation can be converted into a first order equation by taking energy conservation into account

$$m\ddot{r} + V'_{\text{eff}}(t) = \frac{1}{\dot{r}}\frac{d}{dt}\left[\frac{1}{2}m\dot{r}^2 + V_{\text{eff}}(r)\right] = 0\,, \tag{3.98}$$

which enables one to obtain a separable equation for $\dot{r}$. This approach however is rather sophisticated, such that commonly one aims for obtaining an equation for $dr/d\phi$ instead.

Example: Reservoir Relaxation Model (not treated in lecture)

As our last example for nonlinear differential equations, we consider a nonlinear relaxation model describing the evolution of temperature and chemical potential of an always-thermalized finite electronic reservoir. The idea is that the electronic reservoir is coupled to a small system (that itself may be coupled to further reservoirs), through which it experiences a flux of charge I_M and energy I_E. The total electron number and energy in the reservoir are represented as

$$N = \int \mathcal{D}(\omega) f(\omega) d\omega\,, \qquad E = \int \mathcal{D}(\omega)\omega f(\omega) d\omega\,, \tag{3.99}$$

where temperature $T = 1/\beta$ and chemical potential μ enter implicitly in the Fermi [13] function

$$f(\omega) = \frac{1}{e^{\beta(\omega-\mu)}+1}\,. \tag{3.100}$$

Total conservation of charge and energy implies that given charge and energy currents into the reservoir

$$\dot{N} = J_M = \frac{\partial N}{\partial \mu}\dot{\mu} + \frac{\partial N}{\partial \beta}\frac{d\beta}{dT}\dot{T}\,, \qquad \dot{E} = J_E = \frac{\partial E}{\partial \mu}\dot{\mu} + \frac{\partial E}{\partial \beta}\frac{d\beta}{dT}\dot{T} \tag{3.101}$$

one can calculate the change of reservoir charge and energy. Here however, we will be interested in the change of reservoir temperature and chemical potential, for which we can obtain a differential equation by solving the above equations for $\dot{\mu}$ and $\dot{T}$. This requires us to solve for the coefficients first

$$\begin{aligned}
\frac{\partial N}{\partial \mu} &= \int \mathcal{D}(\omega) f(\omega)[1-f(\omega)] d\omega \beta = \mathcal{I}_1 \beta\,, \\
\frac{\partial N}{\partial \beta} &= -\int \mathcal{D}(\omega) f(\omega)[1-f(\omega)](\omega-\mu) d\omega = -\mathcal{I}_2\,, \\
\frac{\partial E}{\partial \mu} &= \int \mathcal{D}(\omega)\omega f(\omega)[1-f(\omega)] d\omega \beta = (\mathcal{I}_2 + \mu\mathcal{I}_1)\beta\,, \\
\frac{\partial E}{\partial \beta} &= -\int \mathcal{D}(\omega)\omega f(\omega)[1-f(\omega)](\omega-\mu) d\omega = -\mathcal{I}_3 - \mu\mathcal{I}_2\,.
\end{aligned} \tag{3.102}$$

Here, we have defined three integrals

$$\begin{aligned}
\mathcal{I}_1 &= \int \mathcal{D}(\omega) f(\omega)[1-f(\omega)] d\omega\,, \qquad \mathcal{I}_2 = \int \mathcal{D}(\omega)(\omega-\mu) f(\omega)[1-f(\omega)] d\omega\,, \\
\mathcal{I}_3 &= \int \mathcal{D}(\omega)(\omega-\mu)^2 f(\omega)[1-f(\omega)] d\omega\,,
\end{aligned} \tag{3.103}$$

which in the wide-band limit $\mathcal{D}(\omega) = D$ can be solved exactly

$$\mathcal{I}_1 = \frac{D}{\beta} = DT\,, \qquad \mathcal{I}_2 = 0\,, \qquad \mathcal{I}_3 = \frac{\pi^2}{3}\frac{D}{\beta^3} = \frac{\pi^2}{3}DT^3\,. \tag{3.104}$$

From these, we obtain a simple relation between currents and thermodynamic parameters

$$\begin{pmatrix} J_M \\ J_E \end{pmatrix} = D \begin{pmatrix} 1 & 0 \\ \mu & \frac{\pi^2}{3}T \end{pmatrix} \begin{pmatrix} \dot{\mu} \\ \dot{T} \end{pmatrix}\,. \tag{3.105}$$

We can directly invert the matrix containing the heat and charge capacities to solve for the first derivatives

$$\begin{pmatrix} \dot{\mu} \\ \dot{T} \end{pmatrix} = \frac{1}{D} \begin{pmatrix} 1 & 0 \\ -\frac{3}{\pi^2}\frac{\mu}{T} & \frac{3}{\pi^2}\frac{1}{T} \end{pmatrix} \begin{pmatrix} J_M \\ J_E \end{pmatrix}\,. \tag{3.106}$$

Although we have represented this using a matrix, we stress that the resulting ODE is highly nonlinear, since the currents may themselves depend in a highly nonlinear fashion on the reservoir temperature. When we have now two reservoirs (labeled L and R) that are connected by some

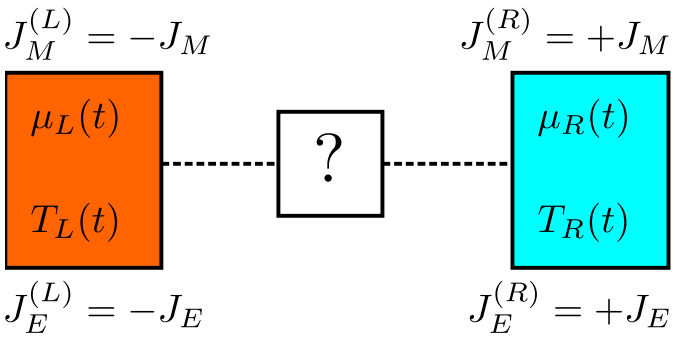

Figure 3.3: Sketch of two reservoirs (boxes left and right) coupled (dashed lines) via an unspecified quantum system (middle). Since particle and energy currents are assumed as conserved, the four thermodynamic variables $\mu_{L/R}(t)$ and $T_{L/R}(t)$ can be reduced to two, e.g. only the difference in chemical potentials and the difference in temperatures.

structure, all parameters become reservoir-specific, see Fig. 3.3. However, any reasonable two-terminal setup should realistically obey particle conservation $J_M^R = -J_M^L = J_M$ and also energy conservation $J_E^R = -J_E^L = J_E$. The two currents will depend on all thermodynamic variables, resulting in

$$\begin{aligned}
\dot{\mu}_L &= -\frac{1}{D_L} J_M(\mu_L, \mu_R, T_L, T_R)\,, \qquad \dot{\mu}_R = +\frac{1}{D_R} J_M(\mu_L, \mu_R, T_L, T_R)\,, \\
\dot{T}_L &= +\frac{1}{D_L}\frac{3}{\pi^2}\frac{\mu_L(t)}{T_L(t)} J_M(\mu_L, \mu_R, T_L, T_R) - \frac{1}{D_L}\frac{3}{\pi^2}\frac{1}{T_L(t)} J_E(\mu_L, \mu_R, T_L, T_R)\,, \\
\dot{T}_R &= -\frac{1}{D_R}\frac{3}{\pi^2}\frac{\mu_R(t)}{T_R(t)} J_M(\mu_L, \mu_R, T_L, T_R) + \frac{1}{D_R}\frac{3}{\pi^2}\frac{1}{T_R(t)} J_E(\mu_L, \mu_R, T_L, T_R)\,.
\end{aligned} \tag{3.107}$$

As an aside, we note that these equations can be further reduced. For example, from the conservation of total particle number $\dot{N}_L + \dot{N}_R = 0 = D_L\dot{\mu}_L + D_R\dot{\mu}_R$ we obtain that e.g. the weighted average of the chemical potentials

$$\frac{D_L}{D_L + D_R}\mu_L(t) + \frac{D_R}{D_L + D_R}\mu_R(t) = \bar{\mu} = \text{const} \tag{3.108}$$

is a constant of motion – where D_α denotes the charge capacity of reservoir α. This equation can be used to represent the chemical potentials $\mu_L(t)$ and $\mu_R(t)$ using only the bias voltage $V(t) = \mu_L(t) - \mu_R(t)$. From the conservation of energy we obtain that

$$\begin{aligned}
E &= \frac{D_L}{2}\mu_L^2(t) + \frac{D_R}{2}\mu_R^2(t) + \frac{\pi^2}{3}\frac{D_L}{2}T_L^2(t) + \frac{\pi^2}{3}\frac{D_R}{2}T_R^2(t) = \text{const} \\
&= \frac{D_L + D_R}{2}\bar{\mu}^2 + \frac{1}{2}\frac{D_L D_R}{D_L + D_R}V^2(t) + \frac{\pi^2}{6}\left[D_L T_L^2(t) + D_R T_R^2(t)\right]
\end{aligned} \tag{3.109}$$

is also a constant of motion.

However, we consider only a simplified limit by setting the capacity of one reservoir to infinity $D_L \to \infty$, such that automatically $\dot{T}_L \to 0$ and $\dot{\mu}_L \to 0$, leaving $\mu_L = \mu$ and $T_L = T$ at their initial values. One is left with just two equations for the evolution of μ_R and T_R. To obtain these, we have to specify the dependence of the currents on the thermal parameters, where a useful example is the single-electron transistor that has been treated previously. Here, we have two reservoirs with

[13] Enrico Fermi (1901 – 1954) was an italian physicist known for many contributions to statistical mechanics, quantum theory and nuclear theory. He also supervised the construction of the worlds first nuclear reactor.

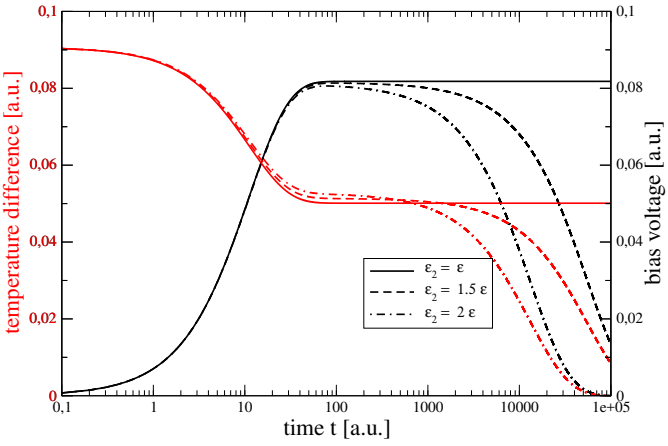

Figure 3.4: Temporal evolution of the bias voltage $V(t)$ (black) and the temperature difference $T_L - T_R$ (red) for different ratios of channel energies $\epsilon_2 = \alpha\epsilon = \epsilon_1$ (solid, dashed, and dash-dotted, respectively). After an initial evolution phase the system reaches a pseudo-equilibrium that is persistent only for $\epsilon_1 = \epsilon_2$ (solid curves). Whenever the channel energies are different, the pseudo-equilibrium eventually relaxes to thermal equilibrium. During the pseudo-equilibrium phase (intermediate plateaus), part of the initial temperature gradient has been converted into a voltage.

temperatures T_L, T_R and chemical potentials μ_L and μ_R, respecively. These are connected via a single quantum dot, through which the current reads

$$J_M = \gamma \left[f_L(\epsilon) - f_R(\epsilon) \right] , \qquad J_E = \epsilon J_M , \tag{3.110}$$

where γ encoded details of the coupling strength to the respective reservoirs into a single factor and where ϵ was the on-site energy of the quantum dot. The so-called tight-coupling property $J_E = \epsilon J_M$ follows from the fact that a single quantum dot only has a single transition frequency ϵ. We see that both currents vanish when $\mu_R = \mu$ and $T_R = T$ as well, since then the Fermi functions agree. Linearizing around this point $\mu_R = \mu + \tilde{\mu}_R$ and $T_R = T + \tilde{T}_R$, we obtain the system

$$\frac{d}{dt} \begin{pmatrix} \tilde{\mu}_R \\ \tilde{T}_R \end{pmatrix} = \gamma \frac{e^{\beta(\epsilon-\mu)}}{e^{\beta(\epsilon-\mu)}+1} \begin{pmatrix} -1 & -\beta(\epsilon-\mu) \\ -\frac{3}{\pi^2}\beta(\epsilon-\mu) & -\frac{3}{\pi^2}\beta^2(\epsilon-\mu)^2 \end{pmatrix} \begin{pmatrix} \tilde{\mu}_R \\ \tilde{T}_R \end{pmatrix} , \tag{3.111}$$

and for the eigenvalues we obtain that one of them is negative whereas the other vanishes, such that the solutions converge toward the fixed point. True stability of the fixed point can be enforced by adding more complicated currents, see below.

More realistically, the system currents will not obey the tight-coupling property, e.g.

$$\begin{aligned} J_M &= \gamma_1 \left[f_L(\epsilon_1) - f_R(\epsilon_1) \right] + \gamma_2 \left[f_L(\epsilon_2) - f_R(\epsilon_2) \right] , \\ J_E &= \epsilon_1\gamma_1 \left[f_L(\epsilon_1) - f_R(\epsilon_1) \right] + \epsilon_2\gamma_2 \left[f_L(\epsilon_2) - f_R(\epsilon_2) \right] , \end{aligned} \tag{3.112}$$

i.e., $J_E \neq \epsilon J_M$ (unless the ϵ_i are equal), which leads to vanishing currents and therefore to fixed points when $\mu_L = \mu_R$ and $T_L = T_R$. By initializing the system e.g. with a temperature gradient in the absence of a charge gradient it is possible to generate (at least temporally) a voltage, i.e., to extract work. The temporal evolution of such a system is depicted in Fig. 3.4. It is visible that in the tight-coupling limit, it is possible to convert e.g. an initial temperature gradient into work (a persistent voltage). However, it should realistically be kept in mind that the tight-coupling property is never exactly fulfilled and relaxation into final equilibrium may thus be expected. Nevertheless, even these more realistic systems show a distinct timescale separation between initial charge separation and discharging of the system.

3.5 Numerical Solution

There are many numerical solution methods for nonlinear ODEs on the market. They can of course also be applied to linear ODEs with time-dependent or constant coefficients. Here, we will just discuss the simplest implementations that are not optimized for a particular problem.

To fix the notation, we will consider systems of first order differential equations (linear or nonlinear with possibly time-dependent coefficients)

$$\dot{\boldsymbol{x}} = \boldsymbol{f}(\boldsymbol{x}(t), t)\,, \tag{3.113}$$

where bold symbols denote vectors – or vector-valued functions, and where $\boldsymbol{f}$ can also explicitly depend on time. In this section, we will for convenience drop the explicit bold notation for vectors. When time is discretized in slices of width Δt, we can also discretize the derivative forward in time

$$t_\ell = \ell \Delta t\,, \qquad x(t_\ell) = x_\ell\,, \qquad \frac{dx}{dt}(t_\ell) = \frac{x_{\ell+1} - x_\ell}{\Delta t}\,. \tag{3.114}$$

Thus, the differential equation can directly be converted into an iterative scheme when the known values x_ℓ and t_ℓ are inserted in the right-hand side

$$x_{\ell+1} = x_\ell + \Delta t f(x_\ell, t_\ell) + \mathcal{O}\{\Delta t^2\}\,. \tag{3.115}$$

This first order forward-time (also called Euler discretization) scheme is however not very accurate and may behave quite unstable, unless the discretization width is chosen extremely small (which implies a large numerical effort). It should not be recommended. In principle one is free to insert values from the future in the right-hand side, too. If the function f permits, one might solve the resulting equation

$$x_{\ell+1} = x_\ell + \Delta t f(x_{\ell+1}, t_{\ell+1}) \tag{3.116}$$

for $x_{\ell+1}$ and obtain another iterative scheme, provided we can solve the resulting equation for $x_{\ell+1}$ either directly or via some numerical algorithm. Such schemes are called implicit ones. Finally, we remark that it is easily possible to mix forward and backward time discretizations, which will become relevant for the numerical solution of partial differential equations.

We will illustrate this issue with the simple differential equation for exponential decay $\dot{x} = -\alpha x(t)$ with $\alpha > 0$. The simple forward-time Euler discretization yields

$$x_{\ell+1} = (1 - \alpha \Delta t)\, x_\ell\,. \tag{3.117}$$

When now the timestep is chosen too large such that $\alpha \Delta t \geq 2$ one can easily see that instead of approaching the value zero – as the exact solution $x(t) = e^{-\alpha t} x_0$ would suggest – the solution explodes as $|x_{\ell+1}| = |1 - \alpha \Delta t||x_\ell|$. A smaller timestep would not exhibit this behaviour.

Alternatively, we could use an implicit scheme by evaluating the right-hand side of the differential equation in the future $x_{\ell+1} - x_\ell = -\alpha \Delta t x_{\ell+1}$, which for this simple equation can be solved for

$$x_{\ell+1} = \frac{1}{1 + \alpha \Delta t} x_\ell\,. \tag{3.118}$$

We note that the solution will not explode for large $\alpha \Delta t$, such that regarding stability, an implicit scheme is favorable.

Finally, the right-hand side can also be evaluated symmetrically $x_{\ell+1} - x_\ell = -\alpha \Delta t (x_{\ell+1} + x_\ell)/2$, which yields

$$x_{\ell+1} = \frac{2 - \alpha \Delta t}{2 + \alpha \Delta t} x_\ell \tag{3.119}$$

and thus also predicts stable behaviour.

3.5.1 Runge-Kutta algorithm

When it is not possible to invert the function f, we will use a forward-time discretization scheme. We see that by simply computing the derivative at an intermediate point between x_ℓ and $x_{\ell+1}$, we can increase the order of the scheme

$$k_1 = \Delta t f(x_\ell, t_\ell)\,, \qquad k_2 = \Delta t f(x_\ell + \frac{1}{2}k_1, t_\ell + \frac{1}{2}\Delta t)\,, \qquad x_{\ell+1} = x_\ell + k_2 + \mathcal{O}\{\Delta t^3\}\,. \quad (3.120)$$

The above scheme is called second order Runge[14] -Kutta[15] (or midpoint) method. The fact that it is second order in Δt is visible from the Taylor-expansion

$$\begin{aligned} x_{\ell+1} &= x_\ell + \left.\frac{dx}{dt}\right|_{t=t_\ell} \Delta t + \left.\frac{d^2x}{dt^2}\right|_{t=t_\ell} \frac{\Delta t^2}{2} + \mathcal{O}\{\Delta t^3\} \\ &= x_\ell + f(x_\ell, t_\ell)\Delta t + \left.\frac{\partial f(x,t)}{\partial x}\frac{dx}{dt}\right|_{t=t_\ell} \frac{\Delta t^2}{2} + \left.\frac{\partial f(x,t)}{\partial t}\right|_{t=t_\ell} \frac{\Delta t^2}{2} + \mathcal{O}\{\Delta t^3\}\,, \end{aligned} \quad (3.121)$$

which coincides with what we would obtain by expanding Eq. (3.120) for small Δt. In effect, it uses two function calls – one at the initial time t_ℓ and one at half a time-step $t_\ell + \Delta t/2$ to propagate the solution by one timestep.

The by far most-used algorithm is however a fourth-order Runge-Kutta method

$$\begin{aligned} k_1 &= \Delta t f(x_\ell, t_\ell)\,, \qquad k_2 = \Delta t f(x_\ell + k_1/2, t_\ell + \Delta t/2)\,, \\ k_3 &= \Delta t f(x_\ell + k_2/2, t_\ell + \Delta t/2)\,, \qquad k_4 = \Delta t f(x_\ell + k_3, t_\ell + \Delta t)\,, \\ x_{\ell+1} &= x_\ell + \frac{k_1}{6} + \frac{k_2}{3} + \frac{k_3}{3} + \frac{k_4}{6} + \mathcal{O}\{\Delta t^5\}\,. \end{aligned} \quad (3.122)$$

It uses four function evaluations to propagate the solution by one timestep but has a much larger accuracy. Nevertheless, it should be used in combination with an adaptive timestep.

3.5.2 Leapfrog integration

Many problems of classical mechanics can be cast into the form $\ddot{x} = F(x)/m = f(x)$ or – equivalently – $\dot{x} = v$ and $\dot{v} = f(x)$. The leapfrog scheme works by evolving position and velocity in an alternating fashion – thus leap-frogging over each other

$$x_i = x_{i-1} + v_{i-1/2}\Delta t\,, \qquad v_{i+1/2} = v_{i-1/2} + f(x_i)\Delta t\,. \quad (3.123)$$

Here, x_i is the position at time t_i and $v_{i+1/2}$ is the velocity at time $t_i + \Delta t/2$. It is also possible to apply the scheme with velocities and positions evaluated at the same times

$$x_{i+1} = x_i + v_i\Delta t + \frac{f(x_i)}{2}\Delta t^2\,, \qquad v_{i+1} = v_i + \frac{f(x_i) + f(x_{i+1})}{2}\Delta t\,. \quad (3.124)$$

The Leapfrog integration is a second order method but has the nice property that it is symmetric in time (provided a constant timestep is used). This implies that the initial conditions can be recovered from any evolved state.

[14] Carl David Tolmé Runge (1856–1927) was a german mathematician and physicist.
[15] Martin Wilhelm Kutta (1867–1944) was a german mathematician.

Figure 3.5: Program flow chart of an adaptive stepsize control in explicit integration schemes, such as e.g. fourth order Runge-Kutta. The overhead for stepsize control in a single loop is about 50% of the computational cost. However, since the increase of the timestep also allows one to proceed much faster through regions where $f(x,t)$ is essentially flat, adaptive stepsize control will quite often lead to a reduced overall runtime.

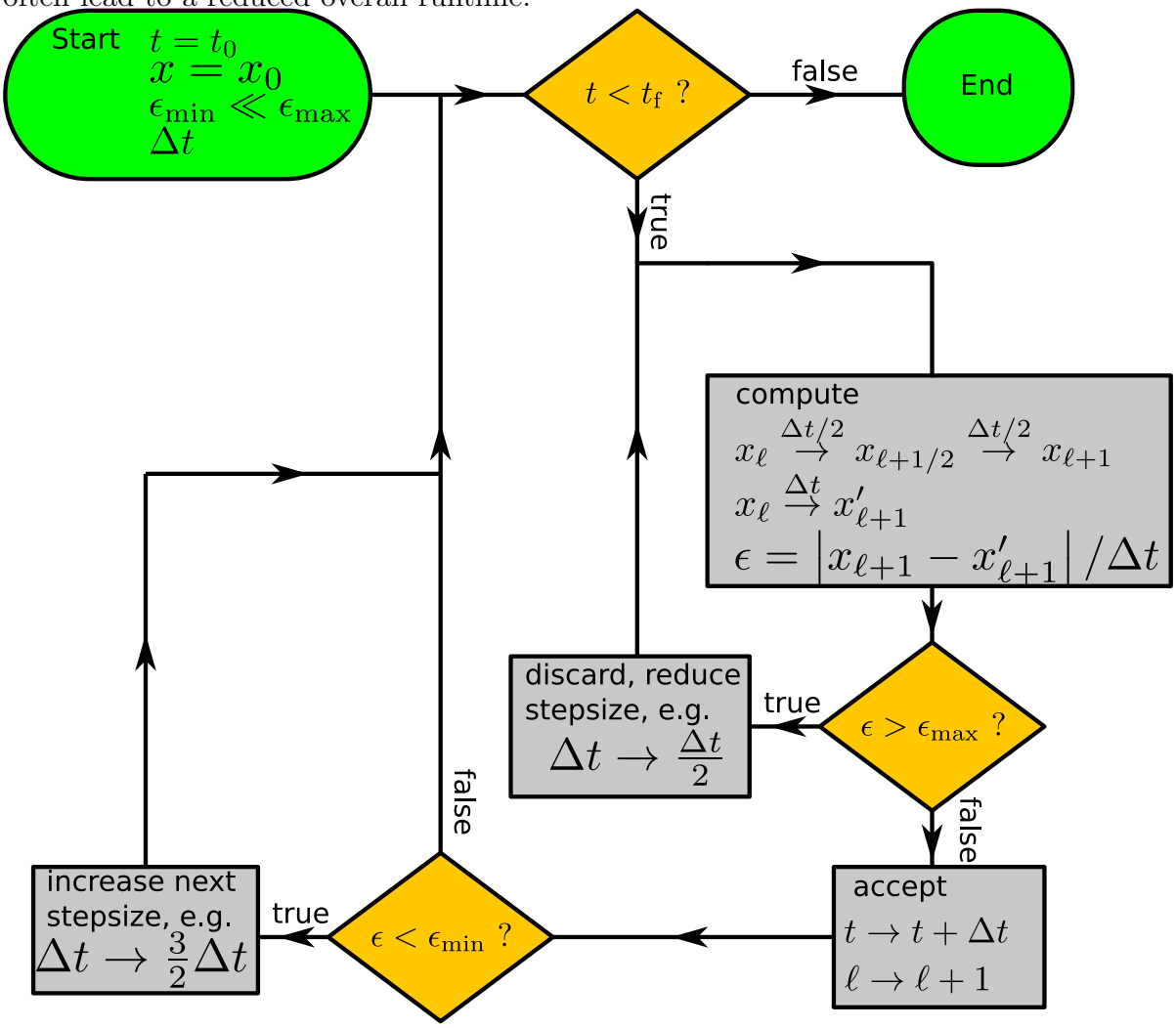

3.5.3 Adaptive stepsize control

To keep a certain promise on the total error, the timestep width in explicit integration schemes can be increased (to proceed faster with less numerical effort) and decreased (to improve accuracy) when applicable. The implementation of an adaptive stepsize requires one to estimate the error for each timestep. Such an estimate can be gained from comparing two small steps of size $\Delta t/2$ and a single large step of size Δt as shown in Fig. 3.5. At first glance, it seems that adaptive stepsize control will triple the computational cost. However, this is not true. Since we keep the solution obtained from the small timesteps $x_{\ell+1}$, the actual discretization width of the algorithm is $\Delta t/2$, and the additional overhead due to the stepsize control is therefore roughly 50% in a single loop. In addition, the possibility to increase the timestep when the error is negligible (which e.g. happens when $f(x,t)$ is flat) mostly leads to a significantly faster solution when stepsize control is applied.

3.6 A note on Large Systems

When the ODE system involves many variables – e.g. in a molecular dynamics simulation of many interacting constituents, stability may become a more and more important issue. For illustration we consider a chain of coupled harmonic oscillators with the equation of motion

$$0 \;=\; m\ddot{z}_i + \frac{\partial}{\partial z_i}\frac{k}{2}(z_i - z_{i-1})^2 + \frac{\partial}{\partial z_i}\frac{k}{2}(z_{i+1} - z_i)^2 = m\ddot{z}_i - k\left(z_{i+1} - 2z_i + z_{i-1}\right) . \quad (3.125)$$

We could now map this to a large system of first order ODEs and try to solve it with some explicit integration scheme. In consequence, timesteps for all oscillators would have to be chosen very small if only a single oscillator was strongly displaced. Thus, it is very likely that such explicit methods are not suitable for large systems. In fact, one can note that the harmonic oscillator chain can also be considered as a differential equation for a function $z(x,t)$ depending on two variables. When we discretize space in intervals Δx, this can be written as

$$0 = \frac{\partial^2 z(x_i,t)}{\partial t^2} - (k\Delta x)\frac{\Delta x}{m}\frac{z(x_{i+1}) - 2z(x_i) + z(x_{i-1})}{\Delta x^2} . \quad (3.126)$$

In the limit $\Delta x \to 0$, $m \to 0$, and $k \to \infty$ such that the average spring constant $k\Delta x$ and the mass density $m/\Delta x$ remain finite implying that $\kappa = k\Delta x^2/m$ remains also finite, this becomes the wave equation

$$0 = \frac{\partial^2 z(x,t)}{\partial t^2} - \kappa\frac{\partial^2 z(x,t)}{\partial x^2} . \quad (3.127)$$

In fact, the wave equation is a simple example for a partial differential equation, where derivatives with respect to more than a single variables occur. This opens a whole class of systems, which we discuss in the next chapter.

Chapter 4

Special Partial Differential Equations

As we have seen before, partial differential equations (PDEs) often arise in the continuum limit from ordinary differential equations. In essence, a partial differential equation can e.g. in two dimensions be defined implicitly by the equation

$$F\left(x, y, g(x,y), \frac{\partial g}{\partial x}, \frac{\partial g}{\partial y}, \frac{\partial^2 g}{\partial x^2}, \dots\right) = 0\,. \tag{4.1}$$

Generally, we can formally write an n-th order PDE this as

$$F\left(\boldsymbol{x}, g(\boldsymbol{x}), Dg(\boldsymbol{x}), D^2 g(\boldsymbol{x}), \dots, D^n g(\boldsymbol{x})\right) = 0\,. \tag{4.2}$$

A partial differential equation should fulfil the following properties

- The sought-after function should depend on at least two variables
- There should be derivatives occuring with respect to all variables
- The equation should only contain derivatives (not integrals) or the function itself.

An important subclass of PDEs are the linear ones of second order, which in case of a function $\phi(x, y)$ we can write as

$$A\frac{\partial^2\phi}{\partial x^2} + B\frac{\partial^2\phi}{\partial x \partial y} + C\frac{\partial^2\phi}{\partial y^2} + D\frac{\partial\phi}{\partial x} + E\frac{\partial\phi}{\partial y} + F\phi(x,y) = G(x,y)\,. \tag{4.3}$$

It is a general feature of a PDE that their solutions may exhibit discontinuities in the function or its derivatives. The surface through which these discontinuities occur are called characteristics of the PDE and depending on the shape of the characteristics one can – depending on the prefactors of the second derivatives – in two-dimensions further classify the PDE:

- When $B^2 - 4AC > 0$, the PDE is called **hyperbolic**. An example for such a PDE is the previously discussed equation that arises in the continuum limit for coupled harmonic oscillators, i.e., the wave equation

  $$\frac{\partial^2\phi}{\partial t^2} - \kappa\frac{\partial^2\phi}{\partial x^2} = 0\,. \tag{4.4}$$

  Here, we obviously have $B^2 - 4AC = 4\kappa > 0$.

- When $B^2 - 4AC = 0$, the PDE is called **parabolic**. An example for such a PDE is the diffusion equation

$$D\frac{\partial^2\phi}{\partial x^2} - \frac{\partial\phi}{\partial t} = 0\,. \tag{4.5}$$

- Finally, when $B^2 - 4AC > 0$, the PDE is called **elliptic**. An example for this is the Poisson equation

$$\frac{\partial^2\phi}{\partial x^2} + \frac{\partial^2\phi}{\partial y^2} = \rho(x,y)\,, \tag{4.6}$$

  where we have $A = C = 1$.

A nice property of PDEs is their uniqueness of solutions. Given that one has found any solution satisfying the PDE and the boundary conditions (treating time and other variables on equal footing, the term boundary conditions may also include the initial condition), then it is the solution. Therefore, any ansatz to find solutions of PDEs is valuable.

4.1 Separation Ansatz

A popular approach to PDE is to reduce their dimension by trying to solve them with a separation ansatz. Here, one assumes that the solution is separable, i.e., that it can be written in a product form. For example, when spatial and temporal contributions separable, the solution could be written as $\Phi(\boldsymbol{x},t) = \phi(\boldsymbol{x})\psi(t)$. One simply inserts this as an ansatz in the PDE and tries to obtain separate differential equations for $\phi(\boldsymbol{x})$ and $\psi(t)$, which due to their reduced dimensionality can be solved much simpler. The general aim is to reduce the PDE to the form

$$F_1(\phi(\boldsymbol{x}), D\phi, D^2\phi, \ldots) = F_2(\psi(t), \dot{\psi}, \ddot{\psi}, \ldots)\,. \tag{4.7}$$

Then, since this relation should hold for all $\boldsymbol{x}$ and t, both sides of the equation should be equal to some constant α. The separate differential equations are then given by

$$\alpha = F_1(\phi(\boldsymbol{x}), D\phi, D^2\phi, \ldots)\,, \qquad \alpha = F_2(\psi(t), \dot{\psi}, \ddot{\psi}, \ldots)\,. \tag{4.8}$$

4.1.1 Diffusion Equation

As an example, we discuss how to reduce the one-dimensional diffusion equation

$$\frac{\partial\rho}{\partial t} = D\frac{\partial^2\rho}{\partial x^2} \tag{4.9}$$

in the domain $x \in \{-L/2, +L/2\}$ with the initial condition $\rho(x,0) = \rho_0(x)$ and von-Neumann[1] boundary conditions

$$\frac{\partial\rho}{\partial x}(-L/2,t) = \frac{\partial\rho}{\partial x}(+L/2,t) = 0 \tag{4.10}$$

[1] John von Neumann (1903 – 1957) was a hungarian mathematician and physicist considered as one of the founding fathers of computing.

using the separation ansatz $\rho(x,t) = X(x)T(t)$. The diffusion equation can then be brought into the form

$$\frac{1}{D}\frac{T'(t)}{T(t)} = \frac{X''(x)}{X(x)} \stackrel{!}{=} -k^2\,, \tag{4.11}$$

and we obtain the two separate equations

$$T'(t) + Dk^2T(t) = 0\,, \qquad X''(x) + k^2X(x) = 0\,. \tag{4.12}$$

These are now ordinary differential equations. The first of these is readily solved by $T(t) = e^{-Dk^2t}$, where we have fixed the constant arising from the initial condition to one. Since $T(t)$ and $X(x)$ enter as a product, we are free to transfer this constant to $X(x)$. The general solution of the second equation is $X(x) = Ae^{+\mathrm{i}kx} + Be^{-\mathrm{i}kx}$, where we have to fix A and B and the unknown k from initial and boundary conditions. The boundary conditions yield two equations

$$\frac{A}{B} = e^{+\mathrm{i}kL}\,, \qquad \frac{A}{B} = e^{-\mathrm{i}kL}\,, \tag{4.13}$$

which can only be satisfied for discrete values of $k \to n\pi/L$. Consequently, we have $B_n = e^{\pm \mathrm{i}n\pi}A_n = (-1)^nA_n$. Therefore, depending on whether n is even or odd, we will have $B = +A$ or $B = -A$, respectively. Since the discreteness of k also maps to the time-dependent part, we first note that the general solution can be written as

$$\begin{aligned}\rho(x,t) &= \sum_n e^{-D(n^2\pi^2/L^2)t}A_n\left[e^{+\mathrm{i}\pi nx/L} + (-1)^n e^{-\mathrm{i}\pi nx/L}\right] \\ &= \sum_n e^{-D(n^2\pi^2/L^2)t}a_n\left[1 + (-1)^n e^{-\mathrm{i}2\pi nx/L}\right] = \sum_n \rho_n(x,t)\,,\end{aligned} \tag{4.14}$$

where n goes in principle over all integers. We note that in the above Fourier-type series, terms with even n will lead to an even contribution of $\rho_n(x,t) = \rho_n(-x,t)$ whereas terms with odd n to odd contributions with $\rho_n(x,t) = -\rho_n(-x,t)$. The above solution is constructed to obey the boundary condition but also has to match the initial condition, e.g.

$$\rho_0(x) = \frac{1}{L} + \frac{1}{L}\cos(2\pi x/L) \stackrel{!}{=} \sum_n A_n\left[e^{+\mathrm{i}\pi nx/L} + (-1)^n e^{-\mathrm{i}\pi nx/L}\right]\,. \tag{4.15}$$

We immediately see that this is an even function of x and can therefore conclude that $A_{2n+1} = 0$. By direct comparison we can directly identify

$$A_0 = 1/(2L)\,, \qquad A_{+2} = 1/(2L)\,, \tag{4.16}$$

whereas all other coefficients must vanish. The full solution is then given by

$$\rho(x,t) = \frac{1}{L} + \frac{1}{L}\cos(2\pi x/L)e^{-D(4\pi^2/L^2)t}\,, \tag{4.17}$$

and it satisfies boundary condition and initial condition (which of course must be chosen compatible with each other), see also Fig. 4.1. We see that the initial unimodal shape quickly decays to the constant value $\frac{1}{L}$.

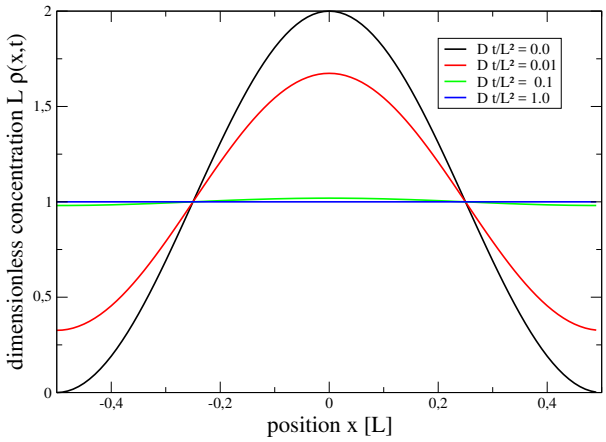

Figure 4.1: Solution of the diffusion equation with (no-flux) von-Neumann boundary conditions. The initial unimodal concentration profile quickly decays into a flat distribution. The area under all curves is the same – implying conservation of total mass.

For general initial conditions we note that by introducing the functions

$$g_n(x) = \frac{e^{+2\pi \mathrm{i} n \frac{x}{L}}}{\sqrt{L}} \tag{4.18}$$

we directly note their orthonormality relation over the interval $[-L/2, +L/2]$

$$\int_{-L/2}^{+L/2} g_n^*(x) g_m(x) dx = \delta_{nm}\,, \tag{4.19}$$

such that we can determine the even Fourier coefficients from general initial conditions as

$$a_n = \frac{1}{L} \int_{-L/2}^{+L/2} \rho_0(x) e^{-\mathrm{i}2\pi n x/L} dx\,. \tag{4.20}$$

Also when we had prescribed not the derivative of the function at the boundaries (to inhibit an unphysical flux out of the considered domain) but the value of the function itself – so called Dirichlet[2] boundary conditions – we would have found a discretizing condition on k.

Now if, alternatively, we wanted to solve the diffusion equation not in a box but in the full space (discarding then the von-Neumann boundary conditions), we would not obtain a discretizing constraint on k. Then, it may assume any continous value, and we can write the solution as

$$\rho(x,t) = \int A(k) e^{+\mathrm{i}kx} e^{-Dk^2 t} dk\,. \tag{4.21}$$

From the initial condition, we can then obtain $A(k)$.

4.1.2 Damped Wave Equation

Things become a bit more complicated when higher derivatives occur, e.g. with respect to time. As an example, we consider the one-dimensional wave equation (4.4) supplemented with a dampening term

$$\frac{\partial^2 z}{\partial t^2} + \gamma \frac{\partial z}{\partial t} - \kappa \frac{\partial^2 z}{\partial x^2} = 0\,. \tag{4.22}$$

[2]Johann Peter Gustav Lejeune Dirichlet (1805 – 1859) was a german mathematician with contributions to number theory and Fourier series.

The function $z(x,t)$ may e.g. describe the transversal displacement of a guitar string, where the dampening γ arises from internal friction and collisions with the air molecules. Consistently with this picture, we assume Dirichlet boundary conditions $z(-L/2,t) = z(+L/2,t) = 0$ at all times and a triangular and stationary displacement initially

$$z(x,0) = a\left\{[1-2x/L]\,\Theta(x) + [1+2x/L]\,\Theta(-x)\right\}\,, \qquad \frac{\partial z}{\partial t}(x,0) = 0\,. \tag{4.23}$$

A separation ansatz $z(x,t) = X(x)T(t)$ yields

$$\frac{T''(t)}{T(t)} + \gamma\frac{T'(t)}{T(t)} = \kappa\frac{X''(x)}{X(x)} \stackrel{!}{=} -\kappa k^2\,. \tag{4.24}$$

Here, we have for convenience multiplied the new parameter k by the coefficient κ, to simplify the resulting separate spatial and temporal equations

$$T''(t) + \gamma T'(t) + \kappa k^2 T(t) = 0\,, \qquad X''(x) + k^2 X(x) = 0\,. \tag{4.25}$$

We first turn our attention to the spatial equation, we have a similiar situation as with the diffusion equation before, i.e., the solution is of the form $X(x) = Ae^{+\mathrm{i}kx} + Be^{-\mathrm{i}kx}$. The Dirichlet boundary conditions now yield

$$\frac{A}{B} = -e^{+\mathrm{i}kL}\,, \qquad \frac{A}{B} = -e^{-\mathrm{i}kL}\,, \tag{4.26}$$

where we have to discretize $k_n = n\pi/L$ with $n = 0,1,2,\ldots$, such that $B = -Ae^{\pm\mathrm{i}n\pi} = (-1)^{n+1}A$.

We can directly solve the temporal equation via $T(t) = t_+e^{\lambda_+ t} + t_-e^{\lambda_- t}$, where

$$\lambda_\pm = -\frac{\gamma}{2} \pm \sqrt{\left(\frac{\gamma}{2}\right)^2 - \kappa k^2} \approx \pm\mathrm{i}k\sqrt{\kappa} - \frac{\gamma}{2} + \mathcal{O}\{\gamma^2\}\,. \tag{4.27}$$

Above, we have expanded the solution for small γ, where the string is still expected to vibrate. As before, we can demand that $T(0) = 1$ to transfer the normalization question to $X(x)$, but due to the initially vanishing transverse string velocity we also have $T'(0) = 0$. This fixes the coefficients

$$\begin{aligned} t_- &= \frac{+\lambda_+}{\lambda_+ - \lambda_-} \approx \frac{1}{2} + \frac{\mathrm{i}\gamma}{4k\sqrt{\kappa}} + \mathcal{O}\{\gamma^2\}\,, \\ t_+ &= \frac{-\lambda_-}{\lambda_+ - \lambda_-} \approx \frac{1}{2} - \frac{\mathrm{i}\gamma}{4k\sqrt{\kappa}} + \mathcal{O}\{\gamma^2\}\,. \end{aligned} \tag{4.28}$$

Since k is dependent on n, all these variables become dependent on n, too, and the temporal solution can be written as

$$T_n(t) = t_+^{(n)}e^{\lambda_+^{(n)}t} + t_-^{(n)}e^{\lambda_-^{(n)}t} \approx e^{-\gamma t/2}\cos(k_n\sqrt{\kappa}t) + \frac{\gamma}{2k_n\sqrt{\kappa}}e^{-\gamma t/2}\sin(k_n\sqrt{\kappa}t)\,, \tag{4.29}$$

which obeys $T_n(0) = 1$ and $T_n'(0) = 0$. The general solution becomes

$$\begin{aligned} z(x,t) &= \sum_n T_n(t)A_n\left[e^{+\mathrm{i}n\pi x/L} + (-1)^{n+1}e^{-\mathrm{i}n\pi x/L}\right] \\ &= \sum_n \left[T_{2n}(t)A_{2n}2\mathrm{i}\sin(2n\pi x/L) + T_{2n+1}(t)A_{2n+1}2\cos((2n+1)\pi x/L)\right]\,. \end{aligned} \tag{4.30}$$

and has to match the initial condition in Eq. (4.23). We can calculate the coefficients A_n from orthonormality of the functions

$$f_n(x) = \sqrt{\frac{2}{L}} \begin{cases} \sin(n\pi x/L) & : \quad n \in \{2,4,6,\ldots\} \\ \cos(n\pi x/L) & : \quad n \in \{1,3,5,\ldots\} \end{cases} \tag{4.31}$$

over the interval $[-L/2, +L/2]$. We show this by relating the function to previous results

$$\begin{aligned} f_{2n}(x) &= \sqrt{\frac{2}{L}} \sin(2n\pi x/L) = \sqrt{\frac{2}{L}} \left(e^{+\mathrm{i}2\pi nx/L} - e^{-\mathrm{i}2\pi nx/L}\right) \frac{1}{2\mathrm{i}} = \frac{1}{\mathrm{i}\sqrt{2}} \left[g_{+n}(x) - g_{-n}(x)\right] , \\ f_{2n+1}(x) &= \sqrt{\frac{2}{L}} \cos((2n+1)\pi x/L) = \frac{e^{\mathrm{i}\pi x/L}}{\sqrt{2}} \left[g_{+n}(x) + g_{-(n+1)}(x)\right] , \end{aligned} \tag{4.32}$$

where we have used the previous orthonormal functions Using the already shown orthonormality relations (4.19) of the $g_n(x)$, we can directly deduce

$$\int_{-L/2}^{+L/2} f^*_{2n}(x) f_{2m}(x) dx = \frac{1}{2} \int_{-L/2}^{+L/2} \left[g^*_{+n}(x) - g^*_{-n}(x)\right] \left[g_{+m}(x) - g_{-m}(x)\right] dx = \delta_{n,m} - \delta_{n,-m} = \delta_{nm} \tag{4.33}$$

where we have only used that both n and m are positive. Similarly, we show

$$\delta_{nm} = \int_{-L/2}^{+L/2} f^*_{2n+1}(x) f_{2m+1}(x) dx \,, \tag{4.34}$$

such that it remains to be shown that

$$\int_{-L/2}^{+L/2} f^*_{2n+1}(x) f_{2m}(x) dx \;=\; 0 \,. \tag{4.35}$$

This follows directly from the observation that $f_{2n}(-x) = -f_{2n}(+x)$ is odd under reflection and $f_{2n+1}(-x) = +f_{2n+1}(+x)$ is even. Their product is consequently odd and the integral over the symmetric interval must vanish.

The Fourier series of the initial condition (4.23) can be written as

$$z(x,0) = \sum_{n=0}^{\infty} \frac{8a}{\pi^2(1+2n)^2} \cos\left[(2n+1)\frac{\pi x}{L}\right] , \tag{4.36}$$

such that by comparing with Eq. (4.30) we can directly read off

$$A_{2n+1} = \frac{4a}{\pi^2(1+2n)^2} \,, \qquad A_{2n} = 0 \,, \tag{4.37}$$

which leads to the PDE solution

$$z(x,t) = \sum_{n=0}^{\infty} T_{2n+1}(t) \frac{8a}{\pi^2(2n+1)^2} \cos\left(\frac{(2n+1)\pi x}{L}\right) . \tag{4.38}$$

The vibration of the guitar string with a symmetric initial excitation in x will thus support half of the eigenmodes of the string, which will follow damped oscillations, see Fig. 4.2.

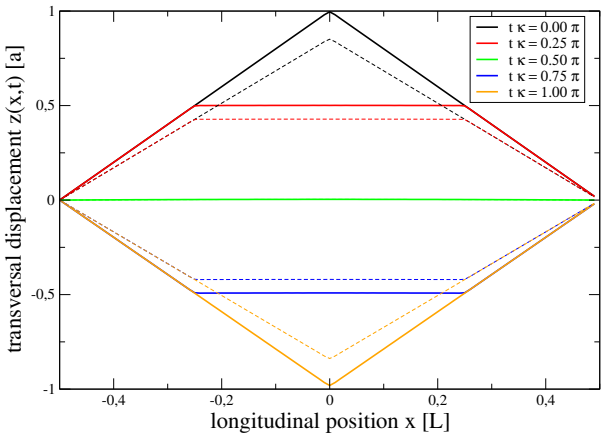

Figure 4.2: Solution of the wave equation with Dirichlet boundary conditions. The initial triangular displacement profile oscillates and is slowly damped (dashed curves: after 5 periods). The points at which the derivative of the function appears discontinuous form a hyperbolic causality cone, consistent with the classification of the wave equation. Parameters: $\gamma = 0.01\kappa$.

4.2 Fourier Transform

We have seen that in finite domains the solutions of PDEs are given by Fourier series. This is connected to the fact that any periodic function – which is equivalent to considering the function only in the interval of one period – can be represented by a Fourier series. The natural consequence is that for unbounded domains one may expect a continuos Fourier representation to hold. Alternatively to the separation ansatz, we may exploit this and use properties of the Fourier transform to reduce derivatives to algebraic equations, similiar to the use of the Laplace transform with ODEs. Of course, we can only expect this to work well when the equation under consideration is linear. The complexity is then transferred to the inversion of the Fourier transform.

4.2.1 Example: Reaction-Diffusion Equation

The separation ansatz does not always work. Consider, for example, the diffusion equation supplemented with a non-separable reaction term

$$\frac{\partial c}{\partial t} = D\frac{\partial^2 c}{\partial x^2} + r(x,t)\,, \tag{4.39}$$

where $c(x,t)$ is the concentration of a substance, D is the diffusion constant, and $r(x,t)$ is the rate at which the substance is produced by some reaction. For $r(x,t) > 0$ one often talks about a source term and for $r(x,t) < 0$ it is called a sink. An alternative interpretation would be that $c(x,t)$ is the temperature, D the heat conductivity, and $r(x,t)$ could describe heat sources and sinks. Since we consider the spatial domain as unbounded, we perform a continous FT of the spatial dimension

$$C(\omega,t) = \frac{1}{\sqrt{2\pi}}\int c(x,t)e^{+\mathrm{i}\omega x}dx\,, \qquad R(\omega,t) = \frac{1}{\sqrt{2\pi}}\int r(x,t)e^{+\mathrm{i}\omega x}dx\,, \tag{4.40}$$

which transfers the reaction-diffusion equation to an inhomogeneous ODE

$$\frac{\partial C}{\partial t} = D(-\mathrm{i}\omega)^2 C(\omega,t) + R(\omega,t)\,. \tag{4.41}$$

Here, we have used property (2.5) of the FT. Since this equation does no longer contain a derivative with respect to ω, it is actually an ODE with ω as a parameter, which we can hopefully solve with a suitable method. For example, considering a Lorentzian and time-independent profile of the

reaction rate (this would actually be a separable problem), we can easily compute the FT from adapting Eq. (2.13)

$$r(x,t) = r(x) = \frac{R_0\delta^2}{x^2+\delta^2} \qquad \Longrightarrow \qquad R(\omega,t) = R(\omega) = \frac{R_0}{\sqrt{2\pi}} e^{-\delta|\omega|}\,. \tag{4.42}$$

When now initially the concentration of the substance vanishes throughout $c(x,0) = 0$, the same holds true for its FT $C(\omega,0) = 0$, and we can write the solution of the ODE as

$$C(\omega,t) = \frac{\left[1-e^{-D\omega^2 t}\right]}{\omega^2} \frac{R_0}{\sqrt{2\pi}D} e^{-\delta|\omega|}\,. \tag{4.43}$$

The solution is then represented via the inverse FT integral

$$c(x,t) = \frac{1}{2\pi}\frac{R_0}{D}\int \frac{\left[1-e^{-D\omega^2 t}\right]}{\omega^2} e^{-\delta|\omega|} e^{-\mathrm{i}\omega x} d\omega\,. \tag{4.44}$$

Since in this case we already know the inverse FT of parts of the solution, it may be helpful to employ the convolution theorem.

4.2.2 Example: Unbounded Wave Equation

As a second example for the use of the Fourier Transform, we consider again the wave equation (4.4) without dampening and with initial conditions $\frac{\partial z}{\partial t}(x,0) = 0$ and $z(x,0) = a\delta(x)$. Such an initial excitation could e.g. correspond to an infinitely large steel bar that is locally excited with a hammer at time $t = 0$. Simple FT $Z(\omega,t) = \mathcal{F}_x(z(x,t))$ converts the equation into an ODE

$$\ddot{Z} + \kappa\omega^2 Z(\omega,t) = 0\,. \tag{4.45}$$

with the initial conditions $Z(\omega,0) = a/\sqrt{2\pi}$ and $\dot{Z}(\omega,0) = 0$. Therefore, we have reduced the problem to an undamped harmonic oscillator, which is solved by

$$Z(\omega,t) = \frac{a}{\sqrt{2\pi}} \cos\left(\sqrt{\kappa}\omega t\right) \tag{4.46}$$

in accordance with the initial conditions. The inverse FT now yields

$$z(x,t) = \frac{1}{\sqrt{2\pi}}\int Z(\omega,t) e^{-\mathrm{i}\omega x} d\omega = \frac{a}{2}\left[\delta(x-\sqrt{\kappa}t) + \delta(x+\sqrt{\kappa}t)\right]\,, \tag{4.47}$$

and we see that the initial pulse propagates with velocity $c = \sqrt{\kappa}$ along the steel bar.

4.2.3 Example: Fokker-Planck equation

We have seen that an undirected motion leads in the continuum representation to the diffusion equation. When for whatever reason the rates at which particles move in a particular direction depends on time and space (varying motility) and possibly also on direction (drift of the medium), we can describe the flow between the compartments with the rate equation

$$\dot{P}_i = R_{i-1}(t)P_{i-1} + L_{i+1}(t)P_{i+1} - [R_i(t) + L_i(t)]P_i\,. \tag{4.48}$$

Here, $R_i(t)$ desribes the rate to move to the right from compartment i to compartment $i+1$, and $L_i(t)$ the rate to move left from compartment i to compartment $i-1$. It is straightforward to see that the total probability is conserved $\sum_i \dot{P}_i = 0$. Furthermore, we can write the rate equation as

$$\begin{aligned}\dot{P}_i &= \{[R_{i-1}(t)+L_{i-1}(t)]P_{i-1} + [R_{i+1}(t)+L_{i+1}(t)]P_{i+1} - 2[R_i(t)+L_i(t)]P_i\} \\ &\quad + \{L_i(t)P_i - L_{i-1}(t)P_{i-1}\} - \{R_{i+1}(t)P_{i+1} - R_i(t)P_i\}\ . \end{aligned} \tag{4.49}$$

Here, we see that the first line appears like a second derivative of a function $[r(x,t)+l(x,t)]P(x,t)$, whereas the second line is the discretized version of the first derivative of $l(x,t)P(x,t)$ and $r(x,t)P(x,t)$, respectively. This motivates us to consider the Fokker[3] -Planck[4] equation as

$$\frac{\partial \rho}{\partial t} = \frac{\partial}{\partial x}\left[v(x,t)\rho(x,t)\right] + \frac{\partial^2}{\partial x^2}\left[d(x,t)\rho(x,t)\right]\ , \tag{4.50}$$

where $v(x,t)$ describes the drift and $d(x,t)$ the undirected part of the motility.

We supplement the Fokker-Planck equation with a self-amplifying term – corresponding e.g. to proliferation of a bacterial species. When we assume that drift v and motility D are constant, the equation becomes

$$\frac{\partial \rho}{\partial t} = D\frac{\partial^2 \rho}{\partial x^2} + v\frac{\partial \rho}{\partial x} + \alpha\rho(x,t)\,. \tag{4.51}$$

This equation could e.g. model a pipe with flow velocity v, at which at time $t=0$ a bacterial population is placed with

$$\rho_0(x,0) = \delta(x-x_0)\,. \tag{4.52}$$

After Fourier transform, the equation assumes the form

$$\frac{\partial \rho(\omega,t)}{\partial t} = \left[\alpha - \mathrm{i}\omega v - \omega^2 D\right]\rho(\omega,t)\,, \tag{4.53}$$

and the initial condition transfers to $\rho_0(\omega) = \frac{e^{\mathrm{i}\omega x_0}}{\sqrt{2\pi}}$. The equation in frequency space is therefore solved by

$$\rho(\omega,t) = e^{(\alpha - \mathrm{i}\omega v - \omega^2 D)t}\frac{e^{\mathrm{i}\omega x_0}}{\sqrt{2\pi}}\,, \tag{4.54}$$

and we can calulate the solution from the inverse FT

$$\rho(x,t) = \frac{1}{2\pi}\int e^{(\alpha - \mathrm{i}\omega v - \omega^2 D)t}e^{-\mathrm{i}\omega(x-x_0)}d\omega = \frac{e^{\alpha t}}{\sqrt{2\pi}\sqrt{2Dt}}e^{-(x-x_0+vt)^2/(4Dt)}\,, \tag{4.55}$$

which is just an inflated Gaussian that propagates with mean $\mu = x_0 - vt$ and at the same time spreads. From the normalization of the Gaussian we conclude that the total bacterial population

$$N(t) = \int \rho(x,t)dx = e^{\alpha t} \tag{4.56}$$

indeed simply follows an exponential growth law.

[3] Adriaan Daniël Fokker (1887 – 1972) was a dutch physicist and musician. He derived the equation in 1913 but also contributed to special and general relativity.

[4] Max Karl Ernst Ludwig Planck (1858 – 1947) was a german theoretical physicist with numerous contributions. His fame rests on his original contributions to quantum theory.

4.3 Green's functions

We have already seen that once inhomogeneous terms appear, the solution of PDEs becomes even more complicated. In a nutshell, the method of Green's[5] functions allows to construct the solution of **linear** inhomogeneous PDEs from simple inhomogeneous PDEs. Let $\boldsymbol{z}$ be a point in the domain we consider and let $\mathcal{D}_{\boldsymbol{z}}$ be a linear differential operator that may contain functions of $\boldsymbol{z}$ and derivatives with respect to all components of $\boldsymbol{z}$. For example, for the diffusion equation $\mathcal{D}_{x,t}\rho(x,t) = \mathcal{D}_{\boldsymbol{z}}\rho(z) = 0$ we would have $\mathcal{D}_{x,t} = \frac{\partial}{\partial t} - D\frac{\partial^2}{\partial x^2}$. To such a linear differential operator we can associated a Green's function as follows.

Box 17 (Green's function) *For a linear differential operator $\mathcal{D}_{\boldsymbol{z}}$, the Green's function $G(\boldsymbol{z},\boldsymbol{s})$ is defined as the solution of the equation*

$$\mathcal{D}_z G(\boldsymbol{z},\boldsymbol{s}) = \delta(\boldsymbol{z}-\boldsymbol{s})\,. \tag{4.57}$$

Then, the inhomogeneous problem

$$\mathcal{D}_{\boldsymbol{z}}\rho(\boldsymbol{z}) = \phi(\boldsymbol{z}) \tag{4.58}$$

is solved by

$$\rho(\boldsymbol{z}) = \int G(\boldsymbol{z},\boldsymbol{s})\phi(\boldsymbol{s})d\boldsymbol{s}\,. \tag{4.59}$$

It is then straightforward to show the claim

$$\mathcal{D}_{\boldsymbol{z}}\rho(\boldsymbol{z}) = \mathcal{D}_{\boldsymbol{z}}\int G(\boldsymbol{z},\boldsymbol{s})\phi(\boldsymbol{s})d\boldsymbol{s} = \int \left[\mathcal{D}_{\boldsymbol{z}}G(\boldsymbol{z},\boldsymbol{s})\right]\phi(\boldsymbol{s})d\boldsymbol{s} = \int \delta(\boldsymbol{z}-\boldsymbol{s})\phi(\boldsymbol{s})d\boldsymbol{s} = \phi(\boldsymbol{z})\,. \tag{4.60}$$

We note that given the Green's function, it may of course be difficult or impossible to solve the integral for arbitrary source terms $\phi(\boldsymbol{s})$. Nevertheless, it provides a straightforward recipe how to obtain the solution and has proven useful in many cases. Many variants of the Green's function formalism exist, tailored to specific problems. Here, we will only discuss a few representatives.

4.3.1 Example: Poisson Equation

When we consider the long-term limit in reaction-diffusion equations or electrostatic problems, one arrives at the Poisson [6] equation, which e.g. in three dimensions assumes the form

$$\left[\frac{\partial^2}{\partial x^2} + \frac{\partial^2}{\partial y^2} + \frac{\partial^2}{\partial z^2}\right]\phi(x,y,z) = 4\pi\rho(x,y,z)\,. \tag{4.61}$$

The Green's function must accordingly obey

$$\left[\frac{\partial^2}{\partial x^2} + \frac{\partial^2}{\partial y^2} + \frac{\partial^2}{\partial z^2}\right]G(x,y,z,x',y',z') = \delta(x-x')\delta(y-y')\delta(z-z')\,, \tag{4.62}$$

[5] George Green (1793 – 1841) was a british mill owner and mathematician. With the heritage of his father he could persue his mathematical interests in his forties but nevertheless contributed strongly.

[6] Siméon Denis Poisson (1781 – 1840) was a french mathematician, geodesist and physicist.

and we perform a three-dimensional FT yielding

$$G(\boldsymbol{\omega}, \boldsymbol{r'}) = -\frac{e^{+\mathrm{i}\boldsymbol{\omega}\cdot\boldsymbol{r'}}}{(2\pi)^{3/2}\boldsymbol{\omega}^2}\,. \tag{4.63}$$

The actual solution is obtained via the inverse FT

$$G(\boldsymbol{r}, \boldsymbol{r'}) \;=\; -\frac{1}{(2\pi)^3}\int d\omega_x d\omega_y d\omega_z \frac{e^{-\mathrm{i}\boldsymbol{\omega}\cdot(\boldsymbol{r}-\boldsymbol{r'})}}{\omega_x^2+\omega_y^2+\omega_z^2} = G(\boldsymbol{r}-\boldsymbol{r'}). \tag{4.64}$$

To perform the inverse FT, it is useful to switch to spherical coordinates with θ chosen as the angle between $\boldsymbol{r}-\boldsymbol{r'}$ and $\boldsymbol{\omega}$. Eventually, the angular and then the radial integrals can be performed and one obtains

$$G(\boldsymbol{r}-\boldsymbol{r'}) = -\frac{1}{4\pi}\frac{1}{|\boldsymbol{r}-\boldsymbol{r'}|}\,. \tag{4.65}$$

Consequently, for an arbitrary source distribution, the potential is determined by

$$\phi(x,y,z) = -\int dx'dy'dz' \frac{\rho(x',y',z')}{\sqrt{(x-x')^2+(y-y')^2+(z-z')^2}}\,. \tag{4.66}$$

We note that the Green's function depends on possible boundary conditions. Fortunately, within electrostatics it is sometimes possible to enforce boundary conditions using the method of image charges.

4.3.2 Example: Wave Equation

The wave equation can also be written with the d'Alembert [7] operator

$$\Box\phi(\boldsymbol{r},t) = \left\{\frac{1}{c^2}\frac{\partial^2}{\partial t^2} - \Delta\right\}\phi(\boldsymbol{r},t)\,, \tag{4.67}$$

where c denotes the wave velocity (when we derive the wave equation from the Maxwell equations c indeed becomes the velocity of light). An inhomogeneous wave equation

$$\Box\phi(\boldsymbol{r},t) = f(\boldsymbol{r},t) \tag{4.68}$$

can arise when e.g. a chain of oscillators is driven or when electromagnetic signals are sent. To find the Green's function, we have to solve

$$\Box G(\boldsymbol{r},t) = \delta(t-t_0)\delta(x-x_0)\delta(y-y_0)\delta(z-z_0)\,. \tag{4.69}$$

We note that the direction of time is not inherent in the above equation. Fundamental principles such as causality therefore will have to be enforced to find the correct Green's function. Since the $\Box$-operator is translationally invariant, we can set $t_0 = 0$ and $\boldsymbol{r}_0 = \boldsymbol{0}$. A four-fold FT yields the equation

$$\left[\frac{-\omega^2}{c^2} + \boldsymbol{k}^2\right] G(\boldsymbol{k},\omega) = \left(\frac{1}{2\pi}\right)^2\,, \tag{4.70}$$

[7] Jean-Baptiste le Rond d'Alembert (1717 – 1783) was a french mathematician, physicist and philosopher also known for his co-authorship of the *Encyclopédie*.

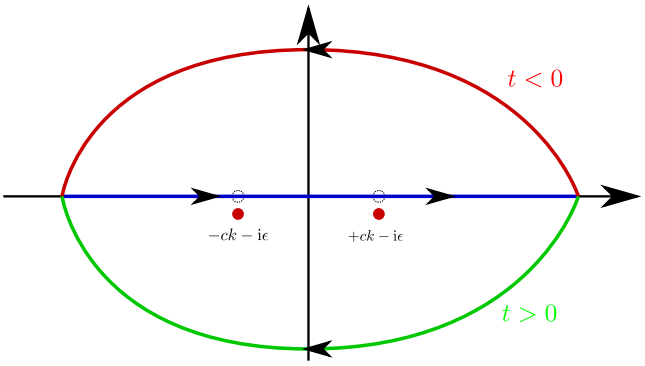

Figure 4.3: Sketch of the integration contour in Eq. (4.72) in the complex plane. To ensure for causality, the poles are shifted by an infinitesimal amount into the lower complex plane (red dots), such that they contribute only for positive times, where the contour has to be closed using the lower arc. For negative times, the contour is closed in the upper half plane, and the Green's function correspondingly vanishes.

and to obtain the original Green's function we have to perform the inverse FT (later-on, we can re-insert $\boldsymbol{r} \to \boldsymbol{r} - \boldsymbol{r}_0$ and $t \to t - t_0$)

$$G(\boldsymbol{r}, t) = \left(\frac{1}{2\pi}\right)^4 \int d\omega \int d^3\boldsymbol{k} \frac{e^{-\mathrm{i}(\boldsymbol{k}\cdot\boldsymbol{r} + \omega t)}}{k^2 - \omega^2/c^2} \,. \tag{4.71}$$

We first consider the temporal integral

$$I(k, t) = \int \frac{e^{-\mathrm{i}\omega t} c^2}{c^2 k^2 - \omega^2} d\omega \,. \tag{4.72}$$

Here, we have the situation that two poles $\omega^* = \pm ck$ lie directly on the real axis, such that one may question the mere existence of the integral. Closer inspection of the integrand however yields that imaginary and real parts separately have positive and negative contributions at the poles that may cancel. Therefore, we consider shifting the integration contour slightly away from the real axis. At this point, we introduce causality as a boundary condition on the Green's function: For $t < 0$, the Green's function should vanish, since a source term should only influence the solution in the future but not in the past. For $t < 0$, the contour will be closed in the upper half plane, and for $t > 0$, the lower half plane will be the correct choice. Therefore, to obtain the so-called **retarded Green's function** [4], we consider the replacement $\omega \to \omega + \mathrm{i}\epsilon$ in the denominator, which moves the poles at $\omega_{1/2} = -\mathrm{i}\epsilon \pm ck$ to the lower complex half plane, see also Fig. 4.3. For $t < 0$, the integral correspondingly vanishes, whereas for positive times we have to take two poles into account (recall the global sign arising from the clockwise orientation)

$$\begin{aligned} I(k, t) &= -\Theta(t) 2\pi\mathrm{i} \lim_{\epsilon \to 0} \left[\operatorname*{Res}_{\omega = +ck - \mathrm{i}\epsilon} \frac{e^{-\mathrm{i}\omega t} c^2}{c^2 k^2 - (\omega + \mathrm{i}\epsilon)^2} + \operatorname*{Res}_{\omega = -ck - \mathrm{i}\epsilon} \frac{e^{-\mathrm{i}\omega t} c^2}{c^2 k^2 - (\omega + \mathrm{i}\epsilon)^2} \right] \\ &= -2\pi\mathrm{i}\Theta(t) c^2 \left[-\frac{e^{-\mathrm{i}ckt}}{2ck} + \frac{e^{+\mathrm{i}ckt}}{2ck} \right] \\ &= +2\pi\Theta(t) \frac{c}{k} \sin(ckt) \,. \end{aligned} \tag{4.73}$$

The retarded Green's function therefore becomes

$$\begin{aligned} G(\boldsymbol{r}, t) &= \left(\frac{1}{2\pi}\right)^3 \Theta(t) \int d^3\boldsymbol{k} \frac{c}{k} \sin(ckt) e^{-\mathrm{i}\boldsymbol{k}\cdot\boldsymbol{r}} \\ &= \left(\frac{1}{2\pi}\right)^2 \Theta(t) \int_0^\infty dk \int_0^\pi d\theta \sin(\theta) ck \sin(ckt) e^{-\mathrm{i}kr\cos\theta} \,, \end{aligned} \tag{4.74}$$

where we have introduced spherical coordinates and already performed a trivial angular integration. Next, we perform the remaining angular integral

$$\int_0^\pi \sin\theta e^{-\mathrm{i}kr\cos\theta} d\theta = \int_{-1}^{+1} e^{-\mathrm{i}krx} dx = 2\frac{\sin(kr)}{kr}\,, \tag{4.75}$$

such that the Green's function becomes

$$\begin{aligned} G(\boldsymbol{r},t) &= 2\left(\frac{1}{2\pi}\right)^2 \Theta(t)\frac{c}{r}\int_0^\infty \sin(ckt)\sin(kr)dk = \left(\frac{1}{2\pi}\right)^2 \Theta(t)\frac{c}{r}\int \sin(ckt)\sin(kr)dk \\ &= \left(\frac{1}{2\pi}\right)^2 \Theta(t)\frac{c}{r}\frac{(-1)}{4}\int \left[e^{+\mathrm{i}ckt} - e^{-\mathrm{i}ckt}\right]\left[e^{+\mathrm{i}kr} - e^{-\mathrm{i}kr}\right] dk \\ &= \frac{1}{2\pi}\Theta(t)\frac{c}{r}\frac{(-1)}{4} 2\left[\delta(r+ct) - \delta(r-ct)\right] \\ &= \frac{\Theta(t)}{4\pi}\frac{c}{r}\delta(r-ct)\,, \end{aligned} \tag{4.76}$$

where in the last step we have used that the first δ-function cannot contribute for $ct > 0$. From translational invariance, we conclude

$$G(\boldsymbol{r},t,\boldsymbol{r}_0,t_0) = \frac{\Theta(t-t_0)}{4\pi}\frac{c}{|\boldsymbol{r}-\boldsymbol{r}_0|}\delta\left[|\boldsymbol{r}-\boldsymbol{r}_0| - c(t-t_0)\right]\,. \tag{4.77}$$

We note that this Green's function obeys causality as the boundary condition. We have not specified any initial condition for the field, implicitly assuming that the field initially vanishes.

The full solution of the inhomogeneous wave equation

$$\Box\phi(\boldsymbol{r},t) = f(\boldsymbol{r},t) \tag{4.78}$$

therefore becomes

$$\phi(\boldsymbol{r},t) = \int \frac{\Theta(t-t')}{4\pi}\frac{c}{|\boldsymbol{r}-\boldsymbol{r'}|}\delta\left[|\boldsymbol{r}-\boldsymbol{r'}| - c(t-t')\right] f(\boldsymbol{r'},t')d^3\boldsymbol{r'}dt'\,. \tag{4.79}$$

For example, for a point-like sender source at $f(\boldsymbol{r},t) = f(t)\delta^{(3)}(\boldsymbol{r}-\boldsymbol{r}_0)$, we obtain

$$\begin{aligned} \phi(\boldsymbol{r},t) &= \int \frac{\Theta(t-t')}{4\pi}\frac{c}{|\boldsymbol{r}-\boldsymbol{r}_0|}\delta(|\boldsymbol{r}-\boldsymbol{r}_0| - c(t-t'))f(t')dt' \\ &= \frac{1}{4\pi}\frac{1}{|\boldsymbol{r}-\boldsymbol{r}_0|}\int_0^\infty \delta(|\boldsymbol{r}-\boldsymbol{r}_0| - \tau)f(t-\tau/c)d\tau \\ &= \frac{1}{4\pi}\frac{f(t-|\boldsymbol{r}-\boldsymbol{r}_0|/c)}{|\boldsymbol{r}-\boldsymbol{r}_0|}\,. \end{aligned} \tag{4.80}$$

Correspondingly, we see that the field at point $\boldsymbol{r}$ can only be influenced by the sender signal that has been sent at time $t - |\boldsymbol{r}-\boldsymbol{r}_0|/c$, which again motivates the name retarded Green's function. Furthermore, we see that the field is suppressed as the distance between sender and receiver is increased. When we send the light velocity to infinity, we recover case of the Poisson equation (up to a sign, which is rooted in the different prefactor of the spatial derivatives in the two differential operators).

4.4 Nonlinear Equations

With a few exceptions, the study of nonlinear PDEs is limited to numerical approaches. In some cases however, one is able to find suitable transformations that reduce the complexity of the problem. Such transformations are often guided by practical experience. For example, it is a well-established approach in this case to look for travelling wave solutions that may either arise exactly or asymptotically. To be more exact, a travelling wave solution has in one spatial dimension the form [5]

$$u(x,t) = u(x - vt) = u(z)\,, \tag{4.81}$$

where v is an a priori unknown wavespeed.

4.4.1 Example: Fisher-Kolmogorov-Equation

A prominent example for an equation exhibiting travelling waves is the Fisher [8]- Kolmogorov [9]-equation

$$\frac{\partial u}{\partial t} = D\frac{\partial^2 u}{\partial x^2} + \alpha u(x,t)\left[1 - \frac{u(x,t)}{C}\right]\,. \tag{4.82}$$

Here, D represents the diffusion constant as usual, α corresponds to a growth rate, and C denotes a (homogeneous) carrying capacity. It is straightforward to bring the equation in dimensionless form by introducing $\tau = \alpha t$, $y = \sqrt{\frac{\alpha}{D}}x$, and $n = u/C$, which yields

$$\frac{\partial n}{\partial \tau} = \frac{\partial^2 n}{\partial y^2} + n(1-n)\,. \tag{4.83}$$

We note that homogeneous stationary solutions are $n(y,\tau) = 0$ and $n(y,\tau) = 1$. A travelling-wave ansatz of the form $n(y,\tau) = n(y - v\tau)$ then transforms the PDE into an ODE of the form

$$n''(z) + vn'(z) + n(z)[1 - n(z)] = 0\,. \tag{4.84}$$

Without loss of generality we constrain ourselves to positive wavespeeds

$$v > 0\,. \tag{4.85}$$

When we find a solution to ODE equation with constant $v > 0$ that is also stable in presence of perturbations, the travelling waves for v and $-v$ are both solutions. We can qualitatively study the equivalent system of coupled first order ODEs

$$n'(z) = m(z)\,, \qquad m'(z) = -vm(z) - n(z)[1 - n(z)] \tag{4.86}$$

near its fixed points $\bar{m}_1 = 0$, $\bar{n}_1 = 0$ and $\bar{m}_2 = 0$, $\bar{n}_2 = 1$ with a nonlinear stability analysis. Near the fixed points, we obtain the linearized systems

$$\frac{d}{dz}\begin{pmatrix}\Delta n_1\\ \Delta m_1\end{pmatrix} = \begin{pmatrix}0 & +1\\ -1 & -v\end{pmatrix}\begin{pmatrix}\Delta n_1\\ \Delta m_1\end{pmatrix}\,, \qquad \frac{d}{dz}\begin{pmatrix}\Delta n_2\\ \Delta m_2\end{pmatrix} = \begin{pmatrix}0 & +1\\ +1 & -v\end{pmatrix}\begin{pmatrix}\Delta n_2\\ \Delta m_2\end{pmatrix}\,. \tag{4.87}$$

[8] Sir Ronald Aylmer Fisher (1890 – 1962) was a british statistician and evolutionary biologist, who contributed to the foundations of population genetics.

[9] Andrey Nikolaevich Kolmogorov (1903 – 1987) was a soviet mathematician with contributions to multiple fields.

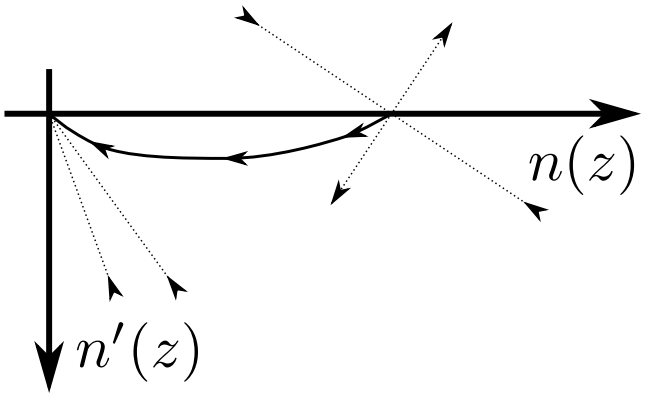

Figure 4.4: Phase plane for Eq. (4.87). For $v \geq 2$, the fixed point at the origin is stable, whereas the other fixed point is always a saddle node. To obtain a trajectory connecting the fixed points that is completely contained in the quadrant $n(z) > 0$ and $n'(z) < 0$, it is necessary that $v \geq 2$.

By studying the eigenvalues of these matrices, we can infer the qualitative behaviour of the solution near the fixed points. At the origin, we obtain the eigenvalues

$$\lambda_1^{\pm} = -\frac{v}{2} \pm \sqrt{\left(\frac{v}{2}\right)^2 - 1}\,, \tag{4.88}$$

which are both negative for $v \geq 2$. For $0 < v < 2$, the real part of the eigenvalues remains negative, but these obtain in addition an imaginary part. In this case, the fixed point a the origin would correspond to a stable spiral. The other fixed point has the eigenvalues

$$\lambda_2^{\pm} = -\frac{v}{2} \pm \sqrt{\left(\frac{v}{2}\right)^2 + 1}\,. \tag{4.89}$$

Since, $\lambda_2^- < 0$ and $\lambda_2^+ > 0$ for all $v > 0$, the second fixed point is a saddle node. Our travelling wave describes the transition from an empty phase with $n = 0$ to a filled phase with $n = 1$, and correspondingly it must decrease across the phase boundary $n'(z) < 0$. Now, to obtain trajectories travelling from the second fixed point to the first in the physically relevant quadrant specified by $m(z) = n'(z) < 0$ and $n(z) > 0$, it is necessary that $v \geq 2$, see Fig. 4.4. This means that a corresponding travelling wave solution should have a (dimensionless) minimum wavespeed $v \geq 2$. In the original frame this implies the condition

$$v_{\text{wave}} \geq 2\sqrt{\alpha D}\,, \tag{4.90}$$

such that the minimum wave speed is given by the product of proliferation rate and diffusion constant. This raises the question which wavespeed is actually obtained for a given initial condition. At the front of the travelling wave, where $n(y,\tau) \ll 1$, we can use the exponential ansatz $n(y,\tau) = Ae^{-a(y-v\tau)}$ (with $A > 0$ and $a > 0$) and neglect the quadratic part in the dimensionless Fisher-Kolmogorov equation (4.83). This yields for the initial condition with slope a a condition for $v = a + 1/a$, and we see that the minimum wavespeed is obtained for $a = 1$.

4.4.2 Example: Korteweg-de-Vries equation

Another prominent nonlinear equation is one proposed by Korteweg [10] and de Vries [11]. It was proposed to describe the dynamics of waves in long channels. These waves were observed to keep

[10] Diederik Johannes Korteweg (1848 – 1941) was a Dutch mathematician.
[11] Gustav de Vries (1866 – 1934) was a Dutch mathematician

their shape over very large distances despite of friction and dispersive forces. In its dimensionless form, the Korteweg-de-Vries (KdV) equation reads

$$\frac{\partial u}{\partial t} + 6u(x,t)\frac{\partial u}{\partial x} + \frac{\partial^3 u}{\partial x^3} = 0 \tag{4.91}$$

and thus constitutes an example of a nonlinear PDE of third order. As before, we are aiming to find travelling wave solutions and therefore use the transformation $z = x - vt$, where v is the wave speed. This yields the ODE

$$u'''(z) + [6u(z) - v]u'(z) = 0\,, \tag{4.92}$$

to which one aims to find a solution. It turns out that multiple solutions exist (the physical one of course is then chosen by the initial and boundary conditions). Here, we just describe one way of constructing such solitonic solutions. A simple ansatz is to assume an exponential dependence, and to prevent the solution to blow off at $z \to \pm\infty$, it is reasonable to use the ansatz

$$u(z) = \frac{\sum_{n=-a}^{+A} a_n e^{nz}}{\sum_{n=-b}^{+B} b_n e^{nz}}\,. \tag{4.93}$$

Since the solution should be finite at $z \to \pm\infty$, it follows that we have to demand $A = B$ and $a = b$.

Then, already with the simplest ansatz with $A = B = 1$ and $a = b = 1$, i.e., with an ansatz of the form

$$u(z) = \frac{a_{-1}e^{-z} + a_0 + a_{+1}e^{+z}}{e^{-z} + b_0 + b_{+1}e^{+z}} \tag{4.94}$$

it is possible to find a solution to Eq. (4.92). Above, we have already eliminated the parameter b_{-1}, since it is redundant. Using this ansatz in the KdV equation, sorting the result in powers of e^{nz}, and equating all coefficients of e^{nz} to zero eventually yields a set of equations for the remaining parameters. One particular solution (which is not simply constant) is

$$u(z) = \frac{4(v-1) + 4b_0(v+5)e^z + b_0^2(v-1)e^{2z}}{6\left(2 + b_0 e^z\right)^2}\,. \tag{4.95}$$

Here, the velocity of the wave v and the parameter b_0 are both arbitrary. The velocity however is related to the baseline of the solution $\lim_{z\to\pm\infty} u(z) = (v-1)/6$. We note that as the dimensionless KdV equation (4.92) is invariant with respect to a shift of the solution when we also change the velocity, we can construct other solutions by adding a constant. In particular, one soliton with compact support is obtained by setting $v = 1$, yielding

$$u(z) = \frac{4b_0 e^z}{(2 + b_0 e^z)^2}\,. \tag{4.96}$$

4.5 Numerical Solution: Finite Differences

The numerical solution of PDEs is usually an enormous challenge, such that the use of supercomputers and parallelization is often advisable. We will discuss a few simple approaches at an introductory level.

Here, we discretize both time and space in equal intervals of size Δt and Δx, Δy, and Δz. As a convention, we will label the solution at discrete sampling points by $u^{(n)}_{abc} = u(x_a, y_b, z_c, t_n)$. Suitable approximations for derivatives occuring in a PDE are then the difference quotients, e.g. in three spatial dimensions

$$\frac{\partial u(x,y,z,t)}{\partial t} \approx \frac{u^{(n+1)}_{a,b,c} - u^{(n)}_{a,b,c}}{\Delta t}\,, \qquad \frac{\partial u(x,y,z,t)}{\partial x} \approx \frac{u^{(n)}_{a+1,b,c} - u^{(n)}_{a-1,b,c}}{2\Delta x} \tag{4.97}$$

would be a forward-time approximation to the time derivative and a centered-space approximation to the spatial derivative. Often, one is given an initial distribution of the solution and wants to evolve it in time. Depending now on which kind of approximation is inserted for the time derivatives, we obtain different numerical solution schemes. We will illustrate this at the example of the 1D diffusion equation (the generalization to higher dimensions is straightforward).

4.5.1 Explicit Forward-Time Discretization

A forward-time approximation would yield

$$\frac{u^{(n+1)}_a - u^{(n)}_a}{\Delta t} = D\frac{u^{(n)}_{a+1} - 2u^{(n)}_a + u^{(n)}_{a-1}}{\Delta x^2}\,, \tag{4.98}$$

which we can immediately convert into an iterative equation for the propagated solution

$$u^{(n+1)}_a = u^{(n)}_a + D\frac{\Delta t}{\Delta x^2}\left[u^{(n)}_{a+1} - 2u^{(n)}_a + u^{(n)}_{a-1}\right]\,. \tag{4.99}$$

Thus, to propagate the solution of the diffusion equation by one timestep, one needs the local value of the function $u^{(n)}_a$ and the value of the next neighbours $u^{(n)}_{a\pm1}$. To encode boundary conditions requires some special care: Assuming a discretization N grid points, where $a \in \{1, 2, \ldots, N-1, N\}$, the boundary conditions will constrain the external nodes $a = 1$ and $a = N$, such that these need not be explicitly evolved:

- To encode e.g. Dirichlet boundary conditions, we simply have to fix the boundary nodes to a constant value $u^{(n)}_1 = u_{\text{left}}$ and $u^{(n)}_N = u_{\text{right}}$ and need to apply the iteration equation only for the internal nodes $u^{(n)}_a$ with $2 \le a \le N-1$.
- To encode e.g. no-flux von-Neumann boundary conditions, we also evolve only the internal nodes and replace in the iteration equation $u^{(n)}_1 = u^{(n)}_2$ and $u^{(n)}_N = u^{(n)}_{N-1}$. For general von-Neumann boundary conditions one can demand the differences $u^{(n)}_1 - u^{(n)}_2$ and $u^{(n)}_N - u^{(n)}_{N-1}$ to be constant.
- For periodic boundary conditions, we can e.g. identify $u^{(n)}_{N+1} = u^{(n)}_1$ and $u^{(n)}_0 = u^{(n)}_N$ and evolve $1 \le a \le N$ with the iteration equation.

We note that for a forward-time and centered space discretization we have not treated time and space on equal footing. This enables one to arrive at a simple iteration equation but unfortunately comes at a costly price: When the timestep is too large or the spatial resolution becomes too fine, the scheme becomes unstable. We see this from a von-Neumann stability analysis of the discretization scheme, where as an ansatz one locally linearizes the PDE (here, this is not necessary since the diffusion equation is linear) and then considers the dynamics of modes of the form

$$u^{(n)}_a = A^n e^{\mathrm{i}ak}\,, \tag{4.100}$$

where $k \in \mathbb{R}$ and A is unknown. Thus, the ansatz is oscillatory in space (note that this simply corresponds to an expansion in Fourier modes) and exponential in time, and if, for any k, we obtain that $|A| > 1$, the solutions may diverge in time and the scheme is considered unstable. Inserting the ansatz in Eq. (4.99) we obtain

$$A^{n+1} e^{\mathrm{i}ka} = \left[1 - 2D\frac{\Delta t}{\Delta x^2}\right] A^n e^{\mathrm{i}ka} + D\frac{\Delta t}{\Delta x^2} A^n e^{\mathrm{i}ka} \left[e^{-\mathrm{i}k} + e^{+\mathrm{i}k}\right] , \tag{4.101}$$

which implies

$$A = 1 + 2D\frac{\Delta t}{\Delta x^2}[\cos(k) - 1] . \tag{4.102}$$

To demand that $|A| \leq 1$ for all k eventually yields the Courant [12]-condition

$$2D\frac{\Delta t}{\Delta x^2} \leq 1 , \tag{4.103}$$

that has to be satisfied to render the iteration (4.99) stable. This condition, unfortunately, is quite prohibitive: For large D, we will have to choose a small timestep and a rough spatial discretization, and if we want to increase the spatial resolution (decrease Δx), we at the same time must also increase the temporal resolution (decrease Δt). Furthermore, it is a necessary condition for stability but not sufficient. When the dimension is increased, the Courant-condition becomes even more prohibitive

$$2D\left(\frac{\Delta t}{\Delta x^2} + \frac{\Delta t}{\Delta y^2} + \frac{\Delta t}{\Delta z^2}\right) \leq 1 . \tag{4.104}$$

4.5.2 Implicit Centered-Time discretization

We can can also center the time derivative around t, which however would involve values from the previous timestep $\frac{\partial u}{\partial t} \approx (u^{(n+1)} - u^{n-1})/(2\Delta t)$. Alternatively, we can also evaluate the r.h.s. of the diffusion equation at time t_n and t_{n+1}. This is called Crank [13]- Nicolson [14] scheme, which for the one-dimensional diffusion equation reads

$$u_a^{(n+1)} = u_a^{(n)} + \frac{D}{2}\frac{\Delta t}{\Delta x^2}[u_{a+1}^{(n)} - 2u_a^{(n)} + u_{a-1}^{(n)}] + \frac{D}{2}\frac{\Delta t}{\Delta x^2}[u_{a+1}^{(n+1)} - 2u_a^{(n+1)} + u_{a-1}^{(n+1)}] . \tag{4.105}$$

We note that the temporal derivative is centered around $t + \Delta t/2$, which has been taken into account by the average on the r.h.s. A von-Neumann stability analysis $u_a^{(n)} = A^n e^{\mathrm{i}ka}$ yields

$$A = \frac{1 - \frac{D\Delta t}{\Delta x^2}(1 - \cos k)}{1 + \frac{D\Delta t}{\Delta x^2}(1 - \cos k)} , \tag{4.106}$$

which for all $k \in \mathbb{R}$ and for all $D\Delta t/\Delta x^2 > 0$ obeys $|A| \leq 1$. The scheme is therefore unconditionally stable. This allows one to choose large timesteps (which would however also lead to decreased accuracy). Unfortunately, the scheme is more diffucult to evolve since it requires to invert a matrix:

[12] Richard Courant (1888 – 1972) was a german mathematician.
[13] John Crank (1916 – 2006) was a british mathematical physicist.
[14] Phyllis Nicolson (1917 – 1968) was a british mathematician.

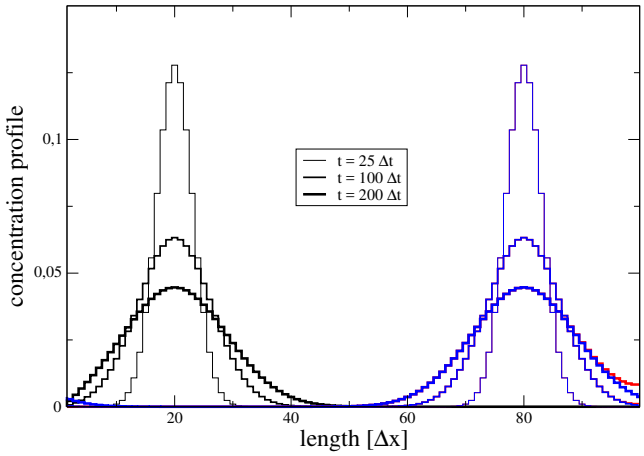

Figure 4.5: Comparison of Crank-Nicolson solutions of the diffusion equation for Dirichlet (black), von-Neumann (red), and periodic (blue) boundary conditions for different times (from bold to thin). Whereas for Dirichlet boundary conditions (initiated with a δ-profile at $x = 20\Delta x$), the total mass is not conserved, this is different for periodic and (no-flux) von-Neumann boundary conditions (initiated at $x = 80\Delta x$). Other parameters: $D\Delta t/\Delta x^2 = 0.1$.

Arranging all terms with $n+1$ on the left and those with n on the right, we obtain for the internal $(1 \leq a \leq N-1)$ nodes the equations

$$-\alpha u_{a-1}^{(n+1)} + (1+2\alpha)u_a^{(n+1)} - \alpha u_{a+1}^{(n+1)} = +\alpha u_{a-1}^{(n)} + (1-2\alpha)u_a^{(n)} + \alpha u_{a+1}^{(n)}\,, \tag{4.107}$$

where we have defined $\alpha = (D/2)\Delta t/\Delta x^2$. When we assume e.g. Dirichlet boundary conditions $u_1^{(n+1)} = u_1^{(n)}$ and $u_N^{(n+1)} = u_N^{(n)}$ for the external nodes, this can be written with a matrix $A(\alpha)$

$$A(+\alpha)\begin{pmatrix} u_1^{(n+1)} \\ \vdots \\ \vdots \\ u_N^{(n+1)} \end{pmatrix} = A(-\alpha)\begin{pmatrix} u_1^{n} \\ \vdots \\ \vdots \\ u_N^{n} \end{pmatrix},$$

$$A(\alpha) = \begin{pmatrix} 1 & 0 & & & & & \\ -\alpha & 1+2\alpha & -\alpha & & & & \\ & -\alpha & \ddots & \ddots & & & \\ & & \ddots & \ddots & -\alpha & & \\ & & & -\alpha & 1+2\alpha & -\alpha & \\ & & & & 0 & 1 & \end{pmatrix}. \tag{4.108}$$

Fortunately, the matrix to be inverted is tri-diagonal. We also note that it is diagonally dominant, such that its inverse will always exist. For other boundary conditions, we would obtain some minor modifications, but in any case, for such matrices, adapted algorithms exist that compute the inverse extremely efficiently. We note that the initial conditions must be chosen consistent with the boundary conditions. When the concentration does not vanish at the boundary, the choice of boundary condition may lead to fundamentally different behaviour, see Fig. 4.5.

The fact that a matrix has to be inverted to propagate the solution is common to all implicit schemes. This is usually compensated by the fact that implicit schemes tend to be more stable than explicit ones. In higher dimensions however, the matrix that has to be inverted will no longer be tri-diagonal but rather band-diagonal. There exist adapted methods to map the band-diagonal matrices to multiple tri-diagonal ones. However, since generally only few next neighbors are involved in the representation of spatial derivatives, the matrix to be inverted will be always extremely sparse. Therefore, an iterative algorithm as e.g. inverse iteration in Eq. (3.38) may be applicable and even quite efficient when the sparsity of the matrix is used in the matrix multiplications. We

also note that when one is interested in a Poisson-type problem

$$\Delta\rho(x) = f(x) \tag{4.109}$$

we can map it to the steady-state problem of a reaction-diffusion equation $\partial_t\rho = D\partial_x^2\rho + Df(x)$. To find the solution to the Poisson equation very quickly, a large timestep is also desirable, such that an implicit scheme would be advisable.

4.5.3 Indexing in higher dimensions

Whereas in one spatial dimension, it is straightforward to collect the discretized values in a single vector and to find the next neighbours of a node, the latter requires a little thought in higher dimensions. To facilitate the construction of such models, we introduce here the **index function**, which takes the indices of a node as an input and returns the position where its value is stored in a vector as an output. Clearly, in one dimension we have

$$I(a) = a\,, \qquad 1 \le a \le N_x\,, \tag{4.110}$$

where N_x is the total number of nodes. In two dimensions, this becomes

$$I(a,b) = (b-1)N_x + a\,, \qquad 1 \le a \le N_x\,, \qquad 1 \le b \le N_y\,, \tag{4.111}$$

which can take all values in $1 \le I(a,b) \le N_xN_y$.

Finally, in three dimensions we have

$$\begin{aligned} I(a,b,c) &= (c-1)N_xN_y + (b-1)N_x + a\,, \\ 1 &\le a \le N_x\,, \qquad 1 \le b \le N_y\,, \qquad 1 \le c \le N_z\,, \end{aligned} \tag{4.112}$$

which takes the values in $1 \le I(a,b,c) \le N_xN_yN_z$. Of course, this is just one possible cartesian representation.

Since next-neighbors in space are in higher dimensions not always mapped to next neighbors in the solution vector, this has the consequence that a tri-diagonal form of the inversion matrix is not always attainable. Nevertheless, the matrix will always be quite sparse.

4.5.4 Nonlinear PDEs

Example: Fisher-Kolmogorov-Equation

When parts of the PDE are nonlinear, it is – at least concerning the nonlinear terms – usually simpler to use forward-time discretization. As an example, we consider the Fisher-Kolmogorov equation (4.83). The linearised version around the fixed values $\bar{n}_1 = 0$ and $\bar{n}_2 = 1$ becomes with $n(y,\tau) = \bar{n}_i + n_i(y,\tau)$

$$\frac{\partial n_1}{\partial\tau} = \frac{\partial^2 n_1}{\partial y^2} + n_1(y,\tau)\,, \qquad \frac{\partial n_2}{\partial\tau} = \frac{\partial^2 n_2}{\partial y^2} - n_2(y,\tau)\,. \tag{4.113}$$

When we use a conventional forward-time discretization on the linearized versions, a von-Neumann stability analysis yields the condition

$$|A| = \left|1 - 2\frac{\Delta\tau}{\Delta y^2}[1-\cos(k)] \pm \Delta\tau\right| \le 1\,. \tag{4.114}$$

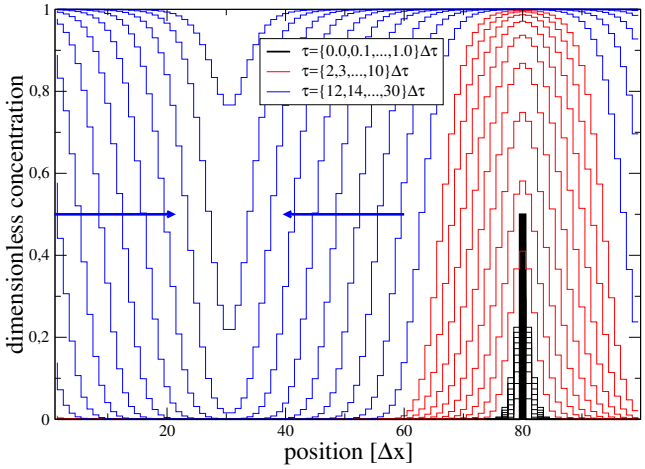

Figure 4.6: Numerical solution of the Fisher-Kolmogorov equation (4.83) dynamics. For small times (black), the initially sharply peaked distribution first smoothens (diffusion-dominated regime). For intermediate times (red), exponential growth in the central region sets in establishing two phases where $n(x,t) \in \{0,1\}$. Afterwards (blue), the phase boundary propagates like a travelling wave at dimensionless speed $v \approx 2$ (length of arrows: $20\Delta x$). Due to the periodic boundary conditions, the two wave fronts collide. Other parameters $\Delta x = 1$, $\Delta\tau = 0.1$

Therefore, it is important to keep in mind that for given discretization width Δy, the timestep Δt must remain bounded. It can actually be tested easily that when the timestep is chosen too large, the solution will diverge. For the full Fisher-Kolmogorov-equation we obtain the iteration scheme

$$u_a^{(n+1)} = u_a^{(n)} + \frac{\Delta\tau}{\Delta y^2}\left[u_{a+1}^{(n)} - 2u_a^{(n)} + u_{a-1}^{(n)}\right] + \Delta\tau u_a^{(n)}(1 - u_a^{(n)})\,. \tag{4.115}$$

When supplemented with periodic boundary conditions, this yields the dynamics shown in Fig. 4.6. We see that the speed of the resulting travelling wave is slightly larger than $v_{\min} = 2$.

Example: Korteweg-de-Vries Equation

Similarly, we can consider the evolution of solitons in the KdV equation (4.91). Here, the **forward-time discretization** yields (we start from the form $\partial_t u = -6u\partial_x u - \partial_x^3 u$)

$$u_a^{(n+1)} = u_a^{(n)}\left[1 - 3\frac{\Delta t}{\Delta x}\left(u_{a+1}^{(n)} - u_{a-1}^{(n)}\right)\right] - \frac{\Delta t}{2\Delta x^3}\left(u_{a+2}^{(n)} - 2u_{a+1}^{(n)} + 2u_{a-1}^{(n)} - u_{a-2}^{(n)}\right)\,. \tag{4.116}$$

When we assume periodic boundary conditions $u_{a+N}^n = u_a^n$, there is no need to find other discretizations of the third derivative at the boundary. Unfortunately, even when we neglect the nonlinear term, a von-Neumann stability analysis $u_a^{(n)} = A^n e^{ika}$ yields that $|A| \geq 1$ for all k, i.e., a forward discretization scheme is always unstable – regardless of the timestep width. Therefore, implicit methods must even be used for these types of problems, but even then there exists a variety of different approaches.

The simplest approach is to use a **semi-implicit** method. Rewriting the nonlinear term in the KdV equation we obtain

$$\frac{\partial u}{\partial t} = -3\frac{\partial u^2}{\partial x} - \frac{\partial^3 u}{\partial x^3}\,. \tag{4.117}$$

Treating all linear terms in a centered fashion and only the non-linear term explicitly (forward-time), we obtain a system that requires only matrix inversion for its propagation. For this, we first

write numerical approximations to the first and third derivative as

$$\begin{aligned}\frac{\partial u^2}{\partial x} &\approx \frac{\left(u_{a+1}^{(n)}\right)^2 - \left(u_{a-1}^{(n)}\right)^2}{2\Delta x}\,,\\ \frac{\partial^3 u}{\partial x^3} &\approx \frac{u_{a+2}^{(n)} - 2u_{a+1}^{(n)} + 2u_{a-1}^{(n)} - u_{a-2}^{(n)}}{4\Delta x^3} + \frac{u_{a+2}^{(n+1)} - 2u_{a+1}^{(n+1)} + 2u_{a-1}^{(n+1)} - u_{a-2}^{(n+1)}}{4\Delta x^3}\,.\end{aligned} \tag{4.118}$$

Sorting all forward-time terms to the left and backward-time terms to the right, we obtain

$$\begin{aligned}&u_a^{(n+1)}\\ &+\tfrac{\Delta t}{4\Delta x^3}\left(u_{a+2}^{(n+1)} - 2u_{a+1}^{(n+1)} + 2u_{a-1}^{(n+1)} - u_{a-2}^{(n+1)}\right)\end{aligned} \quad = \quad \begin{aligned}&u_a^{(n)}\\ &-\tfrac{\Delta t}{4\Delta x^3}\left(u_{a+2}^{(n)} - 2u_{a+1}^{(n)} + 2u_{a-1}^{(n)} - u_{a-2}^{(n)}\right)\\ &-3\tfrac{\Delta t}{2\Delta x}\left[\left(u_{a+1}^{(n)}\right)^2 - \left(u_{a-1}^{(n)}\right)^2\right]\end{aligned} \tag{4.119}$$

When we now apply a von-Neumann stability analysis $u_a^{(n)} = A^n e^{\mathrm{i}ka}$ and neglect the nonlinear terms this yields

$$A = \frac{1 - 2\mathrm{i}\alpha\left[\sin(2k) - \sin(k)\right]}{1 + 2\mathrm{i}\alpha\left[\sin(2k) - \sin(k)\right]}\,, \tag{4.120}$$

where $\alpha = \Delta t/(4\Delta x^3)$. Therefore, we conclude that $|A| = 1$ for all values of k. Unfortunately, any slight modification (recall that we have neglected the nonlinear terms completely) might spoil this fragile stability. Furthermore, we see that – assuming periodic boundary conditions and eliminating the redundant node – to propagate the system from n to $n+1$, we have to invert a matrix of the form

$$A = \begin{pmatrix} 1 & -2\alpha & +\alpha & & -\alpha & +2\alpha \\ +2\alpha & \ddots & \ddots & \ddots & & -\alpha \\ -\alpha & \ddots & \ddots & \ddots & \ddots & \\ & \ddots & \ddots & \ddots & \ddots & +\alpha \\ +\alpha & & \ddots & \ddots & \ddots & -2\alpha \\ -2\alpha & +\alpha & & -\alpha & +2\alpha & 1 \end{pmatrix}. \tag{4.121}$$

Inversion of this matrix is always possible when $|\alpha| = \Delta t/(4\Delta x^3) < 1/6$: In this case, the matrix is diagonally dominant, and the Gershgorin [15] circle theorem guarantees positivity of all eigenvalues. Unfortunately, to obey a reasonable spatial resolution, this requires to keep the timestep quite small.

The next possible improvement would be to treat also the nonlinear terms using a **Crank-Nicolson** discretization scheme. For simplicity, we will assume periodic boundary conditions throughout $u_N^{(n)} = u_0^{(n)}$ and eliminate the node $u_0^{(n)}$ from our considerations. Moving all terms to the right yields the nonlinear equation

$$\begin{aligned}0 &= -u_a^{(n)} + \alpha\left(u_{a+2}^{(n)} - 2u_{a+1}^{(n)} + 2u_{a-1}^{(n)} - u_{a-2}^{(n)}\right) + 3\beta\left[\left(u_{a+1}^{(n)}\right)^2 - \left(u_{a-1}^{(n)}\right)^2\right]\\ &\quad + u_a^{(n+1)} + \alpha\left(u_{a+2}^{(n+1)} - 2u_{a+1}^{(n+1)} + 2u_{a-1}^{(n+1)} - u_{a-2}^{(n+1)}\right) + 3\beta\left[\left(u_{a+1}^{(n+1)}\right)^2 - \left(u_{a-1}^{(n+1)}\right)^2\right]\\ &= f_a(u_1^{(n+1)}, \ldots, u_N^{(n+1)})\,,\end{aligned} \tag{4.122}$$

[15] Semyon Aronovich Gershgorin (1901 – 1933) was a soviet mathematician.

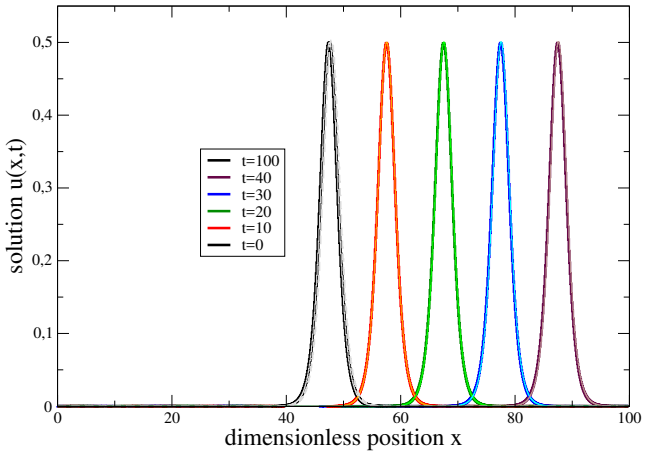

Figure 4.7: Numerical solution of the KdV equation with the soliton (4.96) with $b_0 = 20$. After $t = 100$, the soliton ($v = 1$) has completed one cycle (periodic boundary conditions), and for semi-implicit discretization (4.119) its shape has slightly changed (thin curves in lighter colors, $\Delta x = 0.1$, $\Delta t = 0.00025$). This error is not present in the fully implicit Crank-Nicolson treatment (4.122) with Newton iteration (bold curves, $\Delta x = 0.1$, $\Delta t = 0.25$). Beyond increased accuracy, the fully implicit Crank-Nicolson scheme was also about 1000 times faster.

where $\alpha = \Delta t/(4\Delta x^3)$ as before and $\beta = \frac{\Delta t}{4\Delta x}$. The spatial index obeys $1 \le a \le N$ and the perodic boundary conditions imply $a + N \hat{=} a$. This equation can be solved for $\boldsymbol{x} = \boldsymbol{u}^{(n+1)}$ using a-fixed-point method such as e.g. Newton-iteration. The Jacobian [16] of the vector-valued function $\boldsymbol{f}(\boldsymbol{x})$ becomes

$$\mathcal{J}(\boldsymbol{x}) = \begin{pmatrix} \frac{\partial f_1}{\partial x_1} & \cdots & \frac{\partial f_1}{\partial x_N} \\ \vdots & & \vdots \\ \frac{\partial f_N}{\partial x_1} & \cdots & \frac{\partial f_N}{\partial x_N} \end{pmatrix} = A + 6\beta \begin{pmatrix} 0 & +x_2 & & & -x_N \\ -x_1 & 0 & +x_3 & & \\ & \ddots & \ddots & \ddots & \\ & & \ddots & \ddots & +x_N \\ +x_1 & & & -x_{N-1} & 0 \end{pmatrix}. \quad (4.123)$$

That is, given the vector $\boldsymbol{u}^{(n)}$ we can e.g. define the initial guess $\boldsymbol{x}_0 = \boldsymbol{u}^{(n)}$ and then iterate

$$\boldsymbol{x}_{n+1} = \boldsymbol{x}_n - \mathcal{J}^{-1}(\boldsymbol{x}_n)\boldsymbol{f}(\boldsymbol{x}_n) \quad (4.124)$$

until convergence $|\boldsymbol{x}_N - \boldsymbol{x}_{N-1}| < \epsilon$ is reached. The final value does then correspond to the next timestep $\boldsymbol{u}^{(n+1)} = \boldsymbol{x}_N$. We note that we need not necessarily compute the inverse matrix explicitly but it suffices to solve the system $\mathcal{J}(\boldsymbol{x}_n)\boldsymbol{\Delta x} = -\boldsymbol{f}(\boldsymbol{x}_n)$ for $\boldsymbol{\Delta x}$ and then set $\boldsymbol{x}_{n+1} = \boldsymbol{x}_n + \boldsymbol{\Delta x}$. However, this comes with the advantage of treating all derivatives in a centered fashion, which greatly improves accuracy. Furthermore, we observe numerically that the timestep can now be chosen much larger, compare Fig. 4.7.

[16] Carl Gustav Jacob Jacobi (1804–1851) was a german mathematician.

Chapter 5

Master Equations

Many processes in nature are stochastic. In classical physics, this may be due to our incomplete knowledge of the system. Due to the unknown microstate of e.g. a gas in a box, the collisions of gas particles with the domain wall will appear random. In quantum theory, the evolution equations themselves involve amplitudes rather than observables in the lowest level, such that a stochastic evolution is intrinsic. In order to understand such processes in great detail, a description should include such random events via a probabilistic description. For dynamical systems, probabilities associated with events may evolve in time, and the determining equation for such a process is called master equation.

5.1 Rate Equations

If the master equation is a system of linear ODEs $\dot{\boldsymbol{P}} = T\boldsymbol{P}$, we will call it **rate equation**.

Box 18 (Rate Equation) *A rate equation is a first order differential equation describing the time evolution of probabilities, e.g. for discrete states*

$$\frac{dP_k}{dt} = \sum_\ell \left[T_{k\ell}P_\ell - T_{\ell k}P_k\right] , \qquad \dot{\boldsymbol{P}} = T\boldsymbol{P} , \tag{5.1}$$

where the $T_{k\neq\ell} > 0$ are positive transition rates from states ℓ to state k. In matrix representation, this implies

$$T = \begin{pmatrix} -\sum\limits_{i\neq 1} T_{i1} & T_{12} & \dots & T_{1N} \\ T_{21} & -\sum\limits_{i\neq 2} T_{i2} & & T_{2N} \\ \vdots & & \ddots & \vdots \\ T_{N1} & \dots & \dots & -\sum\limits_{i\neq N} T_{iN} \end{pmatrix} \tag{5.2}$$

The rate equation is said to satisfy **detailed balance**, when for the stationary state $T\bar{\boldsymbol{P}} = 0$ the equality $T_{k\ell}\bar{P}_\ell = T_{\ell k}\bar{P}_k$ holds for all pairs (k, ℓ) separately.

Furthermore, when the transition matrix $T_{k\ell}$ is symmetric, all processes are reversible at the level of the rate equation description.

Here, we will use the term **master equation** in more general terms describing any system of coupled ODEs for probabilities. This is more general than a rate equation, since, for example, the Markovian quantum master equation does in general not only involve probabilities (diagonals of the density matrix) but also coherences (off-diagonals).

It is straightforward to show that rate equations conserve the total probability

$$\sum_k \frac{dP_k}{dt} = \sum_{k\ell} \left(T_{k\ell} P_\ell - T_{\ell k} P_k\right) = \sum_{k\ell} \left(T_{\ell k} P_k - T_{\ell k} P_k\right) = 0\,. \tag{5.3}$$

Beyond this, all probabilities must remain positive, which is also respected by a normal rate equation: Evidently, the solution of a rate equation is continuous, such that when initialized with valid probabilities $0 \leq P_i(0) \leq 1$ all probabilities are non-negative initially. Let us assume that after some time, the probability P_k it the first to approach zero (such that all others are non-negative). Its time-derivative is then always non-negative

$$\left.\frac{dP_k}{dt}\right|_{P_k=0} = +\sum_\ell T_{k\ell} P_\ell \geq 0\,, \tag{5.4}$$

which implies that $P_k = 0$ is repulsive, and negative probabilities are prohibited.

Finally, the probabilities must remain smaller than one throughout the evolution. This however follows immediately from $\sum_k P_k = 1$ and $P_k \geq 0$ by contradiction.

In conclusion, a rate equation of the form (5.1) automatically preserves the sum of probabilities and also keeps $0 \leq P_i(t) \leq 1$ – a valid initialization provided. That is, under the evolution of a rate equation, probabilities remain probabilities.

5.1.1 Example 1: Fluctuating two-level system

Let us consider a system of two possible events, to which we associate the time-dependent probabilities $P_0(t)$ and $P_1(t)$. These events could for example be the two conformations of a molecule, the configurations of a spin, the two states of an excitable atom, etc. To introduce some dynamics, let the transition rate from $0 \to 1$ be denoted by $T_{10} > 0$ and the inverse transition rate $1 \to 0$ be denoted by $T_{01} > 0$. The associated master equation is then given by

$$\frac{d}{dt}\begin{pmatrix} P_0 \\ P_1 \end{pmatrix} = \begin{pmatrix} -T_{10} & +T_{01} \\ +T_{10} & -T_{01} \end{pmatrix}\begin{pmatrix} P_0 \\ P_1 \end{pmatrix} \tag{5.5}$$

5.1.2 Example 2: Interacting quantum dots

Imagine a double quantum dot, where the Coulomb interaction energy is so large that the doubly occupied state can be omitted from the considerations. In essence, only three states remain. Let $|0\rangle$ denote the empty, $|L\rangle$ the left-occupied, and $|R\rangle$ the right-occupied states, respectively. Now assume the two quantum dots to be tunnel-coupled to adjacent reservoirs but not among themselves. When we assume the transition rate to load the system from reservoir $\alpha \in \{L, R\}$ to be given by a product of a bare tunneling rate Γ_α and the occupation probability $0 < f_\alpha < 1$, it is also reasonable to assume that the rate of the inverse process is given by $\Gamma_\alpha(1 - f_\alpha)$, i.e., by

the product of bare tunneling rate and the probability to have a free space in the reservoir $1 - f_\alpha$. The total rate matrix then reads

$$T = \Gamma_L \begin{pmatrix} -f_L & 1-f_L & 0 \\ +f_L & -(1-f_L) & 0 \\ 0 & 0 & 0 \end{pmatrix} + \Gamma_R \begin{pmatrix} -f_R & 0 & 1-f_R \\ 0 & 0 & 0 \\ +f_R & 0 & -(1-f_R) \end{pmatrix} . \tag{5.6}$$

In fact, a microscopic derivation can be used to confirm the above-mentioned assumptions, and the parameters f_α become the Fermi functions

$$f_\alpha = \frac{1}{e^{\beta_\alpha(\epsilon_\alpha - \mu_\alpha)} + 1} \tag{5.7}$$

with inverse temperature β_α, chemical potentials μ_α, and dot level energy ϵ_α.

We recall that for rate matrices, all columns must add up to zero.

5.2 Density Matrix Formalism

5.2.1 Density Matrix

Suppose one wants to describe a quantum system, where the system state is not exactly known. That is, there is an ensemble of known normalized states $\{|\Phi_i\rangle\}$, but there is uncertainty in which of these states the system is. Such systems can be conveniently described by the density matrix formalism [6].

Box 19 (Density Matrix) *The density matrix can be written as*

$$\rho = \sum_i p_i \left|\Phi_i\right\rangle \left\langle\Phi_i\right| , \tag{5.8}$$

where $0 \leq p_i \leq 1$ denote the probabilities to be in the state $|\Phi_i\rangle$ with $\sum_i p_i = 1$. Note that we require the states to be normalized ($\langle\Phi_i|\Phi_i\rangle = 1$) but not generally orthogonal ($\langle\Phi_i|\Phi_j\rangle \neq \delta_{ij}$ is allowed).

Formally, any matrix fulfilling the properties

- *self-adjointness:* $\rho^\dagger = \rho$
- *normalization:* $\mathrm{Tr}\{\rho\} = 1$
- *positivity:* $\langle\Psi|\,\rho\,|\Psi\rangle \geq 0$ *for all vectors* Ψ

can be interpreted as a valid density matrix.

For a pure state one has $p_{\bar{i}} = 1$ for a particular $\bar{i}$ and thereby $\rho = |\Phi_{\bar{i}}\rangle\langle\Phi_{\bar{i}}|$. Evidently, a density matrix is pure if and only if $\rho = \rho^2$.

The expectation value of an operator for a known state $|\Psi\rangle$

$$\langle A\rangle = \langle\Psi|\,A\,|\Psi\rangle \tag{5.9}$$

can be obtained conveniently from the corresponding pure density matrix $\rho = |\Psi\rangle\langle\Psi|$ by simply computing the trace

$$\begin{aligned}\langle A\rangle &\equiv \mathrm{Tr}\{A\rho\} = \mathrm{Tr}\{\rho A\} = \mathrm{Tr}\{A|\Psi\rangle\langle\Psi|\} \\ &= \sum_n \langle n|A|\Psi\rangle\langle\Psi|n\rangle = \langle\Psi|\left(\sum_n |n\rangle\langle n|\right)A|\Psi\rangle \\ &= \langle\Psi|A|\Psi\rangle\ . \end{aligned} \tag{5.10}$$

When the state is not exactly known but its probability distribution, the expectation value is obtained by computing the weighted average

$$\langle A\rangle = \sum_i P_i \langle\Phi_i|A|\Phi_i\rangle\ , \tag{5.11}$$

where P_i denotes the probability to be in state $|\Phi_i\rangle$. The definition of obtaining expectation values by calculating traces of operators with the density matrix is also consistent with mixed states

$$\begin{aligned}\langle A\rangle &\equiv \mathrm{Tr}\{A\rho\} = \mathrm{Tr}\left\{A\sum_i p_i|\Phi_i\rangle\langle\Phi_i|\right\} = \sum_i p_i \mathrm{Tr}\{A|\Phi_i\rangle\langle\Phi_i|\} \\ &= \sum_i p_i \sum_n \langle n|A|\Phi_i\rangle\langle\Phi_i|n\rangle = \sum_i p_i \langle\Phi_i|\left(\sum_n |n\rangle\langle n|\right)A|\Phi_i\rangle \\ &= \sum_i p_i \langle\Phi_i|A|\Phi_i\rangle\ . \end{aligned} \tag{5.12}$$

To summarize, a density matrix formulation is a convenient way to describe the evolution of statistical mixtures (non-pure states).

We finally note that the (real-valued) diagonal entries of the density matrix are often called **populations**, whereas the (complex-valued) off-diagonal entries are termed **coherences**. However, these notions always depend on the chosen basis.

5.2.2 Dynamical Evolution in a closed system

The evolution of a pure state vector in a closed quantum system is described by the evolution operator $U(t)$, as e.g. for the Schrödinger equation

$$\left|\dot{\Psi}(t)\right\rangle = -\mathrm{i}H(t)|\Psi(t)\rangle \tag{5.13}$$

the time evolution operator

$$U(t) = \hat{\tau}\exp\left\{-i\int_0^t H(t')dt'\right\} \tag{5.14}$$

may be defined as the solution to the operator equation

$$\dot{U}(t) = -\mathrm{i}H(t)U(t)\,. \tag{5.15}$$

For constant $H(0) = H$, we simply have the solution $U(t) = e^{-\mathrm{i}Ht}$, but we have also already discussed the case of adiabatic evolution and periodic evolution in Sec. 3.2 and Sec. 3.3, respectively. From this, we conclude that a pure-state density matrix $\rho = |\Psi(t)\rangle \langle\Psi(t)|$ would evolve according to the von-Neumann equation

$$\dot{\rho} = -\mathrm{i}\,[H(t), \rho(t)] \tag{5.16}$$

with the formal solution $\rho(t) = U(t)\rho(0)U^\dagger(t)$, compare Eq. (5.14).

When we naively apply this evolution equation to a density matrix $\rho(0) = \sum_i p_i |\Phi_i\rangle \langle\Phi_i|$ that is not pure, we would obtain

$$\rho(t) = \sum_i p_i U(t) |\Phi_i\rangle \langle\Phi_i| U^\dagger(t)\,. \tag{5.17}$$

Since unitary transformations preserve the scalar product between all ket vectors, it follows that transitions between the (now time-dependent) state vectors $|\Phi_i(t)\rangle = U(t)|\Phi_i\rangle$ are impossible with unitary evolution. This means that the von-Neumann evolution equation does yield the same dynamics as the Schrödinger equation if it is restarted on different initial states $\rho_i^0 = |\Phi_i\rangle \langle\Phi_i|$.

Also the Measurement process can be generalized similarly. For a quantum state $|\Psi\rangle$, measurements are described by a set of measurement operators $\{M_m\}$, each corresponding to a certain measurement outcome, and with the completeness relation $\sum_m M_m^\dagger M_m = \mathbf{1}$. The probability of obtaining result m is given by

$$p_m = \langle\Psi| M_m^\dagger M_m |\Psi\rangle \tag{5.18}$$

and after the measurement with outcome m, the quantum state is collapsed

$$|\Psi\rangle \xrightarrow{m} \frac{M_m |\Psi\rangle}{\sqrt{\langle\Psi| M_m^\dagger M_m |\Psi\rangle}}\,. \tag{5.19}$$

The projective measurement is just a special case of that with $M_m = |m\rangle \langle m|$.

Box 20 (Measurements with density matrix) *For a set of measurement operators $\{M_m\}$ corresponding to different outcomes m and obeying the completeness relation $\sum_m M_m^\dagger M_m = \mathbf{1}$, the probability to obtain result m is given by*

$$p_m = \mathrm{Tr}\left\{M_m^\dagger M_m \rho\right\} \tag{5.20}$$

and action of measurement on the density matrix – provided that result m was obtained – can be summarized as

$$\rho \xrightarrow{m} \rho' = \frac{M_m \rho M_m^\dagger}{\mathrm{Tr}\left\{M_m^\dagger M_m \rho\right\}} \tag{5.21}$$

It is therefore straightforward to see that description by Schrödinger equation or von-Neumann equation with the respective measurement postulates are equivalent. The density matrix formalism conveniently includes statistical mixtures in the description but at the cost of quadratically increasing the number of state variables.

5.2.3 Most general evolution in an open system

A very convenient approach to general linear maps of the density matrix that preserve its properties is the so-called Kraus [1] representation.

Box 21 (Kraus representation) *The Kraus representation of a linear map of the density matrix is given by*

$$\rho' = \sum_\alpha K_\alpha \rho K_\alpha^\dagger \tag{5.22}$$

with $\sum_\alpha K_\alpha^\dagger K_\alpha = \mathbf{1}$ *and otherwise arbitrary Kraus operators* K_α*. It preserves all density matrix properties.*

It is straightforward to show that the properties trace, hermiticity, and positivity of ρ are also inherited by ρ'. That is, under the evolution of a Kraus map, density matrices remain density matrices. Special cases of Kraus maps are the evolution under measurement and also the unitary evolution of closed system. Below, we will see that specific non-unitary differential formulations of the density matrix evolution can also be related to Kraus maps.

5.3 Lindblad Master Equation

Any dynamical evolution equation for the density matrix should (at least in some approximate sense) preserve its interpretation as density matrix, i.e., trace, hermiticity, and positivity must be preserved. By construction, the mesurement postulate and unitary evolution preserve these properties. However, more general evolutions are conceivable. If we constrain ourselves to linear master equations that are local in time and have constant coefficients, the most general evolution that preserves trace, self-adjointness, and positivity of the density matrix is given by a Lindblad [2] form.

Box 22 (Lindblad form) *A master equation of Lindblad form has the structure*

$$\dot\rho = \mathcal{L}\rho = -\mathrm{i}\,[H,\rho] + \sum_{\alpha,\beta=1}^{N^2-1} \gamma_{\alpha\beta}\left(A_\alpha \rho A_\beta^\dagger - \frac{1}{2}\left\{A_\beta^\dagger A_\alpha, \rho\right\}\right), \tag{5.23}$$

where the hermitian operator $H = H^\dagger$ *can be interpreted as an effective Hamiltonian and* $\gamma_{\alpha\beta} = \gamma_{\beta\alpha}^*$ *is a positive semidefinite matrix, i.e., it fulfills* $\sum_{\alpha\beta} x_\alpha^* \gamma_{\alpha\beta} x_\beta \geq 0$ *for all vectors* x *(or, equivalently that all eigenvalues of* $(\gamma_{\alpha\beta})$ *are non-negative* $\lambda_i \geq 0$*).*

An alternative representation is

$$\dot\rho = \mathcal{L}\rho = -\mathrm{i}\,[H,\rho] + \sum_{\alpha=1}^{N^2-1}\left(B_\alpha \rho B_\alpha^\dagger - \frac{1}{2}\left\{B_\alpha^\dagger B_\alpha, \rho\right\}\right). \tag{5.24}$$

[1] Karl Kraus (1938 – 1988) was a german theoretical physicist.
[2] Göran Lindblad (1940–) is a swedish physicist.

We will now show that the Lindblad type master equation can be written in simpler form: As the dampening matrix γ is hermitian, it can be diagonalized by a suitable unitary transformation U, such that $\sum_{\alpha\beta} U_{\alpha'\alpha}\gamma_{\alpha\beta}(U^\dagger)_{\beta\beta'} = \delta_{\alpha'\beta'}\gamma_{\alpha'}$ with $\gamma_\alpha \geq 0$ representing its non-negative eigenvalues. Using this unitary operation, a new set of operators can be defined via $A_\alpha = \sum_{\alpha'} U_{\alpha'\alpha}L_{\alpha'}$. Inserting this decomposition in the master equation, we obtain

$$\begin{aligned}
\dot{\rho} &= -\mathrm{i}\,[H,\rho] + \sum_{\alpha,\beta=1}^{N^2-1} \gamma_{\alpha\beta}\left(A_\alpha \rho A_\beta^\dagger - \frac{1}{2}\left\{A_\beta^\dagger A_\alpha, \rho\right\}\right) \\
&= -\mathrm{i}\,[H,\rho] + \sum_{\alpha',\beta'}\left[\sum_{\alpha\beta}\gamma_{\alpha\beta}U_{\alpha'\alpha}U^*_{\beta'\beta}\right]\left(L_{\alpha'}\rho L_{\beta'}^\dagger - \frac{1}{2}\left\{L_{\beta'}^\dagger L_{\alpha'}, \rho\right\}\right) \\
&= -\mathrm{i}\,[H,\rho] + \sum_{\alpha}\gamma_\alpha\left(L_\alpha \rho L_\alpha^\dagger - \frac{1}{2}\left\{L_\alpha^\dagger L_\alpha, \rho\right\}\right)\,, \qquad (5.25)
\end{aligned}$$

where γ_α denote the N^2-1 non-negative eigenvalues of the dampening matrix. Finally, we can absorb the positive eigenvalues γ_α into the definition of the operators by defining $B_\alpha = \sqrt{\gamma_\alpha}L_\alpha$, which yields the form in Def. 22.

Evidently, the representation of a master equation is not unique. Any other unitary operation would lead to a different non-diagonal form which however describes the same physical dynamics. In addition, we note here that the master equation is not only invariant to unitary transformations of the operators A_α, but in the diagonal representation also to inhomogeneous transformations of the form

$$\begin{aligned}
L_\alpha &\to L'_\alpha = L_\alpha + a_\alpha \\
H &\to H' = H + \frac{1}{2\mathrm{i}}\sum_\alpha \gamma_\alpha\left(a_\alpha^* L_\alpha - a_\alpha L_\alpha^\dagger\right) + b\,, \qquad (5.26)
\end{aligned}$$

with complex numbers a_α and a real number b. The first of the above equations can be exploited to choose the Lindblad operators L_α traceless.

We would like to demonstrate the preservation of positivity here. Since preservation of hermiticity follows directly from the Lindblad form, we can – at any time – formally write the density matrix in its spectral representation

$$\rho(t) = \sum_j P_j(t)\,|\Psi_j(t)\rangle\,\langle\Psi_j(t)| \qquad (5.27)$$

with the eigenvalues $P_j(t) \in \mathbb{R}$ of the density matrix (we still have to show that these remain positive) and time-dependent orthonormal eigenstates obeying

$$\langle\Psi_i(t)|\Psi_j(t)\rangle = \delta_{ij} \qquad \Longrightarrow \qquad \left\langle\dot{\Psi}_i(t)|\Psi_j(t)\right\rangle + \left\langle\Psi_i(t)|\dot{\Psi}_j(t)\right\rangle = 0\,. \qquad (5.28)$$

With this decomposition, the time derivative of the density matrix becomes

$$\dot{\rho} = \sum_j\left[\dot{P}_j\,|\Psi_j\rangle\,\langle\Psi_j| + P_j\left|\dot{\Psi}_j\right\rangle\langle\Psi_j| + P_j\,|\Psi_j\rangle\left\langle\dot{\Psi}_j\right|\right]\,, \qquad (5.29)$$

and sandwiching the time derivative of the density matrix yields $\langle\Psi_j(t)|\,\dot\rho\,|\Psi_j(t)\rangle = \dot P_j(t)$. On the other hand, we can also use the Lindblad equation to obtain

$$\begin{aligned}\dot P_j &= -\mathrm{i}\,\langle\Psi_j|\,H\,|\Psi_j\rangle\,P_j + \mathrm{i}P_j\,\langle\Psi_j|\,H\,|\Psi_j\rangle \\ &\quad + \sum_\alpha \gamma_\alpha\Big[\,\langle\Psi_j|\,L_\alpha(\sum_k P_k\,|\Psi_k\rangle\,\langle\Psi_k|)L_\alpha^\dagger\,|\Psi_j\rangle - \frac{1}{2}\,\langle\Psi_j|\,L_\alpha^\dagger L_\alpha\left(\sum_k P_k\,|\Psi_k\rangle\,\langle\Psi_k|\right)|\Psi_j\rangle \\ &\quad -\frac{1}{2}\,\langle\Psi_j|\left(\sum_k P_k\,|\Psi_k\rangle\,\langle\Psi_k|\right)L_\alpha^\dagger L_\alpha\,|\Psi_j\rangle\,\Big] \\ &= \sum_k\left(\sum_\alpha \gamma_\alpha|\langle\Psi_j|\,L_\alpha\,|\Psi_k\rangle|^2\right)P_k - \left(\sum_\alpha\langle\Psi_j|\,L_\alpha^\dagger L_\alpha\,|\Psi_j\rangle\right)P_j\,. \end{aligned} \tag{5.30}$$

This is nothing but a rate equation with positive but time-dependent transition rates from $k\to j$

$$T_{jk}(t) = \sum_\alpha \gamma_\alpha|\langle\Psi_j(t)|\,L_\alpha\,|\Psi_k(t)\rangle|^2 \geq 0\,, \tag{5.31}$$

which implies for the sum over the reverse rates that

$$\begin{aligned}\sum_k T_{kj}(t) &= \sum_\alpha\gamma_\alpha\sum_k\langle\Psi_k|\,L_\alpha\,|\Psi_j\rangle\,\langle\Psi_j|\,L_\alpha^\dagger\,|\Psi_k\rangle = \sum_\alpha\gamma_\alpha\sum_k\langle\Psi_j|\,L_\alpha^\dagger\,|\Psi_k\rangle\,\langle\Psi_k|\,L_\alpha\,|\Psi_j\rangle \\ &= \sum_\alpha\gamma_\alpha\,\langle\Psi_j|\,L_\alpha^\dagger L_\alpha\,|\Psi_j\rangle\,, \end{aligned} \tag{5.32}$$

such that also the second term matches this representation. With our arguments from Sec. 5.1 it follows that the positivity of the eigenvalues $P_j(t)$ is granted. Unfortunately, the basis within which this simple rate equation holds is time-dependent and also only known after solving the master equation and diagonalizing the solution. It is therefore not very practical in most occasions. However, in many applications a basis admitting a rate equation representation can be found, which we will discuss below. Usually (but not always), the coherences in this case just decay and can therefore be neglected in the long-term limit. However, even in these fortunate cases it may become difficult to find the basis where the long-term density matrix becomes diagonal (i.e., the pointer basis) without solving the full master equation.

Formally, when the density matrix is written as a vector (first containing the populations and then the coherences), a master equation acts like a matrix – often called Liouvillian [3] Then, a rate equation representation means that the Liouvillian simply has block form letting populations and coherences evolve independently. In fact, the most common quantum-optical procedure for deriving a Lindblad master equation (successively applying the Born [4], Markov, and secular approximations) very often (in case of non-degenerate system Hamiltonians) leads to a simplified rate equation description in the energy eigenbasis of the system Hamiltonian.

5.3.1 Example: Master Equation for a driven cavity

When the cavity is driven with a laser and simultaneously coupled to a vaccuum bath $n_B = 0$, one may obtain the master equation

$$\dot\rho_\mathrm{S} = -\mathrm{i}\left[\Omega a^\dagger a + \frac{P}{2}e^{+i\omega t}a + \frac{P^*}{2}e^{-i\omega t}a^\dagger, \rho_\mathrm{S}\right] + \gamma\left[a\rho_\mathrm{S}a^\dagger - \frac{1}{2}a^\dagger a\rho_\mathrm{S} - \frac{1}{2}\rho_\mathrm{S}a^\dagger a\right]\,, \tag{5.33}$$

[3] Joseph Liouville (1809 – 1882) was a french mathematician.
[4] Max Born (1882–1970) was a german physicist and mathematician.

where the Laser frequency is denoted by ω and its amplitude by P. Similar to the Floquet treatent of Sec. 3.3, the transformation $\rho = e^{+\mathrm{i}\omega a^\dagger a t}\rho_S e^{-\mathrm{i}\omega a^\dagger a t}$ maps to a time-independent master equation

$$\dot\rho = -\mathrm{i}\,[H,\rho] + \gamma\left[a\rho a^\dagger - \frac{1}{2}a^\dagger a\rho - \frac{1}{2}\rho a^\dagger a\right], \qquad H = (\Omega-\omega)a^\dagger a + \frac{P}{2}a + \frac{P^*}{2}a^\dagger . \tag{5.34}$$

This equation obviously couples coherences and populations in the Fock space representation where $a\,|n\rangle = \sqrt{n}\,|n-1\rangle$ and $a^\dagger\,|n\rangle = \sqrt{n+1}\,|n+1\rangle$. Nevertheless, it can be mapped to a closed set of equations for certain expectation values, e.g. $\langle a^\dagger a\rangle$, $\langle a\rangle$, and $\langle a^\dagger\rangle$, which we leave as an exercise. To obtain a rate equation representation, we use the invariance of the Lindblad equation under shifts of the Lindblad operators and simultaneous modification of the Hamiltonian. According to Eq. (5.26), the master equation can be written as

$$\dot\rho = -\mathrm{i}\left[H + \frac{\gamma}{2\mathrm{i}}(\alpha^* a - \alpha a^\dagger) + \beta\mathbf{1}, \rho\right] + \gamma\left[(a+\alpha)\rho(a^\dagger+\alpha^*) - \frac{1}{2}\left\{(a^\dagger+\alpha^*)(a+\alpha),\rho\right\}\right] \tag{5.35}$$

with a priori unknown coefficients α and β. Now, by choosing $\alpha = \frac{P^*}{2(\Omega-\omega)-\mathrm{i}\gamma}$ we see that the effective Hamiltonian becomes diagonal $H + \frac{\gamma}{2\mathrm{i}}(\alpha^* a - \alpha a^\dagger) + \beta\mathbf{1} = (\Omega-\omega)\tilde a^\dagger\tilde a - \frac{(\Omega-\omega)|P|^2}{4(\Omega-\omega)^2+\gamma^2}$, where $\tilde a = a + \alpha$ denotes the transformed annihilation operator. In the master equation, we can neglect the constant shift term, such that it reads

$$\dot\rho \;=\; -\mathrm{i}\left[(\Omega-\omega)\tilde a^\dagger\tilde a, \rho\right] + \gamma\left[\tilde a\rho\tilde a^\dagger - \frac{1}{2}\left\{\tilde a^\dagger\tilde a,\rho\right\}\right] . \tag{5.36}$$

In the eigenbasis of $\tilde a^\dagger\tilde a$, the corresponding rate equation reads

$$\dot\rho_n = +\gamma(n+1)\rho_{n+1} - \gamma n\rho_n . \tag{5.37}$$

Here, we observe that there are only transitions from $n \to n-1$ but not opposite transitions. Consequently, the system will relax to the ground state ($n=0$) of the modified Hamiltonian

$$H' \;=\; (\Omega-\omega)\tilde a^\dagger\tilde a - \frac{(\Omega-\omega)|P|^2}{4(\Omega-\omega)^2+\gamma^2}\mathbf{1} . \tag{5.38}$$

The energy of the ground state is given by $E_0 = -\frac{(\Omega-\omega)|P|^2}{4(\Omega-\omega)^2+\gamma^2}$, which is consistent with the result that one would obtain from generating coupled equations of motion.

5.3.2 Superoperator notation

After all, a Lindblad equation is a first order ODE for the elements of the density matrix, which obeys special properties. Since it is linear in the density matrix, it is for many applications convenient to represent it in a superoperator form, where we represent the density matrix elements in a vector and let the action of the dissipator be represented by a matrix

$$\rho = \begin{pmatrix} \rho_{11} & \cdots & \rho_{1N} \\ \vdots & & \vdots \\ \rho_{N1} & \cdots & \rho_{NN} \end{pmatrix} \to \begin{pmatrix} \rho_{11} \\ \vdots \\ \rho_{NN} \\ \rho_{12} \\ \rho_{21} \\ \vdots \\ \rho_{N-1,N} \\ \rho_{N,N-1} \end{pmatrix} . \tag{5.39}$$

Here, we have the freedom of choosing the representation order, in the above example we first sort the populations and then the coherences. This is frequently done in the energy eigenbasis representation. It is customary to represent the matrices encoding the action of the Lindblad superoperator by calligraphic symbols, e.g. we could write the Lindblad equation in short as

$$\dot{\rho} = \mathcal{L}\rho\,. \tag{5.40}$$

Here, the matrix elements of the superoperator can be found by investigating which matrix elements of $\dot{\rho}$ couple to matrix elements of ρ.

A representation where the superoperator notation is more convenient consists in simply sorting the rows of the density matrix as columns

$$\rho = \begin{pmatrix} \rho_{11} & \cdots & \rho_{1N} \\ \vdots & & \vdots \\ \rho_{N1} & \cdots & \rho_{NN} \end{pmatrix} \rightarrow \begin{pmatrix} \rho_{11} \\ \vdots \\ \rho_{1N} \\ \vdots \\ \rho_{N1} \\ \vdots \\ \rho_{NN} \end{pmatrix}. \tag{5.41}$$

In this form, the superoperator representation can be obtained directly: For any operators A_L and A_R one has the relation

$$\mathcal{A}\rho = \left(A_L \otimes A_R^T\right)\rho \hat{=} A_L \rho A_R\,, \tag{5.42}$$

where A_R^T denotes the transpose of A_R. In particular, we note that both A_L and A_R may be the identity.

5.4 Full Counting Statistics in master equations

Very often, one is not only interested in the evolution of probabilities of certain states, but in the statistics of jumps between these states. This makes a big difference: For example, we can reach the ground state of the harmonic oscillator from its first excited state by the emission of a single photon. However, another process would be the absorbtion of e.g. three photons, followed by the sequential emission of four photons. For these two trajectories connecting the same initial and final state, a photo-detector measuring e.g. only the emitted photons would measure completely different signals. To infer the statistics of the latter is known as Full Counting Statistics.

5.4.1 Phenomenologic Identification of Jump Terms

Given a microscopic model, one can derive the statistics of the reservoir microscopically, and the methods for doing this can be combined with the conventional derivation of master equations [7]. However, when one is given a Lindblad master equation without microscopic derivation

$$\dot{\rho} = -\mathrm{i}[H,\rho] + \sum_\alpha \gamma_\alpha \left[L_\alpha \rho L_\alpha^\dagger - \frac{1}{2}\left\{L_\alpha^\dagger L_\alpha, \rho\right\}\right], \tag{5.43}$$

it is essential to interpret the transitions that are induced by the individual terms. Assuming that the density matrix at time t is given by a pure state $\rho(t) = |\Psi_i\rangle\langle\Psi_i|$, the probability to find it in an orthogonal state $P_f = \langle\Psi_f|\,\rho(t+\Delta t)\,|\Psi_f\rangle$ after an infinitesimally short time interval Δt is given by

$$P_f = +\sum_\alpha \gamma_\alpha \Delta t\, \langle\Psi_f|\, L_\alpha\, |\Psi_i\rangle\, \langle\Psi_i|\, L_\alpha^\dagger\, |\Psi_f\rangle\ . \tag{5.44}$$

Therefore, it appears quite natural to define the transition rate as

$$R_{i\to f} = \sum_\alpha \gamma_\alpha |\langle\Psi_f|\, L_\alpha\, |\Psi_i\rangle|^2\,. \tag{5.45}$$

We note that for orthogonal states $\langle\Psi_i|\Psi_f\rangle = 0$, the above definition is invariant with respect to shifts of the Lindblad operators (5.26). Therefore, these terms in the master equation are often also called **jump terms**. The quantum jumps go along with changes in e.g. the particle or energy content of the system

$$\Delta N_S = \langle\Psi_f|\, N\, |\Psi_f\rangle - \langle\Psi_i|\, N\, |\Psi_i\rangle\ , \qquad \Delta E_S = \langle\Psi_f|\, H\, |\Psi_f\rangle - \langle\Psi_i|\, H\, |\Psi_i\rangle\ , \tag{5.46}$$

which – when the system is only coupled to a single reservoir – must have been transferred into the reservoir (conservation of total energy and particle number provided). For multiple reservoirs ν, one often has a simple additive decomposition of the bare rates

$$\gamma_\alpha = \sum_\nu \gamma_\alpha^{(\nu)}\,, \tag{5.47}$$

where $\gamma_\alpha^{(\nu)}$ describes the coupling to reservoir ν only. This allows one to associate to the jump term

$$\mathcal{J}_\alpha^{(\nu)}\rho = \gamma_\alpha^{(\nu)} L_\alpha \rho L_\alpha^\dagger \tag{5.48}$$

in the master equation a transfer of energy and/or particles to the reservoir ν due to jump α. Thereby, one can by analyzing the influence of the jump terms obtain information about the statistics of energy and matter exchanges with the reservoir.

To track these also formally, it is useful to introduce the concept of a **conditional density matrix** $\rho^{(n)}(t)$, which describes the state of the system provided that the detector has counted n particles. By summing over all detector configurations we recover the original density matrix of the system

$$\rho = \sum_n \rho^{(n)}\,, \tag{5.49}$$

and consequently, $P_n(t) = \mathrm{Tr}\left\{\rho^{(n)}(t)\right\}$ describes the probability of the detector being in state n. Since we have identified the jump terms that lead to the exchange of particles with the reservoir, we can set up a differential equation for the conditioned density matrices from the Lindblad master equation

$$\dot\rho^{(n)} = \mathcal{L}_0\rho^{(n)} + \mathcal{L}_+\rho^{(n-1)} + \mathcal{L}_-\rho^{(n+1)}\,. \tag{5.50}$$

Above, we have assumed that at most one particle is transferred in single quantum jumps (which is typical for the weak-coupling limit). Here, $\mathcal{L}_+$ ($\mathcal{L}_-$) describes the part of the Liouvillian that

increases (decreases) the number of particles in the monitored reservoir by one. Consequently, $\mathcal{L}_0$ contains all remaining terms (which either leave the particle number invariant or describe jump processes to other reservoirs), and the total Liouvillian is just given by $\mathcal{L} = \mathcal{L}_0 + \mathcal{L}_- + \mathcal{L}_+$. If one is only interested in the total probability that n particles have been transferred, this is obtained by tracing out the system state

$$P_n(t) = \mathrm{Tr}\left\{\rho^{(n)}(t)\right\} . \tag{5.51}$$

It is in general quite difficult to obtain the $P_n(t)$ explicitly. Very often, a description in terms of moments or cumulants is much simpler to obtain. The translational invariance of the conditioned master equation (5.50) suggests to perform a Fourier transform

$$\rho(\chi, t) = \sum_n \rho^{(n)}(t) e^{+\mathrm{i}n\chi} , \tag{5.52}$$

and the FT variable χ is in this context for obvious reasons called counting field. We note that to obtain **moments** of the distribution $P_n(t)$, it suffices to calculate suitable derivatives with respect to the counting field

$$\left\langle n^k \right\rangle_t = \sum_n n^k P_n(t) = (-\mathrm{i}\partial_\chi)^k \mathrm{Tr}\left\{\rho(\chi, t)\right\}\Big|_{\chi=0} . \tag{5.53}$$

After the FT, the conditioned master equation becomes

$$\dot{\rho}(\chi, t) = \left(\mathcal{L}_0 + \mathcal{L}_+ e^{+\mathrm{i}\chi} + \mathcal{L}_- e^{-\mathrm{i}\chi}\right)\rho(\chi, t) = \mathcal{L}(\chi)\rho(\chi, t) , \tag{5.54}$$

where the counting field only enters as an ordinary parameter. Assuming that $\rho^{(n)}(0) = \delta_{n,0}\rho_0$, this is solved by $\rho(\chi, t) = e^{\mathcal{L}(\chi)t}\rho_0$, and consequently, the moment-generating function for $P_n(t)$ is given by

$$M(\chi, t) = \mathrm{Tr}\left\{e^{\mathcal{L}(\chi)t}\rho_0\right\} , \qquad \left\langle n^k \right\rangle_t = (-\mathrm{i}\partial_\chi)^k M(\chi, t)\Big|_{\chi=0} . \tag{5.55}$$

Alternatively, one may characterize a distribution completely using **cumulants**. These are obtained by derivatives of the cumulant-generating function, which is defined via the logarithm

$$C(\chi, t) = \log \mathrm{Tr}\left\{e^{\mathcal{L}(\chi)t}\rho_0\right\} , \qquad \left\langle\left\langle n^k \right\rangle\right\rangle_t = (-\mathrm{i}\partial_\chi)^k C(\chi, t)\Big|_{\chi=0} . \tag{5.56}$$

Up to now, these expressions are not particularly useful, as computing the exponential of a Liouvillian is cumbersome (it is in general not hermitian and may not admit diagonalization).

In the long-term limit, one may assume that the initial state is not of relevance, such that in practice, one often uses the long-term versions were the initial state is replaced by the stationary one

$$M(\chi, t) \to \mathrm{Tr}\left\{e^{\mathcal{L}(\chi)t}\bar{\rho}\right\} , \qquad C(\chi, t) \to \log \mathrm{Tr}\left\{e^{\mathcal{L}(\chi)t}\bar{\rho}\right\} , \tag{5.57}$$

which is obtained from $\mathcal{L}(0)\bar{\rho} = 0$. Assuming that there exists only a single stationary state (ergodicity), the cumulant-generating function may even be further simplified. To see this, we note that the Liouvillian $\mathcal{L}(0)$ must have eigenvalues with negative real part and a single vanishing eigenvalue describing the unique stationary state. Continuing this for non-vanishing χ, there must

exist one eigenvalue – which we call $\lambda(\chi)$ – with the property $\lambda(0) = 0$. For finite χ, it must have the largest real part of all eigenvalues (at least in a surrounding of $\chi = 0$). Now, we use that this dominant eigenvalue occurs in the Jordan-Block form as a separate entry

$$\begin{aligned} C(\chi,t) &= \log \mathrm{Tr}\left\{\mathcal{Q}(\chi)e^{\mathcal{Q}^{-1}(\chi)\mathcal{L}(\chi)\mathcal{Q}(\chi)}\mathcal{Q}^{-1}(\chi)\rho_0\right\} \to \log \mathrm{Tr}\left\{\mathcal{Q}(\chi)\left(\begin{array}{c|c} e^{\lambda(\chi)t} & 0 \\ \hline 0 & \mathbf{0}\end{array}\right)\mathcal{Q}^{-1}(\chi)\rho_0\right\} \\ &= \log\left[e^{\lambda(\chi)t}f(\chi)\right] = \lambda(\chi)t + \log f(\chi) \approx \lambda(\chi)t\,. \end{aligned} \tag{5.58}$$

Here, $\mathcal{Q}(\chi)$ is the similiarity transformation that maps to the Jordan block form, $f(\chi)$ is determined by the $Q(\chi)$ in a complicated way, and we have used that for sufficiently large times the only surviving eigenvalue is the one with the largest real part. The take-home message is that, to learn about the statistics $P_n(t)$, it suffices to obtain the dominant eigenvalue $\lambda(\chi)$ of the counting-field dependent Liouvillian.

5.4.2 Example: Single-Electron-Transistor

The possibly simplest example for a master equation is the single-electron-transistor, for which we have already discussed the current (1.76). Starting from a microscopic derivation (which we omit here), one obtains a Lindblad master equation acting in the Hilbert space of the central quantum dot (with basis vectors $|0\rangle$ and $|1\rangle$ denoting the empty and filled dot, respectively). For tunnel-couplings to two leads, it can be simplified to the form

$$\begin{aligned} \dot\rho &= -\mathrm{i}\left[\epsilon d^\dagger d,\rho\right] + (\Gamma_L f_L + \Gamma_R f_R)\left[d^\dagger\rho d - \frac{1}{2}\left\{dd^\dagger,\rho\right\}\right] \\ &\quad +(\Gamma_L(1-f_L) + \Gamma_R(1-f_R))\left[d\rho d^\dagger - \frac{1}{2}\left\{d^\dagger d,\rho\right\}\right], \end{aligned} \tag{5.59}$$

where $H = \epsilon d^\dagger d$ is the Hamiltonian of the dot with on-site energy ϵ, d ($d^\dagger$) are fermionic annihilation (creation) operators, Γ_ν are bare tunneling rates and $f_\nu = [e^{\beta_\nu(\epsilon-\mu_\nu)}+1]^{-1}$ are the Fermi functions of reservoir ν. Arranging the matrix elements of the density matrix in a vector

$$\begin{pmatrix} \rho_{00} & \rho_{01} \\ \rho_{10} & \rho_{11}\end{pmatrix} \Longrightarrow \begin{pmatrix} \rho_{00} \\ \rho_{11} \\ \rho_{01} \\ \rho_{10}\end{pmatrix}, \tag{5.60}$$

it is straightforward to see that the Lindblad equation can be represented as a superoperator of the form

$$\mathcal{L} = \sum_{\nu\in\{L,R\}}\begin{pmatrix} -\Gamma_\nu f_\nu & +\Gamma_\nu(1-f_\nu) & 0 & 0 \\ +\Gamma_\nu f_\nu & -\Gamma_\nu(1-f_\nu) & 0 & 0 \\ 0 & 0 & -\Gamma_\nu/2+\mathrm{i}\epsilon/2 & 0 \\ 0 & 0 & 0 & -\Gamma_\nu/2-\mathrm{i}\epsilon/2\end{pmatrix}. \tag{5.61}$$

We observe that here coherences and populations evolve independently, and that the coherences just decay. In fact, the assumptions used in the microscopic derivation of the master equation for this model are not compatible with initial superpositions of empty and filled electronic states, such that we may neglect the coherences completely. In what follows, we will therefore discuss the counting field analysis only for the population block $\mathcal{L}^{\mathrm{pop}}$ of the full dissipator.

Identifying the jump terms e.g. for jumps from the dot into the right reservoir $\Gamma_R(1-f_R)d\rho d^\dagger$ and jumps from the right reservoir into the dot $\Gamma_R f_R d^\dagger \rho d$ we see that these map to off-diagonal terms in the population part of the Liouvillian

$$\begin{aligned}\mathcal{L}_+^{\rm pop} &= \begin{pmatrix} 0 & \Gamma_R(1-f_R) \\ 0 & 0 \end{pmatrix}, \qquad \mathcal{L}_-^{\rm pop} = \begin{pmatrix} 0 & 0 \\ \Gamma_R f_R & 0 \end{pmatrix}, \\ \mathcal{L}_0^{\rm pop} &= \begin{pmatrix} -\Gamma_L f_L - \Gamma_R f_R & +\Gamma_L(1-f_L) \\ +\Gamma_L f_L & -\Gamma_L(1-f_L) - \Gamma_R(1-f_R) \end{pmatrix}. \end{aligned} \tag{5.62}$$

Altogether, this leads after Fourier transformation to the counting-field dependent Liouvillian

$$\mathcal{L}^{\rm pop}(\chi) = \begin{pmatrix} -\Gamma_L f_L - \Gamma_R f_R & +\Gamma_L(1-f_L) + \Gamma_R(1-f_R)e^{+{\rm i}\chi} \\ +\Gamma_L f_L + \Gamma_R f_R e^{-{\rm i}\chi} & -\Gamma_L(1-f_L) - \Gamma_R(1-f_R) \end{pmatrix}. \tag{5.63}$$

In essence, we have got an evolution equation enabling us to calculate the evolution of the joint probability distribution $P_{na}(t)$ describing the probabilities for having transferred n particles to the right reservoir and simultaneously leaving the system in state $a \in \{0,1\}$.

5.5 Entropy and Thermodynamics

5.5.1 Spohn's inequality

We learned that Lindblad equations unconditionally preserve the properties of the density matrix. However, beyond these certainly appealing property, there is more to say about Lindblad equations.

We first recall an early result by Lindblad [8] stating that completely-positive trace-preserving maps (Kraus maps) are contractive. To this end, we first start with some definitions. First, we define the von-Neumann entropy of the system

Box 23 (von-Neumann entropy) *The von-Neumann entropy of a system described by density matrix ρ is defined as*

$$S(\rho) = -{\rm Tr}\left\{\rho \ln \rho\right\}. \tag{5.64}$$

We have $0 \leq S(\rho) \leq \ln N$ for an $N \times N$ density matrix ρ.

The von-Neumann entropy can serve as an entanglement measure for states that are globally pure. It is sometimes used synonymously with the Shannon [5] entropy $S_{\rm Sh} = -\sum_i P_i \ln P_i$ but is strictly speaking not the same. The Shannon entropy is defined for a discrete probability distribution, if it is used in context with the density matrix one should specify what exactly is meant, it only coincides with the von-Neumann entropy when the P_i are the eigenvalues of ρ. The analogous diagonal entropy $S_{\rm D} = -\sum_i \rho_{ii} \ln \rho_{ii}$ is formally basis-dependent, whereas the von-Neumann entropy is not. Furthermore, we introduce a pseudo-distance between density matrices

[5] Claude Elwood Shannon (1916–2001) was an american mathematician and engineer, and the founder of information theory.

Box 24 (Quantum Relative Entropy) *The quantum relative entropy between two density matrices ρ and σ is defined as*

$$D(\rho||\sigma) = \mathrm{Tr}\left\{\rho\left(\ln\rho - \ln\sigma\right)\right\} . \tag{5.65}$$

Obviously, the relative entropy vanishes when the two density matrices are equal $D(\rho||\rho) = 0$. Furthermore, the relative entropy can be shown to be non-negative $D(\rho||\sigma) \geq 0$. However, since it is not symmetric, it is not a real distance. Lindblads result [8] states that Kraus maps $\mathcal{K}\rho = \rho'$ are contractive, i.e., that

$$D(\mathcal{K}\rho||\mathcal{K}\sigma) \leq D(\rho||\sigma) . \tag{5.66}$$

This can be exploited for Lindblad generators $\mathcal{L}$ in the following way: Taking the Kraus map $\mathcal{K} = e^{\mathcal{L}\Delta t}$ and choosing the distance to the steady state $\sigma = \bar{\rho}$, which fulfils $\mathcal{L}\bar{\rho} = 0$, we can expand the inequality

$$D\left(\rho||\bar{\rho}\right) - D\left(e^{\mathcal{L}\Delta t}\rho||\bar{\rho}\right) \geq 0 \tag{5.67}$$

for small Δt to obtain Spohn's [6] inequality [9].

Box 25 (Spohn's inequality) *Let $\mathcal{L}$ be a Lindblad-type generator and $\bar{\rho}$ its stationary state fulfilling $\mathcal{L}\bar{\rho} = 0$. Then, the physical evolution obeys at all times the inequality*

$$-\mathrm{Tr}\left\{[\mathcal{L}\rho][\ln\rho - \ln\bar{\rho}]\right\} \geq 0 . \tag{5.68}$$

We stress again that this inequality requires the evaluation e.g. of the matrix logarithm.

5.5.2 Phenomenologic definition of currents

Strictly speaking, a conventional master equation only tells us about the state of the system and not about the changes in the reservoir. For a system that is coupled to a single reservoir, we might from total conservation laws and the dynamics of the system conclude how much energy or how many particles have passed into the reservoir. This is different however for multiple reservoirs, which at non-equilibrium may give rise to steady-state currents. However, the additive decomposition of the Liouville superoperators allows us to phenomenologically identify contributions to the currents from individual reservoirs.

From the additive decomposition $\mathcal{L} = \sum_\nu \mathcal{L}^{(\nu)}$, we can conclude for the energy of the system

$$\frac{d}{dt}\langle E\rangle = \mathrm{Tr}\left\{H_S\dot{\rho}\right\} = -\mathrm{iTr}\left\{H_S[H_S,\rho]\right\} + \sum_\nu \mathrm{Tr}\left\{H_S(\mathcal{L}^{(\nu)}\rho)\right\} . \tag{5.69}$$

We immediately see that the first term vanishes, and that the contributions of the individual reservoirs are additive. This gives rise to the definition of the energy current entering the system from reservoir ν

$$I_E^{(\nu)} = \mathrm{Tr}\left\{H_S(\mathcal{L}^{(\nu)}\rho)\right\} = \mathrm{Tr}\left\{\mathcal{H}_S\mathcal{L}^{(\nu)}\rho\right\} . \tag{5.70}$$

[6] Herbert Spohn (born 1946) is a german mathematician and physicist at TU Munich.

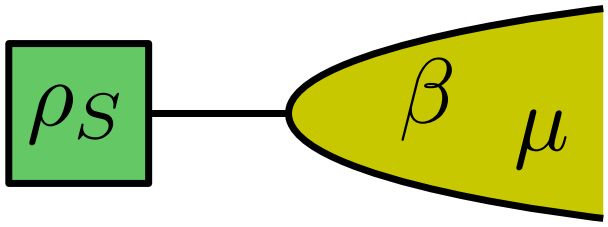

Figure 5.1: Sketch of a system (box) coupled via some generic coupling to a grand-canonical reservoir (5.73), characterized by inverse temperature β and chemical potential μ. There exists a class of master equations that generically predicts a long-term thermalization of the system, where the long-term density matrix $\rho_S \to \bar{\rho}_S$ approaches the system Gibbs state (5.74).

Similarly, we can define a particle current. This only makes sense if the system Hamiltonian conserves the total particle number $[N_S, H_S] = 0$, which leads to

$$\frac{d}{dt}\langle N\rangle = \mathrm{Tr}\left\{N_S\dot{\rho}\right\} = -\mathrm{iTr}\left\{N_S[H_S,\rho]\right\} + \sum_\nu \mathrm{Tr}\left\{N_S(\mathcal{L}^{(\nu)}\rho)\right\} . \tag{5.71}$$

Again, the commutator term vanishes whenever $[H_S, N_S] = 0$ and the particle (or matter) current entering the system from reservoir ν then becomes

$$I_M^{(\nu)} = \mathrm{Tr}\left\{N_S(\mathcal{L}^{(\nu)}\rho)\right\} = \mathrm{Tr}\left\{\mathcal{N}_S\mathcal{L}^{(\nu)}\rho\right\} . \tag{5.72}$$

We note that in these definitions we have mixed superoperator (calligraphic) and operator notations, which explains why we have put some brackets in the expressions.

Alternatively, such definitions of currents can of course be obtained form evaluating the first moments within the counting field formalism.

5.5.3 Thermodynamics of Lindblad equations

There exists a class of Lindblad equations that predicts thermalization of the system when it is only coupled to a single bath (compare Fig. 5.1), characterized by inverse temperature β and chemical potential μ

$$\bar{\rho}_\mathrm{B} = \frac{e^{-\beta(H_\mathrm{B}-\mu N_\mathrm{B})}}{\mathrm{Tr}\left\{e^{-\beta(H_\mathrm{B}-\mu N_\mathrm{B})}\right\}} , \tag{5.73}$$

where H_B denotes the reservoir Hamiltonian and N_B its particle number operator. In particular, this class arises in the weak-coupling limit from microscopic derivations that employ the Born-, Markov-, and secular approximations [10], and we will consequently denote it as the BMS class below. Under certain conditions, one can then prove that the stationary state of such a BMS master equation becomes the Gibbs [7] state

$$\bar{\rho}_\mathrm{S} = \frac{e^{-\beta(H_\mathrm{S}-\mu N_\mathrm{S})}}{\mathrm{Tr}\left\{e^{-\beta(H_\mathrm{S}-\mu N_\mathrm{S})}\right\}} , \tag{5.74}$$

i.e., both temperature β and chemical potential μ must equilibrate with the reservoir.

Finally, we consider the evolution of the system entropy.

[7] Josiah Willard Gibbs (1839–1903) was an american physicist with contributions to statistical mechanics and physical chemistry.

What is the meaning of the Spohn inequality (5.68), apart from its formal meaning as some contraction rate? Clearly, the first term is just the time derivative of the von-Neumann entropy

$$\dot{S}(\rho) \;=\; -\mathrm{Tr}\left\{\dot{\rho}\ln\rho\right\} - \mathrm{Tr}\left\{\rho\frac{d}{dt}\ln\rho\right\} = -\mathrm{Tr}\left\{(\mathcal{L}\rho)\ln\rho\right\}\,. \tag{5.75}$$

Here, we have used that the density matrix is always diagonalizable $\rho = U\rho_D U^\dagger$, leading to

$$\begin{aligned}\mathrm{Tr}\left\{\rho\frac{d}{dt}\ln\rho\right\} &= \mathrm{Tr}\left\{U\rho_D U^\dagger\dot{U}(\ln\rho_D)U^\dagger + U\rho_D U^\dagger U(\ln\rho_D)\dot{U}^\dagger + U\rho_D U^\dagger U\rho_D^{-1}\dot{\rho}_D U^\dagger\right\}\\ &= \mathrm{Tr}\left\{\rho_D U^\dagger\dot{U}(\ln\rho_D) + \rho_D(\ln\rho_D)\dot{U}^\dagger U + \dot{\rho}_D\right\}\\ &= \mathrm{Tr}\left\{\rho_D(\ln\rho_D)\left(\dot{U}^\dagger U + U^\dagger\dot{U}\right) + \dot{\rho}_D\right\} = 0\,,\end{aligned} \tag{5.76}$$

where we have used that $U^\dagger U = \mathbf{1}$, correspondingly $\dot{U}^\dagger U + U^\dagger\dot{U} = \mathbf{0}$, and $\mathrm{Tr}\left\{\dot{\rho}_D\right\} = 0$ (conservation of probabilities).

The interpretation of the remaining term in the time derivative of the entropy is different. When the stationary state of the system is a thermal Gibbs state $\bar{\rho} = e^{-\beta(H_S-\mu N_S)}/Z_S$ with inverse temperature β, chemical potential μ, system Hamiltonian H_S, and system particle number operator N_S, we would get

$$\begin{aligned}\mathrm{Tr}\left\{\rho(\ln\bar{\rho})\right\} &= -\beta\mathrm{Tr}\left\{(\mathcal{L}\rho)(H_S-\mu N_S)\right\} - \ln Z_S\mathrm{Tr}\left\{\mathcal{L}\rho\right\} = -\beta\mathrm{Tr}\left\{(H_S-\mu N_S)\mathcal{L}\rho\right\}\\ &= -\beta(I_E - \mu I_M) = -\beta\dot{Q}\,.\end{aligned} \tag{5.77}$$

where $\dot{Q}$ denotes the heat current entering the system from the reservoir. This terminology also implies that it counts positive when entering the system. Therefore, Spohn's inequality can be written as

$$\dot{S} - \beta\dot{Q} \geq 0\,, \tag{5.78}$$

which bounds the rate at which heat enters the system by the change of its entropy. The arguments we used for the system entropy also hold for the reservoir, such that

$$\dot{S}_{\mathrm{res}} = -\mathrm{Tr}\left\{\dot{\rho}\ln\rho\right\}\,. \tag{5.79}$$

Our simple master equation approach does not allow us to track the reservoir density matrix, such that of course the change of it is formally zero. However, if it were allowed to change, we would get by inserting at a specific time a thermal state $\rho = e^{-\beta(H_B-\mu N_B)}/Z_B$,

$$\dot{S}_{\mathrm{res}} = \beta\mathrm{Tr}\left\{\dot{\rho}(H_B-\mu N_B)\right\} + \ln Z_B\mathrm{Tr}\left\{\dot{\rho}\right\} = \beta\mathrm{Tr}\left\{\dot{\rho}(H_B-\mu N_B)\right\} = \beta\dot{Q}_{\mathrm{res}}\,, \tag{5.80}$$

where in the last equality we have simply inserted the definition of the heat entering the reservoir. Identifying the change of the reservoir energy and particle number with the corresponding negative changes in the system (this neglects effects of the interaction) we would get $-\beta\dot{Q} = \dot{S}_{\mathrm{res}}$, and eventually Spohn's inequality can be read as

$$\dot{S}_{\mathrm{sys}} + \dot{S}_{\mathrm{res}} \geq 0. \tag{5.81}$$

This is the second law of thermodynamics formulated for both system and reservoir (neglecting higher-order interaction effects)! Clearly, the system entropy may decrease (e.g. when a system relaxes down to its ground state), but at the same time, entropy is generated in the reservoirs. Since our master equation treatment is so far incomplete, we can up to now not track this contribution.

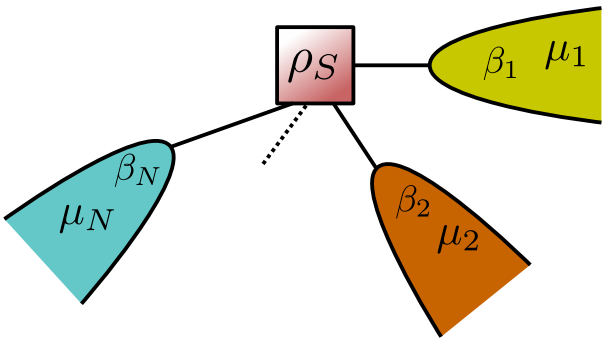

Figure 5.2: A system (box) is coupled to many different grand-canonical reservoirs, characterized by different inverse temperatures β_ν and chemical potentials μ_ν. The stationary state of the system is an unknown non-equilibrium stationary state, but the second law bounds the stationary heat currents exchanged with the reservoirs.

5.5.4 Nonequilibrium thermodynamics

We first phrase the necessary prerequisites. Let us assume that we have a system coupled to many reservoirs ν and subject to slow driving $H_S \to H_S(t)$, see Fig. 5.2. Further, we assume that the coupling to the reservoirs is weak, such that the resulting dissipator can be constructed additively from the dissipator to each reservoir

$$\mathcal{L} = \sum_\nu \mathcal{L}^{(\nu)} \,. \tag{5.82}$$

These assumptions are necessary to ensure that all previous approximations are applicable, such that only the parameters in the dissipators become time-dependent, eventually leading to a master equation of the form

$$\dot\rho = -\mathrm{i}[H_S(t),\rho] + \sum_\nu \mathcal{L}^{(\nu)}(t)\rho \,. \tag{5.83}$$

Looking at the energy balance of the system, we can directly state the first law of thermodynamics

$$\begin{aligned} \dot E &= \frac{d}{dt}\mathrm{Tr}\left\{H_S(t)\rho_S(t)\right\} \\ &= \mathrm{Tr}\left\{\dot H_S\rho_S\right\} + \sum_\nu \mu_\nu \mathrm{Tr}\left\{N_S(\mathcal{L}^{(\nu)}\rho)\right\} + \sum_\nu \mathrm{Tr}\left\{(H_S-\mu_\nu N_S)(\mathcal{L}^{(\nu)}\rho)\right\} \,. \end{aligned} \tag{5.84}$$

Here, the first term can be identified as mechanical work rate

$$\dot W = \mathrm{Tr}\left\{\dot H_S\rho_S\right\} \,, \tag{5.85}$$

the second as chemical work rate injected by reservoir ν

$$\dot W^{(\nu)} = \mu_\nu \mathrm{Tr}\left\{N_S(\mathcal{L}^{(\nu)}\rho)\right\} \,, \tag{5.86}$$

and the third as a heat current entering the system from reservoir ν

$$\dot Q^{(\nu)} = \mathrm{Tr}\left\{(H_S-\mu_\nu N_S)(\mathcal{L}^{(\nu)}\rho)\right\} \,. \tag{5.87}$$

We note that this is not a derivation of the first law. Rather, we have postulated it and used it to classify the individual currents. These definitions remain sensible when H_S is time-dependent.

Furthermore, we assume that also in case of slow time-dependent driving one has that the dissipators $\mathcal{L}^{(\nu)}(t)$ drag towards the **time-local** Gibbs state

$$\mathcal{L}^{(\nu)}(t)\frac{e^{-\beta_\nu(H_S(t)-\mu_\nu N_S)}}{Z} \equiv \mathcal{L}^{(\nu)}(t)\bar{\rho}^{(\nu)}(t) = 0\,. \tag{5.88}$$

In particular, this implies that

$$\ln \bar{\rho}^{(\nu)}(t) = -\beta_\nu(H_S(t) - \mu_\nu N_S) - \ln Z\,, \tag{5.89}$$

where $\ln Z$ is just a number, such that $\mathrm{Tr}\left\{(\mathcal{L}^{(\nu)}\rho)\ln Z\right\} = 0$. Then, we can show the second law in non-equilibrium as follows

$$\begin{aligned}
\dot{S}_{\mathrm{i}} &= \dot{S} - \sum_\nu \beta_\nu \dot{Q}^{(\nu)} \\
&= -\mathrm{Tr}\left\{\dot{\rho}\ln\rho\right\} + \sum_\nu \mathrm{Tr}\left\{[\mathcal{L}^{(\nu)}(t)\rho(t)]\ln\bar{\rho}^{(\nu)}(t)\right\} \\
&= -\sum_\nu \mathrm{Tr}\left\{[\mathcal{L}^{(\nu)}(t)\rho(t)][\ln\rho(t) - \ln\bar{\rho}^{(\nu)}(t)]\right\}\,,
\end{aligned} \tag{5.90}$$

where we have used that $\dot{S} = -\mathrm{Tr}\left\{\dot{\rho}\ln\rho\right\} = -\sum_\nu \mathrm{Tr}\left\{(\mathcal{L}^{(\nu)}\rho)\ln\rho\right\}$, since the commutator term does not contribute. With view on Eq. (5.88), we can for each term in the summation use Spohn's inequality to conclude that the entropy production rate

$$\dot{S}_{\mathrm{i}} = \dot{S} - \sum_\nu \beta_\nu \dot{Q}^{(\nu)} \geq 0\,. \tag{5.91}$$

This denotes the second law in presence of (slow) driving and multiple reservoirs. We stress that we have used only that the total Liouville superoperator is additive in the baths and probability conserving, and that the stationary state of each Lindblad superoperator is the local thermal equilibrium state, possibly depending on time.

To get a feeling for the meaning of this inequality, let us consider an undriven two-terminal setup (with left (L) and right (R) leads) in the long-term limit. Defining matter $I_M = +I_M^{(L)} = -I_M^{(2)}$ and energy $I_E = +I_E^{(L)} = -I_E^{(R)}$ currents from left to right (where we have used matter and energy conservation at steady state), the second law simplifies with $\dot{S} \to 0$ to

$$(\beta_R - \beta_L)I_E + (\beta_L\mu_L - \beta_R\mu_R)I_M \geq 0\,. \tag{5.92}$$

When now e.g. the temperatures are equal $\beta_L = \beta_R = \beta$, the inequality becomes $\beta(\mu_L - \mu_R)I_M \geq 0$. This simply tells us that the current must flow from high chemical potential to low chemical potential. Conversely, when the chemical potentials are equal ($\mu_L = \mu_R = \mu$), the inequality becomes $(\beta_R - \beta_L)(I_E - \mu I_M) = (\beta_R - \beta_L)Q \geq 0$. In this case, we recover the known formulation of the second law that heat Q always flows from hot to cold.

Chapter 6

Canonical Operator Transformations

The study of the dynamics of physical systems is deeply connected to the properties of operators. For example, the harmonic oscillator in quantum physics has an extremely simple form when represented with bosonic creation and annihilation operators $H = \hbar\omega(a^\dagger a + 1/2)$. From knowing the spectrum of the operator $a^\dagger a$, we can infer the full dynamics of the oscillator system. From the realization that, many different of such simple standard cases exist, it becomes obvious that transformations that map complicated Hamiltonians to simple ones can be extremely useful in practice.

6.1 Bogoliubov transformations

So far, we were mainly concerned with simple systems made of only a single constituent. To describe many particles and different modes, we will use creation and annihilation operators $a_k^\dagger$ and a_k specific for each mode k. In a nutshell, Bogoliubov [1] transformations map bosonic (or fermionic) creation and annihilation operators to new bosonic (or fermionic) creation and annihilation operators while leaving their (anti-)commutation relations invariant. We will discuss the bosonic case here, since the treatment of the fermionic case is similar provided the fermionic anticommutation relations are taken into account.

Box 26 (Bosonic Bogoliubov transform) *A bosonic Bogoliubov transform is a linear mapping between bosonic annihilation and creation operators, which preserves the corresponding bosonic commutation relations*

$$a_k = \sum_q \left[u_{kq} b_q + v_{kq} b_q^\dagger\right] , \qquad \begin{aligned} \left[a_k, a_{k'}^\dagger\right] &= \delta_{kk'} , \qquad [a_k, a_{k'}] = 0 , \\ \left[b_k, b_{k'}^\dagger\right] &= \delta_{kk'} , \qquad [b_k, b_{k'}] = 0 , \end{aligned}$$

where $u_{kq}, v_{kq} \in \mathbb{C}$. Similarly, a fermionic Bogoliubov transform is defined completely analogous as a linear transformation between fermionic operators that leaves the fermionic anticommutation relations invariant.

[1] Nikolay Bogoliubov (1909–1992) was an influential russian theoretical physicist with multiple contributions to quantum field theory, statistical mechanics, and dynamical systems.

The demand that the commutation relations must be preserved puts additional constraints on the a priori unknown coefficients u_{kq} and v_{kq}. For example, from the commutation relations we obtain the conditions

$$\begin{aligned}\left[a_k, a_{k'}^\dagger\right] &= \sum_q \left(u_{kq}u_{k'q}^* - v_{kq}v_{k'q}^*\right) = \delta_{kk'}\,,\\ [a_k, a_{k'}] &= \sum_q \left(u_{kq}v_{k'q} - v_{kq}u_{k'q}\right) = 0\,,\end{aligned} \tag{6.1}$$

where we note that the equation $\left[a_k^\dagger, a_{k'}^\dagger\right] = 0$ just adds the conjugate of the second constraint. In case of fermions, we would have equations of similar structure, just with a + instead of the − sign. First of all, we see that a simple but special solution to these equations is to choose $v_{kk'} = 0$. Then, creation and annihilation operators are not mixed, the second of Eq. (6.1) is trivially fulfilled, and the first reduces to a unitarity condition $\sum_q u_{kq}u_{k'q}^* = \delta_{kk'}$ on the matrix formed by the u_{kq}. In this case, the Bogoliubov transform therefore reduces to a **unitary transform between annihilation operators**. An even trivial examples of unitary Bogoliubov transforms are the multiplication of the creation and annihilation operators by a phase factor (absence of any mixing): When discussing operator transforms, we noted that time-dependent phase factors would e.g. arise in the interaction picture.

In the general case, interpreting the coefficients as matrix elements $u_{kq} = (U)_{kq}$ and $v_{kq} = (V)_{kq}$ as elements of matrices, we can also write these relations as

$$UU^\dagger - VV^\dagger = \mathbf{1}\,, \qquad UV^{\mathrm{T}} - VU^{\mathrm{T}} = \mathbf{0}\,. \tag{6.2}$$

Now, arranging the U and V matrices in an enlarged matrix

$$W = \begin{pmatrix} U^{\mathrm{T}} & V^\dagger \\ V^{\mathrm{T}} & U^\dagger \end{pmatrix}\,, \qquad W^{\mathrm{T}} = \begin{pmatrix} U & V \\ V^* & U^* \end{pmatrix}\,, \tag{6.3}$$

where A^{T} denotes the transpose of the matrix A, we see that we can encode the conditions (6.2) – or conjugate (transposes) thereof – into a single relation on the matrix W

$$W^{\mathrm{T}} \begin{pmatrix} \mathbf{0} & +\mathbf{1} \\ -\mathbf{1} & \mathbf{0} \end{pmatrix} W = \begin{pmatrix} \mathbf{0} & +\mathbf{1} \\ -\mathbf{1} & \mathbf{0} \end{pmatrix}\,. \tag{6.4}$$

Such matrices W are called **symplectic**, they have unit determinant and form a group under matrix multiplication. Consequently, in general Bogoliubov transforms are symplectic transforms of the creation and annihilation operators. Fortunately, even in the non-trivial cases, the symplectic transform is not completely fixed, which gives us the freedom to recast the Hamiltonian into a specific form. For fermions, we would again get a +-sign in the above equation.

The Bogoliubov transform can then be written as

$$\left(\begin{array}{c} \vdots \\ a_k \\ \vdots \\ \hline \vdots \\ a_k^\dagger \\ \vdots \end{array}\right) = \left(\begin{array}{c|c} U & V \\ \hline V^* & U^* \end{array}\right) \left(\begin{array}{c} \vdots \\ b_k \\ \vdots \\ \hline \vdots \\ b_k^\dagger \\ \vdots \end{array}\right) = W^{\mathrm{T}} \left(\begin{array}{c} \vdots \\ b_k \\ \vdots \\ \hline \vdots \\ b_k^\dagger \\ \vdots \end{array}\right)\,. \tag{6.5}$$

6.1.1 Example: Diagonalization of a homogeneous chain

Consider the hopping of bosons (or fermions) along a homogeneous but finite-sized chain with N sites

$$\begin{aligned} H &= \omega \sum_{i=1}^{N} a_i^\dagger a_i + T \sum_{i=1}^{N-1} a_i^\dagger a_{i+1} + T \sum_{i=1}^{N-1} a_{i+1}^\dagger a_i \\ &= (a_1^\dagger, \ldots, a_N^\dagger) \begin{pmatrix} \omega & T & & \\ T & \ddots & \ddots & \\ & \ddots & \ddots & T \\ & & T & \omega \end{pmatrix} \begin{pmatrix} a_1 \\ \vdots \\ \vdots \\ a_N \end{pmatrix} . \end{aligned} \tag{6.6}$$

We note that we have taken the freedom to choose T real, since any phase could have been absorbed in the definition of the bosonic operators. Since the Hamiltonian conserves the total number of particles, we choose a unitary Bogoliubov transform ($V = \mathbf{0}$, $\boldsymbol{a} = U\boldsymbol{b}$), which yields

$$H = (b_1^\dagger, \ldots, b_N^\dagger) U^\dagger \begin{pmatrix} \omega & T & & \\ T & \ddots & \ddots & \\ & \ddots & \ddots & T \\ & & T & \omega \end{pmatrix} U \begin{pmatrix} b_1 \\ \vdots \\ \vdots \\ b_N \end{pmatrix} \stackrel{!}{=} \sum_{k=1}^{N} \Omega_k b_k^\dagger b_k \, . \tag{6.7}$$

The special shape of our Bogoliubov transform is therefore given by

$$W = \begin{pmatrix} U^{\mathrm{T}} & \mathbf{0} \\ \mathbf{0} & U^\dagger \end{pmatrix} , \tag{6.8}$$

with a unitary matrix U. The eigenvalues and eigenvectors (composing the sought-after unitary) of such a simple tri-diagonal matrix are

$$\Omega_k = \omega - 2T \cos \frac{\pi k}{N+1} \, , \qquad \boldsymbol{u}_k = \begin{pmatrix} u_{1k} \\ u_{2k} \\ \vdots \\ u_{Nk} \end{pmatrix} = \sqrt{\frac{2}{N+1}} \begin{pmatrix} \sin \frac{1\pi k}{N+1} \\ \vdots \\ \sin \frac{N\pi k}{N+1} \end{pmatrix} , \tag{6.9}$$

where $1 \leq k \leq N$. Thus, we obtain the complete spectrum of the finite chain. Since we have chosen the Bogoliubov transform as unitary (creation and annihilation operators do not mix), the sign difference between fermions and bosons does not matter, and we obtain exactly the same transformation. However, for bosons we stress that in order keep the full spectrum bounded from below, it is necessary that for all k we have $\omega_k > 0$, which requires $|2T| < \omega$. For fermions, this requirement does not exist, since due to the Pauli exclusion principle we can only put N fermionic particles onto a chain with N sites, but an infinite number of bosons.

6.2 Jordan-Wigner Transform

Excursion: Tensor Product and Partial Trace

To properly define the Jordan-Wigner transform, we first provide a reminder of the tensor product. Roughly speaking, the tensor product represents a way to construct a larger vector space from two (or more) smaller vector spaces.

Box 27 (Tensor Product) *Let V and W be Hilbert spaces (vector spaces with scalar product) of dimension m and n with basis vectors $\{|v\rangle\}$ and $\{|w\rangle\}$, respectively. Then $V \otimes W$ is a Hilbert space of dimension $m \cdot n$, and a basis is spanned by $\{|v\rangle \otimes |w\rangle\}$, which is a set combining every basis vector of V with every basis vector of W.*

Mathematical properties

- *Bilinearity* $(z_1 |v_1\rangle + z_2 |v_2\rangle) \otimes |w\rangle = z_1 |v_1\rangle \otimes |w\rangle + z_2 |v_2\rangle \otimes |w\rangle$
- *operators acting on the combined Hilbert space* $A \otimes B$ *act on the basis states as* $(A \otimes B)(|v\rangle \otimes |w\rangle) = (A |v\rangle) \otimes (B |w\rangle)$
- *any linear operator on* $V \otimes W$ *can be decomposed as* $C = \sum_i c_i A_i \otimes B_i$
- *the scalar product is inherited in the natural way, i.e., one has for* $|a\rangle = \sum_{ij} a_{ij} |v_i\rangle \otimes |w_j\rangle$ *and* $|b\rangle = \sum_{k\ell} b_{k\ell} |v_k\rangle \otimes |w_\ell\rangle$ *the scalar product* $\langle a|b\rangle = \sum_{ijk\ell} a^*_{ij} b_{k\ell} \langle v_i|v_k\rangle \langle w_j|w_\ell\rangle = \sum_{ij} a^*_{ij} b_{ij}$

If more than just two vector spaces are combined to form a larger vector space, the dimension of the joint vector space grows rapidly, as e.g. exemplified by the case of a qubit: Its Hilbert space is just spanned by two vectors $|0\rangle$ and $|1\rangle$. The joint Hilbert space of two qubits is four-dimensional, of three qubits 8-dimensional, and of n qubits 2^n-dimensional. Eventually, this exponential growth of the Hilbert space dimension for composite quantum systems is at the heart of quantum computing.

As an example, let $\boldsymbol{\sigma}$ denote the vector of Pauli matrices, i.e.,

$$\sigma^1 = \begin{pmatrix} 0 & +1 \\ +1 & 0 \end{pmatrix} \qquad \sigma^2 = \begin{pmatrix} 0 & -\mathrm{i} \\ +\mathrm{i} & 0 \end{pmatrix} \qquad \sigma^3 = \begin{pmatrix} +1 & 0 \\ 0 & -1 \end{pmatrix} \tag{6.10}$$

Then we can compute the trace of the operator as follows

$$\begin{aligned} \Sigma &= a\mathbf{1} \otimes \mathbf{1} + \sum_{i=1}^{3} \alpha_i \sigma^i \otimes \mathbf{1} + \sum_{j=1}^{3} \beta_j \mathbf{1} \otimes \sigma^j + \sum_{i,j=1}^{3} a_{ij} \sigma^i \otimes \sigma^j \equiv \sum_{\alpha\beta=0}^{3} \Sigma_{\alpha\beta} \sigma^\alpha \otimes \sigma^\beta \,, \\ \mathrm{Tr}\{\Sigma\} &= \sum_{n_1 n_2} \langle n_1, n_2| \Sigma |n_1, n_2\rangle = \sum_{\alpha\beta} \Sigma_{\alpha\beta} \sum_{n_1} \langle n_1| \sigma^\alpha |n_1\rangle \sum_{n_2} \langle n_2| \sigma^\beta |n_2\rangle \\ &= 4\Sigma_{00} = 4a \,. \end{aligned} \tag{6.11}$$

Generally, since the scalar product is inherited, this enables a convenient calculation of the trace in case of a few operator decomposition, e.g., for just two operators

$$\begin{aligned} \mathrm{Tr}\{A \otimes B\} &= \sum_{n_A, n_B} \langle n_A, n_B| A \otimes B |n_A, n_B\rangle \\ &= \left[\sum_{n_A} \langle n_A| A |n_A\rangle\right] \left[\sum_{n_B} \langle n_B| B |n_B\rangle\right] \\ &= \mathrm{Tr}_A\{A\}\mathrm{Tr}_B\{B\} \,, \end{aligned} \tag{6.12}$$

where $\mathrm{Tr}_{A/B}$ denote the trace in the Hilbert space of A and B, respectively.

For composite systems, it is usually not necessary to keep all information of the complete system in the density matrix. Rather, one would like to have a density matrix that encodes all the

information on a particular subsystem only. Obviously, the map $\rho \to \mathrm{Tr}_\mathrm{B}\{\rho\}$ to such a reduced density matrix should leave all expectation values of observables A acting only on the considered subsystem invariant, i.e.,

$$\mathrm{Tr}\{A \otimes \mathbf{1}\rho\} = \mathrm{Tr}\{A\mathrm{Tr}_\mathrm{B}\{\rho\}\} \,. \tag{6.13}$$

If this basic condition was not fulfilled, there would be no point in defining such a thing as a reduced density matrix: Measurement would yield different results depending on the Hilbert space of the experimenters feeling.

Box 28 (Partial Trace) *Let $|a_1\rangle$ and $|a_2\rangle$ be vectors of state space A and $|b_1\rangle$ and $|b_2\rangle$ vectors of state space B. Then, the partial trace over state space B is defined via*

$$\mathrm{Tr}_\mathrm{B}\{|a_1\rangle\langle a_2| \otimes |b_1\rangle\langle b_2|\} = |a_1\rangle\langle a_2|\,\mathrm{Tr}\{|b_1\rangle\langle b_2|\} \,. \tag{6.14}$$

The partial trace is linear, such that the partial trace of arbitrary operators is calculated similarly. By choosing the $|a_\alpha\rangle$ and $|b_\gamma\rangle$ as an orthonormal basis in the respective Hilbert space, one may therefore calculate the most general partial trace via

$$\begin{aligned}
\mathrm{Tr}_\mathrm{B}\{C\} &= \mathrm{Tr}_\mathrm{B}\left\{\sum_{\alpha\beta\gamma\delta} c_{\alpha\beta\gamma\delta}\,|a_\alpha\rangle\langle a_\beta| \otimes |b_\gamma\rangle\langle b_\delta|\right\} \\
&= \sum_{\alpha\beta\gamma\delta} c_{\alpha\beta\gamma\delta}\mathrm{Tr}_\mathrm{B}\{|a_\alpha\rangle\langle a_\beta| \otimes |b_\gamma\rangle\langle b_\delta|\} \\
&= \sum_{\alpha\beta\gamma\delta} c_{\alpha\beta\gamma\delta}\,|a_\alpha\rangle\langle a_\beta|\,\mathrm{Tr}\{|b_\gamma\rangle\langle b_\delta|\} \\
&= \sum_{\alpha\beta\gamma\delta} c_{\alpha\beta\gamma\delta}\,|a_\alpha\rangle\langle a_\beta| \sum_\epsilon \langle b_\epsilon|b_\gamma\rangle\langle b_\delta|b_\epsilon\rangle \\
&= \sum_{\alpha\beta}\left[\sum_\gamma c_{\alpha\beta\gamma\gamma}\right]|a_\alpha\rangle\langle a_\beta| \,.
\end{aligned} \tag{6.15}$$

The definition 28 is the only linear map that respects the invariance of expectation values.

For example, to compute the partial trace of a pure density matrix $\rho = |\Psi\rangle\langle\Psi|$ in the bipartite state

$$|\Psi\rangle = \frac{1}{\sqrt{2}}(|01\rangle + |10\rangle) \equiv \frac{1}{\sqrt{2}}(|0\rangle \otimes |1\rangle + |1\rangle \otimes |0\rangle) \tag{6.16}$$

one would obtain

$$\mathrm{Tr}_2\{|\Psi\rangle\langle\Psi|\} = \frac{1}{2}|0\rangle\langle 0| + \frac{1}{2}|1\rangle\langle 1| \,. \tag{6.17}$$

A consequence of the tensor product construction is that operators acting on different Hilbert spaces must automatically commute, as we have already postulated in using different mode operators for the bosonic commutation relations

$$\left[a_k, a_q^\dagger\right] = \delta_{kq} \,, \qquad [a_k, a_q] = \left[a_k^\dagger, a_q^\dagger\right] = 0 \,. \tag{6.18}$$

For spin systems, this is very similar. In particular, any collection of two-level systems can be described by a spin-1/2 representation, where we simply add an index to the Pauli matrix describing the spin on which it is acting $\sigma^\alpha \to \sigma^\alpha_n$. The commutation relations for the Pauli matrices then become

$$[\sigma^x_n, \sigma^y_m] = 2\mathrm{i}\sigma^z_n \delta_{nm} \tag{6.19}$$

and cyclic permutations.

The Jordan-Wigner transform

The Jordan [2]-Wigner [3] transform maps a system of spin-1/2 particles to a system of fermions. Many different versions exist, each adapted to the particular shape of the problem to which it is applied. These versions are related by simple rotations in the spin basis.

Box 29 (Jordan-Wigner transform) *The Jordan-Wigner transform is given by*

$$\sigma^x_n = (c_n + c^\dagger_n) \prod_{m=1}^{n-1} \left(2c^\dagger_m c_m - \mathbf{1}\right) , \qquad \sigma^y_n = \mathrm{i}(c_n - c^\dagger_n) \prod_{m=1}^{n-1} \left(2c^\dagger_m c_m - \mathbf{1}\right) ,$$
$$\sigma^z_n = 2c^\dagger_n c_n - \mathbf{1} . \tag{6.20}$$

It maps a system of spins described by Pauli matrices σ^α_n acting on the site n two a system of fermionic operators c_n and vice versa. With $\sigma^\pm_n = (\sigma^x_n \pm \mathrm{i}\sigma^y_n)/2$, its inverse is given by

$$c_n = \sigma^z_1 \cdot \ldots \cdot \sigma^z_{n-1}\sigma^-_n = \underbrace{\sigma^z \otimes \ldots \otimes \sigma^z}_{n-1} \otimes \sigma^-_n \otimes \underbrace{\mathbf{1} \otimes \ldots \otimes \mathbf{1}}_{N-n} . \tag{6.21}$$

First, it is useful to see that the transformation indeed respects the fermionic operator anti-commutation relations. In the simplest case, we can consider $n = m$ and compute

$$\left\{c_n, c^\dagger_n\right\} = \sigma^-_n\sigma^+_n + \sigma^+_n\sigma^-_n = \mathbf{1} . \tag{6.22}$$

Here, we have used that $\sigma^z\sigma^z = \mathbf{1}$ and also the explicit representation of the $\sigma^\pm_n$ Pauli matrices. Similarly, we can calculate for $n < m$ (the opposite case can be generated by considering the adjoint equations)

$$\left\{c_n, c^\dagger_m\right\} = \sigma^-_n\sigma^z_n\sigma^z_{n+1} \ldots \sigma^z_{m-1}\sigma^+_m + \sigma^z_n\sigma^-_n\sigma^z_{n+1} \ldots \sigma^z_{m-1}\sigma^+_m = \mathbf{0} . \tag{6.23}$$

Here, we have simply used that $\{\sigma^\pm_n, \sigma^z_n\} = \mathbf{0}$, which follows straightforwardly from the single-site Pauli matrix relation $\left\{\sigma^\alpha, \sigma^\beta\right\} = 2\delta_{\alpha\beta}$. From $(\sigma^\pm)^2 = \mathbf{0}$ it also follows straightforwardly that $\{c_n, c_m\} = \mathbf{0}$ and similarly $\left\{c^\dagger_n, c^\dagger_m\right\} = \mathbf{0}$.

The inverse Jordan Wigner transform can be useful to represent fermionic operators by spins: For example, in computer algebra problems, it may be useful to implement the fermionic anticommutation relations by constructing them from Pauli matrix relations. On the other hand, we can

[2] Ernst Pascual Jordan (1902–1980) was a german theoretical and mathematical physicist.

[3] Eugene Paul Wigner (1902–1995) was a Hungarian-American theoretical physicist and nobel laureate, who studied chemical engineering at TU Berlin.

map spin models – in particular ones where the spins interact with each other along a chain – to non-interacting fermionic models, which can be further treated with methods such as Bogoliubov transforms.

We see that the transformation is actually useful in models that have a next-neighbour interaction along a chain such as

$$H = \sum_n g_n^x \sigma_n^x \sigma_{n+1}^x + \sum_n g_n^y \sigma_n^y \sigma_{n+1}^y + \sum_n g_n^z \sigma_n^z \,. \tag{6.24}$$

Here, we have assumed an infinitely long chain – the treatment of closed chains is also possible – and we have assumed that the interaction acts along the x and y components only. Upon inserting the Jordan-Wigner transform, we see that tails of σ^z operators mostly just cancel due to $(2c_n^\dagger c_n - \mathbf{1})^2 = \mathbf{1}$, and the model becomes

$$\begin{aligned} H &= \sum_n g_n^x (c_n + c_n^\dagger)(2c_n^\dagger c_n - \mathbf{1})(c_{n+1} + c_{n+1}^\dagger) - \sum_n g_n^y (c_n - c_n^\dagger)(2c_n^\dagger c_n - \mathbf{1})(c_{n+1} - c_{n+1}^\dagger) \\ &\quad + \sum_n g_n^z (2c_n^\dagger c_n - \mathbf{1}) \\ &= \sum_n g_n^x (c_n - c_n^\dagger)(c_{n+1} + c_{n+1}^\dagger) - \sum_n g_n^y (c_n + c_n^\dagger)(c_{n+1} - c_{n+1}^\dagger) + \sum_n g_n^z (c_n^\dagger c_n - c_n c_n^\dagger) \,. \end{aligned} \tag{6.25}$$

When now the model is also translationally invariant $g_n^x \to g^x$, $g_n^y \to g^y$, and $g_n^z \to g^z$, we can further treat it with Fourier transforms. It should be noted that translational invariance can for finite chain lengths $0 \leq n \leq N$ only be achieved with periodic boundary conditions, i.e., by closing the chain like a ring. For open chains of finite length, the Jordan-Wigner transform will give rise to fermionic product operators ranging over the complete chain. However, for very long chains we can neglect the boundary effects and try to obtain the spectrum of the chain by comparing with the infinite length limit. For finite chain lengths, we can perform a discrete Fourier transform of the creation and annihilation operators

$$c_n = \frac{1}{\sqrt{N}} \sum_{k=-(N-1)/2}^{+(N-1)/2} c_k e^{-\mathrm{i}2\pi \frac{nk}{N}} \,. \tag{6.26}$$

We note that this is nothing but a special unitary fermionic Bogoliubov transform, automatically preserving the anticommutation relations of the fermionic operators. As the chain length goes to infinity, the above discrete Fourier transform becomes with $\kappa = 2\pi k/N$ a mapping towards continuous operators $c(\kappa)$

$$c_n = \frac{\sqrt{N}}{2\pi} \int_{-\pi}^{+\pi} c(\kappa) e^{-\mathrm{i}n\kappa} d\kappa \,. \tag{6.27}$$

Here, n can take any integer value, and $-\pi \leq \kappa \leq +\pi$. Inserting the transformation, we can after some algebra obtain a form where only positive and negative frequency modes interact

$$\begin{aligned} H &= \frac{N}{2\pi} \int_0^\pi H(\kappa) d\kappa \\ H(\kappa) &= \Big\{ (g^x - g^y) 2\mathrm{i} \sin(\kappa) \left[c(+\kappa)c(-\kappa) + c^\dagger(+\kappa)c^\dagger(-\kappa) \right] \\ &\quad + (g^x + g^y) 2\cos(\kappa) \left[c(+\kappa)c^\dagger(+\kappa) + c(-\kappa)c^\dagger(-\kappa) \right] \\ &\quad + g^z \left[c^\dagger(+\kappa)c(+\kappa) - c(+\kappa)c^\dagger(+\kappa) + c^\dagger(-\kappa)c(-\kappa) - c(-\kappa)c^\dagger(-\kappa) \right] \Big\} \,. \end{aligned} \tag{6.28}$$

A fermionic Bogoliubiov transform can now be used to treat the model further and eventually map it to a Hamiltonian of the form $H = \int \left[\epsilon(\kappa) d^\dagger(\kappa) d(\kappa) + \gamma(\kappa)\mathbf{1}\right] d\kappa$. However, we can already from the above equation compute the ground state of the complete Hamiltonian. Considering only the subspace of pairs of opposite quasi-momenta, we can diagonalize the Hamiltonian $H(\kappa)$ in the four-dimensional subspace spanned by $c(k)$ and $c(-k)$. Its eigenvalues become

$$\begin{aligned}\epsilon_\pm(\kappa) &= 2\left((g^x+g^y)\cos(\kappa) \pm \sqrt{(g^x)^2+(g^y)^2+(g^z)^2-2(g^x+g^y)g^z\cos(\kappa)+2g^xg^y\cos(2\kappa)}\right), \\ \epsilon_{0/1} &= 2(g^x+g^y)\cos(\kappa)\,. \end{aligned} \tag{6.29}$$

From the observation that $\epsilon_-(\kappa) \leq \epsilon_{0/1}(\kappa) \leq \epsilon_+(\kappa)$ we see that the global ground state energy density can be constructed from

$$\begin{aligned}\frac{E_0}{N} &\to \epsilon \\ &= \frac{1}{2\pi}\int_0^\pi \epsilon_-(\kappa) d\kappa \\ &= -\frac{1}{\pi}\int_0^\pi \sqrt{(g^x)^2+(g^y)^2+(g^z)^2-2(g^x+g^y)g^z\cos(\kappa)+2g^xg^y\cos(2\kappa)}d\kappa\,. \end{aligned} \tag{6.30}$$

This integral can be solved analytically in specific cases. An important class of spin models is generated by the choice

$$g^x = -\Omega s\frac{1+\gamma}{2}\,, \qquad g^y = -\Omega s\frac{1-\gamma}{2}\,, \qquad g^z = -\Omega(1-s)\,, \tag{6.31}$$

where $-1 \leq \gamma \leq +1$ and $0 \leq s \leq 1$ are dimensionless parameters and Ω represents an overall energy scale. We see that there are some points where the spectrum changes in a non-analytic way. An analytic understanding, for example, can be obtained when $\gamma = +1$, which reproduces the one-dimensional quantum Ising [4] model in a transverse field

$$H(s) = -(1-s)\Omega\sum_n \sigma_n^z - s\Omega\sum_n \sigma_n^x\sigma_{n+1}^x\,. \tag{6.32}$$

Then, the ground state energy density can in the continuum limit be obtained analytically

$$\frac{E_0}{N} = -\frac{2}{\pi}\varepsilon(4s(1-s))\,, \tag{6.33}$$

where $\varepsilon(x)$ denotes the complete elliptic integral [11]. This approximation agrees well with the brute-force numerical diagonalization when N is large, see Fig. 6.1.

The complete elliptic integral $\varepsilon(4s(1-s))$ has the peculiar property that its second derivative diverges at the critical point $s_{\text{crit}} = 1/2$, whereas the function itself and its first derivative remain finite there, see Fig. 6.2. This serves as a formal classification of the Ising model as a second order quantum phase transition. Particularly, this is the Ising phase transition from paramagnetic ($s = 0$) to the ferromagnetic ($s = 1$) model. The fact that it is the second derivative which shows the first non-analytic behaviour as a function of the control parameter s can be used to classify it as a second order quantum phase transition. Here, the *quantum* terminology reminds us that this phase transition occurs – in stark contrast to classical phase transitions – at zero temperature and is intimitely related to non-analytic changes of the ground state at this point.

[4] Ernst Ising 1900–1998 was a german mathematician and physicist who treated a classical version of this model in his dissertation

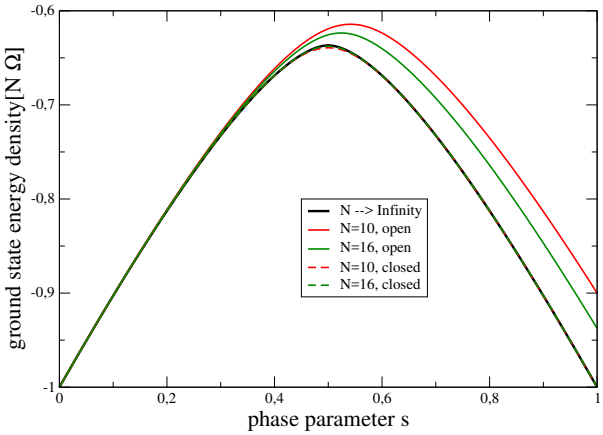

Figure 6.1: Plot of Eq. (6.33) and the numerical calculation of the lowest eigenvalue of Eq. (6.32). The finite-size effects clearly visible an open chain (thin solid curves) for $N = 10$ (Hilbert space dimension 1024) are significantly reduced already for $N = 16$ (Hilbert space dimension 65536). For $s = 1$, the deviation from the $N \to \infty$ ground state solution scales as $1/N$. Indeed, the convergence of the closed-chain calculations (dashed) to the analytic result is much faster.

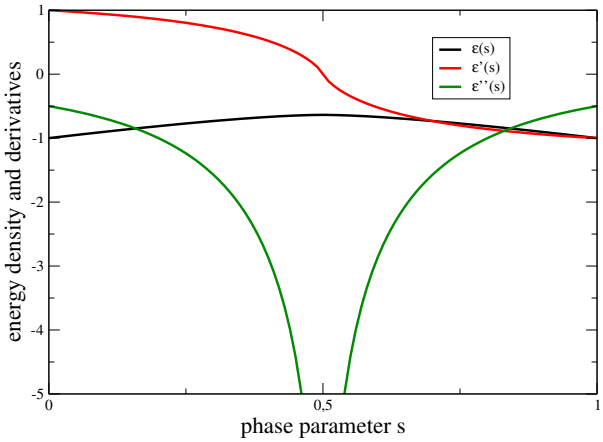

Figure 6.2: Plot of Eq. (6.33) and its first two derivatives. The second derivative diverges at the critical point, signaling the occurrence of a quantum phase transition in the ground state.

6.3 Collective Spin Models

A particular class of models arises from collectively coupling spin operators, as is e.g. apparent in the discussion of the influence of the nuclear spin onto the Schrödinger equation. There, it is customary to introduce **large-spin operators**

$$J^\alpha = \frac{1}{2}\sum_{n=1}^{N} \sigma_n^\alpha \,, \tag{6.34}$$

which obey the commutation relations

$$[J^x, J^y] = \mathrm{i} J^z \tag{6.35}$$

and cyclic permutations. From these in turn it also follows that the total angular momentum commutes with any component

$$[J^2, J^\alpha] = 0 \,, \tag{6.36}$$

which allows one to diagonalize these operators simultaneously. For convenience, we introduce the **ladder operators**

$$J^\pm = J^x \pm \mathrm{i} J^y = \sum_n \sigma_n^\pm \,, \qquad [J^-, J^+] = -2J^z \,. \tag{6.37}$$

It is customary to construct an eigenbasis for both J^2 and J^z with using these ladder operators. Clearly, the ground state of J^z is given by the many-particle state

$$\left|\frac{N}{2}, -\frac{N}{2}\right\rangle = |1\ldots1\rangle \,, \tag{6.38}$$

and it has the eigenvalue

$$J^z \left|\frac{N}{2}, -\frac{N}{2}\right\rangle = -\frac{N}{2}\left|\frac{N}{2}, -\frac{N}{2}\right\rangle \,. \tag{6.39}$$

Now, we could construct the basis of the full Hilbert space by simply looking at the 2^n eigenstates of the σ_i^z Pauli matrices

$$\begin{aligned} |0\rangle &\hat{=} |0\ldots00\rangle \,, \qquad |1\rangle \hat{=} |0\ldots01\rangle \,, \qquad |2\rangle \hat{=} |0\ldots10\rangle \,, \qquad |3\rangle \hat{=} |0\ldots11\rangle \,, \ldots \\ \left|2^N-1\right\rangle &\hat{=} |1\ldots11\rangle \,. \end{aligned} \tag{6.40}$$

This basis is commonly termed the **computational basis** in quantum information contexts [6]. Clearly, these basis states obey the eigenvalue equation

$$\sigma_i^z \,|n_1, \ldots, n_N\rangle = (-1)^{n_i} \,|n_1, \ldots, n_N\rangle \,, \tag{6.41}$$

but they are not eigenstates of the J^2 operator, which renders the basis unsuitable for problems conserving the total angular momentum.

Instead, using the angular momentum eigenstates, characterized by

$$J^2 \,|j,m\rangle = j(j+1)\,|j,m\rangle \,, \qquad J^z \,|j,m\rangle = m\,|j,m\rangle \,, \tag{6.42}$$

where $j \in \{0, \frac{1}{2}, \ldots, \frac{N}{2}\}$ can either assume positive integer or positive half-integer values and similarly $-j \leq m \leq +j$, one can see that the ladder operators can be used to construct an orthonormal basis from just one particular state in each sector with total angular momentum j. In particular, they act on the states $|j, m\rangle$ as

$$J^{\pm} |j, m\rangle = \sqrt{j(j+1) - m(m \pm 1)}\, |j, m \pm 1\rangle \ , \tag{6.43}$$

which one can use to demonstrate with $J^2 = \frac{1}{2} J^+ J^- + \frac{1}{2} J^- J^+ + (J^z)^2$ and $[J^-, J^+] = -2J^z$ that the eigenvalue equations for the large spin (6.42) are preserved. The original computational basis can be seen as the eigenbasis of the individual spins. When we represent the angular momentum eigenstates in the original computational basis, the resulting expansion coefficients are nothing but the well-known Clebsch [5]- Gordon [6] coefficients.

The case is simple for $N = 2$, where the fully symmetric (maximum total angular momentum) subspace reads

$$\begin{aligned} |1, -1\rangle &= |11\rangle \ , \\ |1, 0\rangle &= \frac{1}{\sqrt{2}} [|10\rangle + |01\rangle] && = \frac{1}{\sqrt{2}} J^+ |1, -1\rangle \ , \\ |1, +1\rangle &= |00\rangle && = J^+ |1, 0\rangle \ . \end{aligned} \tag{6.44}$$

To construct the full Hilbert space basis, there is just one state left, which has vanishing total angular momentum

$$|0, 0\rangle \ = \frac{1}{\sqrt{2}} [|10\rangle - |01\rangle] \ , \tag{6.45}$$

and we see that it is annihilated by the raising operator $J^+ |0, 0\rangle = 0$.

Things become more complicated already when $N = 3$, we would in principle have a Hilbert space dimension of $8 = 2^3$. The fully symmetric subspace of maximal angular momentum however has only four states

$$\begin{aligned} \left|\frac{3}{2}, -\frac{3}{2}\right\rangle &= |111\rangle \ , \\ \left|\frac{3}{2}, -\frac{1}{2}\right\rangle &= \frac{1}{\sqrt{3}} [|110\rangle + |101\rangle + |011\rangle] && = \frac{1}{\sqrt{3}} J^+ \left|\frac{3}{2}, -\frac{3}{2}\right\rangle \ , \\ \left|\frac{3}{2}, +\frac{1}{2}\right\rangle &= \frac{1}{\sqrt{3}} [|001\rangle + |010\rangle + |100\rangle] && = \frac{1}{2} J^+ \left|\frac{3}{2}, -\frac{1}{2}\right\rangle \ , \\ \left|\frac{3}{2}, +\frac{3}{2}\right\rangle &= |000\rangle && = \frac{1}{\sqrt{3}} J^+ \left|\frac{3}{2}, +\frac{1}{2}\right\rangle \ . \end{aligned} \tag{6.46}$$

The remaining states are obtained by considering the total angular momentum $j = 1/2$ instead. There, one finds that there are two independent blocks with $j = 1/2$ each supporting $m = \pm 1/2$, such that in total one has again 8 states. For example, we can construct orthogonal states

$$\begin{aligned} \left|\frac{1}{2}, -\frac{1}{2}\right\rangle_a &= \frac{1}{\sqrt{2}} [|110\rangle - |011\rangle] \ , \\ \left|\frac{1}{2}, +\frac{1}{2}\right\rangle_a &= \frac{1}{\sqrt{2}} [|100\rangle - |001\rangle] = J^+ \left|\frac{1}{2}, -\frac{1}{2}\right\rangle_a \end{aligned} \tag{6.47}$$

[5] Rudolf Friedrich Alfred Clebsch (1833–1872) was a german mathematician.
[6] Paul Albert Gordan (1837–1912) was a german mathematician.

and also

$$\left|\frac{1}{2},-\frac{1}{2}\right\rangle_b = \frac{1}{\sqrt{6}}\left[|1110\rangle - 2\,|1101\rangle + |1011\rangle\right] ,$$
$$\left|\frac{1}{2},+\frac{1}{2}\right\rangle_b = \frac{1}{\sqrt{6}}\left[-|1001\rangle + 2\,|1010\rangle - |1100\rangle\right] = J^+\left|\frac{1}{2},-\frac{1}{2}\right\rangle_b . \tag{6.48}$$

When $N = 4$, the symmetric subspace with $j = 2$ contains five states

$$\begin{aligned}
|2,-2\rangle &= |1111\rangle ,\\
|2,-1\rangle &= \frac{1}{2}\left[|1110\rangle + |1101\rangle + |1011\rangle + |0111\rangle\right] &&= \frac{1}{2}J^+\,|2,-2\rangle ,\\
|2,0\rangle &= \frac{1}{\sqrt{6}}\left[|1100\rangle + |1010\rangle + |1001\rangle + |0110\rangle + |0101\rangle + |0011\rangle\right] &&= \frac{1}{\sqrt{6}}J^+\,|2,-1\rangle ,\\
|2,+1\rangle &= \frac{1}{2}\left[|1000\rangle + |0100\rangle + |0010\rangle + |0001\rangle\right] &&= \frac{1}{\sqrt{6}}J^+\,|2,0\rangle ,\\
|2,+2\rangle &= |0000\rangle &&= \frac{1}{2}J^+\,|2,+1\rangle .
\end{aligned} \tag{6.49}$$

Again, we can construct the missing orthogonal states by considering first $j = 1$

$$\begin{aligned}
|1,-1\rangle_a &= \frac{1}{\sqrt{2}}\left[|1110\rangle - |0111\rangle\right] ,\\
|1,0\rangle_a &= \frac{1}{2}\left[|1100\rangle + |1010\rangle - |0101\rangle - |0011\rangle\right] &&= \frac{1}{\sqrt{2}}J^+\,|1,-1\rangle_a ,\\
|1,+1\rangle_a &= \frac{1}{\sqrt{2}}\left[|1000\rangle - |0001\rangle\right] &&= \frac{1}{\sqrt{2}}J^+\,|1,0\rangle_a ,\\
|1,-1\rangle_b &= \frac{1}{\sqrt{2}}\left[|1101\rangle - |1011\rangle\right] ,\\
|1,0\rangle_b &= \frac{1}{2}\left[|1100\rangle - |1010\rangle + |0101\rangle - |0011\rangle\right] &&= \frac{1}{\sqrt{2}}J^+\,|1,-1\rangle_b ,\\
|1,+1\rangle_b &= \frac{1}{\sqrt{2}}\left[|0100\rangle - |0010\rangle\right] &&= \frac{1}{\sqrt{2}}J^+\,|1,0\rangle_b ,\\
|1,-1\rangle_c &= \frac{1}{2}\left[+|1110\rangle - |1101\rangle - |1011\rangle + |0111\rangle\right] ,\\
|1,0\rangle_c &= \frac{1}{\sqrt{2}}\left[-|1001\rangle + |0110\rangle\right] &&= \frac{1}{\sqrt{2}}J^+\,|1,-1\rangle_c ,\\
|1,+1\rangle_c &= \frac{1}{2}\left[-|1000\rangle + |0100\rangle + |0010\rangle - |0001\rangle\right] &&= \frac{1}{\sqrt{2}}J^+\,|1,0\rangle_c .
\end{aligned} \tag{6.50}$$

Eventually, we have only two states left, which are then given by

$$|0,0\rangle_a = \frac{1}{\sqrt{12}}\left[|1100\rangle + |1010\rangle - 2\,|1001\rangle - 2\,|0110\rangle + |0101\rangle + |0011\rangle\right] ,$$
$$|0,0\rangle_b = \frac{1}{2}\left[|1100\rangle - |1010\rangle - |0101\rangle + |0011\rangle\right] . \tag{6.51}$$

Specifically, we see that these are annihilated by acting the the ladder raising operator $J^+\,|0,0\rangle_a = 0$ and $J^+\,|0,0\rangle_b = 0$.

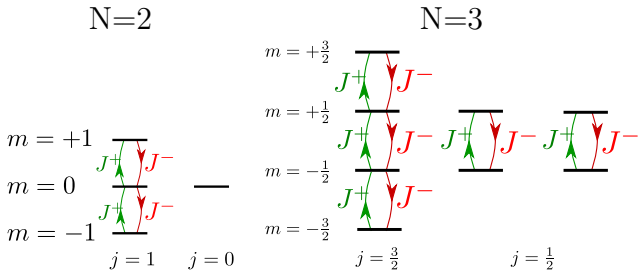

Figure 6.3: Sketch of the $|j, m\rangle$ eigenstates of the angular momentum operators J^2 and J^z for a system formed of $N = 2$, and $N = 3$ qubits. The full Hilbert space dimension is always 2^N, such that there are degenerate angular momentum states.

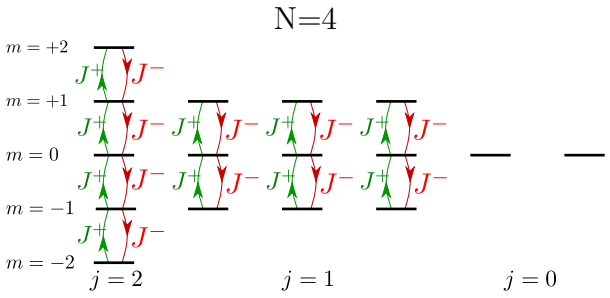

Figure 6.4: Same as Fig. 6.3, just for $N = 4$. The application of the J^+ ladder operator always annihilates the topmost states, the application of J^- the bottom states. States with $j = m = 0$ belong to the kernel of $J^{\pm}$.

The situation is summarized in Figs. 6.3 and 6.4. By looking only at the maximum angular momentum subspace $j = N/2$, we therefore constrain ourselves to the subspace of fully symmetric states. In the general case of N, we can therefore in the fully symmetric (maximum $j = N/2$) subspace construct the eigenstates by acting with J^+ on the global ground state $|1 \dots 1\rangle$ and normalizing afterwards. Then, we look for vectors that are orthonormal to $J^+ |1 \dots 1\rangle$ and take these as the foundation to construct further basis vectors with the ladder operator. This procedure is repeated until a complete basis is found.

6.3.1 Example: The Lipkin-Meshkov-Glick model

The Lipkin [7] -Meshkov-Glick (LMG) model originated in nuclear physics and was used as a toy model to describe the interaction of nuclear spins. Since these are very close together, it is assumed that they essentially interact uniformly with each other and with an external magnetic field

$$H_{\text{LMG}} = -hJ^z - \frac{\gamma}{N}(J^x)^2 = -\frac{h}{2}\sum_{i=1}^{N}\sigma_i^z - \frac{\gamma}{4N}\sum_{i,j=1}^{N}\sigma_i^x\sigma_j^x \tag{6.52}$$

Sometimes, the model is also supplemented with a $(J^y)^2$ term. Clearly, it commutes with the total angular momentum operator J^2. Furthermore, one can check that it commutes with the parity operator

$$P = e^{\mathrm{i}\pi\frac{N}{2}+\mathrm{i}\pi J^z}\,, \tag{6.53}$$

for which one can show that $PJ^xP^\dagger = -J^x$.

We will try to get an estimate for the ground state energy by exploiting the symmetry of the problem. A suitable ansatz for the ground state wave function could be

$$\Psi(\phi) = \bigotimes_{\ell=1}^{N}\left[\cos(\phi)\,|0\rangle_\ell + \sin(\phi)\,|1\rangle_\ell\right]\,, \tag{6.54}$$

[7] Harry Jeannot Lipkin 1921–2015 was an israeli theoretical physicist with notable contributions to nuclear and elementary physics.

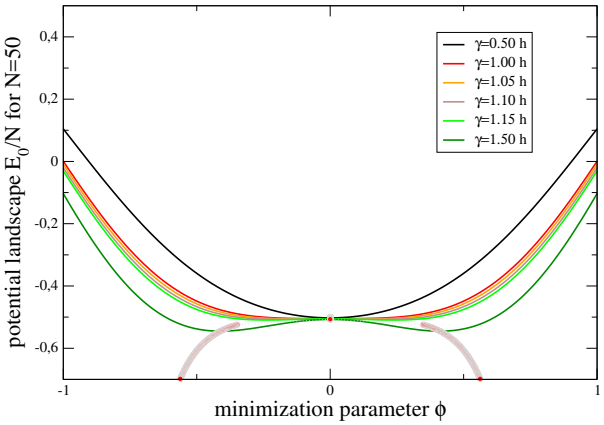

Figure 6.5: Potential landscape (6.56) for $N = 50$ and different values of γ. For $\gamma < h$, the minimum is situated at $\phi = 0$, whereas for $\gamma > h$, it splits into two minima. Symbols mark the trajectory of the minima as γ increases.

where $-\pi/2 < \phi < +\pi/2$ is a yet-to-be determined real parameter (the other values of ϕ would just lead to an overall phase of the wave function). Obviously, this state is well-normalized for all ϕ, and it is a simple product state of N identical single-qubit states. Thereby, it cannot capture effects such as entanglement. However, by minimizing the energy expectation value

$$E_0(h, \gamma, N, \phi) = \langle \Psi(\phi) | \, H_{\mathrm{LMG}} \, | \Psi(\phi) \rangle \tag{6.55}$$

with respect to ϕ, we obtain an upper bound to the true ground state energy. In case of the LMG model, this upper bound turns out to be quite tight, and in addition the potential landscape provides an interpretation of the phase transition. With using that $\langle \Psi(\phi) | \, \sigma_i^z \, | \Psi(\phi) \rangle = \cos^2(\phi) - \sin^2(\phi)$ and $\langle \Psi(\phi) | \, \sigma_i^x \, | \Psi(\phi) \rangle = 2 \sin(\phi) \cos(\phi)$, we can get a simple analytic expression for this function

$$E_0(h, \gamma, N, \phi) = -\frac{hN}{2} \left[\cos^2 \phi - \sin^2 \phi \right] - \gamma \left[\frac{1}{4} + (N-1) \sin^2 \phi \cos^2 \phi \right] . \tag{6.56}$$

Depending on the values of h and γ, the arising potential landscape may assume different shapes as a function of ϕ, see Fig. 6.5. The extrema can be found be minimizing analytically as a function of ϕ

$$\partial_\phi E_0(h, \gamma, N, \phi) = \left[hN - (N-1)\gamma \cos(2\phi) \right] \sin(2\phi) \, , \tag{6.57}$$

which has solutions $\phi_1 = 0$ and $\cos \phi_2 = \frac{N}{N-1} \frac{h}{\gamma}$. Inserting these solutions we get the minimum energies

$$E^1_{\mathrm{min}} = -\frac{hN}{2} - \frac{\gamma}{4} \, , \qquad E^2_{\mathrm{min}} = -\frac{\gamma N}{4} - \frac{h^2 N^2}{4\gamma(N-1)} \, . \tag{6.58}$$

The point where these curves meet marks the position of the phase transition, e.g. considering h as fixed we get

$$\gamma_{\mathrm{crit}} = \frac{N}{N-1} h \, . \tag{6.59}$$

Similar as with the Ising phase transition, the first derivative of the ground state solutions (6.58) is continuous, but the second derivatives do not match, i.e., the true ground state energy is non-analytic at the critical point. This also classifies the model as a second order quantum phase transition.

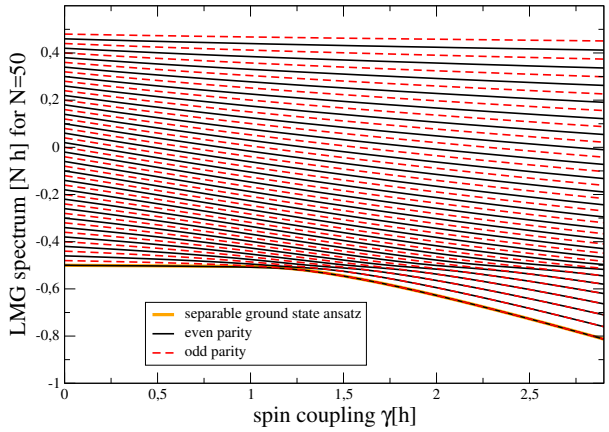

Figure 6.6: Spectrum of the LMG Hamiltonian (6.52) in the subspace of maximum angular momentum $J = \frac{N}{2}$. For $\gamma \ll h$ the ground state energy hardly depends on γ. For large γ, the ground state energy scales with N^2, in very good agreement with the analytic separable estimate (bold blue). Beyond that, we see for large γ some increase in the density of levels around $E/(Nh) = -1/2$, corresponding to an excited state phase transition.

We can separately numerically diagonalize the Hamiltonian within the blocks of fixed total angular momentum and fixed parity. Here, we directly see that the use of the angular momentum eigenbasis yields a huge performance improvement as compared to the computational basis: Whereas for the computational basis, we would have to diagonalize a $2^N \times 2^N$ matrix, with using the angular momentum eigenbasis the largest block that needs to be diagonalized has dimension $(N+1) \times (N+1)$, which is an enormous improvement! Taking the parity into account leads to an additional factor of two. This allows one to treat sizes of N numerically that would be completely intractable in the computational basis representation, the plot in Fig. 6.6 is absolutely no challenge.

6.3.2 Holstein-Primakoff transform

The previous considerations told us an upper bound on the ground state energy. Although Fig. 6.6 demonstrates that the bound appears to be tight, this is not guaranteed. In addition, we know nothing about the corresponding excitations. To get these, we can employ the Holstein [8] -Primakoff [9] transform, which at first maps the LMG model to strongly interacting bosons.

Box 30 (Holstein-Primakoff transform) *The Holstein-Primakoff transform*

$$J^+ = \left[N - a^\dagger a\right]^{1/2} a\,, \qquad J^- = a^\dagger \left[N - a^\dagger a\right]^{1/2}\,, \qquad J^z = \frac{N}{2} - a^\dagger a \tag{6.60}$$

maps large-spin operators $J^\alpha = \frac{1}{2}\sum_{i=1}^N \sigma_i^\alpha$ *to a single bosonic mode* a*. Its inverse formally reads*

$$a = \left[\frac{N}{2} + J^z\right]^{-1/2} J^+\,, \qquad a^\dagger = J^- \left[\frac{N}{2} + J^z\right]^{-1/2}\,. \tag{6.61}$$

We see that the inverse transformation is as it is written actually not always well defined, as the minimum eigenvalue of J^z is given by $-N/2$, such that the operator $N/2 + J^z$ becomes singular. However, to the right of this operator we always have a J^+ large spin operator, such that the inverse Holstein-Primakoff transform should be understood as $a = \lim_{\epsilon\to 0^+} \left[\epsilon + \frac{N}{2} + J^z\right]^{-1/2} J^+$.

[8] Theodore David Holstein (1915–1985) was an american theoretical physicist.
[9] Henry Primakoff (1914–1983) was an american theoretical physicist.

Due to the root in the transformation, we get all kinds of powers of bosonic operators, which means that the arising bosonic particles are interacting. The strength of the method lies in the fact that in the infinite N-limit, the interaction terms can very often be neglected, allowing an exact diagonalization of the underlying model in this limit. First, we show that when we assume bosonic commutation relations for the a operator, the usual spin commutation relations are respected

$$\begin{aligned}[J^x, J^y] &= \left[\frac{1}{2}(J^+ + J^-), -\frac{\mathrm{i}}{2}(J^+ - J^-)\right] = -\frac{\mathrm{i}}{2}\left[J^-, J^+\right] \\ &= -\frac{\mathrm{i}}{2}\left(a^\dagger(N - a^\dagger a)a - (N - a^\dagger a)^{1/2} a a^\dagger (N - a^\dagger a)^{1/2}\right) = -\frac{\mathrm{i}}{2}\left(2a^\dagger a - N\right) \\ &= \mathrm{i}J^z\,. \end{aligned} \tag{6.62}$$

To show this, we have assumed that the bosonic commutation relations hold. Inserting this in the LMG model Hamiltonian (6.52) we arrive at

$$\begin{aligned} H_{\mathrm{LMG}} &= -h\left[\frac{N}{2} - a^\dagger a\right] - \frac{\gamma}{4N}\left(\sqrt{N - a^\dagger a}a + a^\dagger\sqrt{N - a^\dagger a}\right)^2 \\ &= -h\left[\frac{N}{2} - a^\dagger a\right] \\ &\quad - \frac{\gamma}{4}\Big[\left(\sqrt{1 - \frac{a^\dagger a}{N}}a\sqrt{1 - \frac{a^\dagger a}{N}}a + \mathrm{h.c.}\right) + aa^\dagger\left(1 - \frac{a^\dagger a}{N}\right) + a^\dagger\left(1 - \frac{a^\dagger a}{N}\right)a\Big]\,. \end{aligned} \tag{6.63}$$

This is a complicated interacting bosonic system.

Normal phase diagonalization

Being interested in the large N limit, we may simply neglect the suppressed terms, which effectively gets rid of the squareroots

$$\begin{aligned} H^1_{\mathrm{LMG}} &= -h\left[\frac{N}{2} - a^\dagger a\right] - \frac{\gamma}{4}\left[a^2 + a^{\dagger 2} + aa^\dagger + a^\dagger a\right] \\ &= -hN/2 + (h - \gamma/4)a^\dagger a - \gamma/4 aa^\dagger - \frac{\gamma}{4}\left[a^2 + a^{\dagger 2}\right] \\ &= -hN/2 + \Omega b^\dagger b + \omega_0\,. \end{aligned} \tag{6.64}$$

Here, we have neglected terms of $\mathcal{O}\{N^{-1/2}\}$, and in the last step, we have used a single-mode Bogoliubov transform $a = ub + vb^\dagger$, as we did in the exercises. It will work as long as $\gamma < h$ and will yield the solutions

$$\omega_0 = -\frac{h}{2} + \frac{1}{2}\sqrt{h(h-\gamma)}\,, \qquad \Omega = \sqrt{h(h-\gamma)}\,, \tag{6.65}$$

such that we can gather the spectrum of the normal phase as

$$E_n^{\gamma \le h} = -\frac{h}{2}N - \frac{h}{2} + \frac{1}{2}\sqrt{h(h-\gamma)} + n\sqrt{h(h-\gamma)}\,, \qquad n \in \{0, 1, 2, \ldots\}\,. \tag{6.66}$$

From that, we learn that at the critical point, the excitation spectrum vanishes, at least as we approach the critical point from $\gamma < h$.

Superradiant phase diagonalization

When we come from the other side, we soon see that the very same Bogoliubov transform cannot be used here, as the scaling of the spectrum cannot be recovered. Instead, it is necessary to displace the bosonic operators first, to make sure that one expands around the correct vacuum. Scaling of the eigenvalues for $h = 0$ tells us that the correct displacement should scale as

$$a = \sqrt{N}\alpha + b\,, \qquad a^\dagger = \sqrt{N}\alpha^* + b^\dagger\,. \tag{6.67}$$

Here, α is just a complex parameter, which may depend on h and γ, and b is just as bosonic as was a. Inserting this in the LMG Hamiltonian, we can again expand the roots for large N – this is actually a bit tedious and requires careful bookkeeping – and write the LMG Hamiltonian as

$$H^2_{\mathrm{LMG}} = NH_0 + \sqrt{N}H_1 + H_2 + \mathcal{O}\{N^{-1/2}\}\,. \tag{6.68}$$

Here, H_0 is just a number, H_1 is just linear in the creation and annihilation operators and H_2 is quadratic in the annihilation and creation operators. We can fix the value of α by demanding that H_1 vanishes, which yields

$$\alpha = \pm\sqrt{\frac{1}{2} - \frac{h}{2\gamma}}\,, \tag{6.69}$$

which is real for $h < \gamma$. In addition, we have the solution $\alpha = 0$, which recovers the previous case. Inserting this in the Hamiltonian, we get rid of any linear contribution in the bosonic operators, yielding

$$\begin{aligned} H &= -\frac{h^2+\gamma^2}{4\gamma}N + \frac{3}{8}(3\gamma - h)b^\dagger b + \frac{1}{8}(\gamma - 3h)bb^\dagger + \frac{1}{8}(3\gamma - 5h)(b^2 + \text{h.c.}) \\ &= -\frac{h^2+\gamma^2}{4\gamma}N + \Omega c^\dagger c + \omega_0\,, \qquad \Omega = \sqrt{\gamma^2 - h^2}\,, \qquad \omega_0 = \frac{-\gamma}{2} + \frac{1}{2}\sqrt{\gamma^2 - h^2}\,. \end{aligned} \tag{6.70}$$

In the last line, we have used a standard Bogoliubov transform $b = uc + vc^\dagger$ to a diagonal Hamiltonian, which is applicable when $h < \gamma$. Altogether, the spectrum for $\gamma > h$ then reads

$$E_n^{\gamma \geq h} = -\frac{h^2+\gamma^2}{4\gamma}N - \frac{\gamma}{2} + \frac{1}{2}\sqrt{\gamma^2 - h^2} + n\sqrt{\gamma^2 - h^2}\,, \qquad n \in \{0, 1, 2, \ldots\}\,. \tag{6.71}$$

Gathering the results from Eq. (6.66) and (6.71), we get e.g. for the ground state energy in in the continuum limit

$$\frac{E_0}{N} = \begin{cases} -\frac{h}{2} & : \ \gamma \leq h\,, \\ -\frac{h^2+\gamma^2}{4\gamma} & : \ \gamma \geq h \end{cases}$$

Here, we can again discuss the behaviour of the ground state energy density in the continuum limit. Beyond that, we can compare the computed excitation spectra with the numerical solution, see Fig. 6.7.

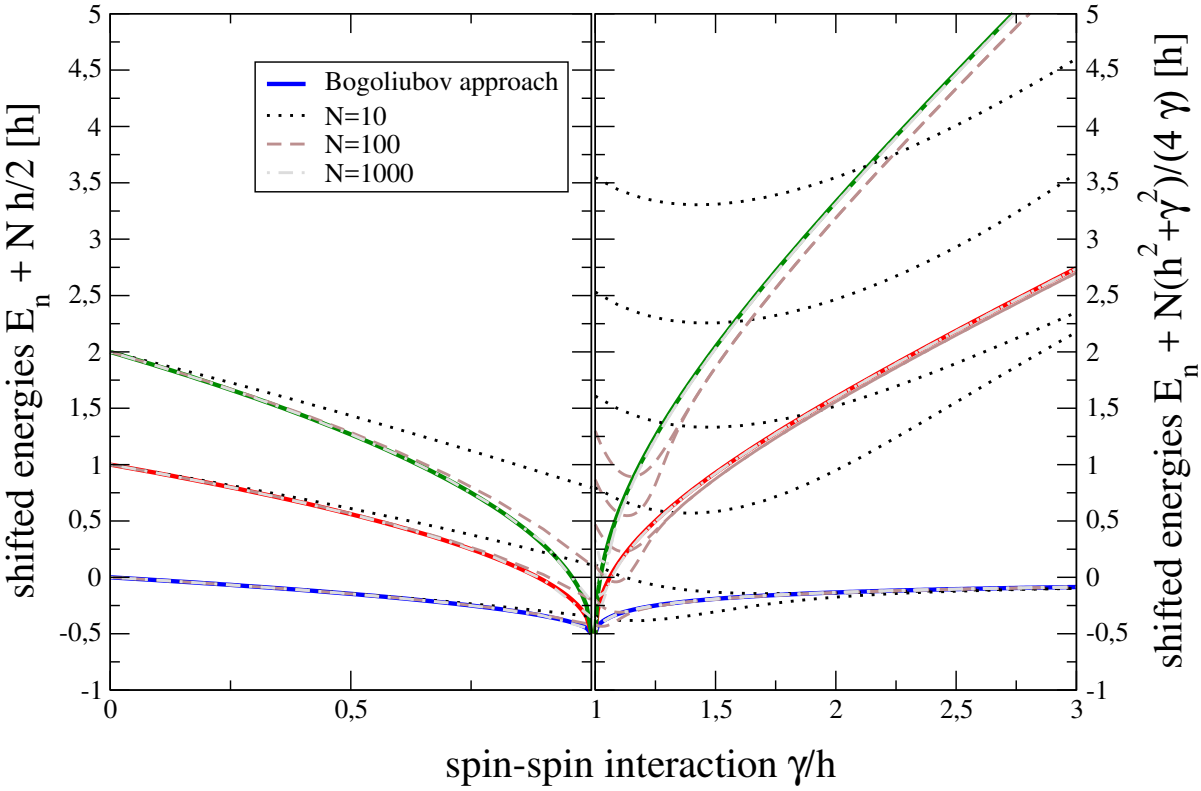

Figure 6.7: Plot of the analytically computed three lowest eigenvalues in the normal phase from Eq. (6.66) (left, solid curves) and in the superradiant phase from Eq. (6.71) (right, solid curves). Different shifts have been applied to both phases to make both phases visible (see left and right vertical axes). The from Eq. (6.52) numerically computed three (left) or six (right) lowest eigenvalues converge for large N (dash-dotted) toward the analytical result (colored solid), whereas for small N (dotted) one can see that the critical point is shifted towards larger γ. On the right, the odd and even parity solutions merge, they are exactly identical as $N \to \infty$ and correspond to the two different opposite sign choices of the displacement α.

Bibliography

[1] William H. Press, Saul A. Teukolsky, William T. Vetterling, and Brian P. Flannery. *Numerical Recipes in C*. Cambridge University Press, 2nd edition, 1994.

[2] Edward Farhi, Jeffrey Goldstone, Sam Gutmann, Joshua Lapan, Andrew Lundgren, and Daniel Preda. A quantum adiabatic evolution algorithm applied to random instances of an NP-complete problem. *Science*, 292:472–476, 2001.

[3] Steven H. Strogatz. *Nonlinear Dynamics and Chaos*. Westview Press, 2000.

[4] John David Jackson. *Classical Electrodynamics*. John Wiley & Sons, 3 edition, 1999.

[5] J. D. Murray. *Mathematical Biology I: An Introduction*. Springer, New York, 2002.

[6] Michael A. Nielsen and Isaac L. Chuang. *Quantum Computation and Quantum Information*. Cambridge University Press, Cambridge, 2000.

[7] M. Esposito, U. Harbola, and S. Mukamel. Nonequilibrium fluctuations, fluctuation theorems, and counting statistics in quantum systems. *Reviews of Modern Physics*, 81:1665–1702, 2009.

[8] Göran Lindblad. Completely positive maps and entropy inequalities. *Communications in Mathematical Physics*, 40:147, 1975.

[9] Herbert Spohn. Entropy production for quantum dynamical semigroups. *Journal of Mathematical Phyics*, 19:1227, 1978.

[10] H.-P. Breuer and F. Petruccione. *The Theory of Open Quantum Systems*. Oxford University Press, Oxford, 2002.

[11] G. B. Arfken and H. J. Weber. *Mathematical Methods For Physicists*. Elsevier LTD, Oxford, 2005.